Universitat Ramon Llull

TESIS DOCTORAL

Título	**Herramientas de cribado virtual aplicadas a inhibidores de entrada del VIH. Diseño de nuevos compuestos anti-VIH.**
Realizada por	Violeta Isabel Pérez Nueno
en el Centro	Escola Tècnica Superior IQS
y en el Departamento	Química Orgánica
Dirigida por	Dr. Jordi Teixidó i Closa, Dr. Xavier Batllori Aguilà

C.Claravall, 1-3
08022 Barcelona
Tel. 936 022 200
Fax. 936 022 249
E-mail: urlsc@sec.url.es
www.url.es

Artículo V

DOI: 10.1002/cmdc.200((will be filled in by the editorial staff))

Biological profiling of anti-HIV agents and insights into CCR5 antagonist binding using *in silico* techniques

Antonio Carrieri*[a], Violeta I. Pérez-Nueno[c], Alessandra Fano[a], Carlo Pistone[a], David W. Ritchie[b], and Jordi Teixidó[c]

Acquired Immune Deficiency Syndrome (AIDS) is responsible for more than 31 million deaths, and many more people world-wide are affected by the disease. Novel ligands capable of blocking virus-cell fusion are emerging as promising candidate molecules towards HIV-1 infection because they promise to overcome the major drawbacks of classical highly active antiretroviral (HAART) drugs. However, due to the paucity of experimentally determined three-dimensional information about the HIV-1 cell surface co-receptors, structure based design continues to be hampered. Using computational techniques based on comparative receptor structure modelling, advanced 3D-QSAR, and protein-ligand docking, we present recent results which define updated molecular requirements and determinants for efficient binding of small molecule ligands to CCR5, a principal biological target for HIV entry blockers. These results are compared with shape and property based virtual screening results for commercially available entry blockers, and will be valuable for predicting new HIV entry-blocking leads.

Introduction

Chemokine receptors (CKRs), integral proteins belonging to the G-protein coupled receptor (GPCR) family, are emerging as novel and promising targets against the human immuno-deficiency virus (HIV-1). In addition to their natural physiological roles, mediated by chemokine binding, the importance of CKRs as anti-HIV targets relies on the fact that CKRs are involved in the early steps of viral entry into the cell. Blocking this interaction could overcome the clinical limits of existing highly active anti-retroviral drug therapies (HAARTs). It has been determined that a critical first step of HIV infection involves fusion of the viral gp120 protein with two particular CKRs, namely CCR5 and CXCR4, and the CD4 co-receptor. [1] However, viral fusion is prevented when chemokines are bound to the extracellular loops of the CKRs. Hence potential candidates to block the disease might be pseudo-peptides or other high molecular weight (MW) entities which can mimic the natural chemokines or, perhaps preferably, which can allosterically modulate the surface shapes of the CCR5 and CXCR4 receptors and hence block the interaction with gp120.

Several structurally diverse agents, pharmacologically defined as CCR5 antagonists, have already been identified.[2] TAK-779 [3] was the first relatively low MW nonpeptide compound found to be capable of antagonizing binding of the RANTES (Regulated upon Activation, Normal T cell Expressed and Secreted) CKR protein. TAK-779 is effective at nanomolar concentrations and its binding to CCR5 has been widely characterized and also interpreted at the three-dimensional (3D) level.[4,5] Recently, the first HIV-1 entry blocker (Maraviroc®) was launched on the market by Pfizer Inc.[6] However, its high molecular complexity, time-consuming and costly synthetic route, together with low yields, seems to limit wide clinical take-up of this and other related drugs. There is therefore a need to develop new CCR5 antagonists with more desirable pharmacological properties. We believe one way to achieve this is to exploit knowledge of existing antagonists using receptor-based and ligand-based *in silico* structural modeling and chemoinformatic techniques. For this reason, we recently studied a set of *easy-to-make* guanylhydrazone [7] and 4-hydroxy-piperidine derivatives, [8] synthesized by Berlex Science (see Chart 1), which have been shown to be functional CCR5 antagonists. The structures and biological data are reported in Table 1.

This article defines some molecular requirements and determinants for efficient binding of antagonists inhibitors to CCR5. The study was carried out by: (i) performing chemometric analyses of the biological activity profile of the Berlex data set by

[a] *Prof. A. Carrieri, Dr. A. Fano, Dr. C. Pistone*
Dipartimento Farmaco-Chimico
Università degli Studi di Bari
Via Orabona 4, 70125, Bari, Italy
Fax: (+) 39 080 5442724
E-mail: carrieri@farmchim.uniba.it
[b] *Dr. D. W. Ritchie*
INRIA
Laboratoire Lorrain de Recherche en Informatique et ses Applications (LORIA)
UMR 7503, BP 239, 54506 Vandoeuvre-les-Nancy, France
[c] *Prof.J. Teixido, Drt. V.I. Pérez-Nueno*
Grup d'Enginyeria Molecular, Institut Químic de Sarrià (IQS), Universitat Ramon Llull
Barcelona, Spain

Supporting information for this article is available on the WWW under http://www.chemmedchem.org or from the author.

developing 3D-QSAR models able to support fresh pharmacophore hypotheses for the rational selection and prediction of potential new leads, (ii) upgrading a previously published three-dimensional (3D) theoretical model of CCR5 and docking selected highly active antagonists to construct a detailed binding site map and hence obtain deeper insights into the 3D determinants of CCR5 antagonist binding, (iii) building a CCR5 pharmacophore model using known high activity ligands, and (iv) performing shape-based virtual screening (VS) using a database of commercially available compounds to identify plausible novel CCR5 antagonists with a view to selecting synthetically accessible low MW candidates for further assay-based analysis. Our results show that a plausible model of the binding mode of known high affinity CCR5 antagonists can be successfully achieved using chemometric information, and receptor-based and ligand-based computational tools.

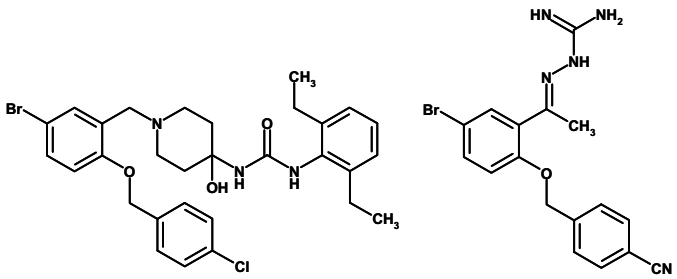

10h 38

Chart 1. Molecular structure of the two most active compounds from the guanylhydrazone (**38**) and 4-hydroxy-piperidine (**10h**) family.

Table 1. Molecular structure and activity data for test and prediction set of Berlex CCR5 antagonists

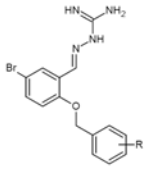

Compound	R	pIC$_{50}$ [(a)]	Compound	R	pIC$_{50}$ [(a)]
1	4–Cl	6.08	**12**	3–COOMe	5.80
3	H	5.72	**14**[(b)]	4–Me	6.30
4	4–F	6.10	**15**	3–Me	5.77
5	4–Br	6.22	**16**	4–Ome	6.15
6	4–CN	6.32	**17**	4–OBn	5.54
7	3–CN	5.70	**18**	4–Ph	5.77
8	4–NO_2	6.05	**19**	2,3	5.96
9	3–NO_2	5.77	**20**[(b)]	2,4–diF	5.43
10	2–NO_2	5.24	**21**	3–NO_2–6–OMe	5.06
11	4–COOMe	5.89			

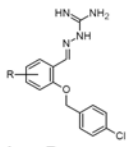

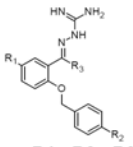

Compound	R	pIC$_{50}$ [(a)]	Compound	R1	R2	R3	pIC$_{50}$ [(a)]
23	5–Cl	6.22	**36**	Br	Cl	Me	6.70
24[(b)]	5–NO_2	5.92	**37Z**	Cl	Cl	Me	5.07
25	5–F	5.47	**37E**	Cl	Cl	Me	6.85
26	3,5–diCl	5.51	**38**	Br	CN	Me	7.03
29	5–CN	6.22	**39**	Br	Cl	Et	6.40
			40	Cl	F	*n*–But	5.38

(a) Inhibition of 125I-labeled MIP-1α binding to human CCR5/CD4 transfected HEK-293 cell.
(b) Included in the prediction set.

Table 1. continued

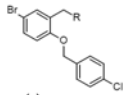

Compound	R	pIC$_{50}$ [(a)]	Compound	R	pIC50 [(a)]
42[(b)]		6.12	**6e**	MeBnN	5.00
43		4.85	**6f**		5.89
44		5.70	**2**[(b)]		6.00
6a	NH_2	5.77	**6i**		6.82
6b	EtNH	5.96	**6j**		6.46
6c	Me_2N	6.22	**6k**[(b)]		7.31
6d	Et_2N	5.85			

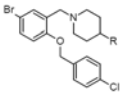

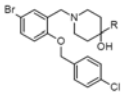

Compound	R	pIC50 [(a)]	Compound	R	pIC50 [(a)]
7a	OEt–	6.35	**9a**	F_3C–	6.24
7b	F–	6.55	**9b**		5.32
7c	–NH_2	5.33	**9c**	H_2NCH_2	6.24
7d[(b)]	–NHEt	5.51	**9d**		5.96
7e	–NHAc	6.41	**9e**		6.68
7f[(b)]	–NH(CO)Ome	6.40			
7g	–CH_2NH_2	5.07			
7h		6.46			
7i	–CO_2Et	5.89			
7j	–CO_2H	5.07			

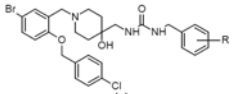

Compound	R	pIC50[(a)]	Compound	R	pIC50[(a)]
10a	4–F	5.82	**10f**	2,4,6–tri Me	7.00
10b	2,6–di F	6.49	**10g**	2,6–di Me	7.33
10c	2,6–di Cl	7.24	**10h**	2,6–di Et	7.96
10d	2,4,6–tri Cl	6.35	**10i**	2,6–di *i*Pr	7.46
10e	4–Br–2,6–di Me	6.77	**10j**	2,6–di MeO	7.57

(a) Inhibition of 125I-labeled MIP-1α binding to human CCR5/CD4 transfected HEK-293 cell.
(b) Included in the prediction set.

Results and Discussion

Chemometric analyses of the biological activity profile of the Berlex data set

Chemometric analyses of the biological activity profile of the Berlex data set were performed by developing 3D-QSAR models for the rational selection and prediction of potential new leads. In order to do this, the antagonist activity of the Berlex dataset, measured as inhibition of 125I-labeled MIP-1α binding to human CCR5/CD4 transfected HEK-293 cells (See Table 1), was first related to GRID independent descriptors (GRINDs) [9] in order to produce statistical models with which to investigate the molecular determinants of function. GRINDs were obtained by a quick and automated procedure involving: (i) calculating the molecular interaction fields (MIFs) induced by selected probe atoms on a 3D grid, (ii) filtering the MIFs in order to extract the most salient chemical information regarding the receptor binding site, and (iii) encoding the spatial relationship within the binding site nodes into new independent 3D variables.

Principal Component Analysis (PCA) was then carried out with MIFs calculated for hydrophobic (DRY), hydrogen bond acceptor (O), hydrogen bond donor (N1), and molecular shape atom probes (TIP), each of which models one aspect of the receptor-ligand interaction, and which together discriminate

between the pharmacological and structural components of the interaction. The first two components of the PCA (PC1 and PC2) were able to explain 33.04% and 25.11% of the variance, respectively. As can be seen in the PCA scores plot in Figure 1, compounds were mostly distinguished correctly according to activity by PC1, with high activity compounds appearing in the right hand quadrant and low actives in the left, and with the most potent ones clustered in the lower part of the plot. Additionally, PC2 generally groups the actives according to their nature and even chemical functional groups, whereby smaller and less hindered molecules which lack charged heterocyclic rings occupy the upper quadrant, and where bulkier ligands with saturated and basic rings are placed in the lower quadrant.

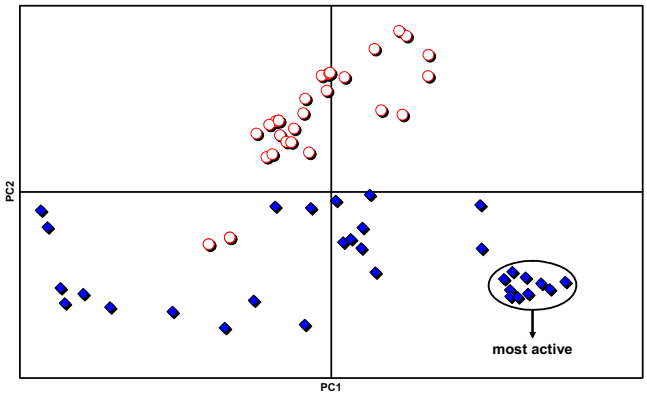

Figure 1. PCA scores plot: amine derivatives are represented by filled diamonds, and hydrazones by empty circles. The most active compounds are mainly placed towards the bottom right, whereas low activity compounds are on the left.

The PCA results show that the GRINDs for this compound set provide a reliable way to understand and interpret the biological data. Hence these descriptors were subsequently used in a Partial Least Squares (PLS) analysis using a training set of sixty derivatives. Additionally, eight molecules selected by PCA as the most descriptive antagonists were used to further validate the model predictively. It can be seen from the figures reported in Table 2 that good PLS statistics were obtained, with the percentage of explained variance being almost 90%. Similarly, the q^2 cross-validated correlation coefficients in both the Leave-one-out and Leave-two-out regression models, as well as using five random groups of compounds in the cross-validation procedure, are well above 0.3 which corresponds to a low probability of chance correlation (i.e. p<5%). To further validate the analysis, the antagonist activity data was shuffled and the PLS was repeated six times. In each case the q2 values were less than zero, indicating the risk of obtaining false positive models by chance is very low.

Table 2. Statistical results of PLS analysis for Berlex test set

n	$r^{2[a]}$	$q^{2[b]}$	$s^{[c]}$	$ONC^{[d]}$
60	0.880	$0.636^{[b_1]}$ $0.634^{[b_2]}$ $0.588^{[b_3]}$	0.2320	5 5 5

[a] Correlation coefficient. [b] Cross validated correlation coefficients: [b_1] Leave-two-out [b_2] Leave-one-out [b_3] Five random groups. [c] Standard error of the calculation. [d] Optimal number of component according to the crossvalidation results.

The quality of the PLS analysis may be also appreciated from the plot of experimental *vs* predicted data reported in Figure 2, in which no significant outliers are observed, and also from the validation set whose data were predicted with an average absolute error of 0.14.

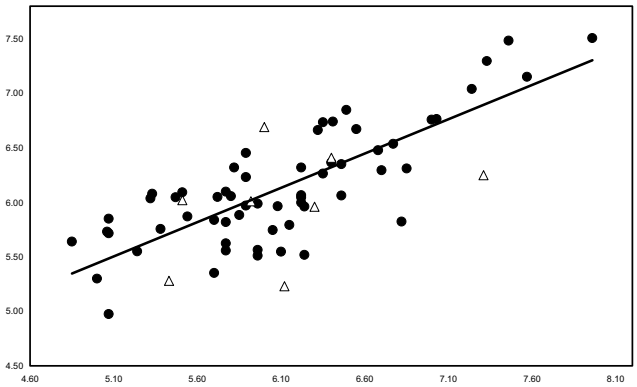

Figure 2. Plot of experimental *vs* predicted data from the non cross-validated model. Filled circles and empty triangles represent test and validation sets respectively.

Further insights into the 3D-QSAR results were gained by considering the signs and magnitudes of the PLS coefficients (see Figure 3) to determine which chemical descriptors are most responsible for antagonist activity. This analysis indicates that the MIFs measured at certain grid nodes and distances with the O-TIP, TIP-TIP, and O-N1 probes have the greatest impact on antagonist potency.

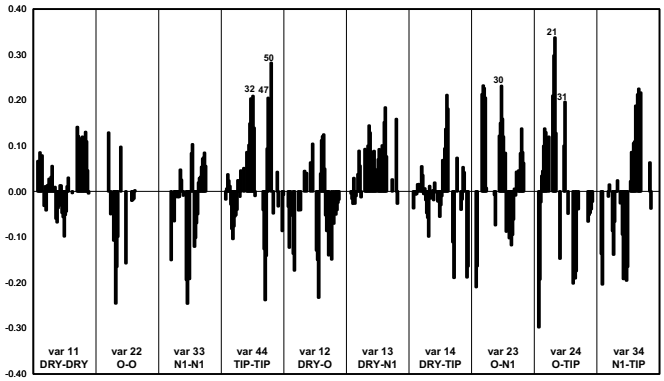

Figure 3. Bar plot of the PLS coefficient for the Berlex test set. Variables mentioned in the text are highlighted.

More specifically, the PLS variables in this study were numbered according to the distances between interacting nodes of a given type using a two-digit variable number (this can be converted to Å distances by multiplying it by the grid spacing and smoothing window, which were 0.5Å and 0.8 Å, respectively). Using this scheme, the variables O-TIP 21 and TIP-TIP 32, 47, and 50 showed the largest coefficients and hence these pharmacophoric moieties are likely to be present in the most active CCR5 antagonists and absent in the least active. Besides these variables, the variables O-N1 30 and O-TIP 31 also emerged as

relevant. These results suggest that certain appropriately spaced structural elements such as convex molecular surfaces and/or polar functional groups are pivotal for this class of HIV-1 entry blocker, and that achieving an optimal geometrical correlation between them could provide an important way to enhance biological activity.

Figure 4 shows graphical representations of the above variables displayed for the two most active compounds from the guanylhydrazone family, **38** (pIC_{50} = 7.03), and from the 4-hydroxy-piperidine family, **10h** (pIC_{50} = 7.96). It can be seen that the most important regions of the MIFs and their corresponding PLS variables are located around the antagonist scaffold in a kind of "L" shape, which is reminiscent of the binding mode calculated previously for known entry blockers,[10] with a first horizontal segment rich in charged and polar groups, and with a second vertical segment which is mostly hydrophobic.

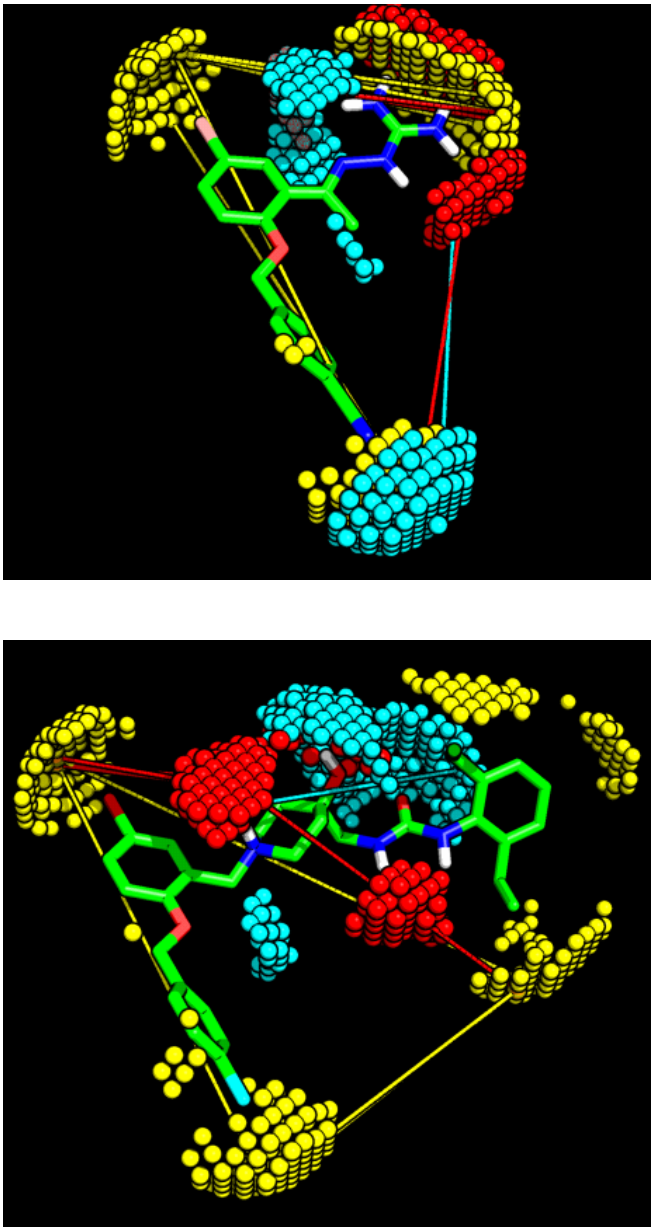

Figure 4. Grid filtered MIFs for high activity compounds **38** (top) and **10h** (bottom). The most significant PLS variables O-TIP, O-N1, and TIP-TIP are represented by red, cyan, and yellow lines, respectively.

Interestingly, two pharmacophoric elements which are shared by both classes of compound and separated by about 18.8–20.0 Å may be identified at the rounded boundaries of the vertical leg of the "L", and these match the para halogen atoms of the diaryl moiety. Perhaps not surprisingly, the SAR results for molecules with longer distances between these points or with bulkier substituents on the aromatic rings generally show significantly lower activities. Additionally, for the guanilhydrazones, the MIFs measures with O-N1 and O-TIP probes mentioned above identified a third polar region around the charged guanidinium group at a short distance (~12.4 Å) from the previously mentioned features. On the other hand, for the 4-hydroxy-piperidines, the presence of longer substituents (i.e. phenyl urea groups) in this region of the scaffold enhances the CCR5 antagonist activity, as might be perceived for favourable MIFs measured with the TIP probes at longer (20.0 Å) distance. The pharmacophoric model for the piperidines also shows the same overall features as described above. However, the piperidines characteristically exhibit a further favourable interaction region with polar probes at the upper face of the molecular skeleton, which distinguishes these two classes of antagonist (see Figure 4).

Overall, the above chemometric results indicate that new candidate CCR5 antagonists should have a relatively inflexible "L" shaped scaffold with polar features similar to those of the above two high affinity Berlex hydroxypiperidine and guanylhydrazone derivatives.

CCR5 antagonist binding mode analysis

A previously published three-dimensional (3D) theoretical model of CCR5 .[11] was upgraded and some highly active antagonists were selected and docked into the CCR5 extra-cellular pocket in order to construct a detailed binding site map (see Experimental Section). This showed a recognition pattern similar to the 3D-QSAR analyses and gave favorably binding energies in the modelled complexes with binding modes consistent with the one we found for TAK-779 in a previous modeling study [12]. In these models, the most hydrophobic tail of both **38** and **10h** is deeply buried within the CCR5 transmembrane cavity which is mainly made up of non-polar residues, with the two aromatic rings making extensive π-π stacking aromatic interactions with Tyr108, Phe112 and Phe113. However, our models exhibit some different interactions involving the remaining parts of those ligands. For example, the guanidinium head of **38** makes a charge transfer complex with the aromatic ring of Tyr108 and an extensive hydrogen bonding network with Thr105, Ser180 and Glu283, while this latter residue is involved with the urea group in the binding of **10h** which fills an empty cleft delimited by Tyr37 and Met287 (see Figure 5). These binding models are corroborated by the site-directed mutagenesis (SMD) results of Dragic et al.[4] which show that all of the above mentioned residues are essential for antagonist binding. Hence, docking results obtained are consistent with the above chemometric analyses showing that new candidate CCR5 antagonists should have a relatively inflexible "L" shaped scaffold with polar features. The binding modes found for the high affinity Berlex hydroxypiperidine and guanylhydrazone ligands are consistent with the grid filtered MIF results obtained, and show the same kinds of interaction with the CCR5 binding pocket.

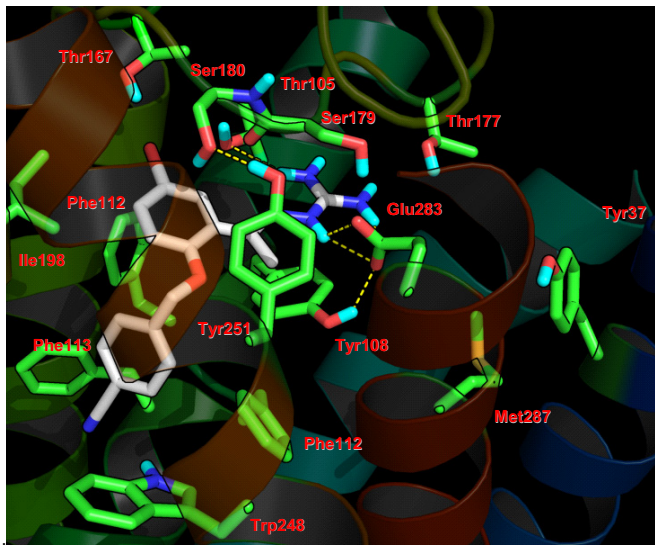

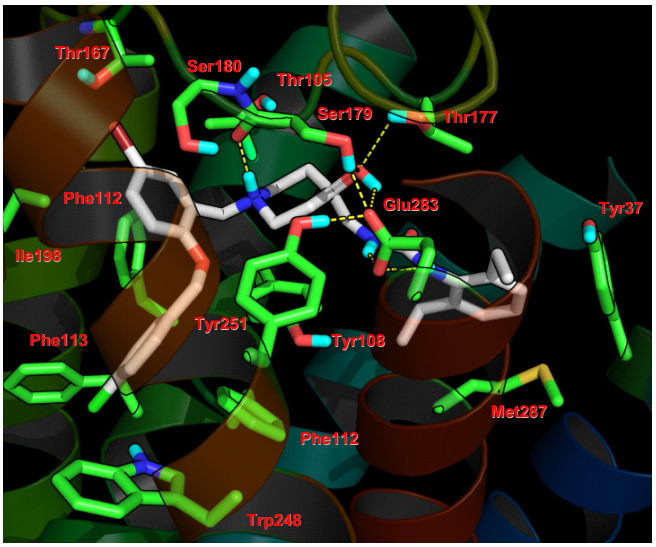

Figure 5. Calculated docking poses for **38** (top) and **10h** (bottom) in the model-built CCR5 extracellular cavity. The Flo+ binding energies are -40.39 and -30.12 kcal/mol, respectively.

Ligand-based pharmacophore modelling

Pharmacophore models were generated with MOE [12] and retrospective analyses were performed in order to select models which achieved an optimal balance between sensitivity and specificity. Several models were proposed (Table 3). Model 1 was built with MOE Pharmacophore Elucidate module and using TAK-220 [13] as the query. Model 2 was built with MOE Pharmacophore Elucidate module and using TAK-779 as the query. Features in Models 3 and 4 were selected from the consensus analysis performed with MOE Pharmacophore Query module of the most active compounds of the AMD3100 derivatives [14] SCH derivatives,[15] 1,3,4-trisubstituted pyrrolidinepiperidines, [16] diketopiperazines, [17] and TAK-779 derivatives. [18] Features in Model 5 were selected from the consensus analysis performed with MOE Pharmacophore Query module of the most active compounds belonging to families AMD3100 derivatives, SCH derivatives, 1,3,4-trisubstituted pyrrolidinepiperidines, diketo-piperazines, TAK-779 derivatives, 4-piperidines, [19] 1-phenyl-1,3-propanodiamines, [20] 4-aminopiperidines, [21] phenylcyclo-hexilamines, [22] and N,N'-diphenylureas. [23] Model 6 was built with MOE Pharmacophore Elucidate module and by constructing the query from the most active compounds belonging to the AMD3100 derivatives, SCH derivatives, 1,3,4-trisubstituted pyrrolidinepiperidines, diketopiper-azines, TAK-779 derivatives, 4-piperidines, 1-phenyl-1,3-propanodiamines, 4-aminopiperidines, phenylcyclohexil-amines and N,N'-diphenylureas.

The retrospective analysis of the models showed that pharmacophore Model 1 (Figure 6) was the most selective with our dataset, identifying 36 false positives and 89 false negatives. It can be seen that the indispensable features found for CCR5 inhibitors coincide with the ones found by the 3D-QSAR and binding mode interactions results. The O-TIP and O-N1 horizontal segment and the vertical hydrophobic segment found in the MIFs analysis are also present in the pharmacophore model (one horizontal segment with an hydrogen bond acceptor feature shown in blue and an hydrogen bond donor feature shown in purple, and one vertical segment with an hydrophobic feature shown in green). This model classified and ranked accurately the known actives and inactive compounds in the dataset. Visual inspection of the hit list of actives in the retrospective analysis showed that the ranking of each compound depended on the model and type of compound. Figure 7 shows the diversity scaffold retrieval analysis obtained with Model 1 at 1%, 5% and 7,6 % of the screened database. It should be noted that because MOE does not give the score of the compounds that do not match the pharmacophore query, the hit analysis can only be performed for the first 7.6 % of the screened database.

Table 3. Validation parameters for different proposed pharmacophore models in a retrospective analysis

Model	1	2	3	4	5	6
A[a]	332	332	332	332	332	332
D[b]	3650	3650	3650	3650	3650	3650
H_a[c]	243	231	173	273	275	261
H_t[d]	279	256	192	440	501	414
FP[e]	36	25	19	167	226	153
FN[f]	89	101	159	59	57	71
EF[g]	9.58	9.92	9.91	6.82	6.03	6.93
Y(%)[h]	87	90	90	62	55	63
A(%)[i]	73	70	52	82	83	79
GH[j]	0.83	0.84	0.80	0.64	0.58	0.64

[[a] The number of active compounds in the database (A). [b] The total number of compounds in the database (D). [c] Active compounds in the hit list (Ha). [d] Total number of compounds in a search hit list (Ht). [e] Number of false positives found (FP). [f] Number of false negatives found (FN). [g] Enrichment (enhancement) factor (EF). [h] Percent yield of actives (Y). [i] Percent ratio of the actives in the hit list. [j] Goodness of Hit list (GH).

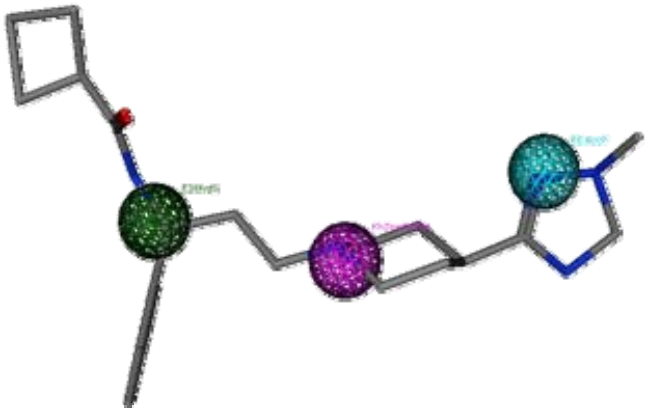

Figure 6. Alignment of the most active hit fitted in the pharmacophore query for Model 1. The feature shown in green is Hyd (hydrophobic), the feature shown in purple is Don (hydrogen bond donor), and the feature shown in blue is Acc (hydrogen bond acceptor).

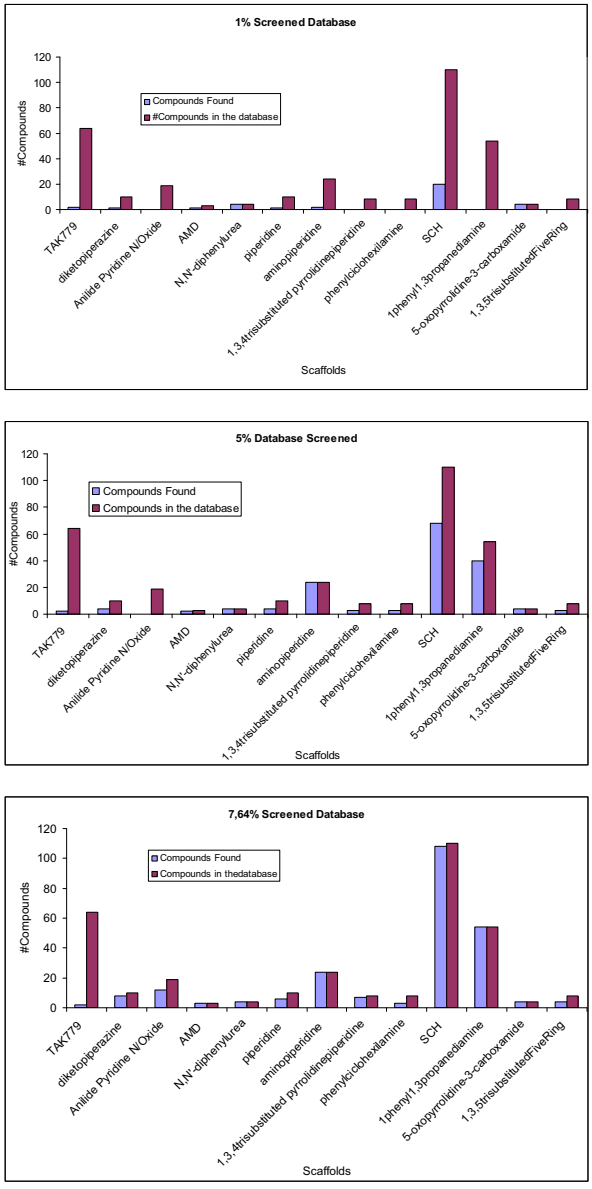

Figure 7. Diversity scaffold retrieval analysis obtained with Model 1 at 1%, 5% and 7,6 % of the screened database.

Shape matching-based virtual screening

As a final test for our hypothesis, shape-based VS was carried out. First, a shape-based inspection was performed in order to analyze the similarity between the docked conformation of TAK-779 from a previous study [11] and the conformations of **10h** obtained here from docking and from the 3D-QSAR analysis. Figure 8 shows that these three molecular shapes occupy similar molecular volumes. Hence these three shapes were used as queries for shape-based VS.

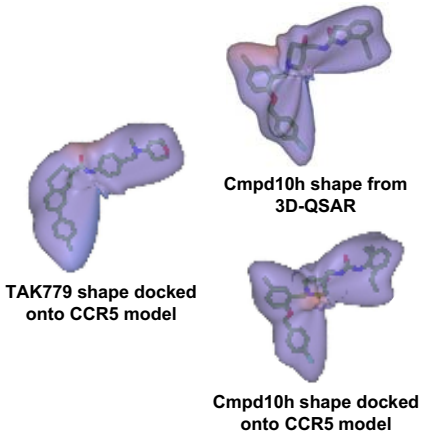

Figure 8. Comparison of molecular shapes of the TAK-779 with 4-hydroxy-piperidine (compound **10h**) in both its docked and 3D QSAR conformations.

Shape-based VS was carried out on the Berlex dataset using receiver-operator-characteristic (ROC) [24] plot and enrichment plot analyses using a variety of ligand-based screening tools. The area under the curve (AUC) of each ROC plot and the enrichment factor (EF) obtained from the enrichment plot were used to provide an objective measure of the ability of each approach to recognize known actives with similar shape to a given active query molecule. In order to avoid potential bias of the VS results due to large differences in basic properties, the 69 Berlex compounds were mixed with 3388 drug-like decoys from the Maybridge Screening Collection [25] which had 1D properties comparable to those of the actives (see Table 3).

Table 3. Summary of the Average 1D Physicochemical Properties of Active and Inactive Molecules in the Screening Database[a]

Molecule	b_1rotN[b]	Weight[c]	a_acc[d]	A_don[e]	a_hyd[f]	S_logP[g]
Actives Berlex	6.07 (1.36)	437.27 (88.81)	2.38 (0.79)	0.77 (1.07)	20.29 (5.65)	3.29 (1.72)
Inactives Maybridge	5.58 (0.71)	410.37 (43.68)	2.62 (0.49)	0.55 (0.50)	20.84 (3.32)	5.26 (1.25)

[a] Standard deviations are given in parentheses. [b] The number of rotatable single bonds. [c] Molecular weight. [d] The number of hydrogen-bond acceptor atoms. [e] The number of hydrogen-bond donor atoms. [f] The number of hydrophobic atoms. [g] Octanol-water partition coefficient.

Figure 9 shows the ROC curves and AUC values obtained for the various shape-based approaches used here. Our recently developed spherical harmonic (SH) consensus shape approach [26] gives the best VS performance (highest AUC values) when

using both the three high activity Berlex compounds (**1**, **2**, and **10h**) from three different scaffold families and the six high affinity PCA-selected compounds (**1**, **6l**, **7g**, **9**, **10j**, and **36**) as the consensus queries (see Figure 11). The next best query is **10h,** identified by the 3D-QSAR calculations, which also scores well with the ROCS and HEX shape-based scoring functions. Nearly all of shape-based scoring functions give better results than the QIKPROP/QIKSIM [27] chemical similarity query calculated from the average of the descriptors for all of the Berlex actives.

Regarding the performance of the three queries used, the **10h** query extracted from 3D-QSAR model identifies very well the compounds with the same scaffold (**10f**, **10g**, **10i**, **10j**, **10c**, **10e**, **10d**, **10b**, **10a**) at the first percentage of database screened, but it does not rank the other Berlex actives as highly as the **10h** query found from docking onto the CCR5 model. For this reason the initial enrichment is better for the query extracted from 3D-QSAR model, but next it is better for the query extracted from docking onto CCR5 model (see Figure 9, Parafit Shape Tanimoto query compound **10h** docked onto CCR5 model and Parafit Shape Tanimoto query compound **10h** from 3D-QSAR). The TAK-779 query extracted from docking onto CCR5 model does not perform so well because this query belongs to a different family of CCR5 inhibitors than the Berlex compounds, so the shape is also a slightly different (Figure 8) and the shape matching scores retrieved between this query and all Berlex compounds are lower (see Figure 9, Parafit Shape Tanimoto query TAK-779 docked onto CCR5 model).

Figure 10 shows the enrichment curves and enrichment factors for the consensus queries compared to the 3D-QSAR query. It can also be seen that the best VS performance (highest AUC values) is achieved using the spherical harmonic (SH) consensus shape approach.

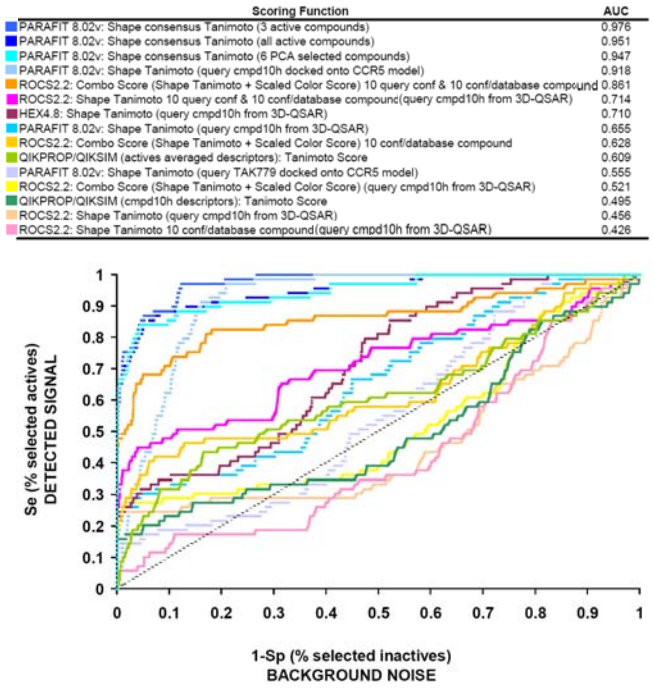

Figure 9. ROC plot evaluation of shape-based virtual screening for 69 Berlex CCR5 antagonists. The dotted black line represents the expected enrichment if actives were selected at random. This figure also reports the AUC values of the corresponding VS ROC curves.

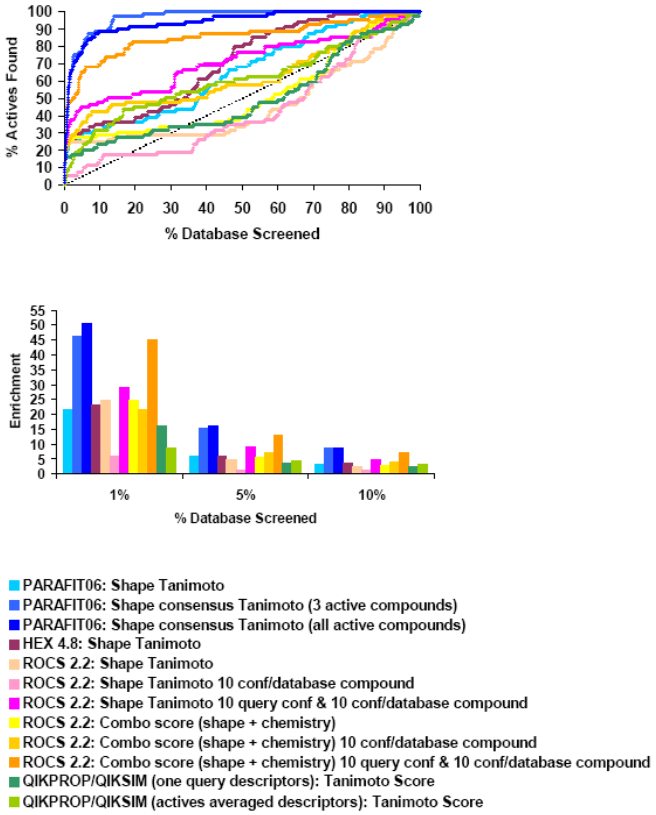

Figure 10. CCR5 shape matching-based enrichments. On the top, enrichment curves obtained using several shape-matching protocols with the Berlex CCR5 inhibitors (the dotted line represents the expected enrichment if actives were selected at random). On the bottom enrichment factor for actives found within the top-ranking 1%, 5%, and 10% fractions of the screened database.

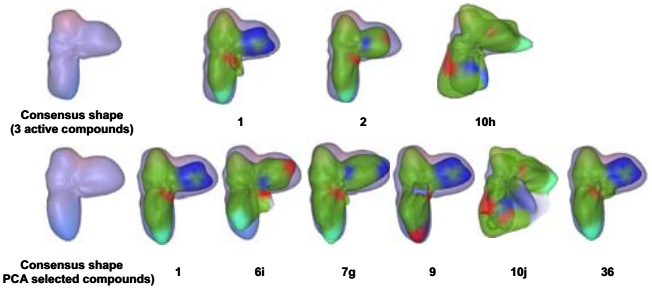

Figure 11. SH consensus shapes of the Berlex compounds. On the left, the consensus shapes calculated from three high activity compounds with different scaffolds (top), and six high affinity PCA-selected compounds (bottom). The remaining images to the right show the superpositions of the selected compounds onto the corresponding consensus shape.

Regarding the scaffold retrieval analysis, the single-ligand **10h** query retrieves compounds with the same scaffold (**10i**, **10g**, **10j**, **10f**, **10e**, **10c**, **10d**, **10b**, **10a**) in the first percentages of the database screened, while the consensus shape query retrieves more diverse scaffold in the first percentages of database screened (e.g. **6k**, **38**, **37E**, **7b**, **39**, **36**, **7a**, **9c**). In all cases, compounds with higher activity are retrieved first. Hence the use of consensus-based queries can be seen to find many CCR5 inhibitors remarkably well.

These results are supported by a large-scale VS experiment carried out by some of us previously, [26] in which 424 known CCR5 antagonists (comprising SCH derivatives, [15] diketopiperazines, [17] anilide piperidine N-oxides, [28] AMD derivatives, [14] 4-piperidines, [19] 4-aminopiperidine or tropanes, [21] 1,3,4-trisubstituted pyrrolidinepiperidines, [16] phenylcyclohexilamines, [22] TAK derivatives, [18] 1-phenyl-1,3- propanodiamines, [20] 1,3,5-trisubstituted pentacyclics, [29] N,N'-diphenylureas, [23] 5-oxopyrrolidine-3-carboxamides, [30] guanylhydrazone derivatives, [7] and 4-hydroxypiperidine derivatives [8]) were mixed with 4696 commercial drug-like compounds from the Maybridge Screening Collection (see Figure 12). In this experiment, the consensus shape of the three most active compounds of different scaffold families in the database (a piperidine derivative, a SCH derivative, and a 1,3,4-trisubstituted pyrrolidinepiperidine) was used as the VS query. Figure 12 shows that the AUC value obtained is high (0.991), thus corroborating the good performance of the consensus shape approach. Furthermore, three well known entry inhibitors (Vicriviroc®, Schering-Plough; Aplaviroc®, GlaxoSmithKline; and Maraviroc®, Pfizer) were included in these calculations. As shown in Figure 12, these actives are all retrieved in the first percentages of database screened. Moreover, visual inspection of the Maybridge compounds selected at the first percentages of database screened show that these compounds present a molecular geometry with polar and charged groups and hydrophobic moieties similar to those of the Berlex compounds.

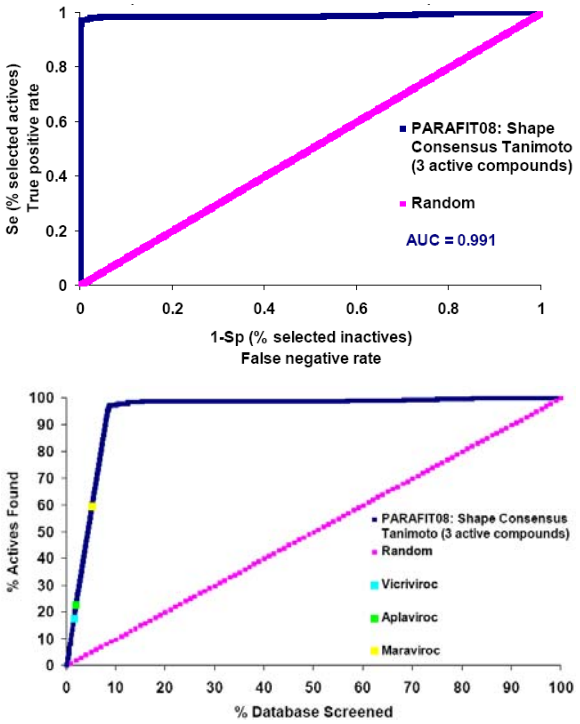

Figure 12. ROC plot (top) and enrichment plot (bottom) of consensus shape-based virtual screening for 424 CCR5 antagonists. The pink line represents the expected enrichment if actives were selected at random. The AUC value is reported in the ROC plot. The enrichment plot shows in blue, green, and yellow, the rank obtained for Vicriviroc®, Aplaviroc®, and Maraviroc®, respectively.

Conclusion

In conclusion, a pharmacophore model for a series of novel CCR5 antagonists has been presented. Chemometric information regarding the molecular determinants most important for anti-HIV-1 activity were combined with results from a structure-based docking study to obtain a highly plausible model of the binding mode of known high affinity CCR5 antagonists. Regarding the ligand-based study, we used CCR5 known binders in conjunction with chemical similarity searches and several shape-matching procedures, including a novel SH consensus shape matching approach, to perform VS. The enrichment and diversity results obtained show that using spherical harmonic consensus shapes as queries provides an effective tool with which to identify multiple CCR5 antagonists by shape-based VS.

Overall, our chemometric analyses, receptor-based and ligand-based computational approaches produce consistent biological profiles of CCR5 antagonists. Hence, the results presented here help build a better picture of the molecular requirements and determinants needed for antagonist inhibitors to bind within the CCR5 extracellular pocket, and will be valuable for predicting new HIV entry-blocking leads.

Experimental Section

Molecular structures of the protonated Berlex compounds were built using the Flo+ [31] suite of software with standard bond distances and valence angles. These were then flexibly superposed on the docked conformation of TAK-779 using fifty thousand cycles of the Flo+ TFIT module and in each case the conformation with the best superposition energy was selected. Compound **6l** was omitted since it was the lone 3-hydroxy-piperidine derivative.

GRINDs were calculated in GRID using the DRY, O, N1, and TIP atom probes to give four auto-correlograms and six cross-correlograms. PCA and PLS analyses were performed using the ALMOND software (version 3.3.0) using default settings and three hundred filtered grid nodes. No initial scaling was applied to the original X-variable matrix which was subsequently filtered by three Fractional Factorial Design runs. Cross-validation was performed using the leave one out (LOO) procedure to select the optimal number of components in the PLS model equal to a significant increase of the cross-validation coefficient q^2 (at least 5%).

The 3D structure of residues 1-320 of CCR5 was built by comparative homology modelling using MODELLER (ver9v2) to upgrade and refine our previously published 3D model [11] based on bovine rhodopsin (PDB code 1U19). The first 100 solutions were generated (refine level = fast, repeat = 100) and afterwards only loops were refined (refine level = slow, repeat = 100). The model with the best DOPE score was selected from this library of 600 models as input for receptor-ligand docking.

Flexible docking of **10h** and **38** was carried out using 100 steps of the Flo+ DYNDOCK module with the CCR5 Cα trace held fixed. The pose with the highest number of hydrogen bonds between the receptor and the antagonists and within and energy window of 100 kJ/mol within the global minimum was selected.

Pharmacophore studies were performed using MOE [12] software with 10 families of known actives: AMD3100 derivatives, SCH derivatives, 1,3,4-trisubstituted pyrrolidinepiperidines, diketopiperazines, TAK-779 derivatives, 4-piperidines, 1-phenyl-1,3-propanodiamines, 4-aminopiperidines, phenylcyclohexilamines and N,N'-diphenylureas. 50 conformations of each compound were calculated (MMFF94 forcefield). The training set consisted on the most active compound from each family of CCR5 inhibitors. The pharmacophore queries were built on the alignment of combinations of these structures with the FlexAlign module [32] in MOE. The pharmacophore scheme of PCH (polarity-charge-hydrophobicity) was applied throughout the MOE study. Chemical features and their tolerance radius were selected, between those suggested by MOE, to achieve better balance between sensitivity and specificity. Validity

of the pharmacophore models was determined by their ability to retrieve known active molecules from the databases using several formulas to score it and provide a quantitative value of goodness. Resulting pharmacophore modelling hit lists were analyzed using these terms (percent yield of actives, percent ratio of the actives in the hit list, enrichment, goodness of hit list, false negatives and false positives). All compounds were sorted into ranked lists based upon their rmsd. These lists were then used to plot the percentage of known actives found versus the percentage of the ranked database screened and to calculate the enrichment factor (EF) at 1%, 5% and 10% of the screened database.

Shape-based VS was performed using PARASURF/PARAFIT 08 [33], ROCS 2.3.1 [34], and HEX 4.8 [35], by superposing each of the database compounds onto a given query molecule. The PARAFIT and HEX superpositions were performed using the **10h** conformation extracted from 3D-QSAR as the query and the conformation computed by the MOE FlexAlign module [32] for each database compound. However, the ROCS shape matching calculations were performed using different query and database compound conformations. OMEGA [36] was used to calculate 10 further conformations of the query molecule, starting from the **10h** 3D-QSAR conformation, as well as 10 different conformations of every compound in the ligand database. Also, a consensus shape-based approach was applied using PARAFIT08, by superposing each of the database compounds onto a consensus SH surface query which combines the most significant features of the related group of Berlex molecules. Two consensus queries were constructed, one by superposing the three different scaffold high activity Berlex compounds (**1**, **2**, and **10h**) and the other by superposing the six high affinity PCA-selected compounds (**1**, **6l**, **7g**, **9**, **10j**, and **36**). In all approaches, the shape Tanimoto objective function was used to rank the ligand database.

The chemical similarity search was carried out using QIKPROP [27] to calculate 46 descriptors and pharmaceutically relevant properties for all database compounds. The Tanimoto similarity coefficient was calculated for all database compounds with respect to a) the compound **10h** descriptors and b) the average of physicochemical and biological properties of the 69 Berlex actives obtained from QIKSIM [27]. The performance of the shape-based VS approaches was assessed using ROC plot analyses.

Acknowledgements

The authors are grateful to OpenEye Scientific Software Inc. and Cepos Insilico Ltd. for providing Academic Licences for ROCS and ParaSurf, respectively. V.I.P.N. thanks the Generalitat de Catalunya-DURSI for a grant within the Formació de Personal Investigador (2008FI) program.

Keywords: HIV-1 infection, CCR5 antagonists, 3D-QSAR, docking, virtual screening

Received: ((will be filled in by the editorial staff))
Published online: ((will be filled in by the editorial staff

[1] S. J. Allen, S. E. Crown, T. M. Handel, *Ann: Rev. Immunol.* **2007**, *25*, 787-820.
[2] S. E. Kuhmann, O. Hartley, *Ann: Rev. Pharmacol. Toxicol.* **2008**, *48*, 425-461.
[3] M. Baba, O. Nishimura, N. Kanzaki, M. Okamoto, H. Sawada, Y. Iizawa, M. Shiraishi, Y. Aramaki, K. Okonogi, Y. Ogawa, K. Meguro, M. Fujino, *Proc. Natl. Acad. Sci. USA* **1999**, *96*, 5698–5703.
[4] T. Dragic, A. Trkola, D. A. D. Thompson, E. G. Cormier, F. A. Kajumo, E. Maxwell, S. W. Lin, W. Ying, S. O. Smith, T. P. Sakmar, J. P. Moore, *Proc. Natl. Acad. Sci. USA* **2000**, *97*, 5639-5644.
[5] C. Seibert, W. Ying, S. Gavrilov, F. Tsamis, S. E: Kuhmann, A. Palani, J. R. Tagat, J. W. Clader, S. W. McCombie, B. M. Baroudy, S. O. Smith, T. Dragic, J. P. Moore, T.P Sakmar. *Virology* **2006**, *349*, 41-54.
[6] Food Drug Adm. (FDA), Center Drug Eval. Res. 2007. Summary Minutes of the Antiviral Drugs Advisory Comm. Meet.
[7] R. G. Wei, D. O. Arnaiz, Y.-L. Chou, D. Davey, L. Dunning, W. Lee, S.-F. Lu, J. Onuffer, B. Ye, G. Phillips, *Bioorg. Med. Chem. Lett.* **2007**, *17*, 231–234.
[8] S.-F. Lu, B. Chen, D. Davey, L. Dunning, S. Jaroch, K. May, J. Onuffer, G. Phillips, B. Subramanyam, J.-L. Tseng, R. G. Wei, M. Wei, B. Ye, *Bioorg. Med. Chem. Lett.* **2007**, *17*, 1883–1887.
[9] M. Pastor, G. Cruciani, I. Mclay, S. Pickett, S. Clementi, *J. Med. Chem.* **2000**, *43*, 3233-4243.
[10] G. Paterlini, *Biophys. J.* **2002**, *83*, 3012-3031.
[11] A. Fano, D. W. Ritchie, A. Carrieri, *J. Chem. Inf. Model.* **2006**, *46*, 1223-1235.
[12] MOE, Molecular Operating Environment, Chemical Computing Group Inc., Montréal, QC (Canada), **2006**.
[13] M. Nishikawa, K. Takashima, T. Nishi, R. A. Furuta, N. Kanzaki, Y. Yamamoto, J.-I. Fujisawa, *Antimicrob. Agents Chemother.* **2005**, *49*, 4708–4715.
[14] K. Princen, S. Hatse, K. Vermeire, S. Aquaro, E. De Clercq, L.-O. Gerlach, M. Rosenkilde, T. W. Schwartz, R. Skerlj, G. Bridger, D. Schols, *J. Virol.* **2004**, *78*, 12996-13006.
[15] F. Tsamis, S. Gavrilov, F. Kajumo, C. Seibert, S. Kuhmann, T. Ketas, A. Trkola, A. Palani, J. W. Clader, J. R. Tagat, S. McCombie, B. Baroudy, J. P. Moore, T. P. Sakmar, T. Dragic, *J. Virol.* **2003**, *77*, 5201-5208.
[16] C. W. Willouhby, K. G. Rosauer, J. J. Hale, R. J. Budhu, S. G. Mills, K. T. Chapman, M. MacCoss, L. Malkowitz, M. S. Springer, S. L. Gould, J. A. DeMartino, S. J. Siciliano, M. A. Cascieri, A. Carella, G. Catver, K. Colmes, W. A. Schlief, R. Danzeisen, D. Hazuda, J. Kessler, J. Lineberger, M. Miller, E. A. Emini, *Bioorg. Med. Chem. Lett.* **2003**, *13*, 427-431.
[17] K. Maeda, K. Yoshimura, S. Shibayama, H. Habashita, H. Tada, K. Sagawa, T. Mikayawa, M. Auki, D. Fukushima, H. Mitsuya, *J. Biol. Chem.* **2001**, *276*, 35194-35200.
[18] Y. Aramaki, M. Seto, T. Okawa, T. Oda, N. Kanzaki, M. Shiraishi, *Chem. Pharm. Bull.* **2004**, *52*, 254-258.
[19] J. Cumming, World Patent WO 2003042178, **2003**.
[20] M. Perros, D. A. Price, B. L. C. Stammen, A. Wood, World Patent WO 2003084954, **2003**.
[21] J. Cumming, J. Winter, World Patent WO 2004018425, **2004**.
[22] W. M. Kazmierski, C. J. Aquino, N. Bifulco, E. E. Boros, B. A. Chauder, P. Y. Chong, M. Duan, F. Jr. Deanada, C. S. Koble, E. W. Malean, J. P. Peckham, A. C. Perkins, J. B. Thompson, D. Vanderwall, World Patent WO 2004054974, **2004**.
[23] S. Imamura, O. Kurasawa, Y. Nara, T. Ichikawa, Y. Nishikawa, T. Iida, S. Hashiguchi, N. Kanzaki, Y. Lizawa, M. Baba, Y. Sugihara, *Bioorg. Med. Chem.* **2004**, *12*, 2295-2306.
[24] N. Triballeau, F. Acher, I. Brabet, J.-P. Pin, H.-O Bertrand, *J. Med. Chem.* **2005**, *48*, 2534-2547
[25] Maybride Bringing life to drug discovery, Maybridge Databases Autumn 2005, Fisher Scientific International, England (UK) **2005**.
[26] V. I. Pérez-Nueno, D. W. Ritchie, J. I. Borrell, J. Teixidó, *J. Chem. Inf. Model.* **2008**, *48*, 2146-2165.
[27] (a) QikProp, version 2.3, Schrödinger Inc., New York (USA) **2005**. (b) W. L. Jorgensen, QikSim, version 2.3, Yale University, New Haven, CT (USA) **2005**.
[28] J. Cumming, H. Tucker, World Patent WO 2003042177, **2003**.
[29] S. Rusconi, A. Scozzafava, A. Mastrolorenzo, T. C. Supuran, *Curr. Drug Targets Infect. Disord.* **2004**, *4*, 339-3553.
[30] S. Imamura, Y. Ishihara, T. Hattori, O. Kurasawa, Y. Matsushita, Y. Sugihara, N. Kanzaki, Y. Lizawa, M. Baba, S. Hashiguchi, *Chem. Pharm. Bull.* **2004**, *52*, 63-73.
[31] C. McMartin, R. S. Bohacek, *J. Comput. Aided Mol. Des.* **1997**, *11*, 333-344.
[32] P. Labute, "Flexible Alignment of Small Molecules", Chemical Computing Group Inc., Montreal (Canada), to be found under http://www.chemcomp.com/journal/malign.htm, **2004**.
[33] ParaSurf and ParaFit, version 8.0, Cepos Insilico Ltd., Erlangen, Germany, to be found under http://www.ceposinsilico.de/Pages/Products.html, **2008.**
[34] A. J. Grant, B. T. Pickup, *J. Comput. Chem.* **1996**, *17*, 1653-1659.
[35] D. W. Ritchie, G. J. L. Kemp, *Proteins: Struct., Funct., Genet.* **2000**, *39*, 178-194.
[36] OMEGA, ersion 2.1.0, OpenEe Scientific Softare Inc., Santa Fe, NM (USA) 2006.

Artículo VI

DOI: 10.1002/cmdc.200800145

Discovery of Novel Non-Cyclam Polynitrogenated CXCR4 Coreceptor Inhibitors

Sofia Pettersson,[a] Violeta I. Pérez-Nueno,[a] Laia Ros-Blanco,[a] Raimon Puig de La Bellacasa,[a] María Obdulia Rabal,[a] Xavier Batllori,[a] Bonaventura Clotet,[b] Imma Clotet-Codina,[b] Mercedes Armand-Ugón,[b] José Esté,[b] José I. Borrell,[a] and Jordi Teixidó*[a]

HIV cell fusion and entry have been validated as targets for therapeutic intervention against infection. Bicyclams were the first low-molecular-weight compounds to show specific interaction with CXCR4. The most potent bicyclam was AMD3100, in which the two cyclam moieties are tethered by a 1,4-phenylenebis(methylene) bridge. It was withdrawn from clinical trials owing to its lack of oral bioavailability and cardiotoxicity. We have designed a combinatorial library of non-cyclam polynitrogenated compounds by preserving the main features of AMD3100. At least two nitrogen atoms on each side of the p*-phenylene moiety, one in the benzylic position and the other(s) in the heterocyclic system were maintained, and the distances between them were similar to the nitrogen atom distances in cyclam. A selection of diverse compounds from this library were prepared, and their in vitro activity was tested in cell cultures against HIV strains. This led to the identification of novel potent CXCR4 coreceptor inhibitors without cytotoxicity at the tested concentrations.*

Introduction

Studies in human immunodeficiency virus (HIV) biology have provided deep knowledge of the molecular events that are involved in the HIV life cycle, which consist of several steps: viral entry,[1,2] reverse transcription,[3–9] integration,[3,10–16] gene expression,[17,18] gene assembly,[19] budding[20] and maturation.[21] There is a need for the development of new drugs that are capable of suppressing HIV strains that are resistant to the currently used reverse transcriptase inhibitors (RTI) or protease inhibitors (PI), and for new drugs that target different stages in the virus life cycle.

HIV cell fusion and entry have been validated as targets for therapeutic intervention against infection.[2] The virus needs a primary receptor (CD4) and a coreceptor, either the chemokine receptor CXCR4 or CCR5, to fuse with the cell. Thus, they became new therapeutic targets for the treatment or prevention of HIV infection.

There are two approved entry and fusion inhibitors: T-20 (Fuzeon or enfuvirtide, developed by Roche–Trimeris), a linear 36 amino acid synthetic peptide with an acetylated N terminus and a carboxamide C terminus that is composed of naturally occurring L-amino acid residues, and maraviroc (Selzentry),[22] a CCR5 inhibitor. The first nonpeptidic CCR5 antagonist was TAK-779[23] (Figure 1), from Takeda Chemicals, although it could not be developed as an anti-HIV-1 drug because of its variable activity and poor oral bioavailability. Later, SCH-D[24] (vicriviroc, Figure 1), was developed by Schering–Plough; it had improved antiviral potency and better pharmacological properties relative to its predecessor SCH-C,[25] and has continued to phase III clinical trials. GW873140 (aplaviroc),[26] a spiroketopiperazine-based agent from Ono Pharmaceutical/GlaxoSmithKline, exhibited potent antiviral activity but has been discontinued for clinical development as an anti-HIV agent. Another class of anti-HIV agents that targets CCR5 includes PRO 140[27] (Progenics Pharmaceuticals), a humanized monoclonal antibody that is designed to block the ability of HIV to enter and infect cells; this antibody is in phase Ib clinical studies. In addition, CCR5 antagonists and monoclonal antibodies have shown potent synergistic antiviral effects by co-binding the receptor.[28]

Bicyclams were the first low-molecular-weight compounds with a specific interaction with CXCR4.[29–32] The most potent bicyclam was AMD3100 (Figure 1) in which the two cyclam moieties are tethered by a 1,4-phenylenebis(methylene) bridge. It has an IC_{50} of 1–10 ng mL^{-1}, which is at least 100 000-fold lower than the cytotoxic concentration. Samples of virus that were recovered from patients whom had been treated with AMD3100 (bicyclam) showed a change in virus phenotype, from X4 to R5; this suggests that AMD3100 blocked selectively those viruses that use CXCR4, although it was not effective in inhibiting CCR5-dependent replication of HIV in vivo. However, AMD3100 has shown poor oral absorption and toxicity, which is related to its high positive charge at physiological

[a] *S. Pettersson, V. I. Pérez-Nueno, L. Ros-Blanco, R. Puig de La Bellacasa, Dr. M. O. Rabal, Dr. X. Batllori, Dr. J. I. Borrell, Dr. J. Teixidó*
Grup d'Enginyeria Molecular
Institut Químic de Sarrià, Universitat Ramon Llull
Via Augusta 390, 08017 Barcelona (Spain)
Fax: (+34) 93-205-6266
E-mail: j.teixido@iqs.url.edu

[b] *Dr. B. Clotet, Dr. I. Clotet-Codina, Dr. M. Armand-Ugón, Dr. J. Esté*
Retrovirology Laboratory IrsiCaixa
Hospital Universitari Germans Trias i Pujol
Universitat Autònoma de Barcelona
08916 Badalona (Spain)

Supporting information for this article is available on the WWW under http://dx.doi.org/10.1002/cmdc.200800145.

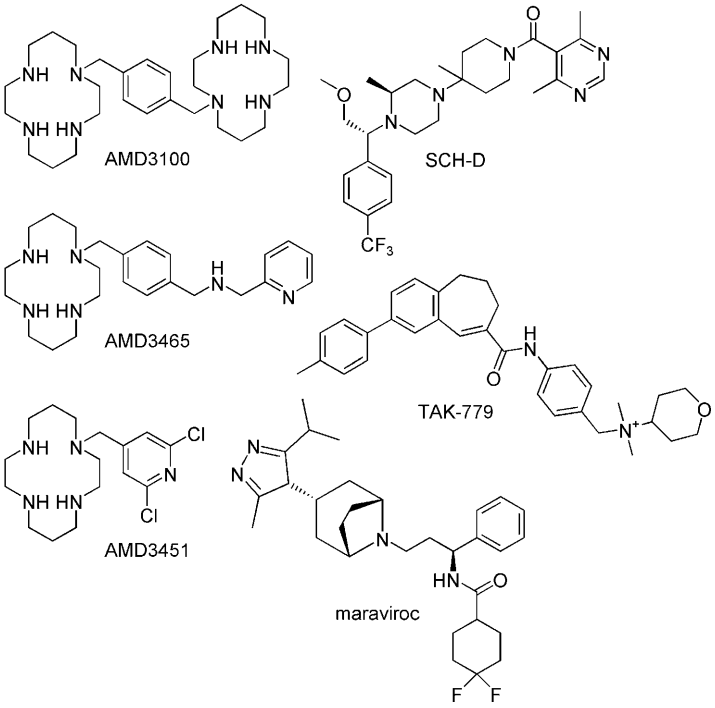

Figure 1. Structures of the main CXCR4 and CCR5 antagonist leads; they have aromatic or aliphatic linkers in polynitrogenated systems.

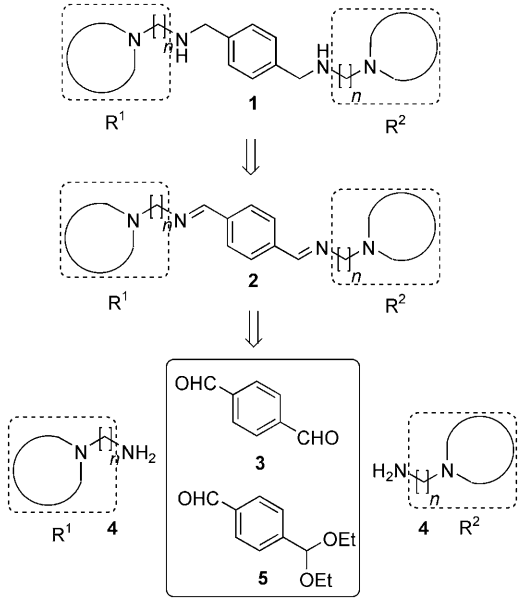

Figure 2. Retrosynthetic analysis for target diamines **1** ($n \geq 1$) and dihydrazones **2** ($n = 0$).

pH, therefore new analogous compounds should improve these characteristics.[33]

CXCR4 and CCR5 antagonist leads, such as AMD3100 (bicyclam), SCH-D or TAK-779 contain aromatic or aliphatic linkers in polynitrogenated systems. Among all of the compounds under study, bicyclams in general, and particularly AMD3100, appear to be the most active. *p*-Phenylenic compounds with a single cyclam moiety have also been developed, such as AMD3465 (Figure 1),[33] which is a CXCR4 antagonist, and AMD3451,[34] which shows antagonist activity against both CXCR4 and CCR5 coreceptors in cell culture studies. This led us to consider the possibility of obtaining symmetrical and nonsymmetrical systems that contain a *p*-phenylenic spacer and nitrogenated cyclic subunits in the search for new compounds that are potentially active against HIV-1. Herein we present the results of these studies.

Library design and compound selection

We designed a combinatorial library[35] by preserving the main features of AMD3100: a) at least two nitrogen atoms on each side of the *p*-phenylene moiety, one in the benzylic position and the other(s) in a heterocyclic system and b) similar distances between these nitrogen atoms as those that are present in cyclam. Such considerations led us to diamines **1** as target compounds (Figure 2). Very recently a similar but less restrictive approach was used by Liotta and colleagues[36] to propose a family of compounds whose general structure, $R^3R^4NCH_2C_6H_4CH_2NR^1R^2$, led to a large scaffold diversity. The most active compound in their library blocks in vitro CXCR4/SDF-1-mediated signaling more effectively than AMD3100, but they found it to be weakly active against HIV propagation in cell culture tests.

A retrosynthetic analysis for target compounds **1** in which $R^1 = R^2$ and $n \geq 1$ led to the symmetrical diimines **2** as precursors, which can be further disconnected to terephthalaldehyde (**3**) and two equivalents of the corresponding amine **4** ($n \geq 1$). When $R^1 = R^2$ and $n = 0$, compounds **2** are in fact symmetrical hydrazones, which can be obtained by condensation of terephthalaldehyde and the corresponding hydrazine **4** ($n = 0$). These dihydrazones were also included in our library.

To obtain nonsymmetrical ($R^1 \neq R^2$) diamines **1** ($n \geq 1$) and dihydrazones **2** ($n = 0$), it was necessary to slightly modify our synthetic approach by using 4-(diethoxymethyl)benzaldehyde (**5**) as the core precursor (Scheme 1). Thus, intermediate hydrazono and aminobenzaldehydes **6** and **7** allowed us to include such nonsymmetrical compounds and nonsymmetrical aminohydrazones **8** as target compounds.

The first selection of nitrogenated building blocks was based on commercial availability; the use of synthetic building blocks is currently under development. A search for available building blocks resulted in 18 commercially available nitrogenated building blocks that consist of a nitrogen-containing heterocyclic system (piperidine, piperazine, morpholine, pyrrolidine, imidazole and triazole), a polymethylene spacer, and a terminal amine group (Figure 3). Consequently, the virtual combinatorial library was built by using three hydrazines **4**{*1–3*} and eight amines **4**{*4–11*} as building blocks for substituents R^1 and R^2 of diamines **1**, dihydrazones **2** and aminohydrazones **8**, and it was subsequently enumerated with Cerius2.[37]

In an attempt to explore the chemical space that is covered by the library, we initially decided to select a reduced set of 19 compounds by using PRALINS[38] (*Program for Rational Analysis of Libraries in silico*) and by applying a diversity criteria, which decreases the number of compounds to be synthesized and

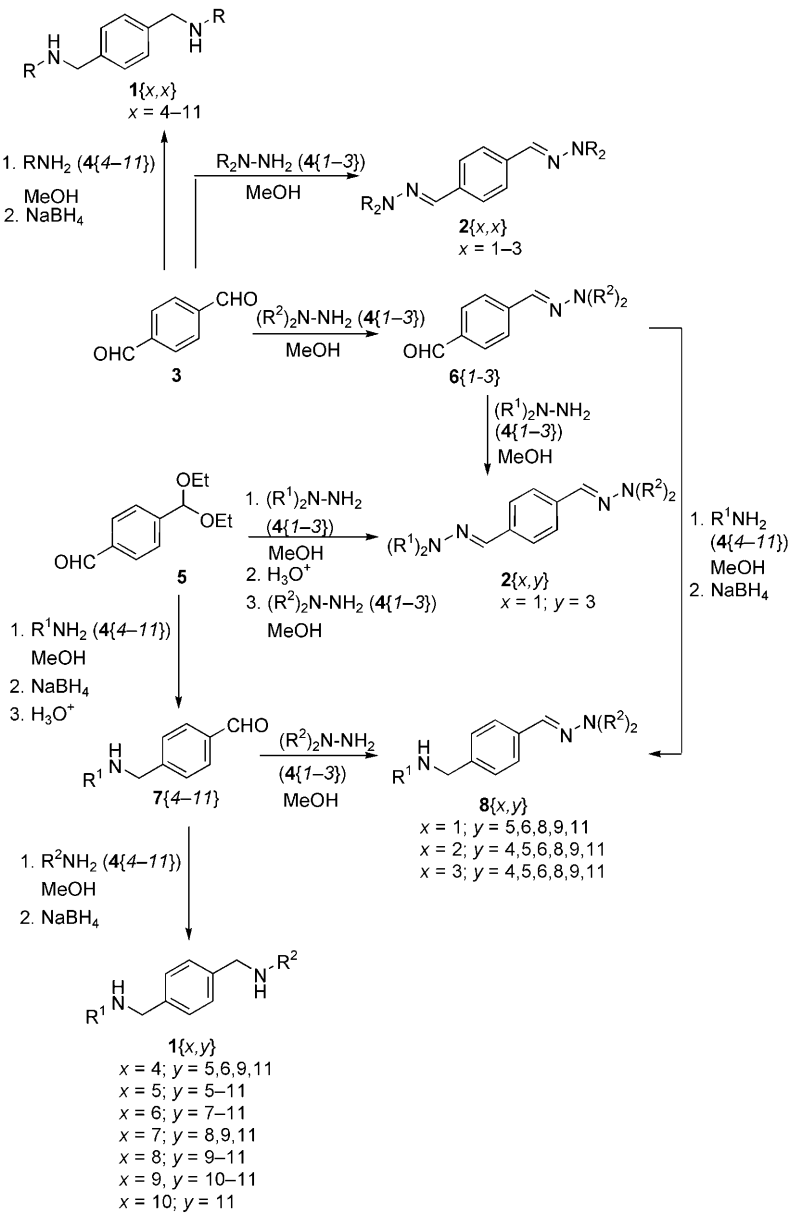

Scheme 1. Synthesis of symmetrical and nonsymmetrical diamines **1**, dihydrazones **2**, and aminohydrazones **8**.

evaluated without decreasing the chance of hit/lead finding. Thus, a series of molecular 2D (physicochemical, topological and topological based on information theory) and 3D (potential energy, surface, shape and volume) descriptors (computed with MOE[39]) were used for the definition of the chemical space. A subsequent principal component analysis decreased the initial set of descriptors to five components (explaining 90% of the variance) which were used as input for the diversity selection with PRALINS; this resulted in the selection of 19 compounds (Table 1).

Chemistry

Combinatorial approaches have been widely used in the identification of novel anti-HIV drugs;[40] in our case, the synthetic strategies that were used to obtain diamines **1**, dihydrazones **2** and aminohydrazones **8** are depicted in Scheme 1. For the synthesis of symmetrical diamines **1** ($R^1 = R^2$), we used a stepwise reductive amination:[41] a) reflux of a mixture of **3** and the corresponding amine **4**{*4–11*} (1:2 molar ratio) in anhydrous methanol by using molecular sieves as a dehydrating agent, and b) subsequent reduction with $NaBH_4$.[35]

Symmetrical dihydrazones **2** ($R^1 = R^2$) were obtained by condensation of **3** with the corresponding hydrazines **4**{*1–3*} in methanol (Scheme 1). Nonsymmetrical ($R^1 \neq R^2$) diamines **1**, dihydrazones **2**, and aminohydrazones **8** needed more complex approaches. Thus, hydrazonobenzaldehydes **6** were synthesized by coupling terephthalaldehyde (**3**) with hydrazines **4**{*1–3*} in a 2:1 molar ratio, followed by chromatographic separation from unreacted **3** and the symmetrical dihydrazone **2** byproduct. The subsequent coupling with a second hydrazine **4**{*1–3*} would afford the nonsymmetrical dihydrazones **2** ($R^1 \neq R^2$) (Scheme 1). This procedure has been used to obtain dihydrazone **2**{*1,3*}.

On the other hand, 4-(diethoxymethyl)benzaldehyde (**5**) was selected as building block to obtain aminobenzaldehydes **7** by reacting equimolar amounts of **5** and the corresponding amine **4**{*4–11*}, followed by reduction of the intermediate iminoacetal and subsequent acetal cleavage with a dilute solution of aqueous hydrochloric acid.[42–44] Treatment of these aminobenzaldehydes **7** with a second amine **4**{*4–11*} in anhydrous MeOH, by using molecular sieves as dehydrating agent, followed by reduction with $NaBH_4$, yielded the nonsymmetrical diamines **1** ($R^1 \neq R^2$) (Scheme 1). Finally, aminohydrazones **8** were accessible either by reductive amination of hydrazonobenzaldehydes **6** with the appropriate amine **4**{*4–11*} or by coupling of the aminobenzaldehydes **7** with the corresponding hydrazine **4**{*1–3*} (Scheme 1).

Results and Discussion

The first subset of compounds synthesized and tested (anti-HIV activity and cytotoxicity) included eight compounds: two dihydrazones (**2**{*1,1*} and **2**{*2,2*}) and six diamines (**1**{*3,4*}, **1**{*5,5*}, **1**{*6,6*}, **1**{*6,11*}, **1**{*9,9*} and **1**{*11,11*}) chosen among the 19 compounds result of the diversity selection. Three of them (**1**{*5,5*}, **1**{*9,9*} and **1**{*6,11*}) showed very promising anti-HIV activities, EC_{50} in the range 0.9–18 μg mL^{-1} (Table 1), so we decided to include structural modifications of them together with the remaining initial 19 candidates.

Thus, the second subset of compounds synthesized and tested was formed by seventeen compounds: one dihydrazone (**2**{*1,3*}), ten diamines (**1**{*6,7*}, **1**{*5,8*}, **1**{*5,10*}, **1**{*5,11*}, **1**{*4,5*}, **1**{*5,6*}, **1**{*5,7*}, **1**{*5,9*}, **1**{*9,10*} and **1**{*9,11*}) and six amino hydrazones (**8**{*3,5*}, **8**{*3,6*}, **8**{*3,8*}, **8**{*3,9*}, **8**{*1,5*} and **8**{*2,5*}). Twelve of these

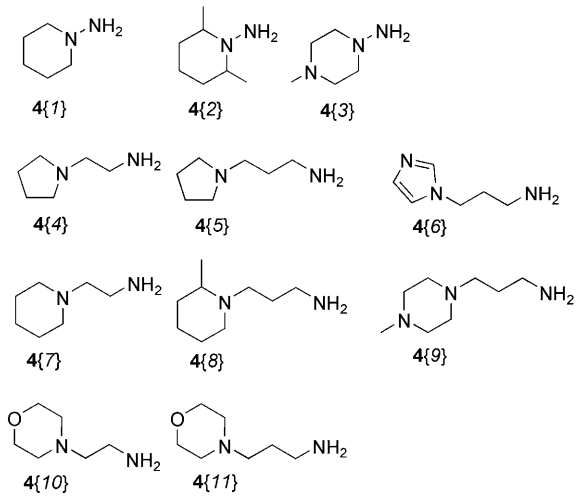

Figure 3. Amine building blocks used in the construction of the virtual combinatorial library.

compounds presented EC_{50} in the range 0.2 to 2.7 μg mL^{-1}, the most potent being **1**{*5,6*} and **1**{*5,8*} (0.2 μg mL^{-1}) (Table 1).

The third and final subset, which included 28 compounds, thus covering the total of 53 compounds synthesized and tested (Table 1), was selected by using computational analysis tools such as quantitative structure–activity relationships (QSAR) techniques and ligand- and structure-based drug design (for CXCR4 and CCR5 modeled HIV-1 entry coreceptors).[45,46] Notable compounds of this subset are **1**{*6,8*} (EC_{50} = 0.03 μg mL^{-1}), **1**{*8,9*} (EC_{50} = 0.03 μg mL^{-1}), and the most active compound in the library, **1**{*8,8*}, which has an EC_{50} value of 0.008 μg mL^{-1} and a CC_{50} > 25 μg mL^{-1}.

Among the different polynitrogenated building blocks, RNH_2, amines **4**{*5*} and **4**{*8*} gave the most active compounds. EC_{50} results suggest that higher activity values could be obtained by using a propylenic spacer between the heterocyclic ring and the nitrogen that supports the *p*-phenylenic moiety, and for heterocyclic systems that contain one nitrogen atom.

To evaluate the results, we determined the EC_{50} and CC_{50} of AMD3100 (EC_{50} = 0.001 μg mL^{-1}; CC_{50} > 5 μg mL^{-1}) and DS (dextran sulfate) (EC_{50} = 0.011 μg mL^{-1}; CC_{50} > 125 μg mL^{-1}) by following the same methodology as for our compounds. As can be seen, compound **1**{*8,8*} presents nearly the same level of activity as the reference compounds, **1**{*8,8*} (EC_{50} = 0.019 μM) and AMD3100 (EC_{50} = 0.002 μM), and shows no cell toxicity at the tested concentrations of up to 25 μg mL^{-1}.

Computational blind docking and ligand binding within the CXCR4 site-directed mutagenesis (SDM)-defined binding pocket[47] were analyzed in detail by using AutoDock[48,49] to study the interactions between **1**{*8,8*} and the CXCR4 coreceptor. To perform these calculations, CXCR4 was first homology modeled with MODELLER[50] and CONGEN[51] by using bovine rhodopsin as a template[52] as described in Pérez-Nueno et al.[53] The compound **1**{*8,8*} structure was built, assigned Gasteiger partial charges,[54] and minimized in MOE with the MMFF94 force field. For the AutoDock blind docking experiment, a 181×181×181 grid with a grid spacing of 0.375 Å was

Table 1. EC_{50} and CC_{50} values of diamines **1**, dihydrazones **2**, and aminohydrazones **8**.

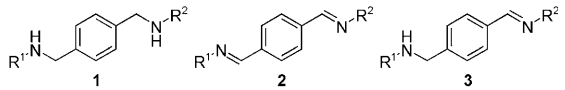

Subset[a]	Compound	R^1NH_2	R^2NH_2	EC_{50} [μg mL^{-1}][b]	CC_{50} [μg mL^{-1}][c]
1	**2**{*1,1*}	**4**{*1*}	**4**{*1*}	> 125	> 125
2	**2**{*1,3*}	**4**{*1*}	**4**{*3*}	> 25	> 25
2	**8**{*1,5*}	**4**{*1*}	**4**{*5*}	2.7	10.1
3	**8**{*1,6*}	**4**{*1*}	**4**{*6*}	> 25	> 25
3	**8**{*1,8*}	**4**{*1*}	**4**{*8*}	> 4.1	4.1
3	**8**{*1,9*}	**4**{*1*}	**4**{*9*}	> 9.8	9.8
3	**8**{*1,11*}	**4**{*1*}	**4**{*11*}	10.6	> 25
1	**2**{*2,2*}	**4**{*2*}	**4**{*2*}	> 125	> 125
3	**8**{*2,4*}	**4**{*2*}	**4**{*4*}	14.7	> 25
2	**8**{*2,5*}	**4**{*2*}	**4**{*5*}	2.0	9.8
3	**8**{*2,6*}	**4**{*2*}	**4**{*6*}	> 25	> 25
3	**8**{*2,8*}	**4**{*2*}	**4**{*8*}	0.6	14.6
3	**8**{*2,9*}	**4**{*2*}	**4**{*9*}	3.8	19.2
3	**8**{*2,11*}	**4**{*2*}	**4**{*11*}	15.7	> 25
3	**2**{*3,3*}	**4**{*3*}	**4**{*3*}	> 125	> 125
1	**8**{*3,4*}	**4**{*3*}	**4**{*4*}	> 84.9	84.9
2	**8**{*3,5*}	**4**{*3*}	**4**{*5*}	1.8	14.3
2	**8**{*3,6*}	**4**{*3*}	**4**{*6*}	11.2	> 25
2	**8**{*3,8*}	**4**{*3*}	**4**{*8*}	1.4	10.3
2	**8**{*3,9*}	**4**{*3*}	**4**{*9*}	11.7	> 25
3	**8**{*3,11*}	**4**{*3*}	**4**{*11*}	8.1	> 25
3	**1**{*4,4*}	**4**{*4*}	**4**{*4*}	10.2	> 25
2	**1**{*4,5*}	**4**{*4*}	**4**{*5*}	1.7	> 25
3	**1**{*4,6*}	**4**{*4*}	**4**{*6*}	4.8	> 25
3	**1**{*4,9*}	**4**{*4*}	**4**{*9*}	8.2	> 25
3	**1**{*4,11*}	**4**{*4*}	**4**{*11*}	> 25	> 25
1	**1**{*5,5*}	**4**{*5*}	**4**{*5*}	0.9	32.4
2	**1**{*5,6*}	**4**{*5*}	**4**{*6*}	0.2	> 25
2	**1**{*5,7*}	**4**{*5*}	**4**{*7*}	1.7	> 25
2	**1**{*5,8*}	**4**{*5*}	**4**{*8*}	0.2	> 25
2	**1**{*5,9*}	**4**{*5*}	**4**{*9*}	0.5	> 25
2	**1**{*5,10*}	**4**{*5*}	**4**{*10*}	2.4	> 25
2	**1**{*5,11*}	**4**{*5*}	**4**{*11*}	1.6	> 25
1	**1**{*6,6*}	**4**{*6*}	**4**{*6*}	> 59.5	59.5
2	**1**{*6,7*}	**4**{*6*}	**4**{*7*}	2.0	> 25
3	**1**{*6,8*}	**4**{*6*}	**4**{*8*}	0.03	> 25
3	**1**{*6,9*}	**4**{*6*}	**4**{*9*}	> 25	> 25
3	**1**{*6,10*}	**4**{*6*}	**4**{*10*}	> 25	> 25
1	**1**{*6,11*}	**4**{*6*}	**4**{*11*}	18.4	> 125
3	**1**{*7,7*}	**4**{*7*}	**4**{*7*}	> 11.7	11.7
3	**1**{*7,8*}	**4**{*7*}	**4**{*8*}	0.5	> 25
3	**1**{*7,9*}	**4**{*7*}	**4**{*9*}	2.5	> 25
3	**1**{*7,11*}	**4**{*7*}	**4**{*11*}	2.7	> 25
3	**1**{*8,8*}	**4**{*8*}	**4**{*8*}	0.008	> 25
3	**1**{*8,9*}	**4**{*8*}	**4**{*9*}	0.03	> 25
3	**1**{*8,10*}	**4**{*8*}	**4**{*10*}	0.4	> 25
3	**1**{*8,11*}	**4**{*8*}	**4**{*11*}	0.5	> 25
1	**1**{*9,9*}	**4**{*9*}	**4**{*9*}	9.5	> 125
2	**1**{*9,10*}	**4**{*9*}	**4**{*10*}	> 25	> 25
2	**1**{*9,11*}	**4**{*9*}	**4**{*11*}	9.1	> 25
3	**1**{*10,10*}	**4**{*10*}	**4**{*10*}	> 85.7	85.7
3	**1**{*10,11*}	**4**{*10*}	**4**{*11*}	> 25	> 25
1	**1**{*11,11*}	**4**{*11*}	**4**{*11*}	> 125	> 125

[a] Subsets of synthesized and tested compounds, in bold for the diversity selection with PRALINS. [b] Effective concentration 50 or the concentration required to inhibit HIV-induced cell death by 50% as evaluated with the MTT method in MT-4 cells. [c] Cytotoxic concentration 50 or the concentration required to induce 50% death of non-infected MT-4 cells as evaluated with the MTT method. Reference compounds: AMD3100: EC_{50} = 0.001 μg mL^{-1}, CC_{50} = > 5 μg mL^{-1}; DS: EC_{50} = 0.011 μg mL^{-1}, CC_{50} = > 125 μg mL^{-1}.

used, and was centered on the SDM-defined ligand-binding site. This grid enclosed the whole protein structure, and the ligand was initially placed far from the protein to include the possibility of finding other binding sites. A smaller (61×61×61) grid was used for the subsequent binding mode analysis calculations. In each case, 100 independent Lamarckian genetic algorithm (LGA) runs were performed and pseudo-Solis and Wets minimization methods were applied by using default parameters. Each docking run was repeated five times. Results from docking analyses were assessed by using the knowledge of the SDM data. They showed two main electrostatic interactions between two positively charged nitrogen atoms in compound **1**{*8,8*} and negatively charged Asp262 and Glu288 residues of the CXCR4 coreceptor (Figure 4). The lowest distances

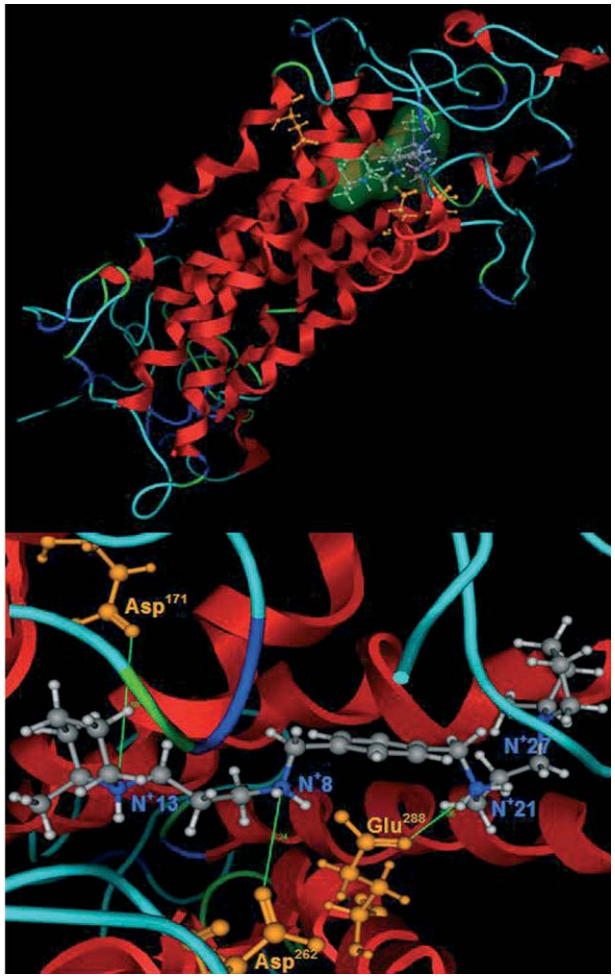

Figure 4. Predicted binding conformation between **1**{*8,8*} and CXCR4 from blind docking analysis. a) Compound **1**{*8,8*} docked within the CXCR4 pocket; b) detailed view of the calculated binding conformation.

from the carboxylic oxygen atoms of the three key binding residues Asp171, Asp262, and Glu288, to the four nitrogen atoms (N27, N21, N8, N13) of **1**{*8,8*} are shown in green: 6.88 Å between N^+13 and O(sp2) Asp171, 5.24 Å between N^+8 and O(sp2) Asp262, and 3.06 Å between N^+21 and O(sp2) Glu288.

Our docking results for **1**{*8,8*} agree with those of Gerlach et al.[55] on the mutagenic substitution of 16 CXCR4 amino acids, in which the three acidic residues, Asp171, Asp262, and Glu288, were identified as the main electrostatic interaction points for positively charged AMD3100 bicyclam rings binding. Moreover, the same study was performed with the AMD3100 ligand as is described in Pérez-Nueno et al.[53] Results with this known active ligand, by using only the same docking protocol as mentioned above, also agree with the **1**{*8,8*} docking results. It is worth mentioning that by using molecular dynamics (MD) it is possible to refine the CXCR4 docking poses to obtain ligand conformations that are closer to the key SDM residues.[56–58] For example, applying 200 ps of AMBER MD to our docking poses by using a protocol as described by Orozco and co-workers[59] gives ligand conformations with an average distance of 2 Å closer to the key binding residues. However, in this work we were more interested in the possibility of predicting a binding site and a binding mode of our more active synthesized molecules by using a docking tool only.

Finally, we carried out time-of-drug-addition experiments to identify the time and site of interaction of our anti-HIV compounds. It is known that the time delay before the addition of a drug is an estimate of its mode of action. Consequently, we determined the time of drug addition for the four most active compounds **1**{*8,8*}, **1**{*6,8*}, **1**{*8,9*} and **1**{*8,10*} compared with a CXCR4 antagonist (AMD3100), a reverse transcriptase inhibitor (AZT; azidothymidine), a fusion inhibitor (C34) and an adhesion inhibitor (DS; dextran sulfate) to confirm the initial hypothesis that the designed compounds act as CXCR4 inhibitors. The results that were obtained (Figure 5) clearly show that these compounds share a time/site of interaction that is similar to that of AMD3100 and act as blockers of the CXCR4 coreceptor. Furthermore, compounds **1**{*8,8*}, **1**{*6,8*}, **1**{*8,9*} completely blocked the binding of the 12G5 monoclonal antibody that targets CXCR4 at 25 μg mL^{-1} as measured by flow cytometry analysis in CXCR4+ cells, but failed to block the binding of antibodies that target CD4, CCR5 or CD45 (data not shown); this

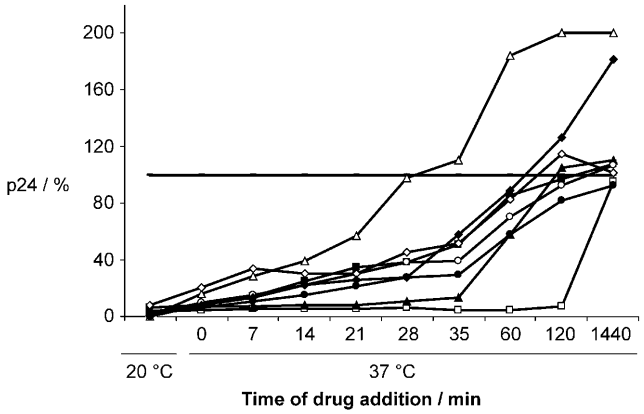

Figure 5. Time of drug addition in MT-4 cells of **1**{*8,8*} (◇), **1**{*6,8*} (●), **1**{*8,9*} (○), and **1**{*8,10*} (◆) in comparison with AZT (□), AMD3100 (■), DS (△), and C34 (▲); control: (——). Virus production was measured by p24 antigen determination in the cell supernatant 30 h post-infection, and is expressed as percentage of control values.

suggests that this class of compounds is very selective for the CXCR4 receptor.

Conclusions

We have designed a combinatorial library of non-cyclam AMD3100 analogues that preserves the main features of AMD3100: a) at least two nitrogen atoms on each side of the *p*-phenylene moiety, one in the benzylic position and the other(s) in a heterocyclic system, and b) similar distances between these nitrogen atoms as those present in cyclam. A diversity-oriented selection has allowed the synthesis of diamines **1**, dihydrazones **2** and aminohydrazones **8**; these compounds cover a broad range of activity values and are useful for calculating QSAR models. This approach led to the synthesis of compounds **1**{*6,8*}, **1**{*8,9*} and **1**{*8,8*}, which show anti-HIV activity values below 0.03 μg mL^{-1} but have displayed no cytotoxic effects at the tested concentrations. Studies on the mode of action of these compounds showed that they inhibited the CXCR4 coreceptor, thus validating the initial target compound design. A combinatorial optimization of the anti-HIV activity of this new family of compounds by using noncommercial amines of general structure **4** is currently on the way.

Experimental Section

Chemistry

IR spectra were recorded in a Nicolet Magna 560 FTIR spectrophotometer. ^{1}H and ^{13}C NMR spectra were recorded in a Varian Gemini 300 spectrometer that was operating at a field strength of 300 and 75.5 MHz, respectively. Chemical shifts were reported in parts per million (δ) and coupling constants (J) were in Hz by using, in the case of ^{1}H NMR spectroscopy, TMS as an internal standard, and in the case of ^{13}C NMR spectroscopy the solvent at 77.0 ppm ($CDCl_3$) as an internal reference. Standard and peak multiplicities are designated as follows: s, singlet; d, doublet; t, triplet; q, quartet; quint, quintet; m, multiplet; br, broad signal. MS data (*m/z* (%), EI, 70 eV) were obtained by using a Hewlett–Packard HP5988A spectrometer, and HRMS data were obtained by using a Micromass Autospec instrument. Elemental microanalyses were obtained on a Carlo–Erba CHNS-O/EA 1108 analyzer. Thin-layer chromatography (TLC) was performed on precoated sheets of silica 60 Polygram SIL N-HR/UV_{254} (Macherey–Nagel, art. 804023). Flash chromatography was performed with silica gel 35–70 μm (SDS, art. 2000027).

***N*-(4-((2-(Pyrrolidin-1-yl)ethylamino)methyl)benzyl)-2-(pyrrolidin-1-yl)ethanamine (1{*4,4*})**. Terephthalaldehyde (**3**) (0.61 g, 4.5 mmol), 1-(2-aminoethyl)pyrrolidine **4**{*4*} (1.04 g, 9.0 mmol) and molecular sieves (4 Å) were mixed in anhydrous MeOH (30 mL) and held at reflux under a N_2 atmosphere for 24 h. The molecular sieves were filtered, and the intermediate imine in MeOH was cooled to 0 °C and treated with solid $NaBH_4$ (0.34 g, 9.0 mmol). The mixture was stirred at RT overnight. Then H_2O was added and the product was extracted with CH_2Cl_2 The organic layers were combined, washed with brine, dried over $MgSO_4$ and the solvent was removed to give **1**{*4,4*} as a yellow oil (1.32 g, 89%). ^{1}H NMR (300 MHz, $CDCl_3$, 25 °C, TMS): δ = 7.27 (s, 4H; Ph), 3.79 (s, 4H; C*H*$_2$Ph), 2.73 (t, $^3J_{H,H}$ = 6.0 Hz, 4H; C*H*$_2$NH), 2.59 (t, $^3J_{H,H}$ = 6.0 Hz, 4H; CH_2N), 2.47 (m, 8H; CH_2N), 2.20 (br s, 2H; NH), 1.75 ppm (quint, $^{33}J_{H,H}$ = 3.3 Hz, 8H; CH_2); ^{13}C NMR (75.5 MHz, $CDCl_3$, 25 °C): δ = 138.8 (Cq), 128.0 (CH), 55.9 (CH_2), 54.2 (CH_2), 53.8 (CH_2), 47.8 (CH_2), 23.5 ppm (CH_2); IR (film): $\tilde{\nu}$ = 3310 (NH), 2962, 2928, 2874, 2794 (CH), 1485, 1444 cm^{-1} (CH); MS (FAB): *m/z* (%): 331.3 (100) $[M+H]^+$, 330.3 (18) $[M]^+$, 329.3 (77) $[M-H]^+$; HRMS calcd for $C_{20}H_{35}N_4$: 331.2862 $[M+H]^+$, found: 331.2867.

***N*-(4-((3-(2-Methylpiperidin-1-yl)propylamino)methyl)benzyl)-3-(2-methylpiperidin-1-yl)propan-1-amine (1{*8,8*})**. The procedure was the same as that stated above for **1**{*4,4*}, but was carried out by using terephthalaldehyde (**3**) (0.43 g, 3.2 mmol), 1-(3-aminopropyl)-2-methyl-piperidine **4**{*8*} (1.04 g, 6.4 mmol) and $NaBH_4$ (0.25 g, 6.4 mmol) to give **1**{*8,8*} as a pale-brown oil (1.33 g, 100%). ^{1}H NMR (300 MHz, $CDCl_3$, 25 °C, TMS): δ = 7.27 (s, 4H; Ph), 3.77 (s, 4H; C*H*$_2$Ph), 2.87 (m, 2H; CH_{eq}N), 2.73 (m, 2H; CH_{eq}), 2.63 (t, $^3J_{H,H}$ = 6.9 Hz, 4H; C*H*$_2$NH), 2.36 (m, 2H; CH_{ax}N), 2.26 (m, 2H; C*H*CH$_3$), 2.14 (br s, 2H; NH), 2.11 (m, 2H; CH_{ax}N),1.68 (quint, $^3J_{H,H}$ = 6.9 Hz, 4H; CH_2), 1.61 (m, 2H; CH_{eq}), 1.58 (m, 2H; CH_{eq}), 1.52 (m, 2H; CH_{eq}), 1.44 (m, 2H; CH_{ax}), 1.28 (m, 4H; CH_{ax}), 1.05 ppm (d, $^3J_{H,H}$ = 6.3 Hz, 6H; CH_3); ^{13}C NMR (75.5 MHz, $CDCl_3$, 25 °C): δ = 138.8 (Cq), 128.0 (CH), 55.9 (CH), 53.7 (CH_2), 52.3 (CH_2), 52.1 (CH_2), 48.3 (CH_2), 34.7 (CH_2), 26.2 (CH_2), 25.7 (CH_2), 24.0 (CH_2), 19.1 ppm (CH_3); IR (film): $\tilde{\nu}$ = 3282 (NH), 2929, 2854, 2793 (CH), 1449, 1372 cm^{-1} (CH); MS (EI): *m/z* (%): 415.4 (0.4) $[M+H]^+$, 112.1 (100) $[C_7H_{14}N]^+$; Anal. ($C_{26}H_{46}N_4$) C, H, N.

((4-(*N*-(Piperidin-1-yl)imino)methyl)phenyl)-*N*-(piperidin-1-yl)methanamine (2{*1,1*}). Terephthalaldehyde (**3**) (0.99 g, 7.3 mmol), 1-aminopiperidine **4**{*1*} (1.51 g, 14.7 mmol) and 4 Å molecular sieves were mixed in anhyd MeOH (30 mL) and held at reflux under a N_2 atmosphere for 16 h. The molecular sieves were filtered, and the solvent was partially removed. The crude oil was cooled, and the resulting precipitate was filtered and rinsed with cold MeOH to give **2**{*1,1*} as a yellow solid (1.42 g, 65%). ^{1}H NMR (300 MHz, $CDCl_3$, 25 °C, TMS): δ = 7.55 (s, 4H; Ph), 7.53 (s, 2H; CH=N), 3.16 (m, 8H; CHN), 1.79–1.71 (m, 8H; CH_2), 1.58–1.50 ppm (m, 4H; CH_2); ^{13}C NMR (75.5 MHz, $CDCl_3$, 25 °C): δ = 136.0 (Cq), 134.3 (CH), 125.9 (CH), 52.1 (CH_2), 25.3 (CH_2), 24.2 ppm (CH_2); IR (film): $\tilde{\nu}$ = 1576 cm^{-1} (C=N); Anal. ($C_{18}H_{26}N_4$) C, H, N.

4-((2-(Pyrrolidin-1-yl)ethylamino)methyl)benzaldehyde (7{*4*}). 4-(Diethoxymethyl)benzaldehyde (**5**) (2.01 g, 9.3 mmol), 1-(2-aminoethyl)pyrrolidine **4**{*4*} (1.09 g, 9.3 mmol) and 4 Å molecular sieves were mixed in anhyd MeOH (30 mL) and held at reflux under a N_2 atmosphere for 36 h. The molecular sieves were filtered and the intermediate imine in MeOH was cooled to 0 °C and treated with solid $NaBH_4$ (0.36 g, 9.3 mmol). The mixture was stirred at RT for 5 h. Then H_2O was added, and the product was extracted with CH_2Cl_2. The organic extracts were combined, washed with brine, dried over $MgSO_4$, and the solvent was removed to give the corresponding 4-(diethoxymethyl)benzylamine as a yellow oil (2.66 g, 93%). This intermediate aminoacetal (2.64 g, 8.6 mmol) was treated with 2 M HCl (20 mL) at RT for 2 h. The resulting mixture was basified with NaOH and extracted with CH_2Cl_2. The CH_2Cl_2 extracts were combined, washed with brine, dried over $MgSO_4$, and the solvent was removed to give the product **7**{*4*} as a brownish oil (1.79 g, 89%). ^{1}H NMR (300 MHz, $CDCl_3$, 25 °C, TMS): δ = 10.00 (s, 1H; CHO), 7.84 (d, $^3J_{H,H}$ = 8.1 Hz, 2H; Ph), 7.51 (d, $^3J_{H,H}$ = 8.1 Hz, 2H; Ph), 3.90 (s, 2H; C*H*$_2$Ph), 2.75 (t, $^3J_{H,H}$ = 6.0 Hz, 2H; C*H*$_2$NH), 2.64 (t, $^3J_{H,H}$ = 6.0 Hz, 2H; CH_2N), 2.51 (m, 4H; CH_2N), 2.01 (br s, 1H; NH), 1.77 ppm (m, 4H; CH_2); ^{13}C NMR (75.5 MHz, $CDCl_3$, 25 °C): δ = 191.8 (CH), 147.6 (Cq), 135.1 (Cq), 129.7 (CH), 128.4 (CH), 55.8 (CH_2), 54.2 (CH_2), 53.7 (CH_2), 47.8 (CH_2), 23.5 ppm (CH_2); IR (film): $\tilde{\nu}$ = 3309 (NH), 2961, 2930, 2875, 2799 (CH), 1700 (C=O), 1606 (CC), 1459, 1446 cm^{-1} (CH); MS (EI): *m/z* (%): 233.2 (1) $[M+H]^+$, 232.2 (22) $[M]^+$

, 84.1 (100) $[C_5H_{10}N]^+$; HRMS: *m/z* calcd for $C_{14}H_{20}N_2O$: 232.1576 $[M+H]^+$, found: 232.1572.

4-((3-(1*H*-Imidazol-1-yl)propylamino)methyl)benzaldehyde (7{*6*}). The procedure was the same as that stated above for **7**{*4*} but by using 4-(diethoxymethyl)benzaldehyde (**5**) (2.01 g, 9.3 mmol), 1-(3-aminopropyl)imidazole **4**{*6*} (1.20 g, 9.3 mmol) and $NaBH_4$ (0.36 g, 9.3 mmol). The intermediate aminoacetal was obtained as a yellow oil (2.68 g, 90%). This acetal (2.68 g, 9.3 mmol) was deprotected to afford **7**{*6*} (1.76 g, 86%) as a yellow oil. ^{1}H NMR (300 MHz, $CDCl_3$, 25 °C, TMS): $\delta = 10.00$ (s, 1H; CHO), 7.85 (d, $^3J_{H,H} = 8.1$ Hz, 2H; Ph), 7.48 (d, $^3J_{H,H} = 8.1$ Hz, 2H; Ph), 7.46 (s, 1H; CHN), 7.05 (s, 1H; CHN), 6.90 (s, 1H; CHN), 4.07 (t, $^3J_{H,H} = 6.9$ Hz, 2H; CH_2N), 3.85 (s, 2H; CH_2Ph), 2.62 (t, $^3J_{H,H} = 6.9$ Hz, 2H; CH_2NH), 1.95 (quint, $^3J_{H,H} = 6.9$ Hz, 2H; CH_2), 1.75 ppm (br s, 1H; NH); ^{13}C NMR (75.5 MHz, $CDCl_3$, 25 °C): $\delta = 191.7$ (CH), 147.2 (Cq), 137.0 (CH), 135.3 (Cq), 129.8 (CH), 129.3 (CH), 128.4 (CH), 118.7 (CH), 53.6 (CH_2), 45.8 (CH_2), 44.6 (CH_2), 31.3 ppm (CH_2). IR (film): $\tilde{\nu} = 3268$ (NH), 3108, 2936, 2831, 2738 (CH), 1696 (C=O), 1606 (C-C), 1508 cm^{-1} (imidazole); MS (EI): *m/z* (%): 244.1 (17) $[M+H]^+$, 243.1 (65) $[M]^+$, 119.0 (100) $[C_8H_7O]^+$; HRMS: *m/z* calcd for $C_{14}H_{17}N_3O$: 243.1372 $[M]^+$, found: 243.1366.

4-((3-(2-Methylpiperidin-1-yl)propylamino)methyl)benzaldehyde (7{*8*}). The procedure was the same as that stated above for **7**{*4*} but by using 4-(diethoxymethyl)benzaldehyde (**5**) (2.01 g, 9.3 mmol), 1-(3-aminopropyl)-2-methylpiperidine **4**{*8*} (1.52 g, 9.3 mmol) and $NaBH_4$ (0.36 g, 9.3 mmol). The intermediate aminoacetal was obtained as a yellow oil (3.18 g, 98%). This acetal (3.18 g, 9.1 mmol) was deprotected to afford **7**{*8*} (2.45 g, 98%) as a yellow oil. ^{1}H NMR (300 MHz, $CDCl_3$, 25 °C, TMS): $\delta = 10.00$ (s, 1H; CHO), 7.85 (d, $^3J_{H,H} = 8.1$ Hz, 2H; Ph), 7.50 (d, $^3J_{H,H} = 8.1$ Hz, 2H; Ph), 3.87 (s, 2H; CH_2NH), 2.87 (m, 1H; $CH_{eq}N$), 2.77 (m, 1H; $CH_{eq}N$), 2.65 (t, $^3J_{H,H} = 6.8$ Hz, 2H; CH_2NH), 2.36 (m, 1H; $CH_{ax}N$), 2.27 (m, 1H; $CHCH_3$), 2.11 (m, 1H; $CH_{ax}N$), 2.00 (br s, 1H; NH), 1.75–1.48 (m, 6H; CH_2), 1.29 (m, 2H; CH_{ax}), 1.06 ppm (d, $^3J_{H,H} = 6.0$ Hz, 3H; CH_3); ^{13}C NMR (75.5 MHz, $CDCl_3$, 25 °C): $\delta = 191.8$ (CH), 147.7 (Cq), 135.2 (Cq), 129.8 (CH), 128.4 (CH), 56.1 (CH), 53.8 (CH_2), 52.3 (CH_2), 52.0 (CH_2), 48.5 (CH_2), 34.6 (CH_2), 26.1 (CH_2), 25.9 (CH_2), 23.9 (CH_2), 19.0 ppm (CH_3); IR (film): $\tilde{\nu} = 3271$ (NH), 2930, 2852, 2793, 2732 (CH), 1702 (C=O), 1606 (C–C), 1449, 1372 cm^{-1} (CH); MS (EI): *m/z* (%): 275.2 (9) $[M+H]^+$, 274.2 (37) $[M]^+$, 112.1 (100) $[C_7H_{14}N]^+$; HRMS: *m/z* calcd for $C_{17}H_{26}N_2O$: 274.2045 $[M]^+$, found: 274.2046.

4-((Piperidin-1-ylimino)methyl)benzaldehyde (6{*1*}). Terephthalaldehyde (**3**) (1.00 g, 7.4 mmol) was dissolved in anhydrous MeOH (30 mL) with 4 Å molecular sieves, followed by the dropwise addition of a solution of 1-aminopiperidine **4**{*1*} (0.38 g, 3.8 mmol) in anhydrous MeOH (5 mL) under a N_2 atmosphere. The mixture was held at reflux for 36 h. Upon removal of the solvent, the residue was separated by chromatography on silica gel by eluting with hexane/EtOAc (5:1). The resulting product was once again separated by chromatography on silica gel by eluting with CH_2Cl_2 /EtOAc (gradient 25:1 to 1:1) to give **6**{*1*} (0.48 g, 60%) as a yellow oil. ^{1}H NMR (300 MHz, $CDCl_3$, 25 °C, TMS): $\delta = 9.96$ (s, 1H; CHO), 7.83 (d, $^3J_{H,H} = 8.4$ Hz, 2H; Ph), 7.71 (d, $^3J_{H,H} = 8.4$ Hz, 2H; Ph), 7.48 (s, 1H; CH=N), 3.25 (t, $^3J_{H,H} = 5.7$ Hz, 4H; CH_2N), 1.76 (quint, $^3J_{H,H} = 5.7$ Hz, 4H; CH_2), 1.61–1.54 ppm (m, 2H; CH_2); ^{13}C NMR (75.5 MHz, $CDCl_3$, 25 °C): $\delta = 191.6$ (CH), 142.8 (Cq), 135.0 (Cq), 131.0 (CH), 130.0 (CH), 125.8 (CH), 51.7 (CH_2), 25.1 (CH_2), 24.0 ppm (CH_2); IR (film): $\tilde{\nu} =$ 2938, 2854, 2818, 2731 (CH), 1694 (C=O), 1605 (C–C), 1579 (C=N), 1549 (C–C), 1448 cm^{-1} (CH); MS (EI): *m/z* (%): 217.0 (17) $[M+H]^+$, 216.0 (100) $[M]^+$; Anal. ($C_{13}H_{16}N_2O$) C, H, N.

4-((2,6-Dimethylpiperidin-1-ylimino)methyl)benzaldehyde (6{*2*}). The procedure was the same as that stated above for **6**{*1*} but terephthalaldehyde (**3**) (3.82 g, 28.2 mmol) and 1-amino-2,6-dimethylpiperidine **4**{*2*} (2.01 g, 14.1 mmol) were used. Upon removal of the solvent, the residue was separated by chromatography on silica gel by eluting with hexane/EtOAc (3:1) to afford **6**{*2*} (2.71 g, 78%) as a yellow oil. ^{1}H NMR (300 MHz, $CDCl_3$, 25 °C, TMS): $\delta = 9.95$ (s, 1H; CHO), 7.81 (d, $^3J_{H,H} = 8.3$ Hz, 2H; Ph), 7.69 (d, $^3J_{H,H} = 8.3$ Hz, 2H; Ph), 7.35 (s, 1H; CH=N), 3.92 (m, 2H; CH-CH_3), 1.87–1.56 (m, 6H; CH_2), 1.15 ppm (d, $^3J_{H,H} = 6.6$ Hz, 6H; CH_3); ^{13}C NMR (75.5 MHz, $CDCl_3$, 25 °C): $\delta = 191.5$ (CH), 143.5 (Cq), 134.4 (Cq), 130.0 (CH), 129.5 (CH), 125.3 (CH), 53.1 (CH), 30.8 (CH_2), 18.3 (CH_3), 15.6 ppm (CH_2); IR (film): $\tilde{\nu} = 2967$, 2935, 2869, 2820, 2728 (C–H), 1693 (C=O), 1604 (C–C), 1572 (C=N), 1539 (C–C), 1468, 1372 cm^{-1} (C-H); MS (EI): *m/z* (%): 245.2 (5) $[M+H]^+$, 244.2 (16) $[M]^+$, 229.2 (100) $[C_{14}H_{17}N_2O]^+$, Anal. ($C_{15}H_{20}N_2O$) C, H, N.

***N*-(4-((2,6-Dimethylpiperidin-1-ylimino)methyl)benzyl)-2-(pyrrolidin-1-yl)ethylamine (8{*2,4*}).** 1-(2-Aminoethyl)pyrrolidine **4**{*4*} (0.52 g, 2.1 mmol) and **6**{*2*} (0.52 g, 2.1 mmol) were dissolved in anhyd MeOH (30 mL). 4 Å Molecular sieves were added, and the mixture was held at reflux under a N_2 atmosphere for 36 h. The molecular sieves were filtered, and the intermediate imine in MeOH was cooled to 0 °C and treated with solid $NaBH_4$ (0.08 g, 2.1 mmol). The reaction was stirred at RT for 16 h. Then H_2O was added, and the product was extracted with CH_2Cl_2. The organic layers were combined, washed with brine, dried over $MgSO_4$, and the solvent was removed to afford **8**{*2,4*} as a yellow oil (0.61 g, 85%). ^{1}H NMR (300 MHz, $CDCl_3$, 25 °C, TMS): $\delta = 8.07$ (s, 1H; CH=N), 7.64 (d, 2H, $^3J = 8.1$ Hz; Ph), 7.34 (d, 2H, $^3J = 8.1$ Hz; Ph), 3.83 (s, 2H; CH_2Ph), 3.06 (m, 2H; $CHCH_3$), 2.77 (t, $^3J_{H,H} = 6.0$ Hz, 2H; CH_2NH), 2.63 (t, $^3J_{H,H} = 6.0$ Hz, 2H; CH_2N), 2.50 (m, 4H; CH_2N), 2.34 (br s, 1H; NH), 1.77 (m, 8H; CH_2), 1.50 (m, 2H; CH_2), 1.00 ppm (d, $^3J_{H,H} = 6.3$ Hz, 6H; CH_3); IR (film): $\tilde{\nu} = 3311$ (NH), 2962, 2931, 2872, 2794 (CH), 1624 (CC), 1584 (C=N), 1556 (C–C), 1459, 1447, 1369 (CH) cm^{-1}; MS (EI): *m/z* (%): 342.3 (0.5) $[M]^+$, 84.0 (100) $[C_5H_{10}N]^+$; HRMS: *m/z* calcd for $C_{21}H_{34}N_4$: 342.2783 $[M]^+$, found: 342.2786.

***N*-(4-((3-(1*H*-Imidazol-1-yl)propylamino)methyl)benzyl)-3-(2-methylpiperidin-1-yl)propan-1-amine (1{*6,8*}).** The procedure was the same as that stated above for **8**{*2,4*}, but 1-(3-aminopropyl)-2-methyl-piperidine **4**{*8*} (0.59 g, 3.6 mmol), **7**{*6*} (0.88 g, 3.6 mmol) and $NaBH_4$ (0.14 g, 3.6 mmol) were used to give **1**{*6,8*} (1.20 g, 86%) as a yellow oil. ^{1}H NMR (300 MHz, $CDCl_3$, 25 °C, TMS): $\delta = 7.44$ (s, 1H; CHN), 7.27 (s, 4H; Ph), 7.03 (s, 1H; CHN), 6.89 (s, 1H; CHN), 4.04 (t, $^3J_{H,H} = 6.9$ Hz, 2H; CH_2N), 3.77 (s, 2H; CH_2Ph), 3.74 (s, 2H; CH_2-Ph), 2.87 (m, 1H; $CH_{eq}N$), 2.74 (m, 1H; $CH_{eq}N$), 2.65 (t, $^3J_{H,H} = 6.9$ Hz, 2H; CH_2NH), 2.60 (t, $^3J_{H,H} = 6.9$ Hz, 2H; CH_2NH), 2.37 (m, 1H; $CH_{ax}N$), 2.27 (m, 1H; $CHCH_3$), 2.12 (m, 1H; $CH_{ax}N$), 2.09 (br s, 2H; NH), 1.92 (quint, $^3J_{H,H} = 6.9$ Hz, 2H; CH_2), 1.72–1.53 (m, 6H; CH_2), 1.29 (m, 2H; CH_{ax}), 1.05 ppm (d, $^3J_{H,H} = 6.3$ Hz, 3H; CH_3); ^{13}C NMR (75.5 MHz, $CDCl_3$, 25 °C): $\delta = 138.9$ (Cq), 138.7 (Cq), 137.1 (CH), 129.2 (CH), 128.2 (CH), 128.0 (CH), 118.7 (CH), 56.0 (CH), 53.7 (CH_2), 52.3 (CH_2), 52.0 (CH_2), 48.3 (CH_2), 45.7 (CH_2), 44.7 (CH_2), 34.6 (CH_2), 31.4 (CH_2), 26.1 (CH_2), 25.7 (CH_2), 23.9 (CH_2), 19.1 ppm (CH_3); IR (film): $\tilde{\nu} = 3277$ (N–H), 3104, 2929, 2853, 2802 (C–H), 1508 (imidazole), 1450, 1373 cm^{-1} (CH); MS (EI): *m/z* (%): 385.3 (2) $[M+2H]^+$, 384.3 (26) $[M+H]^+$, 383.3 (4) $[M]^+$, 112.0 (100) $[C_7H_{14}N]^+$; HRMS: *m/z* calcd for $C_{23}H_{37}N_5$: 383.3049 $[M+H]^+$, found: 383.3048.

***N*-(4-((3-(4-Methylpiperazin-1-yl)propylamino)methyl)benzyl)-3-(2-methylpiperidin-1-yl)propan-1-amine (1{*8,9*}).** The procedure was the same as that stated above for **8**{*2,4*} but 1-(3-aminopropyl)-2-methylpiperidine **4**{*8*} (0.45 g, 2.7 mmol), **7**{*9*} (0.75 g, 2.7 mmol) and $NaBH_4$ (0.10 g, 2.7 mmol) were used to give **1**{*8,9*} (0.45 g, 39%) as a yellow oil. ^{1}H NMR (300 MHz, $CDCl_3$, 25 °C, TMS): $\delta = 7.28$ (s, 4H; Ph), 3.77 (s, 4H; CH_2Ph), 2.88 (m, 1H; $CH_{eq}N$), 2.75

(m, 1H; $CH_{eq}N$), 2.67 (t, $^3J_{H,H}$ = 6.6 Hz, 2H; CH_2NH), 2.65 (t, $^3J_{H,H}$ = 6.6 Hz, 2H; CH_2NH), 2.43 (brs, 12H; CH_2N, $CH_{ax}N$, $CHCH_3$), 2.27 (s, 3H; CH_3N), 2.23 (brs, 2H; NH), 2.12 (m, 1H; $CH_{ax}N$), 1.76–1.53 (m, 8H; CH_2), 1.32–1.21 (m, 2H; $CH_{ax}N$), 1.05 ppm (d, $^3J_{H,H}$ = 6.3 Hz, 3H; CH_3); ^{13}C NMR (75.5 MHz, $CDCl_3$, 25 °C): δ = 138.8 (Cq), 138.6 (Cq), 128.1 (CH), 128.0 (CH), 57.0 (CH_2), 56.0 (CH), 55.1 (CH_2), 53.7 (CH_2), 53.2 (CH_2), 52.3 (CH_2), 52.0 (CH_2), 48.3 (CH_2), 48.1 (CH_2), 46.0 (CH_3), 34.5 (CH_2), 26.9 (CH_2), 26.0 (CH_2), 25.6 (CH_2), 23.9 (CH_2), 19.0 ppm (CH_3); IR (film): $\tilde{\nu}$ = 3280 (N–H), 2931, 2875, 2852, 2793 (C–H), 1458, 1448, 1372 cm^{-1} (C–H); MS (EI): *m/z* (%): 415.4 (0.3) $[M]^+$, 112.2 (100) $[C_7H_{14}N]^+$; HRMS: *m/z* calcd for $C_{25}H_{45}N_5$: 415.3675 $[M]^+$, found: 415.3660.

((4-(*N*-(4-Methylpiperazin-1-yl)imino)methyl)phenyl)-*N*-(piperidin-1-yl)methanamine (2{*1*,*3*}). 1-Amino-4-methylpiperazine **4**{*3*} (0.24 g, 2.3 mmol) and **6**{*3*} (0.53 g, 2.3 mmol) were dissolved in anhydrous MeOH (30 mL). Molecular sieves (4 Å) were added and the mixture was held at reflux under a N_2 atmosphere for 36 h. The molecular sieves were filtered, and the solvent was removed to afford **2**{*1*,*3*} as a yellow solid (0.69 g, 95%). ^1H NMR (300 MHz, $CDCl_3$, 25 °C, TMS): δ = 7.56 (s, 4H; Ph), 7.53 (s, 1H; CH_2Ph), 7.52 (s, 1H; CH_2-Ph), 3.22 (t, $^3J_{H,H}$ = 5.1 Hz, 4H; CH_2N), 3.17 (t, $^3J_{H,H}$ = 5.6 Hz, 4H; CH_2N), 2.62 (t, $^3J_{H,H}$ = 5.1 Hz, 4H; CH_2N), 2.36 (s, 3H; CH_3), 1.75 (m, 4H; CH_2), 1.54 ppm (m, 2H; CH_2); ^{13}C NMR (75.5 MHz, $CDCl_3$, 25 °C): δ = 136.4 (Cq), 135.6 (CH), 135.5 (Cq), 134.0 (CH), 126.2 (CH), 126.0 (CH), 54.6 (CH_2), 52.1 (CH_2), 51.0 (CH_2), 46.0 (CH_3), 25.3 (CH_2), 24.2 ppm (CH_2); IR (film): $\tilde{\nu}$ = 2934, 2837, 2798 (C–H), 1577 (C=N), 1452, 1365 cm^{-1} (C–H); MS (EI): *m/z* (%): 315.2 (2) $[M+2H]^+$, 314.2 (22) $[M+H]^+$, 313.2 (100) $[M]^+$; HRMS: *m/z* calcd for $C_{18}H_{27}N_5$: 313.2266 $[M-H]^+$, found: 313.2266.

4-((2-(Piperidin-1-yl)ethylamino)methyl)benzaldehyde (7{*7*}). 4-(diethoxymethyl)benzaldehyde (**5**) (0.91 g, 4.2 mmol) and 1-(2-aminoethyl)piperidine **4**{*7*} (0.55 g, 4.2 mmol) were dissolved in anhydrous MeOH (3 mL) in a 5 mL microwave reaction vessel. Na_2SO_4 was added and the vessel was sealed. The mixture was heated for 2 h at 100 °C in the microwave. The mixture was filtered and the solvent removed to yield *N*-(4-(diethoxymethyl)benzyliden)-2-(piperidin-1-yl)ethanamine as a reddish oil (1.35 g, 100%). ^1H NMR (300 MHz, $CDCl_3$, 25 °C, TMS): δ = 8.31 (s, 1H; CH=N), 7.71 (d, $^3J_{H,H}$ = 8.1 Hz, 2H; Ph), 7.52 (d, $^3J_{H,H}$ = 8.1 Hz, 2H; Ph), 5.53 (s, 1H; CH), 3.79 (t, $^3J_{H,H}$ = 7.1 Hz, 2H; CH_2N), 3.57 (m, 4H; CH_2CH_3), 2.68 (t, $^3J_{H,H}$ = 7.1 Hz, 2H; CH_2N), 2.51 (brs, 4H; CH_2N), 1.61 (m, 4H; CH_2), 1.45 (m, 2H; CH_2), 1.24 ppm (t, $^3J_{H,H}$ = 7.1 Hz, 6H; CH_3). This imine (1.32 g, 4.1 mmol) was dissolved in anhyd MeOH (30 mL), cooled to 0 °C, and treated with solid $NaBH_4$ (0.16 g, 4.1 mmol). The mixture was stirred at RT for 5 h. Then H_2O was added, and the product was extracted with CH_2Cl_2. The organic extracts were combined, washed with brine, dried over $MgSO_4$, and the solvent was removed to give *N*-(4-(diethoxymethyl)benzyl)-2-(piperidin-1-yl)-ethanamine as a yellow oil (1.23 g, 92%). ^1H NMR (300 MHz, $CDCl_3$, 25 °C, TMS): δ = 7.42 (d, $^3J_{H,H}$ = 8.1 Hz, 2H; Ph), 7.31 (d, $^3J_{H,H}$ = 8.1 Hz, 2H; Ph), 5.49 (s, 1H; CH), 3.80 (s, 2H; CH_2Ph), 3.57 (m, 4H; CH_2CH_3), 2.71 (t, $^3J_{H,H}$ = 6.3 Hz, 2H; CH_2NH), 2.46 (t, $^3J_{H,H}$ = 6.3 Hz, 2H; CH_2N), 2.36 (br, 4H; CH_2N), 2.24 (brs, 1H; NH), 1.56 (quint, $^3J_{H,H}$ = 5.7 Hz, 4H; CH_2), 1.43 (m, 2H; CH_2), 1.23 ppm (t, $^3J_{H,H}$ = 7.1 Hz, 3H, CH_3). This aminoacetal (2.64 g, 8.6 mmol) was treated with 2 M HCl (20 mL) at RT for 2 h. The resulting mixture was basified with NaOH and extracted with CH_2Cl_2. The CH_2Cl_2 extracts were combined, washed with brine, dried over $MgSO_4$, and the solvent was removed to afford aldehyde **7**{*7*} as a brownish oil (0.87 g, 94%). ^1H NMR (300 MHz, $CDCl_3$, 25 °C, TMS): δ = 10.00 (s, 1H; CHO), 7.84 (d, $^3J_{H,H}$ = 8.1 Hz, 2H; Ph), 7.50 (d, $^3J_{H,H}$ = 8.1 Hz, 2H; Ph), 3.89 (s, 2H; CH_2-Ph), 2.70 (t, $^3J_{H,H}$ = 6.2 Hz, 2H; CH_2NH), 2.47 (t, $^3J_{H,H}$ = 6.2 Hz, 2H; CH_2N), 2.36 (br, 4H; CH_2N), 2.18 (brs, 1H; NH), 1.57 (quint, $^3J_{H,H}$ = 5.7 Hz, 4H; CH_2), 1.43 ppm (m, 2H; CH_2).

***N*-(4-((2-(Piperidin-1-yl)ethylamino)methyl)benzyl)-3-(2-methylpiperidin-1-yl)propan-1-amine (1{*7*,*8*})**. 1-(3-aminopropyl)-2-methylpiperidine **4**{*8*} (0.44 g, 2.7 mmol) and **7**{*7*} (0.66 g, 2.7 mmol) were dissolved in anhyd MeOH (3 mL) in a 5 mL microwave vessel, Na_2SO_4 was added, and the vessel was sealed. The mixture was heated for 2 h at 100 °C in the microwave. Then it was filtered, diluted with MeOH (10 mL), cooled to 0 °C, and treated with solid $NaBH_4$ (0.10 g, 2.7 mmol). The mixture was stirred at RT for 4 h. Then H_2O was added and the product was extracted with CH_2Cl_2. The organic extracts were combined, washed with brine, dried over $MgSO_4$ and the solvent was removed to give **1**{*7*,*8*} as a yellow oil (0.98 g, 95%). ^1H NMR (300 MHz, $CDCl_3$, 25 °C, TMS): δ = 7.27 (s, 4H; Ph), 3.78 (s, 2H; CH_2-Ph), 3.77 (s, 2H; CH_2-Ph), 2.86 (m, 1H; $CH_{eq}N$), 2.78 (m, 1H; $CH_{eq}N$), 2.69 (t, $^3J_{H,H}$ = 6.3 Hz, 2H; CH_2NH), 2.63 (t, $^3J_{H,H}$ = 6.9 Hz, 4H; CH_2NH), 2.44 (t, $^3J_{H,H}$ = 6.3 Hz, 2H; CH_2N), 2.34 (m, 5H; $CH_{ax}N$, CH_2N), 2.25 (m, 1H; $CHCH_3$), 2.11 (m, 1H; $CH_{ax}N$), 2.07 (brs, 2H; NH), 1.68 (quint, $^3J_{H,H}$ = 6.9 Hz, 2H; CH_2), 1.55 (m, 8H; CH_2), 1.42 (m, 2H; CH_2), 1.28 (m, 2H; CH_{ax}), 1.05 ppm (d, $^3J_{H,H}$ = 6.3 Hz, 3H; CH_3); ^{13}C NMR (75.5 MHz, $CDCl_3$, 25 °C): δ = 139.0 (Cq), 138.8 (Cq), 128.0 (CH), 58.6 (CH_2), 55.9 (CH), 54.7 (CH_2), 53.7 (CH_2), 52.3 (CH_2), 52.1 (CH_2), 48.3 (CH_2), 45.9 (CH_2), 34.7 (CH_2), 26.2 (CH_2), 26.1 (CH_2), 25.7 (CH_2), 24.5 (CH_2), 24.0 (CH_2), 19.1 ppm (CH_3); IR (film): $\tilde{\nu}$ = 3301 (N–H), 2932, 2852, 2802 (C–H), 1467, 1443, 1373 cm^{-1} (C–H); Anal. ($C_{24}H_{42}N_4$) C, H, N.

Biological evaluation

Antiviral activity: HIV-1 strains were titered in MT-4 cells after acute infection, and infectivity was measured by evaluating the cytopathic effect that was induced after 5 day cultures as described.[60] Anti-HIV activity (EC_{50}) and cytotoxicity (CC_{50}) measurements in MT-4 cells were based on the viability of cells that had been infected or not infected with HIV-1, all were exposed to various concentrations of the test compound. After the MT-4 cells were allowed to proliferate for 5 days, the number of viable cells was quantified by a tetrazolium-based colorimetric method (MTT method) as described.

Time-of-drug-addition studies: MT-4 cells were infected with HIV-1 NL4–3 at a multiplicity of infection of 0.5 and incubated for 1 h at 20 °C in the presence or absence of test compounds. Cells were then washed twice in cool PBS and seeded in 96-well plates at a concentration of 2×10^5 cells per well (final volume 200 μL) at a temperature of 37 °C. Test compounds, dextran sulfate, AMD3100, C34 or AZT were added at various times post-infection, or the cells were cultured in the absence of drug (control). Test compounds were added at concentrations that completely block HIV replication (roughly 100-fold higher than the determined EC_{50}) of each drug in the standard assay performed with MT-4 cells. Virus production was measured by p24 antigen determination in the cell supernatant 30 h post-infection with a commercial p24 antigen ELISA (Innogenetics, Barcelona, Spain).[61]

Acknowledgements

This work was supported in part by the Fundació Marató de TV3 project 020930 and the Spanish Ministerio de Educación y Ciencia project SAF-2007-6322 (J.I.B. and B.C.) and BFU-200600966 (J.A.E.). I. Clotet-Codina, R. Puig de la Bellacasa, L. Ros-Blanco,

and V. Pérez-Nueno hold an FI scholarship from Generalitat de Catalunya and S. Pettersson, from IQS.

Keywords: antiviral agents · heterocycles · medicinal chemistry · molecular modeling · reductive amination

[1] J. A. Este, *Curr. Med. Chem.* **2003**, *10*, 1617–1632.
[2] J. A. Este, A. Telenti, *Lancet* **2007**, *370*, 81–88.
[3] N. J. Anthony, *Curr. Top. Med. Chem.* **2004**, *4*, 979–990.
[4] E. De Clercq, *Chem. Biodiversity* **2004**, *1*, 44–64.
[5] T. Imamichi, *Curr. Pharm. Des.* **2004**, *10*, 4039–4053.
[6] G. A. Locatelli, R. Cancio, S. Spadari, G. Maga, *Curr. Drug Metab.* **2004**, *5*, 283–290.
[7] A. Milinkovic, E. Martinez, *Expert Rev. Anti-Infect. Ther.* **2004**, *2*, 367–373.
[8] C. F. Pereira, T. M. L. Paridaen Judith, *Curr. Pharm. Des.* **2004**, *10*, 4005–4037.
[9] C. M. Tarby, *Curr. Top. Med. Chem.* **2004**, *4*, 1045–1057.
[10] M. L. Andreola, *Curr. Pharm. Des.* **2004**, *10*, 3713–3723.
[11] T. K. Chiu, D. R. Davies, *Curr. Top. Med. Chem.* **2004**, *4*, 965–977.
[12] S. P. Gupta, A. N. Nagappa, *Curr. Med. Chem.* **2003**, *10*, 1779–1794.
[13] A. A. Johnson, C. Marchand, Y. Pommier, *Curr. Top. Med. Chem.* **2004**, *4*, 1059–1077.
[14] A. L. Parrill, *Curr. Med. Chem.* **2003**, *10*, 1811–1824.
[15] F. Turlure, E. Devroe, P. A. Silver, A. Engelman, *Front. Biosci.* **2004**, *9*, 3187–3208.
[16] M. Witvrouw, B. Van Maele, J. Vercammen, A. Hantson, Y. Engelborghs, E. De Clercq, C. Pannecouque, Z. Debyser, *Curr. Drug Metab.* **2004**, *5*, 291–304.
[17] M. Baba, *Curr. Top. Med. Chem.* **2004**, *4*, 871–882.
[18] K. Devadas, S. Dhawan, *Recent Res. Dev. Biochem.* **2003**, *4*, 447–466.
[19] I. Schiavoni, C. Muratori, V. Piacentini, A. M. Giammarioli, M. Federico, *Curr. Drug Targets Immune Endocr. Metab. Disord.* **2004**, *4*, 19–27.
[20] E. Morita, W. I. Sundquist, *Annu. Rev. Cell Dev. Biol.* **2004**, *20*, 395–425.
[21] A. G. Bukrinskaya, *Arch. Virol.* **2004**, *149*, 1067–1082.
[22] P. Dorr, M. Westby, S. Dobbs, P. Griffin, B. Irvine, M. Macartney, J. Mori, G. Rickett, C. Smith-Burchnell, C. Napier, R. Webster, D. Armour, D. Price, B. Stammen, A. Wood, M. Perros, *Antimicrob. Agents Chemother.* **2005**, *49*, 4721–4732.
[23] M. Baba, O. Nishimura, N. Kanzaki, M. Okamoto, H. Sawada, Y. Iizawa, M. Shiraishi, Y. Aramaki, K. Okonogi, Y. Ogawa, K. Meguro, M. Fujino, *Proc. Natl. Acad. Sci. USA* **1999**, *96*, 5698–5703.
[24] J. R. Tagat, S. W. McCombie, D. Nazareno, M. A. Labroli, Y. Xiao, R. W. Steensma, J. M. Strizki, B. M. Baroudy, K. Cox, J. Lachowicz, G. Varty, R. Watkins, *J. Med. Chem.* **2004**, *47*, 2405–2408.
[25] J. M. Strizki, S. Xu, N. E. Wagner, L. Wojcik, J. Liu, Y. Hou, M. Endres, A. Palani, S. Shapiro, J. W. Clader, W. J. Greenlee, J. R. Tagat, S. W. McCombie, K. Cox, A. B. Fawzi, C.-C. Chou, C. Pugliese-Sivo, L. Davies, M. E. Moreno, D. D. Ho, A. Trkola, C. A. Stoddart, J. P. Moore, G. R. Reyes, B. M. Baroudy, *Proc. Natl. Acad. Sci. USA* **2001**, *98*, 12718–12723.
[26] K. Maeda, H. Nakata, Y. Koh, T. Miyakawa, H. Ogata, Y. Takaoka, S. Shibayama, K. Sagawa, D. Fukushima, J. Moravek, Y. Koyanagi, H. Mitsuya, *J. Virol.* **2004**, *78*, 8654–8662.
[27] A. Trkola, T. J. Ketas, K. A. Nagashima, L. Zhao, T. Cilliers, L. Morris, J. P. Moore, P. J. Maddon, W. C. Olson, *J. Virol.* **2001**, *75*, 579–588.
[28] C. Ji, J. Zhang, M. Dioszegi, S. Chiu, E. Rao, A. Derosier, N. Cammack, M. Brandt, S. Sankuratri, *Mol. Pharmacol.* **2007**, *72*, 18–28.
[29] K. De Vresse, D. Reymen, P. Griffin, A. Steinkasserer, G. Werner, G. J. Bridger, J. Esté, W. James, G. W. Henson, J. Desmyter, J. Anné, E. De Clercq, *Antiviral Res.* **1996**, *29*, 209–219.
[30] D. Schols, J. A. Esté, G. Henson, E. De Clercq, *Antiviral Res.* **1997**, *35*, 147–156.
[31] E. De Clercq, *Mol. Pharmacol.* **2000**, *57*, 833–839.
[32] J. A. Esté, C. Cabrera, E. De Clercq, S. Struyf, J. Van Damme, G. Bridger, R. T. Skerlj, M. J. Abrams, G. Henson, A. Gutierrez, B. Clotet, D. Schols, *Mol. Pharmacol.* **1999**, *55*, 67–73.
[33] S. Hatse, K. Princen, E. De Clercq, M. M. Rosenkilde, T. W. Schwartz, P. E. Hernandez-Abad, R. T. Skerlj, G. J. Bridger, D. Schols, *Biochem. Pharmacol.* **2005**, *70*, 752–761.
[34] K. Princen, S. Hatse, K. Vermeire, S. Aquaro, E. De Clercq, L.-O. Gerlach, M. Rosenkilde, T. W. Schwartz, R. Skerlj, G. Bridger, D. Schols, *J. Virol.* **2004**, *78*, 12996–13006.
[35] J. Teixidó, J. I. Borrell, S. Nonell, S. Pettersson, L. Ros, R. Puig de La Bellacasa, M. O. Rabal, V. Pérez, J. Esté, I. Clotet-Codina, M. Armand-Ugón, ES Patent ES200602764, **2006** (filing date: October 26, 2006).
[36] W. Zhan, Z. Liang, A. Zhu, S. Kurtkaya, H. Shim, J. P. Snyder, D. C. Liotta, *J. Med. Chem.* **2007**, *50*, 5655–5664.
[37] Cerius2, Version 6.6, Accelrys Inc., San Diego, CA (USA) **2001**.
[38] R. Pascual, J. I. Borrell, J. Teixidó, *Mol. Diversity* **2000**, *6*, 121–133.
[39] MOE, Molecular Operating Environment, Chemical Computing Group Inc., Montréal, QC (Canada) **2006**.
[40] S. Pettersson, I. Clotet-Codina, J. A. Esté, J. I. Borrell, J. Teixidó, *Mini-Rev. Med. Chem.* **2006**, *6*, 91–108.
[41] A. F. Abdel-Magid, K. G. Carson, B. D. Harris, C. A. Maryanoff, R. D. Shah, *J. Org. Chem.* **1996**, *61*, 3849–3862.
[42] T. H. Fife, L. H. Brod, *J. Org. Chem.* **1968**, *33*, 4136–4140.
[43] J. L. Jensen, R. Siegel, *J. Org. Chem.* **1988**, *53*, 6105–6106.
[44] C. Yue, I. Gauthier, J. Royer, H.-P. Husson, *J. Org. Chem.* **1996**, *61*, 4949–4954.
[45] R. Pascual, PhD Thesis, Universitat Ramon Llull (Barcelona, Spain), **2003**.
[46] M. O. Rabal, PhD Thesis, Universitat Ramon Llull (Barcelona, Spain), **2006**.
[47] A. Brelot, N. Heveker, M. Montes, M. Alizon, *J. Biol. Chem.* **2000**, *275*, 23736–23744.
[48] AutoDock 3.0, Department of Molecular Biology, The Scripps Research Institute, MB-5, La Jolla, CA (USA) **1989**.
[49] G. M. Morris, D. S. Goodsell, R. Halliday, R. Huey, W. E. Hart, R. K. Belew, A. J. Olson, *J. Comput. Chem.* **1998**, *19*, 1639–1662.
[50] A. Sali, T. L. Blundell, *J. Mol. Biol.* **1993**, *234*, 779–815.
[51] R. E. Bruccoleri, *Mol. Simul.* **1993**, *10*, 151–174.
[52] C. Seibert, T. P. Sakmar, *Curr. Pharm. Des.* **2004**, *10*, 2041–2062.
[53] V. I. Pérez-Nueno, D. W. Ritchie, M. O. Rabal, R. Pascual, J. I. Borrell, J. Teixidó, *J. Chem. Inf. Model.* **2008**, *48*, 509–533.
[54] J. Gasteiger, M. Marsili, *Tetrahedron* **1980**, *36*, 3219–3228.
[55] L.-O. Gerlach, R. Skerlj, G. Bridger, T. W. Schwartz, *J. Biol. Chem.* **2001**, *276*, 14153–14160.
[56] C. Bissantz, G. Folkers, D. Rognan, *J. Med. Chem.* **2000**, *43*, 4759–4767.
[57] H. Gutiérrez-de-Terán, M. Pastor, N. B. Centeno, J. Aqvist, F. Sanz, *ChemBioChem* **2004**, *5*, 841–849.
[58] X. Huang, J. Shen, M. Cui, L. Shen, X. Luo, K. Ling, G. Pei, H. Jiang, K. Chen, *Biophys. J.* **2003**, *84*, 171–184.
[59] G. C. Shields, C. A. Laguthton, M. Orozco, *J. Am. Chem. Soc.* **1997**, *119*, 7463–7469.
[60] G. Moncunill, M. Armand-Ugón, B. Clotet, J. A. Este, *AIDS* **2008**, *22*, 23–31.
[61] G. Moncunill, M. Armand-Ugón, I. Clotet, E. Pauls, E. Ballana, A. Llano, B. Romagnoli, J. W. Vrijbloed, F. O. Gombert, B. Clotet, S. De Marco, J. A. Este, *Mol. Pharmacol.* **2008**, *73*, 1264–1273.

Received: May 9, 2008
Revised: June 3, 2008
Published online on July 31, 2008

Supporting Information

Blind docking and binding pocket docking analyses for the calculated CXCR4-compound **1**{*8,8*} complex and experimental details and spectral data for compounds **1**{*5,5*}, **1**{*6,6*}, **1**{*7,7*}, **1**{*9,9*}, **1**{*10,10*}, **1**{*11,11*}, **2**{*2,2*}, **2**{*3,3*}, **7**{*5*}, **7**{*7*}, **7**{*9*}, **7**{*10*}, **7**{*11*}, **6**{*3*}, **8**{*2,6*}, **8**{*2,8*}, **8**{*2,9*}, **8**{*2,11*}, **8**{*3,4*}, **1**{*4,5*}, **1**{*4,6*}, **1**{*4,9*}, **1**{*4,11*}, **1**{*5,6*}, **1**{*5,7*}, **1**{*5,8*}, **1**{*5,9*}, **1**{*5,10*}, **1**{*5,11*}, **1**{*6,7*}, **1**{*6,9*}, **1**{*6,10*}, **1**{*6,11*}, **1**{*7,9*}, **1**{*7,11*}, **1**{*8,10*}, **1**{*8,11*}, **1**{*9,10*}, **1**{*9,11*}, **1**{*10,11*}, **8**{*1,5*}, **8**{*1,6*}, **8**{*1,8*}, **8**{*1,9*}, **8**{*1,11*}, **8**{*2,5*}, **8**{*3,5*}, **8**{*3,6*}, **8**{*3,8*}, **8**{*3,9*} and **8**{*3,11*}.

Table. Blind docking and binding pocket docking analyses for the calculated CXCR4-compound **1**{8,8} complex. This table shows the distances from the carboxylic oxygens of the three key binding residues Asp171, Asp262, and Glu288, to the four nitrogens (N27, N21, N8, N13) of **1**{8,8}. The lowest interaction distances are shown in bold. The nitrogen atoms of **1**{8,8} are charged according to physiological pH.

	Blind docking [a]	Binding pocket docking [b]
Distance to O^- (sp3) Asp^{171} (Å)	10.11 (N+27) 9.36 (N+13) 12.84 (N+27) 11.06 (N+27) 7.98 (N+13) 9.08 (N+N+27)	10.25 (N+8) 7.22 (N+27) 8.00 (N+13) 8.98 (N+27) 9.70 (N+8)
Average	10.07	8.83
Distance to O (sp2) Asp^{171} (Å)	8.22 (N+21) 7.18 (N+13) 10.82 (N+27) 8.93 (N+27) **6.88 (N+13)** **6.97 (N+27)**	8.08 (N+8) **5.87 (N+27)** **5.81 (N+13)** **6.80 (N+27)** 7.51 (N+8)
Average	8.17	6.81
Distance to O^- (sp3) Asp^{262} (Å)	8.02 (N+27) **5.42 (N+21)** **3.74 (N+21)** **4.45 (N+21)** 6.72 (N+8) 6.74 (N+21)	**4.80 (N+21)** 8.63 (N+13) 7.39 (N+21) **3.86 (N+21)** 4.87 (N+21)
Average	5.85	5.91
Distance to O (sp2) Asp^{262} (Å)	6.64 (N+27) 5.83 (N+21) **4.88 (N+21)** **4.72 (N+21)** **5.24 (N+8)** 5.28 (N+21)	**4.90 (N+21)** 6.86 (N+27) 6.23 (N+8) **5.43 (N+21)** **4.81 (N+21)**
Average	**5.43**	**5.65**
Distance to O^- (sp3) Glu^{288} (Å)	6.28 (N+27) **4.10 (N+8)** **4.75 (N+27)** 6.31 (N+21) **3.95 (N+8)** 5.37 (N+8)	4.93 (N+13) **3.90 (N+8)** **4.34 (N+27)** 7.86 (N+13) **4.04 (N+13)**
Average	**5.13**	**4.96**
Distance to O (sp2) Glu^{288} (Å)	**3.83 (N+8)** 5.84 (N+21) **4.94 (N+8)** 5.09 (N+8) **3.06 (N+21)** **3.63 (N+8)**	4.83 (N+13) **3.01 (N+8)** **4.05 (N+27)** 8.60 (N+13) **4.30 (N+13)**
Average	**4.42**	**4.96**

[a] For blind docking analysis all distances refer to the AUTODOCK pose with the lowest overall distance between the compound nitrogens and the three key binding residues.

[b] For binding pocket docking analysis all distances refer to the lowest energy AUTODOCK pose.

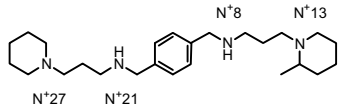

***N*-(4-((3-(pyrrolidin-1-yl)propylamino)methyl)benzyl)-3-(pyrrolidin-1-yl)propan-1-amine (1{*5,5*}).** The procedure was the same as that stated for **1**{*4,4*} but using terephthalaldehyde (**3**) (1.47 g, 11.1 mmol), 1-(3-aminopropyl)pyrrolidine **4**{*5*} (1.47 g, 11.1 mmol) and $NaBH_4$ (0.43 g, 11.1 mmol) to give **1**{*5,5*} as a yellow oil (1.98 g, 99%). IR (film): *ν*=3282 (N-H), 2936, 2789 (C-H), 1458 cm^{-1} (C-H); ^{1}H-NMR (300 MHz, $CDCl_3$, 25 ºC, TMS): *d*=7.26 (s, 4H; Ph), 3.77 (s, 4H; C$\underline{H}_2$-Ph), 2.69 (t, ^3J (H,H)=7.0 Hz, 4H; C$\underline{H}_2$-NH), 2.49 (m, 12H; CH_2-N), 2.08 (br, 2H; NH), 1.75 ppm (m, 12H; CH_2); ^{13}C-NMR (75.5 MHz, $CDCl_3$, 25 ºC): *d*=138.5 (Cq), 128.0 (CH), 54.6 (CH_2), 54.1 (CH_2), 53.5 (CH_2), 47.9 (CH_2), 28.8 (CH_2), 23.4 ppm (CH_2); MS (EI): *m/z* (%): 359.2 (1) [M^++H], 84.0 (100) [$C_5H_{10}N^+$]; HRMS: Calcd for ($C_{22}H_{39}N_4$): 359.3175. Found: 359.3169.

***N*-(4-((3-(1*H*-imidazol-1-yl)propylamino)methyl)benzyl)-3-(1*H*-imidazol-1-yl)propan-1-amine (1{*6,6*}).** The procedure was the same as that stated for **1**{*4,4*} but using terephthalaldehyde (**3**) (0.54 g, 3.9 mmol), 1-(3-aminopropyl)imidazole **4**{*6*} (1.00 g, 7.8 mmol) and $NaBH_4$ (0.30 g, 7.8 mmol) to afford **1**{*6,6*} as a yellow oil (1.38 g, 100%). IR (film): *ν*=3277 (N-H), 3103, 2935, 2815 (C-H), 1508 (imidazol), 1453 cm^{-1} (C-H); ^{1}H-NMR (300 MHz, $CDCl_3$, 25 ºC, TMS): *d*=7.41 (s, 2H; CH-N), 7.26 (s, 4H; Ph), 7.02 (s, 2H; CH-N), 6.88 (s, 2H; CH-N), 4.04 (t, ^3J (H,H)=6.9 Hz, 4H; CH_2-N), 3.74 (s, 4H; C$\underline{H}_2$-Ph), 2.60 (t, ^3J (H,H)=6.9 Hz, 4H; C$\underline{H}_2$-NH), 2.05 (s, 2H; NH), 1.92 ppm (quint, ^3J (H,H)=6.9 Hz, 4H; CH_2); ^{13}C-NMR (75.5 MHz, $CDCl_3$, 25 ºC): *d*=138.8 (CH), 137.1 (Cq), 129.2 (CH), 128.2 (CH), 118.7 (CH), 53.6 (CH_2), 45.6 (CH_2), 44.6 (CH_2), 31.3 ppm (CH_2); MS (EI): *m/z* (%): 353.0 (1) [M^++H], 228.9 (100) [$C_{14}H_{18}N_3^+$]; HRMS: Calcd for $C_{20}H_{28}N_6$ [M+1H]$^+$: 352.2454. Found: 353.2448.

***N*-(4-((2-(piperidin-1-yl)ethylamino)methyl)benzyl)-2-(piperidin-1-yl)ethanamine (1{*7,7*}).** The procedure was the same as that stated for **1**{*4,4*} but using terephthalaldehyde (**3**) (0.29 g, 2.1 mmol), 1-(2-aminoethyl)piperidine **4**{*7*} (0.56 g, 4.3 mmol) and $NaBH_4$ (0.16 g, 4.3 mmol) to give **1**{*7,7*}as a yellow oil (0.76 g, 100%). IR (film): *ν*=3310 cm^{-1} (N-H); ^{1}H-NMR (300MHz, $CDCl_3$, 25 ºC, TMS): *d*=7.32 (s, 4H; Ph), 3.75 (s, 4H; C$\underline{H}_2$-Ph), 2.69 (t, ^3J (H,H)=7.0 Hz, 4H; C$\underline{H}_2$-NH), 2.47 (t, ^3J (H,H)=7.0 Hz, 4H; CH_2-N), 2.39 (m, 8H; CH_2-N), 1.62-1.39 ppm (m, 12H; CH_2); ^{13}C-NMR (75.5MHz, $CDCl_3$, 25 ºC): *d*=139.4 (Cq), 129.6 (CH), 59.0 (CH_2), 55.7 (CH_2), 54.1 (CH_2), 46.1 (CH_2), 26.7 (CH_2), 25.2 ppm (CH_2); Anal. ($C_{22}H_{38}N_4$) C, H, N.

***N*-(4-((3-(4-methylpiperazin-1-yl)propylamino)methyl)benzyl)-3-(4-methylpiperazin-1-yl)propan-1-amine (1{*9,9*}).** The procedure was the same as that stated for **1**{*4,4*} but using terephthalaldehyde (**3**) (0.48 g, 3.5 mmol), 1-(3-aminopropyl)-4-methylpiperazine **4**{*9*} (1.14 g, 7.0 mmol) and $NaBH_4$ (0.27 g, 7.0 mmol) to give **1**{*9,9*} as a brown oil (1.28 g, 87%). IR (film): *ν*=3281 (N-H), 2935, 2793 (C-H), 1458 cm^{-1} (C-H); ^{1}H-NMR (300 MHz, $CDCl_3$, 25 ºC, TMS): *d*=7.26 (s, 4H; Ph), 3.76 (s, 4H; C$\underline{H}_2$-Ph), 2.66 (t, ^3J (H,H)=6.9 Hz, 4H; C$\underline{H}_2$-NH), 2.42 (m, 22H; CH_2-N, NH), 2.27 (s, 6H; CH_3), 1.70 ppm (quint, ^3J (H,H)=6.9 Hz, 4H; CH_2); ^{13}C-NMR (75.5 MHz, $CDCl_3$, 25 ºC): *d*=138.8 (Cq), 128.0 (CH), 57.0 (CH_2), 55.1 (CH_2), 53.7 (CH_2), 53.2 (CH_2), 48.1 (CH_2), 46.0 (CH_3), 26.9 ppm (CH_2); MS (EI): *m/z* (%): 417.0 (9) [M^++H], 416.0 (28) [M^+], 113.0 (100) [$C_6H_{13}N_2^+$]; HRMS: Calcd for $C_{24}H_{44}N_6$ [M+1H]$^+$: 417.3706. Found: 417.3700.

***N*-(4-((2-morpholinoethylamino)methyl)benzyl)-2-morpholinoethylamine (1{*10,10*}).** The procedure was the same as that stated for **1**{*4,4*} but using terephthalaldehyde (**3**) (0.54 g, 4.0 mmol), 2-morpholinoethylamine **4**{*10*} (1.05 g, 8.0 mmol) and $NaBH_4$ (0.31 g, 8.0 mmol) to give **1**{*10,10*} as a white solid (0.93 g, 64%). IR (film): *ν*=3341 (N-H), 2968, 2930, 2817 (C-H), 1446 (C-H), 1117, 830 & 862 cm^{-1} (C-O-C); ^{1}H-NMR (300 MHz, $CDCl_3$, 25 ºC, TMS): *d*=7.27 (s, 4H; Ph), 3.79 (s, 4H; C$\underline{H}_2$-Ph), 3.69 (t, ^3J (H,H)=4.6 Hz, 8H; CH_2-O), 2.70 (t, ^3J (H,H)=6.0 Hz, 4H; C$\underline{H}_2$-NH), 2.50 (t, ^3J (H,H)=6.0 Hz, 4H; CH_2-N), 2.403 (t, ^3J (H,H)=4.6 Hz, 8H; CH_2-N), 1.82 ppm (s, 2H; NH); ^{13}C-NMR (75.5 MHz, $CDCl_3$, 25 ºC): *d*=139.0 (Cq), 128.0 (CH), 67.0 (CH_2), 58.3 (CH_2), 53.7 (CH_2), 45.3 ppm (CH_2); Anal. ($C_{20}H_{34}N_4O_2$) C, H, N. MS (EI): *m/z* (%) 363.4 (5) [M^++H], 362.4 (6) [M^+], 100.0 (100) [$C_5H_{10}NO^+$].

***N*-(4-((3-morpholinopropylamino)methyl)benzyl)-3-morpholinopropan-1-amine (1{*11,11*}).** The procedure was the same as that stated for **1**{*4,4*} but using terephthalaldehyde (**3**) (0.47 g, 3.5 mmol), 3-morpholinopropylamine **4**{*11*} (1.00 g, 7.0 mmol) and $NaBH_4$ (0.27 g, 7.0 mmol) to give **1**{*11,11*} as a yellow oil (1.16 g, 85%). IR (film): *ν*=3301(N-H), 2948, 2852, 2806 (C-H), 1456 (C-H), 1118, 862 cm^{-1} (C-O-C); ^{1}H-NMR (300 MHz, $CDCl_3$, 25 ºC, TMS): *d*=7.27 (s, 4H; Ph), 3.79 (s, 4H; C$\underline{H}_2$-Ph), 3.70 (t, ^3J (H,H)=4.6 Hz, 8H; CH_2-O), 2.68 (t, ^3J (H,H)=7.0 Hz, 4H; C$\underline{H}_2$-NH), 2.41 (m, 12H; CH_2-N), 1.81 (s, 2H; NH), 1.70 ppm (quint, ^3J (H,H)=7.0 Hz, 4H; CH_2); ^{13}C-NMR (75.5 MHz, $CDCl_3$, 25 ºC): *d*=138.9 (Cq), 128.0 (CH), 67.0 (CH_2), 57.4 (CH_2), 53.8 (CH_2), 48.0 (CH_2), 26.8 ppm (CH_2). MS (EI): *m/z* (%) 390.3 (2) [M^+], 100.0 (100) [$C_5H_{10}NO^+$]; HRMS: Calcd for $C_{22}H_{38}N_4O_2$: 390.2995. Found: 390.3007.

((4-(*N*-(2,6-dimethylpiperidin-1-yl)imino)methyl)phenyl)-*N*-(2,6-dimethylpiperidin-1-yl)methanamine (2{*2,2*}). The procedure was the same as that stated for **2**{*1,1*} but using terephthalaldehyde (**3**) (0.57 g, 4.2 mmol) and 1-amino-2,6-dimethylpiperidine **4**{*2*} (1.20 g, 8.4 mmol) to give **2**{*2,2*} as a yellow solid (1.05 g, 65%). IR (film): *ν*=1684 cm^{-1} (C=N); ^{1}H-NMR (300MHz, $CDCl_3$, 25 ºC, TMS): *d*=7.87 (s, 2H; CH=N), 7.64 (s, 4H; Ph), 3.31-3.27 (m, 4H; C$\underline{H}$-CH_3), 1.83-1.51 (m, 12H; CH_2), 1.03 ppm (d, ^3J (H,H)=6.0 Hz, 12H; CH_3); ^{13}C-NMR (75.5 MHz, $CDCl_3$, 25 ºC): *d*=146.6 (CH), 136.0 (Cq), 126.8 (CH), 56.1 (CH), 32.4 (CH_2), 20.0 (CH_3), 19.9 ppm (CH_2); Anal. ($C_{22}H_{34}N_4$) C, H, N.

((4-(*N*-(4-methylpiperazin-1-yl)imino)methyl)phenyl)-*N*-(4-methylpiperazin-1-yl)methanamine (2{*3,3*}). The procedure was the same as that stated for **2**{*1,1*} but using terephthalaldehyde (**3**) (0.37 g, 2.7 mmol) and 1-amino-4-methylpiperazine **4**{*3*} (0.64 g, 5.4 mmol) to give **2**{*3,3*} as a yellow solid (0.67 g, 75%). IR (film): *ν*=1579 cm^{-1} (C=N); ^{1}H-NMR (300MHz, $CDCl_3$): *d*=7.57 (s, 4H; Ph), 7.53 (s, 2H; CH=N), 3.23 (m, 8H; CH_2-N), 2.62 (m, 8H; CH_2-N), 2.36 ppm (s, 6H; CH_3); ^{13}C-NMR (75.5MHz, $CDCl_3$, 25 ºC): *d*=135.8 (Cq), 135.4 (CH), 126.2 (CH), 54.5 (CH_2), 51.0 (CH_2), 46.0 ppm (CH_3); Anal. ($C_{18}H_{28}N_6$) C, H, N.

4-((3-(pyrrolidin-1-yl)propylamino)methyl)benzaldehyde (7{*5*}). The procedure was the same as that stated for **7**{*4*} but using 4-(diethoxymethyl)benzaldehyde (**5**) (6.01 g, 28.0 mmol), 1-(3-aminopropyl)pyrrolidine **4**{*5*} (3.70 g, 28.0 mmol) and $NaBH_4$ (1.07 g, 28.0 mmol). The intermediate aminoacetal was obtained as a yellow oil (8.01 g, 89%). This acetal (7.98 g, 24.9 mmol) was deprotected to afford **7**{*5*} (4.59 g, 75%) as a red oil. IR (film): *v*=3276 (N-H), 2934, 2874, 2790 (C-H), 1700 (C=O), 1606 (C-C), 1458 cm^{-1} (C-H); ^{1}H-NMR (300 MHz, $CDCl_3$, 25 ºC, TMS): *d*=10.00 (s, 1H; CHO), 7.84 (d, ^3J (H,H)=8.1 Hz, 2H; Ph), 7.50 (d, ^3J (H,H)=8.1 Hz, 2H; Ph), 3.88 (s, 2H; C$\underline{H}_2$-Ph), 2.70 (t, ^3J (H,H)=7.0 Hz, 2H; C$\underline{H}_2$-NH), 2.51 (m, 6H; CH_2-N), 1.87 (br, 1H; NH), 1.75 ppm (m, 6H; CH_2); ^{13}C-NMR (75.5 MHz, $CDCl_3$, 25 ºC): *d*=191.8 (CH), 147.7 (Cq), 135.2 (Cq), 129.8 (CH), 128.3 (CH), 54.7 (CH_2), 54.3 (CH_2), 53.7 (CH_2), 48.2 (CH_2), 29.2 (CH_2), 23.5 ppm (CH_2); Anal. ($C_{15}H_{22}N_2O$) C, H, N; MS (EI): *m/z* (%): 247.2 (2) [M^++H], 246.2 (21) [M^+], 84.1 (100) [$C_5H_{10}N^+$].

4-((2-(piperidin-1-yl)ethylamino)methyl)benzaldehyde (7{*7*}). The procedure was the same as that stated for **7**{*4*} but using 4-(diethoxymethyl)benzaldehyde (**5**) (2.01 g, 9.4 mmol), 1-(2-aminoethyl)piperidine **4**{*7*} (1.23 g, 9.4 mmol) and $NaBH_4$ (0.36 g, 9.4 mmol). The intermediate aminoacetal was obtained as a yellow oil (2.79 g, 93%). This acetal (2.75 g, 8.6 mmol) was deprotected to afford **7**{*7*} (2.11 g, quantitative) as a yellow oil. IR (film): *v*=3308 (N-H), 3050, 2934, 2851, 2809 (C-H), 1701 (C=O), 1606 (C-C), 1453 cm^{-1} (C-H); ^{1}H-NMR (300 MHz, $CDCl_3$, 25 ºC, TMS): *d*=10.00 (s, 1H; CHO), 7.84 (d, ^3J (H,H)=8.1 Hz, 2H; Ph), 7.50 (d, ^3J (H,H)=8.1 Hz, 2H; Ph), 3.89 (s, 2H; C$\underline{H}_2$-Ph), 2.70 (t, ^3J (H,H)=6.2 Hz, 2H; C$\underline{H}_2$-NH), 2.47 (t, ^3J (H,H)=6.2 Hz, 2H, CH_2-N), 2.36 (br, 4H; CH_2-N), 2.18 (br, 1H; NH), 1.57 (quint, ^3J (H,H)=5.7 Hz, 4H; CH_2), 1.43 ppm (m, 2H; CH_2); ^{13}C-NMR (75.5 MHz, $CDCl_3$, 25 ºC): *d*=191.8 (CH), 147.7 (Cq), 135.2 (Cq), 129.8 (CH), 128.4 (CH), 58.4 (CH_2), 54.7 (CH_2), 53.7 (CH_2), 45.9 (CH_2), 25.9 (CH_2), 24.4 ppm (CH_2); Anal. ($C_{15}H_{22}N_2O$) C, H, N; MS (EI): *m/z* (%): 246.2 (8) [M^+], 98.1 (100) [$C_6H_{12}N^+$]; HRMS: Calcd for $C_{15}H_{22}N_2O$: 246.1732. Found: 246.1731.

4-((3-(4-methylpiperazin-1-yl)propylamino)methyl)benzaldehyde (7{*9*}). The procedure was the same as that stated for **7**{*4*} but using 4-(diethoxymethyl)benzaldehyde (**5**) (2.00 g, 9.3 mmol), 1-(3-aminopropyl)-4-methylpiperazine **4**{*9*} (1.49 g, 9.3 mmol) and $NaBH_4$ (0.36 g, 9.3 mmol). The intermediate aminoacetal was obtained as a yellow oil (2.94 g, 90%). This acetal (2.93 g, 8.4 mmol) was deprotected to afford **7**{*9*} (2.31 g, quantitative) as a brown oil. IR (film): *v*=3276 (N-H), 2936, 2875, 2794, 2769, 2740 (C-H), 1700 (C=O), 1606 (C-C), 1458 cm^{-1} (C-H); ^{1}H-NMR (300 MHz, $CDCl_3$, 25 ºC, TMS): *d*=10.00 (s, 1H; CHO), 7.85 (d, ^3J (H,H)=8.1 Hz, 2H; Ph), 7.50 (d, ^3J (H,H)=8.1 Hz, 2H; Ph), 3.87 (s, 2H; C$\underline{H}_2$-Ph), 2.69 (t, ^3J (H,H)=6.9 Hz, 2H; C$\underline{H}_2$-NH), 2.45 (br, 8H; CH_2-N), 2.42 (t, ^3J (H,H)=6.9 Hz, 2H; CH_2-N), 2.27 (s, 3H; CH_3), 2.08 (br, 1H; NH), 1.72 ppm (quint, ^3J (H,H)=6.9 Hz, 2H; CH_2); ^{13}C-NMR (75.5 MHz, $CDCl_3$, 25 ºC): *d*=191.8 (CH), 147.7 (Cq), 135.2 (Cq), 129.8 (CH), 128.3 (CH), 57.0 (CH_2), 55.1 (CH_2), 53.7 (CH_2), 53.2 (CH_2), 48.3 (CH_2), 46.0 (CH_3), 27.0 ppm (CH_2); MS (EI): *m/z* (%): 276.2 (4) [M^++H], 275.2 (26) [M^+], 231.2 (100) [$C_{14}H_{21}N_3^+$]; HRMS: Calcd for $C_{16}H_{25}N_3O$: 275.1998. Found: 275.2001.

4-((2-morpholinoethylamino)methyl)benzaldehyde (7{*10*}). The procedure was the same as that stated for **7**{*4*} but using 4-(diethoxymethyl)benzaldehyde (**5**) (2.00 g, 9.3 mmol), 2-morpholinoethylamine **4**{*10*} (1.23 g, 9.3 mmol) and $NaBH_4$ (0.36 g, 9.3 mmol). The intermediate aminoacetal was obtained as a yellow oil (2.55 g, 85%). This acetal (2.52 g, 7.8 mmol) was deprotected to afford **7**{*10*} (1.94 g, quantitative) as a brown oil. IR (film): *v*=3309 (N-H), 2954, 2917, 2894, 2852, 2818 (C-H), 1698 (C=O), 1607 (C-C), 1455 (C-H), 1117, 852 cm^{-1} (C-O-C); ^{1}H-NMR (300 MHz, $CDCl_3$, 25 ºC, TMS): *d*=10.00 (s, 1H; CHO), 7.86 (d, ^3J (H,H)=8.1 Hz, 2H; Ph), 7.50 (d, ^3J (H,H)=8.1 Hz, 2H; Ph), 3.90 (s, 2H; C$\underline{H}_2$-Ph), 3.70 (t, ^3J (H,H)=4.5 Hz, 4H; CH_2-O), 2.71 (t, ^3J (H,H)=6.0 Hz, 2H; C$\underline{H}_2$-NH), 2.51 (t, ^3J (H,H)=6.0 Hz, 2H; CH_2-N), 2.42 (t, ^3J (H,H)=4.5 Hz, 4H; CH_2-N), 1.93 ppm (br, 1H; NH); ^{13}C-NMR (75.5 MHz, $CDCl_3$, 25 ºC): *d*=191.7 (CH), 147.5 (Cq), 135.2 (Cq), 129.8 (CH), 128.4 (CH), 66.9 (CH_2), 58.2 (CH_2), 53.7 (CH_2), 45.4 ppm (CH_2); MS (IE): *m/z* (%) 249.2 (0.3) [M^++H], 248.2 (8) [M^+], 100.0 (100) [$C_5H_{10}NO^+$]; HRMS: Calcd for $C_{14}H_{20}N_2O_2$: 248.1525. Found: 248.1531.

4-((3-morpholinopropylamino)methyl)benzaldehyde (7{*11*}). The procedure was the same as that stated for **7**{*4*} but using 4-(diethoxymethyl)benzaldehyde (**5**) (2.01 g, 9.3 mmol), 3-morpholinopropylamine **5**{*11*} (1.35 g, 9.3 mmol) and $NaBH_4$ (0.36 g, 9.3 mmol). The intermediate aminoacetal was obtained as a yellow oil (2.91 g, 92%). This acetal (2.86 g, 8.5 mmol) was deprotected to afford **7**{*11*} (1.60 g, 72%) as a yellow oil. IR (film): *v*=3307 (N-H), 2950, 2892, 2853, 2814 (C-H), 1698 (C=O), 1607 (C-C), 1457 (C-H), 1117, 861 cm^{-1} (C-O-C); ^{1}H-NMR (300 MHz, $CDCl_3$, 25 ºC, TMS): *d*=10.00 (s, 1H; CHO), 7.85 (d, ^3J (H,H)=8.1 Hz, 2H; Ph), 7.50 (d, ^3J (H,H)=8.1 Hz, 2H; Ph), 3.88 (s, 2H; C$\underline{H}_2$-Ph), 3.70 (t, ^3J (H,H)=4.7 Hz, 4H; CH_2-O), 2.70 (t, ^3J (H,H)=6.9 Hz, 2H; C$\underline{H}_2$-NH), 2.45-2.39 (m, 6H; CH_2-N), 1.81 (br, 1H; NH), 1.72 ppm (quint, ^3J (H,H)=6.9 Hz, 2H; CH_2); ^{13}C-NMR (75.5 MHz, $CDCl_3$, 25 ºC): *d*=191.2 (CH), 147.6 (Cq), 135.2 (Cq), 129.8 (CH), 128.3 (CH), 66.9 (CH_2), 57.3 (CH_2), 53.8 (CH_2), 53.7 (CH_2), 48.1 (CH_2), 26.7 ppm (CH_2); MS (EI): *m/z* (%) 262.2 (3) [M^+], 84.0 (100) [$C_5H_{10}N^+$]; HRMS: Calcd for $C_{15}H_{22}N_2O_2$: 262.1681. Found: 262.1682.

4-((4-methylpiperazin-1-ylimino)methyl)benzaldehyde (6{*3*}). The procedure was the same as that stated for **6**{*1*} but using terephthalaldehyde (**3**) (1.14 g, 8.4 mmol) and 1-amino-4-methylpiperazine **4**{*3*} (0.50 g, 4.2 mmol). Upon removal of the solvent, the residue was chromatographed on silica gel, eluting with DCM/MeOH (gradient from 10:0 to 9:1) to afford **6**{*3*} (0.80 g, 82%) as a yellow solid. IR (film): *v*= 2941, 2843, 2799, 2728 (C-H), 1692 (C=O), 1605 (C-C), 1581 (C=N), 1551 (C-C), 1451, 1364 cm^{-1} (C-H); ^{1}H-NMR (300MHz, $CDCl_3$, 25 ºC, TMS): *d*=9.98 (s, 1H; CHO), 7.84 (d, ^3J (H,H)=7.7 Hz, 2H; Ph), 7.72 (d, ^3J (H,H)=7.7 Hz, 2H; Ph), 7.50 (s, 1H; CH=N), 3.30 (t, ^3J (H,H)=5.1 Hz, 4H; CH_2-N), 2.62 (t, ^3J (H,H)=5.1 Hz, 4H; CH_2-N), 2.37 ppm (s, 3H; CH_3); ^{13}C-NMR (75.5 MHz, $CDCl_3$, 25 ºC): *d*=191.6 (CH), 142.1 (Cq), 135.3 (Cq), 132.6 (CH), 130.0 (CH), 126.1 (CH), 54.3 (CH_2), 50.6 (CH_2), 46.0 ppm (CH_3); MS (EI): *m/z* (%): 232.1 (12) [M^++H], 99.0 (100) [$C_5H_{11}N_2^+$]; HRMS: Calcd for $C_{13}H_{17}N_3O$: 231.1372. Found: 231.1376.

***N*-(4-((2,6-dimethylpiperidin-1-ylimino)methyl)benzyl)-3-(1*H*-imidazol-1-yl)propan-1-amine (8{*2,6*}).** The procedure was the same as that stated for **8**{*2,4*} but using 1-(3-aminopropyl)imidazole **4**{*6*} (0.26 g, 2.0 mmol), **6**{*2*} (0.26 g, 2.0 mmol) and $NaBH_4$ (0.08 g, 2.0 mmol) to give **8**{*2,6*} (0.70 g, 100%) as a yellow oil. IR (film): *v*=3284 (N-H), 3106, 2961, 2931, 2867, 2856, 2824 (C-H), 1624 (C-C), 1582 (C=N), 1552 (C-C), 1508 (imidazol), 1449, 1369 cm^{-1} (C-H); ^{1}H-NMR (300 MHz, $CDCl_3$, 25 ºC, TMS): *d*=8.04 (s, 1H; CH=N), 7.65 (d, ^3J (H,H)=8.1 Hz, 2H; Ph), 7.46 (s, 1H; CH-N), 7.31 (d, ^3J (H,H)=8.1 Hz, 2H; Ph), 7.04 (s, 1H; CH-N), 6.89 (s, 1H; CH-N), 4.05 (t, ^3J (H,H)=6.9 Hz, 2H; CH_2-N), 3.77 (s, 2H; CH_2-Ph), 3.10 (m, 2H; C$\underline{H}$-CH_3), 2.61 (t, ^3J (H,H)=6.9 Hz, 2H; C$\underline{H}_2$-NH), 1.93 (quint, ^3J (H,H)=6.9 Hz, 2H; CH_2), 1.85 (br, 1H; NH), 1.77 (m, 4H; CH_2), 1.51 (m, 2H; CH_2), 1.00 ppm (d, ^3J (H,H)=6.6 Hz, 6H; CH_3); ^{13}C-NMR (75.5 MHz, $CDCl_3$, 25 ºC): *d*=151.7 (CH), 141.4 (Cq), 137.0, (CH) 134.0 (Cq), 129.2 (CH), 128.2 (CH), 127.3 (CH), 118.7 (CH), 57.2 (CH), 53.7 (CH_2), 45.7 (CH_2), 44.7 (CH_2), 32.8 (CH_2), 31.4 (CH_2), 21.2 (CH_2), 20.5 ppm (CH_3); MS (EI): *m/z* (%): 354.2 (5) [M^++H], 112.1 (100) [$C_7H_{14}N^+$]; HRMS: Calcd for $C_{21}H_{32}N_5$ [M+1H]$^+$: 354.2658. Found: 354.2666.

***N*-(4-((2,6-dimethylpiperidin-1-ylimino)methyl)benzyl)-3-(2-methylpiperidin-1-yl)propan-1-amine (8{*2,8*}).** The procedure was the same as that stated for **8**{*2,4*} but using 1-(3-aminopropyl)-2-methyl-piperidine **4**{*8*} (0.35 g, 2.1 mmol), **6**{*2*} (0.52 g, 2.1 mmol) and $NaBH_4$ (0.08 g, 2.1 mmol) to give **8**{*2,8*} (0.77 g, 93%) as a yellow oil. IR (film): *v*=3281 (N-H), 2961, 2930, 2855, 2808 (C-H), 1625 (C-C), 1584 (C=N), 1554 (C-C),

1449, 1370 cm^{-1} (C-H); ^{1}H-NMR (300 MHz, $CDCl_3$, 25 ºC, TMS): *d*=8.06 (s, 1H; CH=N), 7.64 (d, ^3J (H,H)=8.1 Hz, 2H; Ph), 7.34 (d, ^3J (H,H)=8.1 Hz, 2H; Ph), 3.81 (s, 2H; C$\underline{H}_2$-NH), 3.08 (m, 2H; C$\underline{H}$-CH_3), 2.88 (m, 1H; CH_{eq}-N), 2.76 (m, 1H; CH_{eq}-N), 2.65 (t, ^3J (H,H)=6.8 Hz, 4H; C$\underline{H}_2$-NH), 2.35 (br, 1H; NH), 2.34 (m, 1H; CH_{ax}-N), 2.25 (m, 1H; C$\underline{H}$-CH_3), 2.10 (m, 1H; CH_{ax}-N), 1.79-1.32 (cs, 12H; CH_2), 1.27 (m, 2H; CH_{ax}), 1.06 (d, ^3J (H,H)=6.3 Hz, 3H; CH_3), 1.00 ppm (d, ^3J (H,H)=6.3 Hz, 6H; CH_3); ^{13}C-NMR (75.5 MHz, $CDCl_3$, 25 ºC): *d*=152.3 (CH), 141.6 (Cq), 133.8 (Cq), 128.2 (CH), 127.2 (CH), 57.3 (CH), 56.0 (CH), 53.7 (CH_2), 52.3 (CH_2), 52.0 (CH_2), 48.3 (CH_2), 34.6 (CH_2), 32.9 (CH_2), 26.1 (CH_2), 25.6 (CH_2), 23.9 (CH_2), 21.4 (CH_2), 20.6 (CH_3), 19.0 ppm (CH_3).

***N*-(4-((2,6-dimethylpiperidin-1-ylimino)methyl)benzyl)-3-(4-methylpiperazin-1-yl)propan-1-amine (8{*2,9*}).** The procedure was the same as that stated for **8**{*2,4*} but using 1-(3-aminopropyl)-4-methylpiperazine **4**{*9*} (0.31 g, 1.9 mmol), **6**{*2*} (0.47 g, 1.9 mmol) and $NaBH_4$ (0.07 g, 1.9 mmol) to give **8**{*2,9*} (0.72 g, 97%) as a yellow oil. IR (film): *v*=3286 (N-H), 2932, 2872, 2837, 2794 (C-H), 1625 (C-C), 1584 (C=N), 1554 (C-C), 1458, 1370 cm^{-1} (C-H); ^{1}H-NMR (300 MHz, $CDCl_3$, 25 ºC, TMS): *d*=8.05 (s, 1H; CH=N), 7.65 (d, ^3J (H,H)=8.1 Hz, 2H; Ph), 7.34 (d, ^3J (H,H)=8.1 Hz, 2H; Ph), 3.81 (s, 2H; C$\underline{H}_2$-Ph), 3.08 (m, 2H; C$\underline{H}$-CH_3), 2.69 (t, ^3J (H,H)=6.9 Hz, 2H; C$\underline{H}_2$-NH), 2.44 (br, 8H; CH_2-N), 2.41 (t, ^3J (H,H)=6.9 Hz, 2H; CH_2-N), 2.30 (br, 1H; NH), 2.27 (s, 3H; CH_3-N), 1.81-1.68 (m, 6H; CH_2), 1.51 (m, 2H; CH_2), 1.00 ppm (d, ^3J (H,H)=6.3 Hz, 6H; CH_3); ^{13}C-NMR (75.5 MHz, $CDCl_3$, 25 ºC): *d*=152.1 (CH), 141.3 (Cq), 133.8 (Cq), 128.2 (CH), 127.3 (CH), 57.2 (CH), 57.0 (CH_2), 55.1 (CH_2), 53.6 (CH_2), 53.2 (CH_2), 48.1 (CH_2), 46.0 (CH_3), 32.9 (CH_2), 26.7 (CH_2), 21.4 (CH_2), 20.6 ppm (CH_3); MS (EI): *m/z* (%): 386.3 (1) [M^++H], 385.3 (1) [M^+], 113.0 (100) [$C_6H_{13}N^+$]; HRMS: Calcd for $C_{23}H_{39}N_5$: 385.3205. Found: 385.3211.

***N*-(4-((2,6-dimethylpiperidin-1-ylimino)methyl)benzyl)-3-morpholinopropan-1-amine (8{*2,11*}).** The procedure was the same as that stated for **8**{*2,4*} but using 3-morpholinopropylamine **4**{*11*} (0.27 g, 1.9 mmol), **6**{*2*} (0.46 g, 1.9 mmol) and $NaBH_4$ (0.07 g, 1.9 mmol) to give **8**{*2,11*} (0.63 g, 91%) as a yellow oil. IR (film): *v*=3293 (N-H), 2930, 2854, 2808 (C-H), 1625 (C-C), 1584 (C=N), 1554 (C-C), 1456, 1369 (C-H), 1118, 863 cm^{-1} (C-O-C); ^{1}H-NMR (300 MHz, $CDCl_3$, 25 ºC, TMS): *d*=8.06 (s, 1H; CH=N), 7.65 (d, ^3J (H,H)=8.1 Hz, 2H; Ph), 7.33 (d, ^3J (H,H)=8.1 Hz, 2H; Ph), 3.81 (s, 2H; C$\underline{H}_2$-Ph), 3.70 (t, ^3J (H,H)=4.7 Hz, 4H; CH_2-O), 3.08 (m, 2H; C$\underline{H}$-CH_3), 2.69 (t, ^3J (H,H)=6.9 Hz, 2H; C$\underline{H}_2$-NH), 2.45-2.38 (m, 6H; CH_2-N), 2.06 (br, 1H; NH), 1.81-1.66 (m, 6H; CH_2), 1.51 (m, 2H; CH_2), 1.00 ppm (d, ^3J (H,H)=6.3 Hz, 6H; CH_3); ^{13}C-NMR (75.5 MHz, $CDCl_3$, 25 ºC): *d*=152.2 (CH), 141.6 (Cq), 133.8 (Cq), 128.1 (CH), 127.3 (CH), 66.9 (CH_2), 57.4 (CH_2), 57.3 (CH), 53.8 (CH_2), 53.7 (CH_2), 47.9 (CH_2), 32.9 (CH_2), 26.6 (CH_2), 21.4 (CH_2), 20.6 ppm (CH_3); MS (EI): *m/z* (%): 372.2 (2) [M^+], 100.0 (100) [$C_5H_{10}NO^+$]; HRMS: Calcd for $C_{22}H_{36}N_4O$: 372.2889. Found: 372.2895.

***N*-(4-((4-methylpiperazin-1-ylimino)methyl)benzyl)-2-(pyrrolidin-1-yl)ethanamine (8{3,4}).** The procedure was the same as that stated for **8**{*2,4*} but using 1-(2-aminoethyl)pyrrolidine **4**{*4*} (1.16 g, 1.4 mmol), **6**{*3*} (0.32 g, 1.4 mmol) and $NaBH_4$ (0.053 g, 1.4 mmol) to give **8**{*3,4*} (0.42 g, 92%) as a yellow oil. IR (film): *v*=3309 (N-H), 2935, 2875, 2795 (C-H), 1592 (C=N), 1452 cm^{-1} (C-H); ^{1}H-NMR (300 MHz, $CDCl_3$, 25 ºC, TMS): *d*=7.55 (d, ^3J (H,H)=8.0 Hz, 2H; Ph), 7.55 (s, 1H; CH=N), 7.29 (d, ^3J (H,H)=8.0 Hz, 2H; Ph), 3.80 (s, 2H; C$\underline{H}_2$-Ph), 3.21 (t, ^3J (H,H)=5.0 Hz, 4H; CH_2-N), 2.73 (t, ^3J (H,H)=6.0 Hz, 2H; C$\underline{H}_2$-NH), 2.61 (m, 6H; CH_2-N), 2.48 (m, 4H; CH_2-N), 2.36 (s, 3H; CH_3), 1.87 (s, 1H; NH), 1.75 ppm (m, 4H; CH_2); ^{13}C-NMR (75.5 MHz, $CDCl_3$, 25 ºC): *d*=140.4 (Cq), 135.8 (CH), 134.8 (Cq), 128.2 (CH), 126.0 (CH), 55.9 (CH_2), 54.5 (CH_2), 54.2 (CH_2), 53.8 (CH_2), 51.1 (CH_2), 47.8 (CH_2), 46.0 (CH_3), 23.5 ppm (CH_2); Anal. ($C_{19}H_{31}N_5$) C, H, N; MS (EI): *m/z* (%): 330.4 (4) [M^++H], 329.3 (12) [M^+], 84.0 (100) [$C_5H_{10}N^+$].

***N*-(4-((2-(pyrrolidin-1-yl)ethylamino)methyl)benzyl)-3-(pyrrolidin-1-yl)propan-1-amine (1{*4,5*}).** The procedure was the same as that stated for **8**{*2,4*} but using 1-(3-aminopropyl)pyrrolidine **4**{*5*} (0.46 g, 3.5 mmol), **7**{*4*} (0.46 g, 3.5 mmol) and $NaBH_4$ (0.13 g, 3.5 mmol) to give **1**{*4,5*} (1.11 g, 92%) as a yellowish oil. IR (film): *v*=3281 (N-H), 2961, 2930, 2874, 2790 (C-H), 1458, 1445 cm^{-1} (C-H); ^{1}H-NMR (300 MHz, $CDCl_3$, 25 ºC, TMS): *d*=7.27 (s, 4H; Ph), 3.79 (s, 2H; C$\underline{H}_2$-Ph), 3.77 (s, 2H; C$\underline{H}_2$-Ph), 2.73 (m, 4H; C$\underline{H}_2$-NH), 2.61 (t, ^3J (H,H)=6.0 Hz, 2H; CH_2-N), 2.49 (m, 10H; CH_2-N), 2.14 (br, 2H; NH), 1.79-1.71 ppm (m, 10H; CH_2); ^{13}C-NMR (75.5 MHz, $CDCl_3$, 25 ºC): *d*=139.0 (Cq), 138.8 (Cq), 128.1 (CH), 128.0 (CH), 55.9 (CH_2), 54.7 (CH_2), 54.2 (CH_2), 53.8 (CH_2), 53.7 (CH_2), 48.0 (CH_2), 29.2 (CH_2), 23.5 ppm (CH_2); MS (EI): *m/z* (%): 345.3 (0.3) [M^++H], 84.1 (100) [$C_5H_{10}N^+$]; HRMS: Calcd for $C_{21}H_{37}N_4$ [M^++H]: 345.3018. Found: 345.3022.

***N*-(4-((2-(pyrrolidin-1-yl)ethylamino)methyl)benzyl)-3-(1*H*-imidazol-1-yl)propan-1-amine (1{*4,6*}).** The procedure was the same as that stated for **8**{*2,4*} but using 1-(2-aminoethyl)pyrrolidine **4**{*4*} (0.43 g, 3.7 mmol), **7**{*6*} (0.89 g, 3.7 mmol) and $NaBH_4$ (0.14 g, 3.7 mmol) to give **1**{*4,6*} (1.14 g, 91%) as a yellow oil. IR (film): *v* =3279 (N-H), 3104, 2929, 2875, 2799 (C-H), 1508 (imidazol), 1458, 1446 cm^{-1} (C-H); ^{1}H-NMR (300 MHz, $CDCl_3$, 25 ºC, TMS): *d*=7.44 (s, 1H; CH-N), 7.27 (s, 4H; Ph), 7.03 (s, 1H; CH-N), 6.88 (s, 1H; CH-N), 4.04 (t, ^3J (H,H)=6.9 Hz, 2H; CH_2-N), 3.79 (s, 2H; C$\underline{H}_2$-Ph), 3.73 (s, 2H; C$\underline{H}_2$-Ph), 2.74 (t, ^3J (H,H)=5.9 Hz, 2H; C$\underline{H}_2$-NH), 2.61 (m, 4H; C$\underline{H}_2$-NH, CH_2-N), 2.48 (m, 4H; CH_2-N), 2.18 (br, 2H; NH), 1.92 (quint, ^3J (H,H)=6.9 Hz, 2H; CH_2), 1.76 ppm (quint, ^3J (H,H)=3.3 Hz, 4H; CH_2); ^{13}C-NMR (75.5 MHz, $CDCl_3$, 25 ºC): *d*=139.1 (Cq), 138.6 (Cq), 137.0 (CH), 129.2 (CH), 128.2 (CH), 128.0 (CH), 118.7 (CH), 55.9 (CH_2), 54.2 (CH_2), 53.8 (CH_2), 53.7 (CH_2), 47.9 (CH_2), 45.6 (CH_2), 44.7 (CH_2), 31.4 (CH_2), 23.5 ppm (CH_2); MS (EI): *m/z* (%): 342.2 (4) [M^++H], 257.2 (100) [$C_{15}H_{21}N_4^+$]; HRMS: Calcd for $C_{20}H_{32}N_5$ [M^++H]: 342.2658. Found: 342.2666.

***N*-(4-((2-(pyrrolidin-1-yl)ethylamino)methyl)benzyl)-3-(4-methylpiperazin-1-yl)propan-1-amine (1{*4,9*}).** The procedure was the same as that stated for **8**{*2,4*} but using 1-(2-aminoethyl)pyrrolidine **4**{*4*} (0.39 g, 3.3 mmol), **7**{*9*} (0.91 g, 3.3 mmol) and $NaBH_4$ (0.13 g, 3.3 mmol) to give **1**{*4,9*} (0.96 g, 77%) as a yellow oil. IR (film): *v*=3288 (N-H), 2934, 2875, 2793 (C-H), 1458, 1447, 1372, 1354 cm^{-1} (C-H); ^{1}H-NMR (300 MHz, $CDCl_3$, 25 ºC, TMS): *d*=7.27 (s, 4H; Ph), 3.79 (s, 2H; C$\underline{H}_2$-Ph), 3.76 (s, 2H; C$\underline{H}_2$-Ph), 2.74 (t, ^3J (H,H)=6.5 Hz, 2H; C$\underline{H}_2$-NH), 2.67 (t, ^3J (H,H)=6.9 Hz, 2H; C$\underline{H}_2$-NH), 2.61 (t, ^3J (H,H)=6.5 Hz, 2H; CH_2-N), 2.50-2.38 (m, 14H; CH_2-N), 2.27 (s, 3H; CH_3), 2.11 (br, 2H; NH), 1.77-1.66 ppm (m, 6H; CH_2); ^{13}C-NMR (75.5 MHz, $CDCl_3$, 25 ºC): *d*=138.9 (Cq), 138.8 (Cq), 128.1 (CH), 128.0 (CH), 57.0 (CH_2), 55.9 (CH_2), 55.1 (CH_2), 54.2 (CH_2), 53.8 (CH_2), 53.7 (CH_2), 53.2 (CH_2), 48.1 (CH_2), 47.9 (CH_2), 46.0 (CH_3), 27.0 (CH_2), 23.5 ppm (CH_2); MS (EI): *m/z* (%): 374.3 (0.4) [M^++H], 84.0 (100) [$C_5H_{10}N^+$]; HRMS: Calcd for $C_{22}H_{40}N_5$ [M^++H]: 374.3284. Found: 374.3276.

***N*-(4-((2-(pyrrolidin-1-yl)ethylamino)methyl)benzyl)-3-morpholinopropan-1-amine (1{*4,11*}).** The procedure was the same as that stated for **8**{*2,4*} but using 1-(2-aminoethyl)pyrrolidine **4**{*4*} (0.37 g, 3.2 mmol), **7**{*11*} (0.84 g, 3.2 mmol) and $NaBH_4$ (0.12 g, 3.2 mmol) to give **1**{*4,11*} (1.05 g, 91%) as a yellow oil. IR (film): *v*=3305 (N-H), 2953, 2932, 2872, 2852, 2802 (C-H), 1457, 1446 (C-H), 1118, 862 cm^{-1} (C-O-C); ^{1}H-NMR (300 MHz, $CDCl_3$, 25 ºC, TMS): *d*=7.27 (s, 4H; Ph), 3.79 (s, 2H; C$\underline{H}_2$-Ph), 3.77 (s, 2H; C$\underline{H}_2$-Ph'), 3.69 (t, ^3J (H,H)=4.7 Hz, 4H; CH_2-O), 2.74 (t, ^3J (H,H)=5.9 Hz, 2H; C$\underline{H}_2$-NH), 2.68 (t, ^3J (H,H)=6.9 Hz, 2H; C$\underline{H}_2$-NH), 2.61 (t, ^3J (H,H)=5.9 Hz, 2H; CH_2-N), 2.50-2.37 (m, 10H; CH_2-N), 2.04 (br, 2H; NH), 1.80-1.68 ppm (m, 6H; CH_2); ^{13}C-NMR (75.5 MHz, $CDCl_3$, 25 ºC): *d*=139.0 (Cq), 138.7 (Cq), 128.1 (CH), 128.0 (CH), 67.0 (CH_2), 57.4

(CH_2), 55.9 (CH_2), 54.2 (CH_2), 53.8 (CH_2), 53.7 (CH_2), 48.0 (CH_2), 47.9 (CH_2), 26.7 (CH_2), 23.5 ppm (CH_2); MS (EI): *m/z* (%): 361.2 (0.5) [M^++H], 84.0 (100) [$C_5H_{10}N^+$]; HRMS: Calcd for $C_{21}H_{37}N_4O$ [M^++H]: 361.2967. Found: 361.2965.

***N*-(4-((3-(1*H*-imidazol-1-yl)propylamino)methyl)benzyl)-3-(pyrrolidin-1-yl)propan-1-amine (1{*5,6*}).** The procedure was the same as that stated for **8**{*2,4*} but using 1-(3-aminopropyl)pyrrolidine **4**{*5*} (0.49 g, 3.7 mmol), **7**{*6*} (0.91 g, 3.7 mmol) and $NaBH_4$ (0.14 g, 3.7 mmol) to give **1**{*5,6*} (1.33 g, 100%) as a yellow oil. IR (film): *v*=3281 (N-H), 3104, 2931, 2875, 2794 (C-H), 1508 (imidazol), 1458 cm^{-1} (C-H); ^{1}H-NMR (300 MHz, $CDCl_3$, 25 ºC, TMS): *d*=7.43 (s, 1H; CH-N), 7.27 (s, 4H; Ph), 7.03 (s, 1H; CH-N), 6.88 (s, 1H; CH-N), 4.04 (t, ^3J (H,H)=6.9 Hz, 2H; CH_2-N), 3.78 (s, 2H; C$\underline{H}_2$-Ph), 3.74 (s, 2H; C$\underline{H}_2$-Ph), 2.70 (t, ^3J (H,H)=6.9 Hz, 2H; C$\underline{H}_2$-NH), 2.60 (t, ^3J (H,H)=6.6 Hz, 2H; C$\underline{H}_2$-NH), 2.50 (m, 6H; CH_2-N), 2.05 (br, 2H; NH), 1.92 (quint, ^3J (H,H)=6.6 Hz, 2H; CH_2), 1.79-1.10 ppm (m, 6H; CH_2); ^{13}C-NMR (75.5 MHz, $CDCl_3$, 25 ºC): *d*=139.1 (Cq), 138.6 (Cq), 137.0 (CH), 129.2 (CH), 128.1 (CH), 128.0 (CH), 118.7 (CH), 54.7 (CH_2), 54.2 (CH_2), 53.7 (CH_2), 48.0 (CH_2), 45.6 (CH_2), 44.7 (CH_2), 31.4 (CH_2), 29.2 (CH_2), 23.4 ppm (CH_2). MS (EI): *m/z* (%): 357.4 (0.2) [M^++2H], 356.4 (1), 355.5 (0.2) [M^+], 84.2 (100) [$C_5H_{10}N^+$]; HRMS: Calcd for $C_{21}H_{33}N_5$: 355.2736. Found: 355.2740.

***N*-(4-((2-(piperidin-1-yl)ethylamino)methyl)benzyl)-3-(pyrrolidin-1-yl)propan-1-amine (1{*5,7*}).** The procedure was the same as that stated for **8**{*2,4*} but using 1-(3-aminopropyl)pyrrolidine **4**{*5*} (0.46 g, 3.5 mmol), **7**{*7*} (0.85 g, 3.5 mmol) and $NaBH_4$ (0.13 g, 3.5 mmol) to give **1**{*5,7*} (1.13 g, 92%) as a yellowish oil. IR (film): *v*=3298 (N-H), 2933, 2876, 2851, 2792 (C-H), 1454, 1443 cm^{-1} (C-H); ^{1}H-NMR (300 MHz, $CDCl_3$, 25 ºC, TMS): *d*=7.27 (s, 4H; Ph),3.78 (s, 2H; C$\underline{H}_2$-Ph), 3.77 (s, 2H; C$\underline{H}_2$-Ph), 2.69 (t, ^3J (H,H)=6.3 Hz, 4H; C$\underline{H}_2$-NH), 2.52 (m, 6H; CH_2-N), 2.44 (t, ^3J (H,H)=6.3 Hz, 2H; CH_2-N), 2.33 (br, 4H; CH_2-N), 2.08 (br, 2H; NH), 1.79-1.70 (m, 6H; CH_2), 1.55 (m, 4H; CH_2), 1.42 ppm (m, 2H; CH_2). ^{13}C-NMR (75.5 MHz, $CDCl_3$, 25 ºC): *d*=138.9 (Cq), 138.7 (Cq), 128.0 (CH), 58.5 (CH_2), 54.7 (CH_2), 54.2 (CH_2), 53.7 (CH_2), 53.6 (CH_2), 48.0 (CH_2), 45.9 (CH_2), 29.2 (CH_2), 26.0 (CH_2), 24.5 (CH_2), 23.4 ppm (CH_2); MS (EI): *m/z* (%): 359.3 (1) [M^++H], 98.2 (100) [$C_6H_{12}N^+$]; HRMS: Calcd for $C_{22}H_{39}N_4$ [M^++H]: 359.3175. Found: 359.3175.

***N*-(4-((3-(pyrrolidin-1-yl)propylamino)methyl)benzyl)-3-(2-methylpiperidin-1-yl)propan-1-amine (1{*5,8*}).** The procedure was the same as that stated for **8**{*2,4*} but using 1-(3-aminopropyl)-2-methyl-piperidine **4**{*8*} (0.63 g, 3.9 mmol), **7**{*5*} (0.96 g, 3.9 mmol) and $NaBH_4$ (0.15 g, 3.9 mmol) to give **1**{*5,8*} (1.24 g, 83%) as a yellowish oil. IR (film): *v*=3281 (N-H), 2930, 2874, 2855, 2790 (C-H), 1448, 1372 cm^{-1} (C-H); ^{1}H-NMR (300 MHz, $CDCl_3$, 25 ºC, TMS): *d*=7.27 (s, 4H; Ph), 3.77 (s, 2H; C$\underline{H}_2$-Ph), 3.76 (s, 2H; C$\underline{H}_2$-Ph), 2.86 (m, 1H; CH_{eq}-N), 2.68 (m, 5H; CH_{eq}-N, C$\underline{H}_2$-NH), 2.49 (m, 6H; CH_2-N), 2.36 (m, 1H; CH_{ax}-N), 2.26 (m, 1H; C$\underline{H}$-CH_3), 2.11 (m, 1H; CH_{ax}-N), 2.02 (br, 2H; NH), 1.79-1.58 (m, 12H; CH_2), 1.27 (m, 2H; CH_{ax}), 1.05 ppm (d, ^3J (H,H)=6.3 Hz, 3H; CH_3); ^{13}C-NMR (75.5 MHz, $CDCl_3$, 25 ºC): *d*=138.9 (Cq), 138.8 (Cq), 128.1 (CH), 128.0 (CH), 56.0 (CH), 54.8 (CH_2), 54.3 (CH_2), 53.8 (CH_2), 53.7 (CH_2), 52.3 (CH_2), 52.1 (CH_2), 48.3 (CH_2), 48.0 (CH_2), 34.7 (CH_2), 29.3 (CH_2), 26.2 (CH_2), 25.8 (CH_2), 24.0 (CH_2), 23.5 (CH_2), 19.1 ppm (CH_3); MS (EI): *m/z* (%): 387.3 (8) [M^++H]. 386.3 (6) [M^+], 112.1 (100) [$C_7H_{14}N^+$]; HRMS: Calcd for $C_{24}H_{42}N_4$: 386.3409. Found: 386.3412.

***N*-(4-((3-(4-methylpiperazin-1-yl)propylamino)methyl)benzyl)-3-(pyrrolidin-1-yl)propan-1-amine (1{*5,9*}).** The procedure was the same as that stated for **8**{*2,4*} but using 1-(3-aminopropyl)pyrrolidine **4**{*5*} (0.45 g, 3.4 mmol), **7**{*9*} (0.93 g, 3.4 mmol) and $NaBH_4$ (0.13 g, 3.4 mmol) to give **1**{*5,9*} (1.25 g, 95%) as a yellowish oil. IR (film): *v*=3284 (N-H), 2935, 2875, 2792 (C-H), 1458, 1372, 1353 cm^{-1} (C-H); ^{1}H-NMR (300 MHz, $CDCl_3$, 25 ºC, TMS): *d*=7.27 (s, 4H; Ph), 3.77 (s, 2H; C$\underline{H}_2$-Ph), 3.76 (s, 2H; C$\underline{H}_2$-Ph), 2.68 (m, 4H; C$\underline{H}_2$-NH), 2.53-2.38 (m, 16H; CH_2-N), 2.27 (s, 3H; CH_3), 1.91 (br, 2H; NH), 1.79-1.68 ppm (m, 8H; CH_2); ^{13}C-NMR (75.5 MHz, $CDCl_3$, 25 ºC): *d*=138.9 (Cq), 128.0 (CH), 56.9 (CH_2), 55.1 (CH_2), 54.7 (CH_2), 54.2 (CH_2), 53.7 (CH_2), 53.2 (CH_2), 48.1 (CH_2), 48.0 (CH_2), 46.0 (CH_3), 29.3 (CH_2), 27.0 (CH_2), 23.5 ppm (CH_2); MS (EI): *m/z* (%): 387.4 (1) [M^+], 259.2 (100) [$C_{16}H_{25}N_3^+$]; HRMS: Calcd for $C_{23}H_{41}N_5$: 387.3362. Found: 387.3347.

***N*-(4-((2-morpholinoethylamino)methyl)benzyl)-3-(pyrrolidin-1-yl)propan-1-amine (1{*5,10*}).** The procedure was the same as that stated for **8**{*2,4*} but using 2-morpholinoethylamine **4**{*10*} (0.51 g, 3.9 mmol), **7**{*5*} (0.96 g, 3.9 mmol) and $NaBH_4$ (0.15 g, 3.9 mmol) to give **1**{*5,10*} (1.27 g, 90%) as a yellowish oil. IR (film): *v*=3304 (N-H), 2935, 2872, 2852, 2800 (C-H), 1454 (C-H), 1118, 868 cm^{-1} (C-O-C); ^{1}H-NMR (300 MHz, $CDCl_3$, 25 ºC, TMS): *d*=7.28 (s, 4H; Ph), 3.79 (s, 4H; C$\underline{H}_2$-Ph), 3.69 (t, ^3J (H,H)=4.5 Hz, 4H; CH_2-O), 2.71 (m, 4H; C$\underline{H}_2$-NH), 2.51 (m, 8H; CH_2-N), 2.40 (t, ^3J (H,H)=4.5 Hz, 4H; CH_2-N), 2.18 (br, 2H; NH), 1.78 ppm (m, 6H; CH_2); ^{13}C-NMR (75.5 MHz, $CDCl_3$, 25 ºC): *d*=139.0 (Cq), 138.6 (Cq), 128.1 (CH), 67.0 (CH_2), 58.2 (CH_2), 54.8 (CH_2), 54.2 (CH_2), 53.7 (CH_2), 53.6 (CH_2), 48.0 (CH_2), 45.3 (CH_2), 28.9 (CH_2), 23.5 ppm (CH_2); MS (EI): *m/z* (%): 361.3 (3) [M^++H], 360.3 (4) [M^+], 230.3 (100) [$C_{15}H_{22}N_2^+$]; HRMS: Calcd for $C_{21}H_{36}N_4O$: 360.2889. Found: 360.2879.

***N*-(4-((3-(pyrrolidin-1-yl)propylamino)methyl)benzyl)-3-morpholinopropan-1-amine (1{*5,11*}).** The procedure was the same as that stated for **8**{*2,4*} but using 3-morpholinopropylamine **4**{*11*} (0.55 g, 3.8 mmol), **7**{*5*} (0.94 g, 3.8 mmol) and $NaBH_4$ (0.15 g, 3.8 mmol) to give **1**{*5,11*} (1.33 g, 93%) as a yellow oil. IR (film): *v*=3288 (N-H), 2935, 2872, 2853, 2802 (C-H), 1457, 1447 (C-H), 1118, 862 cm^{-1} (C-O-C); ^{1}H-NMR (300 MHz, $CDCl_3$, 25 ºC, TMS): *d*=7.27 (s, 4H; Ph), 3.78 (s, 2H; C$\underline{H}_2$-Ph), 3.77 (s, 2H; C$\underline{H}_2$-Ph), 3.69 (t, ^3J (H,H)=4.8 Hz, 4H; CH_2-O), 2.70 (m, 4H; C$\underline{H}_2$-NH), 2.51 (m, 6H; CH_2-N), 2.41 (m, 6H; CH_2-N), 2.04 (br, 2H; NH), 1.73 ppm (m, 8H; CH_2); ^{13}C-NMR (75.5 MHz, $CDCl_3$, 25 ºC): *d*=138.9 (Cq), 128.0 (CH), 67.0 (CH_2), 57.4 (CH_2), 54.8 (CH_2), 54.3 (CH_2), 53.8 (CH_2), 53.7 (CH_2), 48.1 (CH_2), 48.0 (CH_2), 29.3 (CH_2), 26.8 (CH_2), 23.5 ppm (CH_2); MS (EI): *m/z* (%): 374.3 (18) [M^++H], 373.2 (19) [M^+], 230.2 (100) [$C_{15}H_{22}N_2^+$]; HRMS: Calcd for $C_{22}H_{38}N_4O$: 388.3202. Found: 388.3202.

***N*-(4-((2-(piperidin-1-yl)ethylamino)methyl)benzyl)-3-(1*H*-imidazol-1-yl)propan-1-amine (1{*6,7*}).** The procedure was the same as that stated for **8**{*2,4*} but using 1-(2-aminoethyl)piperidine **4**{*7*} (0.48 g, 3.7 mmol), **7**{*6*} (0.90 g, 3.7 mmol) and $NaBH_4$ (0.14 g, 3.7 mmol) to give **1**{*6,7*} (1.23 g, 94%) as a yellow oil. IR (film): *v*=3279 (N-H), 2935, 2850, 2793 (C-H), 1508 (imidazol), 1446 cm^{-1} (C-H); ^{1}H-NMR (300 MHz, $CDCl_3$, 25 ºC, TMS): *d*=7.43 (s, 1H; CH-N), 7.28 (m, 4H; Ph), 7.03 (s, 1H; CH-N), 6.89 (s, 1H; CH-N), 4.04 (t, ^3J (H,H)=6.8 Hz, 2H; CH_2-N), 3.81 (s, 2H; C$\underline{H}_2$-Ph), 3.74 (s, 2H; C$\underline{H}_2$-Ph), 2.73 (t, ^3J (H,H)=5.9 Hz, 2H; C$\underline{H}_2$-NH), 2.60 (t, ^3J (H,H)=6.8 Hz, 2H; C$\underline{H}_2$-NH), 2.48 (t, ^3J (H,H)=5.9 Hz, 2H; CH_2-N), 2.46 (br, 2H; NH), 2.37 (m, 4H; CH_2-N), 1.92 (quint, ^3J (H,H)=6.8 Hz, 2H; CH_2), 1.56 (m, 4H; CH_2), 1.43 ppm (m, 2H; CH_2); ^{13}C-NMR (75.5 MHz, DMSO-d_6, 25 ºC): *d*=137.0 (Cq, CH), 128.6 (CH), 128.3 (CH), 128.1 (CH), 119.1 (CH), 55.8 (CH_2), 53.7 (CH_2), 51.8 (CH_2), 51.3 (CH_2), 44.8 (CH_2), 43.9 (CH_2), 43.7 (CH_2), 29.9 (CH_2), 25.0 (CH_2), 23.6 ppm (CH_2); MS (EI): *m/z* (%): 356.1 (0.05) [M^++H], 98.0 (100) [$C_6H_{12}^+$]; HRMS: Calcd for $C_{21}H_{34}N_5$: 356.2814. Found: 356.2809.

***N*-(4-((3-(4-methylpiperazin-1-yl)propylamino)methyl)benzyl)-3-(1*H*-imidazol-1-yl)propan-1-amine (1{*6,9*}).** The procedure was the same as that stated for **8**{*2,4*} but using 1-(3-aminopropyl)imidazole **4**{*6*} (0.35 g, 2.8 mmol), **7**{*9*} (0.76 g, 2.8 mmol) and $NaBH_4$ (0.11 g, 2.8 mmol) to give **1**{*6,9*} (0.36 g, 34%) as a yellow oil. IR (film): *v*=3278 (N-H), 3102, 2934, 2875, 2795 (C-H), 1508 (imidazol), 1458, 1372, 1356 cm^{-1} (C-H);

^{1}H-NMR (300 MHz, $CDCl_3$, 25 ºC, TMS): *d*=7.43 (s, 1H; CH-N), 7.27 (s, 4H; Ph), 7.03 (s, 1H; CH-N), 6.88 (s, 1H; CH-N), 4.04 (t, ^3J (H,H)=6.9 Hz, 2H; CH_2-N), 3.77 (s, 2H; C$\underline{H}_2$-Ph), 3.74 (s, 2H; C$\underline{H}_2$-Ph), 2.68 (t, ^3J (H,H)=7.2 Hz, 2H; C$\underline{H}_2$-NH), 2.61 (t, ^3J (H,H)=6.6 Hz, 2H; C$\underline{H}_2$-NH), 2.43 (br, 8H; CH_2-N), 2.41 (t, ^3J (H,H)=7.2 Hz, 2H; CH_2-N), 2.27 (s, 3H; CH_3), 1.93 (br, 2H; NH), 1.92 (quint, ^3J (H,H)=6.6 Hz, 2H; CH_2), 1.71 ppm (quint, ^3J (H,H)=7.2 Hz, 2H; CH_2); ^{13}C-NMR (75.5 MHz, $CDCl_3$, 25 ºC): *d*=139.0 (Cq), 138.7 (Cq), 137.1 (CH), 129.2 (CH), 128.1 (CH), 128.0 (CH), 118.7 (CH), 56.9 (CH_2), 55.1 (CH_2), 53.7 (CH_2), 53.2 (CH_2), 48.1 (CH_2), 46.0 (CH_3), 45.7 (CH_2), 44.7 (CH_2), 31.4 (CH_2), 26.9 ppm (CH_2); MS (EI): *m/z* (%): 385.3 (2) [M^++H], 70.0 (100) [$C_4H_8N^+$]; HRMS: Calcd for $C_{22}H_{36}N_6$: 384.3001. Found: 384.3004.

***N*-(4-((2-morpholinoethylamino)methyl)benzyl)-3-(1*H*-imidazol-1-yl)propan-1-amine (1{*6,10*}).** The procedure was the same as that stated for **8**{*2,4*} but using 2-morpholinoethylamine **4**{*10*} (0.43 g, 3.2 mmol), **7**{*6*} (0.79 g, 3.2 mmol) and $NaBH_4$ (0.12 g, 3.2 mmol) to give **1**{*6,10*} (1.11 g, 96%) as a yellowish oil. IR (film): *v*=3299 (N-H), 3105, 2934, 2890, 2851, 2811 (C-H), 1508 (imidazol), 1454 (C-H), 1117, 854 cm^{-1} (C-O-C); ^{1}H-NMR (300 MHz, $CDCl_3$, 25 ºC, TMS): *d*=7.43 (s, 1H; CH-N), 7.28 (s, 4H; Ph), 7.03 (s, 1H; CH-N), 6.88 (s, 1H; CH-N), 4.05 (t, ^3J (H,H)=6.9 Hz, 2H; CH_2-N), 3.79 (s, 2H; C$\underline{H}_2$-Ph), 3.74 (s, 2H; C$\underline{H}_2$-Ph), 3.69 (t, ^3J (H,H)=4.7 Hz, 4H; CH_2-O), 2.71 (t, ^3J (H,H)=6.0 Hz, 2H; C$\underline{H}_2$-NH), 2.60 (t, ^3J (H,H)=6.9 Hz, 2H; C$\underline{H}_2$-NH), 2.50 (t, ^3J (H,H)=6.0 Hz, 2H; CH_2-N), 2.41 (t, ^3J (H,H)=4.7 Hz, 4H; CH_2-N), 1.95 (br, 2H; NH), 1.93 ppm (quint, ^3J (H,H)=6.9 Hz, 2H; CH_2); ^{13}C-NMR (75.5 MHz, $CDCl_3$, 25 ºC): *d*=139.0 (Cq), 138.7 (Cq), 137.0 (CH), 129.2 (CH), 128.1 (CH), 128.0 (CH), 118.7 (CH), 67.0 (CH_2), 58.2 (CH_2), 53.7 (CH_2), 45.6 (CH_2), 45.3 (CH_2), 44.6 (CH_2), 31.2 ppm (CH_2). MS (EI): *m/z* (%): 358.2 (1) [M^++H], 100.0 (100) [$C_5H_{10}NO^+$]; HRMS: Calcd for $C_{20}H_{31}N_5O$: 357.2529. Found: 357.2517.

***N*-(4-((3-morpholinopropylamino)methyl)benzyl)-3-(1*H*-imidazol-1-yl)propan-1-amine (1{*6,11*}).** The procedure was the same as that stated for **8**{*2,4*} but using 1-(3-aminopropyl)imidazole **4**{*6*} (0.56 g, 4.4 mmol), **7**{*11*} (0.56 g, 4.4 mmol) and $NaBH_4$ (0.17 g, 4.4 mmol) to give **1**{*6,11*} (1.36 g, 85%) as a yellow oil. IR (film): *v*=3282 (N-H), 3104, 2935, 2852, 2808 (C-H), 1509 (imidazol), 1456 (C-H), 1117, 861 cm^{-1} (C-O-C); ^{1}H-NMR (300 MHz, $CDCl_3$, 25 ºC, TMS): *d*=7.42 (s, 1H; CH-N), 7.27 (m, 4H; Ph), 7.03 (s, 1H; CH-N), 6.88 (s, 1H; CH-N), 4.04 (t, ^3J (H,H)=6.9 Hz, 2H; CH_2-N), 3.79 (s, 2H; C$\underline{H}_2$-Ph), 3.74 (s, 2H; C$\underline{H}_2$-Ph), 3.69 (t, ^3J (H,H)=4.7 Hz, 4H; CH_2-O), 2.71 (t, ^3J (H,H)=6.9 Hz, 2H; C$\underline{H}_2$-NH), 2.60 (t, ^3J (H,H)=6.9 Hz, 2H; C$\underline{H}_2$-NH), 2.42 (m, 6H; CH_2-N), 1.92 (quint, ^3J (H,H)=6.9 Hz, 2H; CH_2), 1.88 (s, 2H; NH), 1.72 ppm (quint, ^3J (H,H)=6.9 Hz, 2H; CH_2); ^{13}C-NMR (75.5 MHz, $CDCl_3$, 25 ºC): *d*=138.9 (Cq), 138.2 (Cq), 137.0 (CH), 129.1 (CH), 128.2 (CH), 118.7 (CH), 66.9 (CH_2), 57.4 (CH_2), 53.7 (CH_2), 53.6 (CH_2), 53.4 (CH_2), 48.0 (CH_2), 45.5 (CH_2), 44.6 (CH_2), 31.3 (CH_2), 26.1 ppm (CH_2); MS (EI): *m/z* (%): 373.0 (2) [M^++2H], 372.0 (8) [M+H^+], 100.0 (100) [$C_5H_{10}NO^+$]; HRMS: Calcd for $C_{21}H_{34}N_5O$ [M^++H]: 372.2763. Found: 372.2758.

***N*-(4-((2-(piperidin-1-yl)ethylamino)methyl)benzyl)-3-(4-methylpiperazin-1-yl)propan-1-amine (1{*7,9*}).** The procedure was the same as that stated for **8**{*2,4*} but using 1-(2-aminoethyl)piperidine **4**{*7*} (0.34 g, 2.6 mmol), **7**{*9*} (0.73 g, 2.6 mmol) and $NaBH_4$ (0.10 g, 2.6 mmol) to give **1**{*7,9*} (0.48 g, 47%) as a yellowish oil. IR (film): *v*=3285 (N-H), 2934, 2878, 2849, 2794 (C-H), 1457, 1446, 1372, 1349 cm^{-1} (C-H); ^{1}H-NMR (300 MHz, $CDCl_3$, 25 ºC, TMS): *d*=7.27 (s, 4H; Ph), 3.78 (s, 2H; C$\underline{H}_2$-Ph), 3.77 (s, 2H; C$\underline{H}_2$-Ph), 2.69 (m, 4H; C$\underline{H}_2$-NH), 2.47-2.34 (m, 16H; CH_2-N), 2.27 (s, 3H; CH_3), 2.22 (br, 2H; NH), 1.72 (quint, ^3J (H,H)=6.9 Hz, 2H; CH_2), 1.55 (m, 4H; CH_2), 1.42 ppm (m, 2H; CH_2); ^{13}C-NMR (75.5 MHz, $CDCl_3$, 25 ºC): *d*=139.0 (Cq), 138.5 (Cq), 128.1 (CH), 128.0 (CH), 58.5 (CH_2), 57.0 (CH_2), 55.1 (CH_2), 54.7 (CH_2), 53.7 (CH_2), 53.6 (CH_2), 53.2 (CH_2), 48.1 (CH_2), 46.0 (CH_3), 45.9 (CH_2), 26.8 (CH_2), 26.0 (CH_2), 24.5 ppm (CH_2); MS (FAB): *m/z* (%) 389.2 (5) [M^++2H], 388.2 (100) [M^++H], 387.2 (17) [M^+]; HRMS: Calcd for $C_{21}H_{34}N_5O$ [M^++H]: 88.3440. Found: 388.3454.

***N*-(4-((2-(piperidin-1-yl)ethylamino)methyl)benzyl)-3-morpholinopropan-1-amine (1{*7,11*}).** The procedure was the same as that stated for **8**{*2,4*} but using 1-(2-aminoethyl)piperidine **4**{*7*} (0.44 g, 3.4 mmol), **7**{*11*} (0.89 g, 3.4 mmol) and $NaBH_4$ (0.13 g, 3.4 mmol) to give **1**{*7,11*} (1.24 g, 98%) as a yellow oil. IR (film): *v*=3304 (N-H), 2933, 2852, 2806 (C-H), 1454, 1444 (C-H), 1119, 862 cm^{-1} (C-O-C); ^{1}H-NMR (300 MHz, $CDCl_3$, 25 ºC, TMS): *d*=7.27 (s, 4H; Ph), 3.78 (s, 2H; C$\underline{H}_2$-Ph), 3.77 (s, 2H; C$\underline{H}_2$-Ph), 3.69 (t, ^3J (H,H)=4.7 Hz, 4H; CH_2-O), 2.69 (m, 4H; C$\underline{H}_2$-NH), 2.47-2-34 (m, 12H; CH_2-N), 2.11 (br, 2H; NH), 1.71 (quint, ^3J (H,H)=7.2 Hz, 2H; CH_2), 1.55 (m, 4H; CH_2), 1.42 ppm (m, 2H; CH_2); ^{13}C-NMR (75.5 MHz, $CDCl_3$, 25 ºC): *d*=139.0 (Cq), 138.6 (Cq), 128.1 (CH), 128.0 (CH), 66.9 (CH_2), 58.5 (CH_2), 57.4 (CH_2), 54.7 (CH_2), 53.8 (CH_2), 53.7 (CH_2), 48.0 (CH_2), 45.9 (CH_2), 26.6 (CH_2), 26.0 (CH_2), 24.5 ppm (CH_2); Anal. ($C_{22}H_{38}N_4O$) C, H, N; MS (EI): *m/z* (%): 373.3 (1) [M^+- H], 98.0 (100) [$C_6H_{12}N^+$].

***N*-(4-((2-morpholinoethylamino)methyl)benzyl)-3-(2-methylpiperidin-1-yl)propan-1-amine (1{*8,10*}).** The procedure was the same as that stated for **8**{*2,4*} but using 2-morpholinoethylamine **4**{*10*} (1.12 g, 8.5 mmol), **7**{*8*} (1.35 g, 8.5 mmol) and $NaBH_4$ (0.33 g, 8.5 mmol) to give **1**{*8,10*} (2.46 g, 74%) as a yellow oil. IR (film): *v*=3305 (N-H), 2930, 2853, 2807 (C-H), 1453 (C-H), 1119, 868 cm^{-1} (C-O-C); ^{1}H-NMR (300 MHz, $CDCl_3$, 25 ºC, TMS): *d*=7.27 (s, 4H; Ph), 3.79 (s, 2H; C$\underline{H}_2$-Ph), 3.77 (s, 2H; C$\underline{H}_2$-Ph), 3.69 (t, ^3J (H,H)=4.5 Hz, 4H; CH_2-O), 2.86 (m, 1H; CH_{eq}-N), 2.74 (m, 1H; CH_{eq}-N), 2.70 (t, ^3J (H,H)=6.0 Hz, 2H; C$\underline{H}_2$-NH), 2.63 (t, ^3J (H,H)=6.9 Hz, 2H; C$\underline{H}_2$-NH), 2.49 (t, ^3J (H,H)=6.0 Hz, 2H; CH_2-N), 2.40 (m, 4H; CH_2-N), 2.34 (m, 1H; CH_{ax}-N), 2.25 (m, 1H; C$\underline{H}$-CH_3), 2.11 (m, 1H; CH_{ax}-N), 1.91 (br, 2H; NH), 1.68 (quint, ^3J (H,H)=6.9 Hz, 2H; CH_2), 1.63 (m, 4H; CH_2), 1.27 (m, 2H; CH_{ax}) 1.05 ppm (d, ^3J (H,H)=6.0 Hz, 3H; CH_3); ^{3}C-NMR (75.5 MHz, $CDCl_3$, 25 ºC): *d*=139.0 (Cq), 138.9 (Cq), 128.0 (CH), 67.0 (CH_2), 58.3 (CH_2), 55.9 (CH), 53.8 (CH_2), 53.7 (CH_2), 52.3 (CH_2), 52.1 (CH_2), 48.4 (CH_2), 45.3 (CH_2), 34.7 (CH_2), 26.2 (CH_2), 25.8 (CH_2), 24.0 (CH_2), 19.2 ppm (CH_3); MS (EI): *m/z* (%): 389.3 (1) [M^++H], 100.0 (100) [$C_5H_{10}NO^+$]; HRMS: Calcd for $C_{23}H_{40}N_4O$: 374.3046. Found: 374.3049.

***N*-(4-((3-morpholinopropylamino)methyl)benzyl)-3-(2-methylpiperidin-1-yl)propan-1-amine (1{*8,11*}).** The procedure was the same as that stated for **8**{*2,4*} but using 1-(3-aminopropyl)-2-methyl-piperidine **4**{*8*} (0.62 g, 3.8 mmol), **7**{*11*} (1.00 g, 3.8 mmol) and $NaBH_4$ (0.15 g, 3.8 mmol) to give **1**{*8,11*} (1.54 g, 100%) as a yellow oil. IR (film): *v*=3286 (N-H), 2929, 2853, 2806 (C-H), 1448, 1372 (C-H), 1119, 862 cm^{-1} (C-O-C); ^{1}H-NMR (300 MHz, $CDCl_3$, 25 ºC, TMS): *d*=7.27 (s, 4H; Ph), 3.77 (s, 4H; C$\underline{H}_2$-Ph), 3.70 (t, ^3J (H,H)=4.7 Hz, 4H; CH_2-O), 2.87 (m, 1H; CH_{eq}-N), 2.79-2.62 (m, 5H; C$\underline{H}_2$-NH, CH_{eq}-N), 2.43-2.32 (m, 7H; CH_{ax}-N, CH_2-N), 2.27 (m, 1H; C$\underline{H}$-CH_3), 2.12 (br, 2H; NH), 2.11 (m, 1H; CH_{ax}-N), 1.75-1.52 (m, 8H; CH_2), 1.30 (m, 2H; CH_{ax}), 1.05 ppm (d, ^3J (H,H)=6.0 Hz, 3H; CH_3); ^{13}C-NMR (75.5 MHz, $CDCl_3$, 25 ºC): *d*=138.9 (Cq), 138.7 (Cq), 128.1 (CH), 128.0 (CH), 67.0 (CH_2), 57.4 (CH_2), 56.0 (CH), 53.8 (CH_2), 53.7 (CH_2), 52.3 (CH_2), 52.0 (CH_2), 48.3 (CH_2), 48.0 (CH_2), 34.6 (CH_2), 27.0 (CH_2), 26.1 (CH_2), 25.7 (CH_2), 23.9 (CH_2), 19.1 ppm (CH_3); MS (EI): *m/z* (%): 403.4 (0.5) [M^++H], 112.0 (100) [$C_7H_{14}N^+$]; HRMS: Calcd for $C_{24}H_{42}N_4O$: 402.3359. Found: 402.3354.

***N*-(4-((2-morpholinoethylamino)methyl)benzyl)-3-(4-methylpiperazin-1-yl)propan-1-amine (1{*9,10*}).** The procedure was the same as that stated for **8**{*2,4*} but using 1-(3-aminopropyl)-4-methylpiperazine **4**{*9*} (0.44 g, 2.7 mmol), **7**{*10*} (0.68 g, 2.7 mmol) and $NaBH_4$ (0.10 g, 2.7 mmol) to give **1**{*9,10*} (0.92 g, 86%) as a yellow oil. IR (film): *v*=3300 (N-H), 2935, 2872, 2796 (C-H), 1456, 1372, 1355 (C-H), 1118, 868 cm^{-1} (C-O-C); ^{1}H-NMR (300 MHz, $CDCl_3$, 25 ºC, TMS): *d*=7.27 (s, 4H; Ph), 3.79 (s, 2H; C$\underline{H}_2$-Ph), 3.77 (s, 2H; C$\underline{H}_2$-Ph), 3.68 (t, ^3J (H,H)=4.7 Hz, 4H; CH_2-O), 2.69 (m, 4H; C$\underline{H}_2$-NH), 2.52-2.39 (m, 16H; CH_2-N), 2.27 (s, 3H; CH_3), 2.11 (br, 2H; NH), 1.72 ppm (quint, ^3J (H,H)=6.9 Hz, 2H; CH_2); ^{13}C-NMR

(75.5 MHz, $CDCl_3$, 25 ºC): *d*=138.9 (Cq), 138.7 (Cq), 128.0 (CH), 67.0 (CH_2), 58.2 (CH_2), 57.0 (CH_2), 55.1 (CH_2), 53.7 (CH_2), 53.2 (CH_2), 48.1 (CH_2), 46.0 (CH_3), 45.3 (CH_2), 26.9 ppm (CH_2); MS (EI): *m/z* (%): 389.4 (1) [M^+], 100.1 (100) [$C_5H_{10}NO^+$]; HRMS: Calcd for $C_{22}H_{39}N_5O$: 389.3155. Found: 389.3153.

***N*-(4-((3-morpholinopropylamino)methyl)benzyl)-3-(4-methylpiperazin-1-yl)propan-1-amine (1{*9,11*}).** The procedure was the same as that stated for **8**{*2,4*} but using 1-(3-aminopropyl)-4-methylpiperazine **4**{*9*} (0.43 g, 2.7 mmol), **7**{*11*} (0.71 g, 2.7 mmol) and $NaBH_4$ (0.10 g, 2.7 mmol) to give **1**{*9,11*} (0.91 g, 84%) as a yellow oil. IR (film): *v*=3288 (N-H), 2935, 2872, 2851, 2795 (C-H), 1476, 1372, 1356 (C-H), 1118, 862 cm^{-1} (C-O-C); ^{1}H-NMR (300 MHz, $CDCl_3$, 25 ºC, TMS): *d*=7.27 (s, 4H; Ph), 3.77 (s, 4H; C$\underline{H}_2$-Ph), 3.69 (t, ^3J (H,H)=4.8 Hz, 4H; CH_2-O), 2.68 (t, ^3J (H,H)=6.9 Hz, 2H; C$\underline{H}_2$-NH), 2.67 (t, ^3J (H,H)=6.9 Hz, 2H; C$\underline{H}_2$-NH), 2.45-2.37 (m, 16H; CH_2-N), 2.27 (s, 3H; CH_3), 2.03 (br, 2H; NH), 1.71 ppm (quint, ^3J (H,H)=6.9 Hz, 4H; CH_2); ^{13}C-NMR (75.5 MHz, $CDCl_3$, 25 ºC): *d*=138.8 (Cq), 128.0 (CH), 127.9 (CH), 66.9 (CH_2), 57.3 (CH_2), 56.9 (CH_2), 55.1 (CH_2), 53.7 (CH_2), 53.2 (CH_2), 48.1 (CH_2), 47.9 (CH_2), 46.0 (CH_3), 26.9 (CH_2), 26.7 ppm (CH_2); MS (EI): *m/z* (%): 403.4 (4) [M^+], 100.1 (100) [$C_5H_{10}NO^+$]; HRMS: Calcd for $C_{23}H_{41}N_5O$: 403.3311. Found: 403.3311.

***N*-(4-((2-morpholinoethylamino)methyl)benzyl)-3-morpholinopropan-1-amine (1{*10,11*}).** The procedure was the same as that stated for **8**{*2,4*} but using 2-morpholinoethylamine **4**{*10*} (0.44 g, 3.3 mmol), **7**{*11*} (0.88 g, 3.3 mmol) and $NaBH_4$ (0.13 g, 3.3 mmol) to give **1**{*10,11*} (1.16 g, 92%) as an orange oil. IR (film): *v*=3307 (N-H), 2950, 2891, 2852, 2808 (C-H), 1455 (C-H), 1118, 863 cm^{-1} (C-O-C); ^{1}H-NMR (300 MHz, $CDCl_3$, 25 ºC, TMS): *d*=7.27 (s, 4H; Ph), 3.79 (s, 2H; C$\underline{H}_2$-Ph), 3.77 (s, 2H; C$\underline{H}_2$-Ph), 3.69 (m, 8H; CH_2-O), 2.69 (m, 4H; C$\underline{H}_2$-NH), 2.50 (t, ^3J (H,H)=6.0 Hz, 2H; CH_2-N), 2.45-2.38 (m, 10H; CH_2-N), 1.96 (br, 2H; NH), 1.71 ppm (quint, ^3J (H,H)=6.9 Hz, 2H; CH_2); ^{13}C-NMR (75.5 MHz, $CDCl_3$, 25 ºC): *d*=138.9 (Cq), 138.8 (Cq), 128.1 (CH), 128.0 (CH), 67.0 (CH_2), 58.2 (CH_2), 57.4 (CH_2), 53.8 (CH_2), 53.7 (CH_2), 48.0 (CH_2), 45.3 (CH_2), 26.7 ppm (CH_2). MS (EI): *m/z* (%): 376.2 (0.7) [M^+], 100.0 (100) [$C_5H_{10}NO^+$]; HRMS: Calcd for $C_{21}H_{36}N_4O_2$: 376.2838. Found: 376.2849.

***N*-(4-((piperidin-1-ylimino)methyl)benzyl)-3-(pyrrolidin-1-yl)propan-1-amine (8{*1,5*}).** The procedure was the same as that stated for **2**{*1,3*} but using 1-aminopiperidine **4**{*1*} (0.44 g, 4.2 mmol) and **7**{*5*} (1.04 g, 4.2 mmol) to give **8**{*1,5*} (1.17 g, 84%) as a yellow oil. IR (film): *v*=3287 (N-H), 2935, 2874, 2854, 2793 (C-H), 1591 (C=N), 1450 cm^{-1} (C-H); ^{1}H-NMR (300 MHz, $CDCl_3$, 25 ºC, TMS): *d*=7.55 (d, ^3J (H,H)=8.1 Hz, 2H; Ph), 7.54 (s, 1H; CH=N), 7.27 (d, ^3J (H,H)=8.1 Hz, 2H; Ph), 3.78 (s, 2H; C$\underline{H}_2$-Ph), 3.15 (t, ^3J (H,H)=5.7 Hz, 4H; CH_2-N), 2.28 (t, ^3J (H,H)=6.9 Hz, 2H; C$\underline{H}_2$-NH), 2.50 (m, 6H; CH_2-N), 2.03 (br, 1H; NH), 1.79-1.69 (m, 10H; CH_2), 1.55 ppm (m, 2H; CH_2); ^{13}C-NMR (75.5 MHz, $CDCl_3$, 25 ºC): *d*=139.7 (Cq), 135.3 (Cq), 134.5 (CH), 128.1 (CH), 125.9 (CH), 54.8 (CH_2), 54.2 (CH_2), 53.7 (CH_2), 52.1 (CH_2), 48.0 (CH_2), 29.1 (CH_2), 25.2 (CH_2), 24.2 (CH_2), 23.5 ppm (CH_2); MS (EI): *m/z* (%): 328.3 (0.5) [M^+], 84.1 (100) [$C_5H_{10}N^+$]; HRMS: Calcd $C_{20}H_{32}N_4$: 328.2627. Found: 328.2624.

***N*-(4-((piperidin-1-ylimino)methyl)benzyl)-3-(1*H*-imidazol-1-yl)propan-1-amine (8{*1,6*}).** The procedure was the same as that stated for **2**{*1,3*} but using 1-aminopiperidine **4**{*1*} (0.42 g, 4.0 mmol) and **7**{*6*} (0.98 g, 4.0 mmol) to give **8**{*1,6*} (1.31 g, 100%) as a reddish oil. IR (film): *v*=3282 (N-H), 3105, 2935, 2853, 2809 (C-H), 1590 (C=N), 1508 (imidazol), 1450 cm^{-1} (C-H); ^{1}H-NMR (300 MHz, $CDCl_3$, 25 ºC, TMS): *d*=7.56 (s, 1H; CH=N), 7.55 (d, ^3J (H,H)=8.1 Hz, 2H; Ph), 7.45 (s, 1H; CH-N), 7.26 (d, ^3J (H,H)=8.1 Hz, 2H; Ph), 7.03 (s, 1H; CH-N), 6.88 (s, 1H; CH-N), 4.03 (t, ^3J (H,H)=6.9 Hz, 2H; CH_2-N), 3.74 (s, 2H; C$\underline{H}_2$-Ph), 3.15 (t, ^3J (H,H)=5.7 Hz, 4H; CH_2-N), 2.60 (t, ^3J (H,H)=6.9 Hz, 2H; C$\underline{H}_2$-NH), 2.07 (br, 1H; NH), 1.92 (quint, ^3J (H,H)=6.9 Hz, 2H; CH_2), 1.75 (quint, ^3J (H,H)=5.7 Hz, 4H; CH_2), 1.54 ppm (quint, ^3J (H,H)=5.7 Hz, 2H; CH_2); ^{13}C-NMR (75.5MHz, $CDCl_3$, 25 ºC): *d*=139.5 (Cq), 137.0 (CH), 135.5 (Cq), 134.2 (CH), 129.2 (CH), 128.1 (CH), 125.9 (CH), 118.7 (CH), 53.7 (CH_2), 52.1 (CH_2), 45.6 (CH_2), 44.7 (CH_2), 31.3 (CH_2), 25.2 (CH_2), 24.2 ppm (CH_2); MS (EI): *m/z* (%): 327.2 (4) [M^++2H], 326.2 (18) [M^++H], 243.2 (100) [$C_{15}H_{21}N_3^+$]; HRMS: Calcd for $C_{19}H_{27}N_5$: 325.2266. Found: 325.2277.

***N*-(4-((piperidin-1-ylimino)methyl)benzyl)-3-(2-methylpiperidin-1-yl)propan-1-amine (8{*1,8*}).** The procedure was the same as that stated for **2**{*1,3*} but using 1-aminopiperidine **4**{*1*} (0.19 g, 1.9 mmol) and **7**{*8*} (0.51 g, 1.9 mmol) to give **8**{*1,8*} (0.67 g, 100%) as a reddish oil. IR (film): *v*=3282 (N-H), 2932, 2854, 2804 (C-H), 1591 (C=N), 1450, 1364 cm^{-1} (C-H); ^{1}H-NMR (300 MHz, $CDCl_3$, 25 ºC, TMS): *d*=7.55 (d, ^3J (H,H)=8.1 Hz, 2H; Ph), 7.54 (s, 1H; CH=N), 7.28 (d, ^3J (H,H)=8.1 Hz, 2H; Ph), 3.78 (s, 2H; C$\underline{H}_2$-Ph), 3.15 (t, ^3J (H,H)=5.4 Hz, 4H; CH_2-N), 2.87 (m, 1H; CH_{eq}-N), 2.74 (m, 1H; CH_{eq}-N), 2.65 (t, ^3J (H,H)=6.9 Hz, 2H; C$\underline{H}_2$-NH), 2.42 (br, 1H; NH), 2.37 (m, 1H; CH_{ax}-N), 2.28 (m, 1H; C$\underline{H}$-CH_3), 2.13 (m, 1H; CH_{ax}-N), 1.79-1.52 (m, 12H; CH_2), 1.29 (m, 2H; CH_{ax}), 1.05 ppm (d, ^3J (H,H)=6.3 Hz, 3H; CH_3); ^{13}C-NMR (75.5 MHz, $CDCl_3$, 25 ºC): *d*=139.5 (Cq), 135.4 (Cq), 134.4 (CH), 128.2 (CH), 125.9 (CH), 56.0 (CH), 53.7 (CH_2), 52.3 (CH_2), 52.1 (CH_2), 52.0 (CH_2), 48.3 (CH_2), 34.6 (CH_2), 26.1 (CH_2), 25.5 (CH_2), 25.3 (CH_2), 24.2 (CH_2), 23.9 (CH_2), 19.0 ppm (CH_3); MS (EI): *m/z* (%): 356.2 (2) [M^+], 112.0 (100) [$C_7H_{14}N^+$]; HRMS: Calcd for $C_{22}H_{36}N_4$: 356.2940. Found: 356.2942.

***N*-(4-((piperidin-1-ylimino)methyl)benzyl)-3-(4-methylpiperazin-1-yl)propan-1-amine (8{*1,9*}).** The procedure was the same as that stated for **2**{*1,3*} but using 1-aminopiperidine **4**{*1*} (0.36 g, 3.5 mmol) and **7**{*9*} (0.96 g, 3.5 mmol) to give **8**{*1,9*} (1.21 g, 97%) as a yellow oil. IR (film): *v*=3286 (N-H), 2935, 2875, 2853, 2794 (C-H), 1591 (C=N), 1451, 1357 cm^{-1} (C-H); ^{1}H-NMR (300 MHz, $CDCl_3$, 25 ºC, TMS): *d*=7.55 (d, ^3J (H,H)=8.1 Hz, 2H; Ph), 7.54 (s, 1H; CH=N), 7.27 (d, ^3J (H,H)=8.1 Hz, 2H; Ph), 3.77 (s, 2H; C$\underline{H}_2$-Ph), 3.15 (t, ^3J (H,H)=5.7 Hz, 4H; CH_2-N), 2.67 (t, ^3J (H,H)=6.9 Hz, 2H; C$\underline{H}_2$-NH), 2.42 (br, 8H; CH_2-N), 2.40 (t, ^3J (H,H)=6.9 Hz, 2H; CH_2-N), 2.27 (s, 3H; CH_3), 2.16 (br, 1H; NH), 1.79-1.66 (m, 6H; CH_2), 1.54 ppm (m, 2H; CH_2); ^{13}C-NMR (75.5 MHz, $CDCl_3$, 25 ºC): *d*=139.7 (Cq), 135.4 (Cq), 134.5 (CH), 128.1 (CH), 125.9 (CH), 57.0 (CH_2), 55.1 (CH_2), 53.7 (CH_2), 53.2 (CH_2), 52.1 (CH_2), 48.1 (CH_2), 46.0 (CH_3), 26.9 (CH_2), 25.3 (CH_2), 24.2 ppm (CH_2); MS (EI): *m/z* (%): 358.3 (2) [M^++H], 201.1 (100) [$C_{13}H_{17}N_2^+$]; HRMS: Calcd for $C_{21}H_{35}N_5$: 357.2892. Found: 357.2903.

***N*-(4-((piperidin-1-ylimino)methyl)benzyl)-3-morpholinopropan-1-amine (8{*1,11*}).** The procedure was the same as that stated for **2**{*1,3*} but using 1-aminopiperidine **4**{*1*} (0.37 g, 3.6 mmol) and **7**{*11*} (0.93 g, 3.6 mmol) to give **8**{*1,11*} (1.21 g, 99%) as a yellow oil. IR (film): *v*=3298 (N-H), 2936, 2853, 2807 (C-H), 1591 (C=N), 1451 (C-H), 1118, 861 cm^{-1} (C-O-C); ^{1}H-NMR (300 MHz, $CDCl_3$, 25 ºC, TMS): *d*=7.55 (d, ^3J (H,H)=8.1 Hz, 2H; Ph), 7.54 (s, 1H; CH=N), 7.27 (d, ^3J (H,H)=8.1 Hz, 2H; Ph), 3.77 (s, 2H; C$\underline{H}_2$-Ph), 3.69 (t, ^3J (H,H)=4.7 Hz, 4H; CH_2-O), 3.15 (t, ^3J (H,H)=5.6 Hz, 4H; CH_2-N), 2.67 (t, ^3J (H,H)=6.9 Hz, 2H; C$\underline{H}_2$-NH), 2.44-2.37 (m, 6H; CH_2-N), 1.99 (br, 1H; NH), 1.79-1.65 (m, 6H; CH_2), 1.54 ppm (quint, ^3J (H,H)=5.7 Hz, 2H; CH_2); ^{13}C-NMR (75.5 MHz, $CDCl_3$, 25 ºC): *d*=139.8 (Cq), 135.4 (Cq), 134.4 (CH), 128.1 (CH), 125.9 (CH), 67.0 (CH_2), 57.4 (CH_2), 53.8 (CH_2), 52.1 (CH_2), 47.9 (CH_2), 26.6 (CH_2), 25.3 (CH_2), 24.2 ppm (CH_2); MS (EI): *m/z* (%): 345.2 (2) [M^++H], 344.2 (3) [M^+], 100.0 (100) [$C_5H_{10}NO^+$]; HRMS: Calcd for $C_{20}H_{32}N_4O$: 344.2576. Found: 344.2580.

***N*-(4-((2,6-dimethylpiperidin-1-ylimino)methyl)benzyl)-3-(pyrrolidin-1-yl)propan-1-amine (8{*2,5*}).** The procedure was the same as that stated for **2**{*1,3*} but using 1-amino-2,6-dimethylpiperidine **4**{*2*} (0.58 g, 4.1 mmol) and **7**{*5*} (1.00 g, 4.1 mmol) to give **8**{*2,5*} (1.18 g, 81%) as a yellow oil. IR (film): *v*=3283 (N-H), 2961, 2931, 2872, 2794 (C-H), 1625 (C-C), 1584 (C=N), 1554 (C-C), 1449, 1369 cm^{-1} (C-H); ^{1}H-NMR (300

MHz, $CDCl_3$, 25 ºC, TMS): *d*=8.06 (s, 1H; CH=N), 7.64 (d, ^3J (H,H)=8.1 Hz, 2H; Ph), 7.33 (d, ^3J (H,H)=8.1 Hz, 2H; Ph), 3.81 (s, 2H; C$\underline{H}_2$-Ph), 3.07 (br, 2H; C$\underline{H}$-CH_3), 2.69 (t, ^3J (H,H)=6.9 Hz, 2H; C$\underline{H}_2$-NH), 2.51 (m, 6H; CH_2-N), 2.08 (br, 1H; NH), 1.79-1.69 (m, 10H; CH_2), 1.53 (m, 2H; CH_2), 1.00 ppm (d, ^3J (H,H)=6.3 Hz, 6H; CH_3); ^{13}C-NMR (75.5 MHz, $CDCl_3$, 25 ºC): *d*=152.4 (CH), 141.7 (Cq), 133.7 (Cq), 128.1 (CH), 127.3 (CH), 57.3 (CH), 54.8 (CH_2), 54.2 (CH_2), 53.7 (CH_2), 48.0 (CH_2), 32.9 (CH_2), 29.1 (CH_2), 23.5 (CH_2), 21.5 (CH_2), 20.6 ppm (CH_3); MS (EI): *m/z* (%): 356.3 (1) [M^+], 84.1 (100) [$C_5H_{10}N^+$]; HRMS: Calcd for $C_{22}H_{36}N_4$: 356.2940. Found: 356.2934.

***N*-(4-((4-methylpiperazin-1-ylimino)methyl)benzyl)-3-(pyrrolidin-1-yl)propan-1-amine (8{*3,5*}).** The procedure was the same as that stated for **2**{*1,3*} but using 1-amino-4-methylpiperazine **4**{*3*} (0.50 g, 4.2 mmol) and **7**{*5*} (1.03 g, 4.2 mmol) to give **8**{*3,5*} (1.43 g, 100%) as a brown oil. IR (film): *v*=3288 (N-H), 2937, 2876, 2794 (C-H), 1592 (C=N), 1452, 1365, 1355 cm^{-1} (C-H); ^{1}H-NMR (300 MHz, $CDCl_3$, 25 ºC, TMS): *d*=7.55 (d, ^3J (H,H)=8.1 Hz, 2H; Ph), 7.54 (s, 1H; CH=N), 7.28 (d, ^3J (H,H)=8.1 Hz, 2H; Ph), 3.78 (s, 2H; C$\underline{H}_2$-Ph), 3.21 (t, ^3J (H,H)=5.1 Hz, 4H; CH_2-N), 2.70 (t, ^3J (H,H)=6.6 Hz, 2H; C$\underline{H}_2$-NH), 2.62 (t, ^3J (H,H)=5.1Hz, 4H; CH_2-N), 2.49 (m, 6H; CH_2-N), 2.35 (s, 3H; CH_3), 2.02 (br, 1H; NH), 1.76 ppm (m, 6H; CH_2); ^{13}C-NMR (75.5 MHz, $CDCl_3$, 25 ºC): *d*=140.3 (Cq), 135.8 (CH), 134.8 (Cq), 128.1 (CH), 126.0 (CH), 54.8 (CH_2), 54.5 (CH_2), 54.3 (CH_2), 53.7 (CH_2), 51.0 (CH_2), 48.0 (CH_2), 46.0 (CH_3), 29.2 (CH_2), 23.5 ppm (CH_2); MS (EI): *m/z* (%): 343.2 (1) [M^+], 84.2 (100) [$C_5H_{10}N^+$]; HRMS: Calcd for $C_{20}H_{33}N_5$: 343.2736. Found: 343.2736.

***N*-(4-((4-methylpiperazin-1-ylimino)methyl)benzyl)-3-(1*H*-imidazol-1-yl)propan-1-amine (8{*3,6*}).** The procedure was the same as that stated for **2**{*1,3*} but using 1-amino-4-methylpiperazine **4**{*3*} (0.45 g, 3.8 mmol) and **7**{*6*} (0.92 g, 3.8 mmol) to give **8**{*3,6*} (1.23 g, 96%) as a yellow oil. IR (film): *v*=3282 (N-H), 3104, 2937, 2880, 2828, 2797 (C-H), 1592 (C=N), 1508 (imidazol), 1452, 1365, 1356 cm^{-1} (C-H); ^{1}H-NMR (300 MHz, $CDCl_3$, 25 ºC, TMS): *d*=7.56 (d, ^3J (H,H)=8.1 Hz, 2H; Ph), 7.55 (s, 1H; CH=N), 7.45 (s, 1H; CH-N), 7.27 (d, ^3J (H,H)=8.1 Hz, 2H; Ph), 7.04 (s, 1H; CH-N), 6.89 (s, 1H; CH-N), 4.04 (t, ^3J (H,H)=6.9 Hz, 2H; CH_2-N), 3.75 (s, 2H; C$\underline{H}_2$-Ph), 3.22 (t, ^3J (H,H)=5.1 Hz, 4H; CH_2-N), 2.64-2.58 (m, 6H; C$\underline{H}_2$-NH, CH_2-N), 2.36 (s, 3H; CH_3), 1.92 (quint, ^3J (H,H)=6.9 Hz, 2H; CH_2), 1.70 ppm (br, 1H; NH); ^{13}C-NMR (75.5 MHz, $CDCl_3$, 25 ºC): *d*=140.0 (Cq), 137.0 (CH), 135.6 (CH), 135.1 (Cq), 129.2 (CH), 128.1 (CH), 126.1 (CH), 118.7 (CH), 54.5 (CH_2), 53.7 (CH_2), 51.0 (CH_2), 45.9 (CH_3), 45.6 (CH_2), 44.7 (CH_2), 31.4 ppm (CH_2); MS (EI): *m/z* (%): 341.3 (2) [M^++H], 98.2 (100) [$C_5H_{11}N_2^+$]; HRMS: Calcd for $C_{19}H_{28}N_6$: 340.2375. Found: 340.2374.

***N*-(4-((4-methylpiperazin-1-ylimino)methyl)benzyl)-3-(2-methylpiperidin-1-yl)propan-1-amine (8{*3,8*}).** The procedure was the same as that stated for **2**{*1,3*} but using 1-amino-4-methylpiperazine **4**{*3*} (0.40 g, 3.4 mmol) and **7**{*8*} (0.93 g, 3.4 mmol) to give **8**{*3,8*} (1.05 g, 84%) as a red oil. IR (film): *v*=3279 (N-H), 2932, 2881, 2841, 2795 (C-H), 1593 (C=N), 1452, 1366 cm^{-1} (C-H); ^{1}H-NMR (300 MHz, $CDCl_3$, 25 ºC, TMS): *d*=7.56 (d, ^3J (H,H)=8.1 Hz, 2H; Ph), 7.55 (s, 1H; CH=N), 7.29 (d, ^3J (H,H)=8.1 Hz, 2H; Ph), 3.77 (s, 2H; C$\underline{H}_2$-Ph), 3.21 (t, ^3J (H,H)=5.1 Hz, 4H; CH_2-N), 2.87 (m, 1H; CH_{eq}-N), 2.73 (m, 1H; CH_{eq}-N), 2.65-2.60 (m, 6H; C$\underline{H}_2$-NH, CH_2-N), 2.36 (s, 3H; CH_3-N), 2.36 (m, 1H; CH_{ax}-N), 2.29 (m, 1H; C$\underline{H}$-CH_3), 2.11 (m, 1H; CH_{ax}-N), 1.95 (br, 1H; NH), 1.67 (quint, ^3J (H,H)=6.9 Hz, 2H; CH_2), 1.61-1.48 (m, 4H; CH_2), 1.27 (m, 2H; CH_{ax}), 1.04 ppm (d, ^3J (H,H)=6.0 Hz, 3H; CH-C$\underline{H}_3$); ^{13}C-NMR (75.5 MHz, $CDCl_3$, 25 ºC): *d*=140.3 (Cq), 135.8 (CH), 134.8 (Cq), 128.2 (CH), 126.1 (CH), 56.0 (CH), 54.5 (CH_2), 53.8 (CH_2), 52.3 (CH_2), 52.1 (CH_2), 51.1 (CH_2), 48.3 (CH_2), 46.0 (CH_3), 34.7 (CH_2), 26.2 (CH_2), 25.8 (CH_2), 24.0 (CH_2), 19.1 ppm (CH_3); MS (EI): *m/z* (%): 372.4 (1) [M^++H], 371.4 (2) [M^+], 112.2 (100) [$C_7H_{14}N^+$]; HRMS: Calcd for $C_{22}H_{37}N_5$: 371.3049. Found: 371.3053.

***N*-(4-((4-methylpiperazin-1-ylimino)methyl)benzyl)-3-(4-methylpiperazin-1-yl)propan-1-amine (8{*3,9*}).** The procedure was the same as that stated for **2**{*1,3*} but using 1-amino-4-methylpiperazine **4**{*3*} (0.40 g, 3.4 mmol) and **7**{*9*} (0.93 g, 3.4 mmol) to give **8**{*3,9*} (1.25 g, 99%) as a yellowish oil. IR (film): *v*=3283 (N-H), 2936, 2877, 2836, 2794, 2768 (C-H), 1593 (C=N), 1453, 1365, 1356 cm^{-1} (C-H); ^{1}H-NMR (300 MHz, $CDCl_3$, 25 ºC, TMS): *d*=7.55 (d, ^3J (H,H)=8.1 Hz, 2H; Ph), 7.55 (s, 1H; CH=N), 7.28 (d, ^3J (H,H)=8.1 Hz, 2H; Ph), 3.77 (s, 2H; C$\underline{H}_2$-Ph), 3.21 (t, ^3J (H,H)=5.1 Hz, 4H; CH_2-N), 2.66 (t, ^3J (H,H)=6.9 Hz, 2H; C$\underline{H}_2$-NH), 2.62 (t, ^3J (H,H)=5.1 Hz, 4H; CH_2-N), 2.42 (br, 8H; CH_2-N), 2.40 (t, ^3J (H,H)=6.9 Hz, 2H; CH_2-N), 2.36 (s, 3H; CH_3), 2.27 (s, 3H; CH_3), 1.82 (br, 1H; NH), 1.70 ppm (quint, ^3J (H,H)=6.9 Hz, 2H; CH_2); ^{13}C-NMR (75.5 MHz, $CDCl_3$, 25 ºC): *d*=140.2 (Cq), 135.8 (CH), 134.8 (Cq), 128.1 (CH), 126.0 (CH), 57.0 (CH_2), 55.1 (CH_2), 54.5 (CH_2), 53.7 (CH_2), 53.2 (CH_2), 51.0 (CH_2), 48.0 (CH_2), 46.0 (CH_3), 45.9 (CH_3), 26.9 ppm (CH_2); MS (EI): *m/z* (%) 373.4 (0.6) [M^++H], 372.3 (0.7) [M^+], 56.0 (100) [$C_4H_8^+$]; HRMS: Calcd for $C_{21}H_{36}N_6$: 372.3001. Found: 372.2990.

***N*-(4-((4-methylpiperazin-1-ylimino)methyl)benzyl)-3-morpholinopropan-1-amine (8{*3,11*}).** The procedure was the same as that stated for **2**{*1,3*} but using 1-amino-4-methylpiperazine **4**{*3*} (0.40 g, 3.4 mmol) and **7**{*11*} (0.89 g, 3.4 mmol) to give **8**{*3,11*} (1.22 g, 100%) as a yellow oil. IR (film): *v*=3293 (N-H), 2939, 2888, 2844, 2799 (C-H), 1592 (C=N), 1453, 1364, 1356 (C-H), 1118, 806 cm^{-1} (C-O-C); ^{1}H-NMR (300 MHz, $CDCl_3$, 25 ºC, TMS): *d*=7.56 (s, 1H; CH=N), 7.56 (d, ^3J (H,H)=8.1 Hz, 2H; Ph), 7.28 (d, ^3J (H,H)=8.1 Hz, 2H; Ph), 3.77 (s, 2H; C$\underline{H}_2$-Ph), 3.69 (t, ^3J (H,H)=4.7 Hz, 4H; CH_2-O), 3.21 (t, ^3J (H,H)=5.1 Hz, 4H; CH_2-N), 2.67 (t, ^3J (H,H)=6.9 Hz, 2H; C$\underline{H}_2$-NH), 2.62 (t, ^3J (H,H)=5.1 Hz, 4H; CH_2-N), 2.44-2.37 (m, 6H; CH_2-N), 2.35 (s, 3H; CH_3), 2.05 (br, 1H; NH), 1.70 ppm (quint, ^3J (H,H)=6.9 Hz, 2H; CH_2); ^{13}C-NMR (75.5 MHz, $CDCl_3$, 25 ºC): *d*=140.2 (Cq), 135.7 (CH), 134.9 (Cq), 128.1 (CH), 126.1 (CH), 66.9 (CH_2), 57.4 (CH_2), 54.5 (CH_2), 53.8 (CH_2), 51.0 (CH_2), 47.9 (CH_2), 45.9 (CH_3), 26.6 ppm (CH_2); MS (EI): *m/z* (%): 359.2 (2) [M^+], 100.0 (100) [$C_5H_{10}NO^+$]; HRMS: Calcd for $C_{20}H_{33}N_5O$: 359.2685. Found: 359.2685.

Conclusiones

Los avances conseguidos en el presente trabajo son:

- Se ha conseguido mejorar la caracterización estructural de los modelos de los coreceptores CXCR4 y CCR5 mediante la modelización de los *loops* según la técnica de análisis conformacional sistemático implementada en el programa Congen. Se ha confirmado el sitio de unión y el modo de unión supuesto a partir de los datos experimentales obtenidos por mutagénesis dirigida mediante *docking* convencional, *docking* ciego y dinámica molecular.
- Se ha compilado una quimioteca virtual de 248 inhibidores de CXCR4 y 424 inhibidores de CCR5 extraídos de bibliografía, y 4696 compuestos tipo fármaco supuestamente inactivos, sobre la que se han realizado los estudios de cribado virtual restrospectivos.
- Se ha demostrado que los modelos de los coreceptores construidos pueden ser utilizados en un cribado virtual *structure-based docking*, siendo capaces de enriquecer una base de datos distinguiendo, de una manera mejor a la aleatoria, *hits* virtuales más activos de menos activos independientemente de la función de *scoring* utilizada.
- Asimismo, se han aplicado técnicas de cribado virtual *ligand-based* basadas en *shape matching*, modelos farmacofóricos y búsquedas de similitud a la quimioteca compilada con el fin de distinguir compuestos activos de inactivos. La comparación de estas técnicas con las herramientas de *docking* muestra que se obtienen mejores resultados utilizando las aproximaciones *ligand-based*, concretamente *shape matching* (Parafit, Rocs, Hex), para las dianas de estudio CXCR4 y CCR5.
- Se ha diseñado una nueva aproximación *shape matching* basada en el uso de una *query* promedio de las formas esféricas harmónicas de un conjunto representativo de ligandos activos de estudio. Los resultados del cribado virtual utilizando esta aproximación superan los factores de enriquecimiento obtenidos con otras técnicas de *shape matching*.
- Se ha estudiado la hipótesis propuesta de la multi-región de unión para el coreceptor CCR5 mediante la construcción de diversas estructuras *consensus query* esféricas harmónicas. Se ha medido su utilidad en el cribado virtual de la base de datos de inhibidores de CCR5 compilada. El resultado de este estudio muestra cuatro *shape consensus clusters*, los miembros de los cuales se predice que se unen a tres subsitios solapados diferentes dentro de la cavidad de unión de CCR5.
- Con respecto al análisis prospectivo del cribado virtual, se han obtenido buenos resultados mediante las técnicas *ligand-based* utilizadas. Asimismo, los modelos farmacofóricos diseñados y la función de *scoring* de *docking* Docked Energy proporcionan la mejor correlación con los datos de actividad experimentales. Los compuestos seleccionados mediante el consenso de los filtros de cribado utilizados han rendido actividades satisfactorias.
- Se ha diseñado *de novo structure-based* una quimioteca de posibles compuestos inhibidores de CXCR4 según las características del sitio activo de dicho coreceptor.
- Se ha validado el *fingerprint* de interacción APIF diseñado en el laboratorio de diseño molecular del IQS mediante un cribado virtual *docking* frente a cinco dianas terapéuticas cristalográficas. Los resultados muestran que dicho *fingerprint* es útil como filtro en el cribado virtual *docking* y en la selección de poses/*hits* virtuales que satisfagan una interacción de referencia proteína-ligando.

Conclusions

The advances afforded in the present work are:

- The structural characterization of CXCR4 and CCR5 co-receptor models has been improved by means of systematic conformational analysis implemented in Congen. Both co-receptors models have been validated by molecular dynamics, blind docking, and conventional docking of high-affinity antagonists. The docking modes obtained with these ligands are compatible with the available SDM data on key ligand binding residues.
- A virtual combinatorial library of 248 CXCR4 and 424 CCR5 inhibitors, and 4696 presumed inactive compounds, has been compiled from the literature to perform retrospective virtual screening of antagonists against these co-receptors.
- The co-receptors models built have been used in a structure-based docking virtual screening, yielding reasonable database enrichment by distinguishing virtual hits from decoys, independently of the scoring function, better than random.
- Shape matching, similarity searches, and pharmacophore models ligand-based virtual screening tools have also been applied to the compiled library in order to distinguish active compounds from decoys. The comparison of these approaches with docking tools shows that ligand-based searches, especially shape matching (Parafit, Rocs, Hex), are superior to docking-based approaches for the CXCR4 and CCR5 targets studied.
- A novel spherical harmonic consensus shape-based approach has been developed. This study has shown that using spherical harmonic consensus shapes as queries can be a useful strategy to improve hit enrichments in shape-based virtual screening. ROC plot analyses show an improvement of virtual screening results using the new approach.
- The CCR5 multiple-binding-region hypothesis has been quantitatively explored by constructing different trial spherical harmonic consensus query structures and by measuring their virtual screening utility against our CCR5 inhibitor database. This study found four main super consensus clusters whose members are predicted to bind to three different but somewhat overlapping sites within the CCR5 pocket. Pseudomolecules corresponding to these super consensus clusters were docked into the CCR5 pocket, and the locations of these positions were related to the locations predicted by previous docking studies. Several compounds within each consensus group have experimentally supported or computationally predicted binding modes which are consistent with the locations of the super consensus clusters docked here.
- Regarding the prospective virtual screening, ligand-based approaches used give good results. Also, pharmacophore models and Autodock Docked Energy scoring function give the best correlation with experimental activity data. Molecules found at the first positions of the consensus ranked hit list showed satisfactory activity values.
- A library of possible CXCR4 inhibitors has been de novo structure-based designed according to the CXCR4 binding site features.
- The new interaction fingeprint APIF, developed in the molecular design laboratory in IQS, has been validated by docking virtual screening of estrogen receptor-alpha, trypsin, rhinovirus, HIV protease, and carboxypeptidase experimentally determined X-ray crystal structures. Results obtained show that APIF has proven to be suitable for ranking and filtering docking virtual screening results and selecting virtual poses/hits satisfying a defined ligand-protein interaction reference.

Referencias

1. Drews, J. Drug Discovery: A Historical Perspective. *Science* **2000**, *287*, 1960-1964.
2. Glick, M.; Robinson, D. D.; Grant, G. H.; Graham, R. W. Identification of Ligand Binding Sites on Protein Using a Multi-Scale Approach. *J. Am. Chem. Soc.* **2002**, *124*, 2337-2344.
3. Langer, T.; Wolber, G. Virtual combinatorial chemistry and in silico screening: Efficient tools for lead structure discovery? *Pure Appl. Chem.* **2004**, *76*, 991–996.
4. Muegge, I.; Rarey, M. Small Molecule Docking and Scoring. En *Reviews in Computational Chemistry*; Lipkowitz, K. B.; Boyd, D. B., Ed.; Wiley and Sons: New York, **2001**; Vol 17, pp 1-60.
5. Terfloth, L. *Drug Design*. En *Chemoinformatics*; Gasteiger, J.; Engels, T., Ed.; Wiley-VCH: Weinheim, **2003**. pp 597-618.
6. Keller, T. H.; Pichota, A.; Yin, Z. A practical view of 'druggability'. *Curr. Opin. Chem. Biol.* **2006**, *10*, 357-361.
7. Sperandio, O.; Miteva, M. A.; Delfaud, F.; Villoutreix, B. O. Receptor-Based Computational Screening of Compound Databases: The Main Docking-Scoring Engines. *Curr. Prot. Peptide Sci.* **2006**, *7*, 1-25.
8. Lipinski, C. A.; Lombardo, F.; Dominy, B.W.; Feeny, P. J. Experimental and computacional approaches to estimate solubility and permeability in drug discovery and development settings. *Adv. Drug Deliv. Rev.* **1997**, *23*, 3-25.
9. Oprea, T. I. Property distribution of drug-related chemical databases. *J. Comput. Aided Mol. Des.* **2000**, *14*, 251-264.
10. Muegge, I.; Heald, S. L.; Brittelli, D. Simple selection criteria properties for drug-like chemical matter. *J. Med. Chem.* **2001**, *44*, 1841–1846.
11. Walters, W.; Murcko, M. A. Prediction of 'drug-likeness'. *Adv. Drug Deliv. Rev.* **2002**, *54*, 255-271.
12. Ajay, W.; Walters, P.; Murcko, M. A. Can we learn to distinguish between 'drug-like' and 'non drug-like' molecules. *J. Med. Chem.* **1998**, *41*, 3314–3324.
13. Sadowski, J.; Kubinyi, H. A scoring scheme for discriminating between drugs and nondrugs. *J. Med. Chem.* **1998**, *41*, 3325–3329.
14. Gillet, V. J.; Willett, P.; Bradshaw, J. Identification of Biological Activity Profiles Using Substructural Analysis and Genetic algorithms. *J. Chem. Inf. Comput. Sci.* **1998**, *38*, 165-179.
15. Oprea, T. I.; Matter, H. Integrating virtual screening in lead discovery. *Curr. Opin. Chem. Biol.* **2004**, *8*, 349-358.
16. Johnson, M. A.; Maggiora, G. M. En *Concepts and Application of Molecular Similarity*. Ed.; Wiley: New York, **1990**.
17. Martin, Y. C.; Kofron J. L.; Traphagen L. M. Do structurally similar molecules have similar biological activity?. *J. Med. Chem.* **2002**, *45*, 4350-4358.
18. Martin, Y. C. Diverse viewpoints on computational aspects of molecular diversity. *J. Comb. Chem.* **2001**, *3*, 231-50.
19. Willet, P. Chemical Similarity Searching. *J. Chem. Inf. Comput. Sci.* **1998**, *38*, 983-996.
20. Downs, G. M.; Willett, P. Similarity Searching in Databases of Chemical Structures. En *Reviews in Computational Chemistry*, Lipkowitz, K. B.; Boyd, D. B., Ed.; Wiley and Sons: New York, **1995**; Vol 7, pp 1-66.

21. Todeschini, R.; Consonni, V. *Handbook of Molecular Descriptors*; Ed.; Wiley-VCH: Weinheim, **2000**.

22. Brown, R. D.; Martin, Y. C. Use of Structure-Activity Data To Compare Structure-Based Clustering Methods and Descriptors for Use in Compound Selection. *J. Chem. Inf. Comput. Sci.* **1996**, *36*, 572-584.

23. Patterson, D. E.; Cramer, R. D.; Ferguson, A. M.; Clark, R. D.; Weinberger, L. E. Neighborhood behavior: a useful concept for validation of "molecular diversity" descriptors. *J. Med. Chem.* **1996**, *39*, 3049-3059.

24. Gund, P. En *Pharmacophore Perception, Development, and Use in Drug Design*; Güner, O. F., Ed.; International University Line: La Jolla, **2000**, Chapter 1, pp 3-11.

25. Kuntz, I. D. Structure-based strategies for drug design and discovery. *Science* **1992**, *257*, 1078–1082.

26. Hetényi, C.; Van der Spoel, D. Efficient docking of peptides to proteins without prior knowledge of the binding site. *Prot. Sci.* **2002**, *11*, 11729-1737.

27. Fradera, X.; Mestres, J. Guided Docking Approaches to Structure-Based Design and Screening. *Curr. Top. Med. Chem.* **2004**, *4*, 687-700.

28. Lewis, R. M.; Leach, A. R. Current Methods for Site-Direted Structure Generation. *J. Comput. Aid. Mol. Des.* **1994**, *8*, 467-475.

29. Gasteiger, J.; Ihlenfeldt, W. D.; Fick, R.; Rose, J. R. Similarity Concepts for the Planning of Organic Reactions and Synthesis. *J. Chem. Inf. Comput. Sci.* **1994**, *15*, 793-813.

30. Pascual, R. Tesis Doctoral, Universitat Ramon Llull (Barcelona, Spain),**2003**.

31. Pascual, R.; Borrell, J.I.; Teixido, J. Analysis of selection methodologies for combinatorial library design. *Molecular Diversity* **2003**, *6*, 121-133.

32. Pascual, R.; Mateu, M.; Gasteiger, J.; Borrell, J.I.; Teixido, J. Design and Analysis of a Combinatorial Library of HEPT: Comparison of Selection Methodologies and Inspection of the Actually Covered Chemical Space. *J. Chem. Inf. Comput. Sci.* **2003**, *43*, 199-207.

33. Esté, J. A.; Cabrera, C.; De Clercq, E.; Struyf, S.; Van Damme, J.; Bridger, G.; Skerlj, R. T.; Abrams, M. J.; Henson, G.; Gutierrez, A.; Clotet, B.; Schols; D. Activity of Different Bicyclam Derivatives against Human Immunodeficiency Virus Depends on Their Interaction with the CXCR4 Chemokine Receptor. *Mol. Pharmacol.* **1999**, *55*, 67-73.

34. Teixidó, J.; Borrell, J. I.; Nonell, S.; Pettersson, S.; Ros, L; Puig de la Bellacasa, R.; Rabal, M. O.; Pérez-Nueno, V. I.; Esté, J.; Clotet-Codina, I.; Armand-Ugón, M. ES Patent ES200602764, **2006** (filing date: October 26, 2006).

35. Rabal, M. O. Tesis Doctoral, Universitat Ramon Llull (Barcelona, Spain),**2006**.

36. Rabal, M. O.; Schneider, G.; Borrell, J. I.; Teixidó, J. Structure-Based Virtual Screening of FGFR Inhibitors. Cross-Decoys and Induced-Fit Effect. *Biodrugs* **2007**, *21*, 31-45.

37. Rabal, O.; Gardiner, E.; Gillet, V.; Comparison of Alignment Methods: FieldAlign and ROCS. Presented at the Fourth Joint Sheffield Conference on Chemoinformatics [Online], Sheffield, UK, 18th-20th June 2007. University of Sheffiled, The Octagon Centre. Web site http://cisrg.shef.ac.uk/shef2007/conference.htm (accessed Dec 12, 2008).

38. UNAIDS. AIDS epidemic update: December **2007**. En línea (2/12/08). Accesible a través de http://www.unaids.org/en/KnowledgeCentre/HIVData/EpiUpdate/EpiUpdArchive/2007/default.asp

39. Laurence, J. Sida y sistema inmunitario. *Investigación y ciencia* **1986**, *113*, 44-54.

40. Mathews, C. K.; Van Holde, K. E. Bioquímica. Ed. Mc Graw Hill. 2ª edición. Madrid, **2001**. Pág. 275 -276.

41. Dagleish, A. G.; Beverley, P. C.; Clapham, P. R. The CD4 (T4) antigen is a essential component of the receptor of the AIDS retrovirus. *Nature* **1984**, *312*, 763-767.

42. Gallo, R. C. El virus del SIDA. *Investigación y ciencia* **1987**, *126*, 31-4.

43. Garg, R.; Gupta, S. P.; Gao, H.; Babu, M. S.; Debnath, A. K.; Hansch, C. Comparative Quantitative Structure-Activity Relationship Studies on Anti-HIV Drugs. *Chem. Rev.* **1999**, *99*, 3525-3601.

44. Pardo, F. VIH y SIDA. Revisión **1998**. En línea (2/12/08). Accesible a través de http://www.ctv.es/USERS/fpardo/virus.htm

45. Shaheen, F.; Collman, R. G. Co-receptor antagonist as HIV-1 entry inhibitors. *Curr. Opin. Infect. Dis.* **2004**, *17*, 7-16.

46. Daar, E.; Ling Li, X.; Moudgil, T.; Ho, D. D. High concentrations of recombinant soluble CD4 are required to neutralize primary human immunodeficiency virus type 1 isolates. *Proc. Natl. Acad. Sci. USA* **1990**, *87*, 6574-6578.

47. Jacobson, J. M.; Lowy, I.; Fletcher, C. V.; *et al.* Single-dose safety, pharmacology, and antiviral activity of the human immunodeficiency virus (HIV) type 1 entry inhibitor PRO 542 in HIV-infected adults. *J. Infect. Dis.* **2000**, *182*, 326-329.

48. Vaidehi, N.; Floriano, W. B.; Trabanino, R.; May, E. S.; Freddolino, P.; Choi, E. J.; Zamanakos, G.; Goddard, W. A. Prediction of structure and function of G protein coupled receptors. *PNAS* **2002**, *99*, 12622-12627.

49. Bissantz, C. Tesis Doctoral, University of Freiburg (Alemania), **2002**.

50. Klabunde, T.; Hessler, G. Drug design strategies for targeting G-protein-coupled receptors. *Chembiochem* **2002**, *3*, 928-944.

51. Kenakin, T. Nuevas dianas farmacológicas. *Investigación y ciencia* **2005**, *351*, 15-21.

52. Evers, A.; Klabunde, T. Structure-based Drug Discovery Using GPCR Homology Modeling: Successful Virtual Screening for Antagonists of the Alpha1A Adregenic Receptor. *J. Med. Chem.* **2005**, *48*, 1088-1097.

53. Woodmac PharmaView2001. En línea (2/12/08). Accesible a través de http://www.woodmacresearch.com/phview

54. Trabanino, R. J.; May, E. S.; Vaidehi, N.; Floriano, B. W.; Kam, T. V.; Goddard, W. A. First principles predictions of the structure and function of G-Protein-Coupled Receptors: validation for bovine rhodopsine. *Biophys. J.* **2004**, *86*, 1904-1921.

55. Palczewski, K; Kumasa, T.; Hori, T.; Behnke, C. A.; Motoshima, H.; Fox, B. A.; Le Trong, I.; Teller, D. C.; Okada, T.; Stenkamp, R. E.; Yamamoto, M; Miyano, M. Crystal Structure of Rhodopsin: A G Protein-Coupled Receptor. *Science* **2000**, *289*, 739-745.

56. Teller, D. C.; Okada, T.;Behnke, C. A.; Palczewski, K.; Stenkamp, R. E. Advances in determination of a high-resolution three-dimensional structure of rhodopsin, a model of G-protein-coupled receptors (GPCRs). *Biochemistry* **2001**, *40*, 7761-7772.

57. Rasmussen, S.G.; Choi, H.J.; Rosenbaum, D.M.; Kobilka, T.S.; Thian, F.S.; Edwards, P.C.; Burghammer, M.; Ratnala, V.R.; Sanishvili, R.; Fischetti, R.F.; Schertler, G.F.; Weis, W.I.; Kobilka, B.K. Crystal structure of the human 2 adrenergic G-protein-coupled receptor. *Nature* **2007**,*450*, 383-387.

58. Cherezov, V.; Rosenbaum, D.M.; Hanson, M.A.; Rasmussen, S.G.; Thian, F.S.; Kobilka, T.S.; Choi, H.J.; Kuhn, P.; Weis, W.I.; Kobilka, B.K.; Stevens, R.C. High-Resolution Crystal Structure of an Engineered Human {beta}2-Adrenergic G Protein Coupled Receptor. *Science* **2007**, *318*, 1258-1265.

59. Strader, C. D.; Fong, T. M.; Tota, M. R.; Underwood, D.; Dixon, R. A. F. Structure and function of G protein-coupled receptors. *Annu. Rev. Biochem* **1994**, *63*, 101-132.

60. Shacham, S.; Topf, M.; Avisar, N.; Glaser, F.; Marantz, Y.; Bar-Haim, S.; Norman, S.; Naor, Z.; Becker, O. M. Modeling the 3D structure of GPCRs from sequence. *Med. Res. Rev.* **2001**, *21*, 472-483.

61. Bissantz,C.; Logean, A.; Rognan, D. High-Throughput Modeling of Human G-Protein Coupled Receptors: Amino Acid Sequence Alignement, Three-Dimensional Model Building, and Receptor Library Screening. *J. Chem. Inf. Comput. Sci* **2004**, *44*, 1162-1176.

62. Fredriksson, R.; Lagerstrom, M. C.; Lundin, L. G.; Schioth, H. B. The G-Protein-Coupled Receptors in the Human Genome Form Five Main Families. Phylogenetic Analysis, Paralogon Groups, and Fingerprints. *Mol. Pharmacol.* **2003**, *63*, 1256-1272.

63. Wise, A.; Gearing, K.; Rees, S. Target Validation of G-Protein Coupled Receptors. *Drug Discovery Today* **2002**, *7*, 235-246.

64. Bleul, C. C.; Farzan M.; Choe, H.; Parolin, C.; Clarck-Lewis, I.; Sodroski, J.; Springer, T. A. The lymphocyte chemoattractant SDF-1 is a ligand for LESTR/fusin and blocks HIV-1 entry. *Nature* **1996**, *382*, 829-833.

65. Número de acceso y entrada del coreceptor CXCR4 en SWISS-PROT. En línea (3/12/08). Accesible a través de http://us.expasy.org/uniprot/P61073

66. Zhou, N.; Zhaowen, L.; Jiansong, L.; Dongxiang, H.; James, W.; Pomerantz, R. J. Structural and functional caracterization of human CXCR4 as a chemokine receptor and HIV-1 co-receptor by mutagenesis and molecular modeling studies. *J. Biol. Chem.* **2001**, *276*, 42826-42833.

67. Número de acceso y entrada del coreceptor CCR5 en SWISS-PROT. En línea (3/12/08). Accesible a través de http://us.expasy.org/uniprot/P51681

68. Scohols, D. HIV Co-receptors as Targets for Antiviral Therapy. *Curr. Topics Med. Chem.* **2004**, *4*, 883-893.

69. Pierson, T. C.; Doms, R. W.; Pöhlmann, S. Prospects of HIV-1 entry inhibitors as novel therapeutics. *Rev. Med. Virol.* **2004**, *14*, 255-270.

70. Alkhatib, G.; Combadieri C.; Broder C. C. CC-CKR5: A RANTE, MIP-1α, MIP-1β receptor as fusion cofactor for macrophage-tropic HIV-1. *Science* **1996**, *272*, 1955-1958.

71. Pontow, S.; Ratner, L. Evidence for common structural determinants of human immunodeficiency virus type 1 coreceptor activity proceeded through functional analysis of CCR5/CXCR4 chimeric coreceptors. *J. Virol.* **2001**, *75*, 11503-11514.

72. Berson, J.F.; Long, D.; Doranz, B.J.; Rucker, J.; Jirik, F.R.; Doms, R.W. A seven-transmembrane domain receptor involved in fusion and entry of T-cell-tropic human immunodeficiency virus type 1 strains. *J Virol.* **1996**, *70*, 6288-6295.

73. De Clercq, E. Novel compounds in preclinical/early clinical development for the treatment of HIV infections. *Rev. Med. Virol.* **2000**, *10*, 255-277.

74. De Clercq, E. Emerging anti-HIV drugs. *Expert Opin. Emerg. Drugs* **2005**, *10*, 241-274.

75. De Clercq, E. New antiviral agents in preclinical or clinical development. *Adv. Antivir. Drug Des.* **2004**, *4*, 1-62.

76. De Clercq, E. New Anti-HIV Agents and Targets. *Med. Res. Rev.* **2002**, *22*, 531-565.

77. U.S. Food and Drug Administration. Drugs Used in the Treatment of HIV Infection. Update January **2008**. En línea (3/12/08). Accesible a través de http://www.fda.gov/oashi/aids/virals.html

78. Nelson, M. R. AIDS 2008: Update on Antiretroviral Therapy: Resistance Issues and Investigational Agents (Mexico City, Mexico) **2008**, "AIDS 2008: Investigational Antiretroviral Drugs". En línea (3/12/08). Accesible a través de http://www.medscape.com/viewarticle/582064

79. Brenner, B.G.; Turner, D.; Wainberg, M.A. HIV-1 drug resistance: can we overcome? *Expert Opin. Biol. Ther.* **2002**, *2*, 751–61.

80. De Clercq, E. Anti-HIV chemotherapy: current state of the art. *Med. Chem. Res.* **2004**, *13*, 439-478.

81. Bean, P. New Drugs Targets for HIV. *Clin. Infect. Dis.* **2005**, *41*, 96-100.

82. Kazmierski, W. M.; Peckman, J. P.; Duan, M; Kenakin, T. P.; Jenkinson, S.; Gudmundsson, K. S.; Piscitelli, S. C.; Feldman, P. L. Recent Progress in the Discovery of New CCR5 and CXCR4 Chemokine Receptor Antagonists as Inhibitors of HIV-1 Entry. Part 2. *Curr. Med. Chem. Anti-Infect. Agents* **2005**, *4*, 133-152.

83. Markovic, I.; Clouse, K.A. Recent advances in understanding the molecular mechanisms of HIV-1 entry and fusion: revisiting current targets and considering new options for therapeutic intervention. *Curr. HIV Res.* **2004**, *2*, 223-34.

84. Kaleab, A.; Ameha, S.; Ciddi, V.; Franz, B.; Simon, G. Naturally Derived Anti-HIV Agents. *Phytother. Res.* **2005**, *19*, 557-581.

85. Tauzin, B. Informe 2007. Medicamentos en desarrollo para VIH/SIDA. Presentado por las compañías farmacéuticas americanas. En línea (3/12/08). Accesible a través de http://www.phrma.org/files/meds_in_dev/AIDS2007SP.pdf

86. ClinicalTrials.gov. United States National Library of Medicine National Institutes of Health, Health & Human Services. En línea (3/12/08). Accesible a través de http://clinicaltrials.gov/

87. Pierson, T.C.; Doms, R.W. HIV-1 entry inhibitors: new targets, novel therapies. *Immunol. Lett.* **2003**, *85*, 113-118.

88. Kazmiersky W.; Bifulco N.; Yang H.; Boone, L.; DeAnda, F.; Watson, C.; Kenakin, T. Recent progress in discovery of small-molecule CCR5 chemokine receptor ligands as HIV-1 inhibitors. *Bioorg. Med. Chem.* **2003**, *11*, 2663-2676.

89. Kilby, J.M.; Eron, J.J. Novel therapies based on mechanisms of HIV-1 cell entry. *N. Engl. J. Med.* **2003**, *348*, 2228-2238.

90. Starr-Spirres, L. D.; Collman, R. G. HIV-1 entry and entry inhibitors as therapeutic agents. *Clin. Lab. Med.* **2002**, *22*, 681-701.

91. Tamamura, H.; Hori, A.; Kanzaki, N.; Hiramatsu, K.; Mizumoto, M.; Nakashima, H.; Yamamoto, N.; Otaka, A.; Fujii, N. T140 analogs as CXCR4 antagonists identified as anti-metastatic agents in the treatment of breast cancer. *FEBS Lett.* **2003**, *550*, 79-83.

92. Yang, Y. F.; Mukai, T.; Gao, P.; Yamaguchi, N.; Ono, S.; Iwaki, H.; Obika, S.; Imanishi, T.; Tsujimura, T.; Hamaoka, T.; Fujiwara, H. A non-peptide CCR5 antagonist inhibits collagen-induced artritis by modulating T cell migration without affecting anti-collagen T cell responses. *Eur. J. Immunol.* **2002**, *32*, 2124-2132.

93. Zou, Y. R.; Kottmann, A. H.; Kuroda, M.; Taniuchi, I.; Littman, D. R. Function of the chemokine receptor CXCR4 in haematopoiesis and in cerebellar development. *Nature* **1998**, *393*, 595-599.

94. Tachibana, K.; Hirota, S.; Lizasa, H.; Yoshida, H.; Kawabata, K.; Kataoka, Y.; Kitamura, Y.; Matsushima, K.; Yoshida, N.; Nishikawa, S.; Kishimoto, T.; Nagasawa, T. The chemokine receptor CXCR4 is essential for vascularization of the gastrointestinal tract. *Nature* **1998**, *393*, 591-594.

95. Campbell, D. J.; Kim, C. H.; Butcher, E. C. Chemokines in the systemic organization of immunity. *Immunol. Rev.* **2003**, *195*, 58-71.

96. De Clercq, E. Inhibition of HIV Infection by Bicyclams, Highly Potent and Specific CXCR4 Antagonists. *Mol. Pharmacol.* **2000**, *57*, 833-839.

97. Egberink, H. E.; De Clercq, E.; Van Vliet, A. L. W.; Balzarini, J.; Bridger, G. J.; Henson, G.; Horzinek, M. C.; Schols, D. Bicyclams, Selective Antagonists of the Human Chemokine Receptor CXCR4, Potently Inhibit Feline Immunodeficiency Virus Replication. *J. Virol.* **1999**, *73*, 6346-6352.

98. Hatse, S.; Princen, K.; De Clercq, E.; Rosenkilde, M. M.; Schwartzb, T. W.; Hernandez-Abad, P. E.; Skerlj, R. T.; Bridger, G. J.; Schols, D. AMD3465, a monomacrocyclic CXCR4 antagonist and potent HIV entry inhibitor. *Biochem. Pharmacol.* **2005**, *70*, 752-761.

99. Princen, K.; Hatse, S.; Vermeire, K.; Aquaro, S.; De Clercq, E.; Gerlach, L.-O.; Rosenkilde, M.; Schwartz, T. W.; Skerlj, R.; Bridger, G.; Schols, D. Inhibition of Human Immunodeficiency Virus Replication by a Dual CCR5/CXCR4 Antagonist. *J. Virol.* **2004**, *78*, 12996-13006.

100. Bridger, G. J.; Skerlj, R. T.; Padmanabhan, S.; Martellucci, S. A.; Henson, G. W.; Struyf, S.; Witvrouw, M.; Schols, D.; De Clercq, E. Synthesis and Structure-Activity Relationships of Phenylenebis(methylene)-Linked Bis-azamacrocycles That Inhibit HIV-1 and HIV-2 Replication by Antagonism of the Chemokine Receptor CXCR4. *J. Med. Chem.* **1999**, *42*, 3971-3981.

101. Bridger, G.; Skerlj R.; Kaller A.; Harwing C.; Bogucki D.; Wilson T. R.; Crawford J.; McEachern E. J.; Atsma B.; Nan S.; Zhou Y.; WO 0022600, **2002**.

102. Bridger, G.; Skerlj R.; Kaller A.; Harwing C.; Bogucki D.; Wilson T. R.; Crawford J.; McEachern E. J.; Atsma B.; Nan S.; Zhou Y.; WO 0022599, **2002**.

103. Bridger, G.; Skerlj R.; Kaller A.; Harwing C.; Bogucki D.; Wilson T. R.; Crawford J.; McEachern E. J.; Atsma B.; Nan S.; Zhou Y.; WO 00234745, **2002**.

104. Bridger, G.; Skerlj R.; Kaller A.; Harwing C.; Bogucki D.; Wilson T. R.; Crawford J.; McEachern E. J.; Atsma B.; Nan S.; Zhou Y.; WO 055876, **2003**.

105. Bridger, G.; Skerlj R.; Kaller A.; Harwing C.; Bogucki D.; Wilson T. R.; Crawford J.; McEachern E. J.; Atsma B.; Nan S.; Zhou Y.; Smith C. D.; Di Fluir R. M. US 0019058, **2004**.

106. Ichiyama, K.; Yokohama-Kumakura S.; Tanaka Y.; Tanaka R.; Hirose K.; Bannai K.; Edamatsu T.; Yanaka M.; Niitani Y.; Miyako-Kurosaki N.; Takaku H.; Koyanagi Y.; Yamamoto N. A duodenally absorbable CXC chemokine receptor 4 antagonist, KRH-1636, exhibits a potent and selective anti-HIV-1 activity. *Proc. Natl. Acad. Sci. USA* **2003**, *100*, 4185-4190.

107. Murakami, T.; Yoshida, A.; Tanaka, R.; Mitsuhashi, S.; Hirose, K.; Yanaka, M.; Yamamato, N.; Tanaka, Y.; 11th Conference on Retroviruses and Opportunistic Infections 2 February 8-11, **2004**. San Francisco, CA, Abstract #541.

108. Yamazaki, T.; Saitou, A.; Ono, M.; Yokohama, S.; Bannai, K.; Hiroswe, K.; Yanaka, M.; WO 029218, **2003**.

109. Yamazaki, T.; Kikumoto, S.; Ono, M.; Saitou, A.; Takahashi, H.; Kumakura, S.; Hirose, K.; WO 024697, **2004**.

110. Tamamura, H.; Ojida, A.; Ogawa, T.; Tsutsumi, H.; Masuno, H.; Nakashima, H.; Yamamoto, N.; Hamachi, I.; Fujii, N. Identification of a new class of low molecular weight antagonists against the chemokine receptor CXCR4 having the dipicolylamine-zinc(II) complex structure. *J. Med. Chem.* **2006**, *49*, 3412-3415.

111. Masuda, M.; Nakashima, H.; Murakami, T.; Koyanaki, Y.; Matsumoto, A.; Fujii, N.; Yamamoto, N.; Anti-human immunodeficiency virus activity of a novel synthetic peptide, T22([Tyr-5,12,Lys7]-polyphemusin II): a posible inhibitor of virus cell fusion. *Antimicrob. Agents Chemother.* **1992**, *36*, 1249-1255.

112. Masuda, M.; Nakashima, H.; Ueda, T.; Naba, H.; Ikoma, R.; Otaka, A.; Terakawa, Y.; Tamamura, H.; Ibuka, T.; Murakami, T. A novel anti-HIV synthetic peptide T-22 ([Tyr5, 12, Lys7]-polyphemusin II. *Biochem. Biophys. Res. Comm.* **1992**, *189*, 845-850.

113. Arakaki, R.; Tamamura, H.; Premanathan, M.; Kanbara, K.; Remanan, S.; Mochizuki, K.; Baba, M.; Fujii, N.; Nakashima, H. T134, a small molecule CXCR4 inhibitor, has no cross-drug resistance with AMD3100, a CXCR4 antagonist with a different structure. *J. Virol.* **1999**, *73*, 1719-1723.

114. Tamamura, H.; Omagari, A.; Hiramatsu, K.; Gotoh, K.; Kamamoto, T.; Xu, Y.; Kodama, E.; Matsuoka, M.; Hattori, T.; Yamamoto, N.; Nakashima, H.; Otaka, A.; Fujii, N. Development of

specific CXCR4 inhibitors possessing high selectivity indexes as well as complete stability in serum based on an anti-HIV peptide T140. *Bioorg. Med. Chem. Lett.* **2001**, *11*, 1897-1902.

115. Tamamura, H.; Araki, T.; Ueda, S.; Wang, Z.; Oishi, S.; Esaka, A.; Trent, J.O.; Nakashima, H.; Yamamoto, N.; Peiper, S.C.; Otaka, A.; Fujii, N. Identification of novel low molecular weight CXCR4 antagonists by structural tuning of cyclic tetrapeptide scaffolds. *J. Med. Chem.* **2005**, *48*, 3280-3289

116. Summer-Smith, M.; Zheng, Y.; Zhang, Y. P.; Twist, F. M.; Climie, S. C. Antiherpetic activities of N-α-acetyl-nona-D-arginine amide acetate. *Drugs Exp. Clin. Res.* **1995**, *21*, 1-6.

117. Hamy, F.; Fólder, E. R.; Eximan, G.; Lazdins, J.; Aboul-Ela, F.; Varani, G.; Karn, J.; Klimkait, T. An inhibitor of the Tat/TAR RNA interaction that effectively supresses HIV-1 replication. *Proc. Natl. Acad. Sci. USA* **1997**, *94*, 3548-3553.

118. Doranz, B.J.; Grovit-Ferbas, K.; Sharron, M.P.; Mao, S.H.; Goetz, M.B.; Daar, E.S.; Doms, R.W.; O'Brien, W.A. A small-molecule inhibitor directed against the chemokine receptor CXCR4 prevents its use as and HIV-1 coreceptor. *J. Exp. Med.* **1997**, *186*, 1395–1400.

119. Doranz, B.J.; Filion, L.G.; Diaz-Mitoma, F. *et al.* Safe use of the CXCR4 inhibitor ALX40-4C in humans. *AIDS Res. Hum. Retroviruses* **2001**, *17*, 475-486.

120. Daelemans, D.; Schols, D.; Witvrouw, M.; Pannecouque, C.; Hatse, S.; Van Dooren, S.; Ois Hamy, F.; Klimkait, T.; De Clercq, E.; Vandamme, A-M. A Second Target for the Peptoid Tat/Transactivation Response Element Inhibitor CGP64222: Inhibition of Human Immunodeficiency Virus Replication by Blocking CXCChemokine Receptor 4-Mediated Virus Entry. *Mol. Pharmacol.* **2000**, *57*, 116-124.

121. Kledal, T.N.; Rosenkilde, M.M.; Coulin, F. *et al.* A broad-spectrum chemokine antagonist encoded by Kaposi's sarcoma-associated herpesvirus. *Science* **1997**, *277*, 1656-1659.

122. Zhou, N.; Luo, Z.; Luo, J.; Fan, X.; Cayabyab, M.; Hiraoka, M.; Liu, D.; Han, X.; Pesavento, J.; Dong, C.-Z.; Wang, Y.; An, J.; Kaji, H.; Sodroski, J. G.; Huang, Z. Exploring the stereochemistry of CXCR4-peptide recognition and inhibiting HIV-1 entry with D-peptides derived from chemokines. *J. Biol. Chem.* **2002**, *277*, 17476-17485.

123. Kazmierski, W. M.; Aquino, C. J.; Bifulco, N.; Boros, E. E.; Chauder, B. A.; Chong, P. Y.; Duan, M.; Deanada, F. Jr.; Koble, C. S.; Malean, E. W.; Peckham, J. P.; Perkins, A. C.; Thompson, J. B.; Vanderwall, D. WO 2004054974, **2004**.

124. Duan, M., Kazmierski, W. M.; Aquino, C. J.; WO 200405481, **2004**.

125. Peckham, J. P.; Aquino, C. J.; Kazmierski, W. M. WO2004055010, **2004**.

126. Aquino, C. J.; Chong, P. Y.; Duan, M.; Kazmierski, W. M.; WO 2004055011, **2004**.

127. Youngman, M.; Kazmierski, W. M.; Yang, H.; Aquino, C. J.; WO 2004055012, **2004**.

128. Yang, H.; Kazmierski, W. M.; Aquino, C. J.; WO 2004055016, **2004**.

129. Maeda, K.; Yoshimura, K.; Shibayama, S.; Habashita, H.; Tada, H.; Sagawa, K.; Mikayawa, T.; Auki, M.; Fukushima, D.; Mitsuya, H. Novel low molecular weight spirodiketopiperazine derivatives potently inhibit R5 HIV-1 infection through their antagonistic effects on CCR5. *J. Biol. Chem*. **2001**, *276*, 35194-35200.

130. Shibayama, S.; Sagawa, K.; Watanabe, N.; Takeda, K.; Tada, H.; Fukushima, D. WO 2004054616, **2004**.

131. Takaoka, Y.; Okamoto, M.; Genba, Y. WO 2004026874, **2004**.

132. Takaoka, Y.; Nishizawa, R.; Shibayama, S.; Sagawa, K.; Matsuo, M. Y. WO 2002074770, **2002**.

133. Imawaka, H.; Shibayama, S.; Takaoka, Y.; WO 2003035074, **2003**.

134. Palani, A.; Shapiro, S.; CLADES, J. W.; Greenlee, W. J.; Blythin, D.; Cox, K.; Wagner, N. E.; Strizki, J.; Baroudy, B. M.; Dan N. Biological Evaluation and Interconversion Studies of

Rotamers of SCH 351125, an Orally Bioavailable CCR5 Antagonist. *Bioorg. Med. Chem. Lett.* **2003**, *13*, 705-708.

135. Tsamis, F.; Gavrilov, S.; Kajumo, F.; Seibert, C.; Kuhmann, S.; Ketas, T.; Trkola, A.; Palani, A.; Clader, J. W.; Tagat, J. R.; McCombie, S.; Baroudy, B.; Moore, J. P.; Sakmar, T. P.; Dragic, T. Analysis of the Mechanism by Which the Small-Molecule CCR5 Antagonists SCH- 351125 and SCH-350581 Inhibit Human Immunodeficiency Virus Type 1 Entry. *J. Virol.* **2003**, *77*, 5201-5208.

136. Billick, E.; Seibert, C.; Pugach, P.; Ketas, T.; Trkola, A.; Endres, M. J.; Murgolo, N. J.; Coates, E.; Reyes, G. R.; Baroudy, B. M.; Sakmar, T. P.; Moore, J. P.; Kuhmann, S. E. The Differential Sensitivity of Human and Rhesus Macaque CCR5 to Small-Molecule Inhibitors of Human Immunodeficiency Virus Type 1 Entry Is Explained by a Single Amino Acid Difference and Suggests a Mechanism of Action for These Inhibitors. *J. Virol.* **2004**, *78*, 4134-4144.

137. Aramaki, Y.; Seto, M.; Okawa, T.; Oda, T.; Kanzaki, N.; Shiraishi, M. Synthesis of 1-benzothiepine and 1-benzazepine derivatives as orally active CCR5 antagonists. *Chem. Pharm. Bull.* **2004**, *52*, 254-258.

138. Seto, M.; Aramaki, Y.; Okawa.; T.; Miyamoto, N.; Aikawa, K.; Kanzaki, N.; Shiraishi, M. Orally Active CCR5 Antagonists as Anti-HIV-1 Agents: Synthesis and Biological Activity of 1-Benzothiepine 1,1-Dioxide and 1-Benzazepine Derivatives Containing a Tertiary Amine Moiety *Chem. Pharm. Bull.* **2004**, *52*, 577-590.

139. Imamura, S.; Ishihara, Y.; Hattori, T.; Kurasawa, O.; Matsushita, Y.; Sugihara, Y.; Kanzaki, N.; Lizawa, Y.; Baba, M.; Hashiguchi, S. CCR5 antagonists as anti-HIV-1 agents. 1. Synthesis and biological evaluation of 5-oxopyrrolidine-3-carboxamide derivatives. *Chem. Pharm. Bull.* **2004**, *52*, 63-73.

140. Imamura, S.; Kurasawa, O.; Nara, Y.; Ichikawa, T.; Nishikawa, Y.; Iida, T.; Hashiguchi, S.; Kanzaki, N.; Lizawa, Y.; Baba, M.; Sugihara, Y. CCR5 antagonists as anti-HIV-1 agents. Part 2: Synthesis and biological evaluation of *N*-[3-(4-benzylpiperidin-1-yl)propyl]-*N,N'*- diphenylureas *Bioorg. Med. Chem.* **2004**, *12*, 2295-2306.

141. Willouhby, C. W.; Rosauer, K. G.; Hale, J. J.; Budhu, R. J.; Mills, S. G.; Chapman, K. T.; MacCoss, M.; Malkowitz, L.; Springer, M. S.; Gould, S. L.; DeMartino, J. A.; Siciliano, S. J.; Cascieri, M. A.; Carella, A.; Catver, G.; Colmes, K.; Schlief, W. A.; Danzeisen, R.; Hazuda, D.; Kessler, J.; Lineberger, J.; Miller, M.; Emini, E. A. 1,3,4 Trisubstituted Pyrrolidine CCR5 Receptor Antagonists Bearing 4-Aminoheterocycle Substituted Piperidine Side Chains. *Bioorg. Med. Chem. Lett.* **2003**, *13*, 427-431.

142. Rusconi S., Scozzafava A., Mastrolorenzo A., Supuran T. C. New Advances in HIV Entry Inhibitors Development. *Curr. Drug Targets Infect. Disord.* **2004**, *4*, 339-355.

143. Perros, M.; Price, D. A.; Stammen, B. L. C.; Wood, A. WO 2003084954, **2003**.

144. Basford, P. A.; Stephenson, P. T.; Taylor, S. C. J.; Wood, A. WO 2003084954, **2003**.

145. Armour, D. R.; Price, D. A.; Stammen, B. L. C.; Wood, A.; Perros, M.; Edwards, M. P. WO 2000038680, **2000**.

146. Cumming, J.; Winter, J. WO 2004018425, **2004**.

147. Burrows, J.; Cumming, J. WO 2002076, **2002**.

148. Cumming, J. WO 2003042178, **2003**.

149. Cumming, J. WO 2003080574, **2003**.

150. Cumming, J.; Tucker, H.; WO 2003042177, **2003**.

151. Wei, R. G.; Arnaiz, D. O.; Chou, Y.-L.; Davey, D.; Dunning, L.; Lee, W.; Lu, S.-F.; Onuffer, J.; Ye, B.; Phillips, G. CCR5 receptor antagonists: Discovery and SAR study of guanylhydrazone derivatives. *Bioorg. Med. Chem. Lett.* **2007**, *17*, 231–234.

152. Lu, S.-F.; Chen, B.; Davey, D.; Dunning, L.; Jaroch, S.; May, K.; Onuffer, J.; Phillips, G.; Subramanyam, B.; Tseng, J.-L.; Wei, R. G.; Wei, M.; Ye, B. CCR5 receptor antagonists: Discovery and SAR of novel 4-hydroxypiperidine derivatives. *Bioorg. Med. Chem. Lett.* **2007**, *17*, 1883–1887.

153. Corner, E. G.; Ketas, T. J.; Sullivan, B. M.; Nagashima, K. A.; Huang, W.; Moore, J. P.; Petropoulos, C. J.; Maddon, P. J.; Olson, W. C. Baseline viral susceptibility to the CCR5 co-receptor inhibitor PRO 140. In: The 2nd IAS Conference on HIV Patogenesis and Treatment. Abstract No. 530, Paris, France, July 13-16, **2003**.

154. Pastore, C.; Picchio, G. R.; Galimi, F.; Fish, R.; Hartley, O.; Offord, R. E.; Mosier, D. E. Two mechanisms for human immunodeficiency virus type 1 inhibition by N-terminal modifications of RANTES. *Antimicrob. Agents Chemother.* **2003**, *47*, 509-517.

155. Paliard, X.; Lee, A. Y.; Fraud, N.; Low, D.; Song, D.; Turpin, J.; Kung, A. H. Performance-enhaced synthetic nonakine is a highly potent inhibitor of HIV-1 infection. In: The 2nd IAS Conference on HIV Patogenesis and Treatment. Abstract No. 530, Paris, France, July 13-16, **2003**.

156. Kumar, S.; Kwei, G.Y.; Poon, G.K.; Iliff, S. A.; Wang, Y.; Chen, Q.; Franklin, R.B.; Didolkar, V.; Wang, R.; Yamazaki, M.; Chiu, S-H. L.; Lin, J.H.; Pearson, P.G.; Baillie, T.A. Pharmacokinetics and Interactions of a Novel Antagonist of Chemokine Receptor 5 (CCR5) with Ritonavir in Rats and Monkeys: Role of CYP3A and P-Glicoprotein. *J. Pharmacol. Exp. Ther.* **2003**, *304*, 1161-1171.

157. Debnath, A. K. Generation of predictive pharmacophore models for CCR5 antagonists: Study with piperidine- and piperazine-based compounds as a new class of HIV-1 entry inhibitors. *J. Med. Chem.* **2003**, *46*, 4501–4515.

158. Schröder, C.; Pierson, R.N.; Nguyen, B.N.; Kawka, D.W.; Peterson, L.B.; Wu, G.; Zhang, T.; Springer, M.S.; Siciliano, S.J.; Iliff, S.; Ayala, J.M.; Lu, M.; Mudgett, J.S.; Lyons, K.; Mills, S.G.; Miller, G.G.; Singer, I.I.; Azimzadeh, A.M.; DeMartino, J.A. CCR5 blockade modulates inflammation and alloimmunity in primates. *J. Immunol.* **2007**, *179*, 2289-2299.

159. Pulley, S. R. CCR5 antagonists: from discovery to clinical efficacy. Para: *Progress in Inflamatoion Research*. Chemokine Biology-Basic Research and Clinical Application. Volume II: Pathophysiology of Chemokines. Editado por Kuldeep Neote, Gordon L. Letts and Bernhard Moser; Ed. Birkhäuser Basel,, Switzerland, **2007**. Pág. 145 -163.

160. Donzella, G. A.; Schols, D.; Lin, S. W.; Este, J. A.; Nagashima, K. A.; Maddon, P. J.; Allaway, G. P.; Sakmar, T. P.; Henson, G.; De Clercq, E.; Moore, J. P. AMD3100, a small molecule inhibitor of HIV-1 entry via the CXCR4 co-receptor. *Nat. Med.* **1998**, *4*, 72-77.

161. De Clercq, E.; Yamamoto, N.; Pauwels, R.; Baba, M.; Schols, D.; Nakashima, H.; Balzarini, J.; Debyser, Z.; Murrer, B. A.; Schwartz, D. Potent and selective inhibition of human immunodeficiency virus (HIV)-1 and HIV-2 replication by a class of bicyclams interacting with a viral uncoating event. *Proc. Natl. Acad. Sci. USA* **199**2, *89*, 5286-5290.

162. Zhang, W. B.; Navenot, J. M.; Haribabu, B.; Tamamura, H.; Hiramatu, K.; Omagari, A.; Pei, G.; Manfredi, J. P.; Fujii, N.; Broach, J. R.; Peiper, S. C. A. Point Mutation That Confers Constitutive Activity to CXCR4 Reveals That T140 Is an Inverse Agonist and That AMD3100 and ALX40-4C Are Weak Partial Agonists. *J. Biol. Chem.* **2002**, *277*, 24515-24521.

163. Brelot, A.; Heveker, N.; Montes, M.; Alizon, M. Identification of Residues of CXCR4 Critical for Human Immunodeficiency Virus Coreceptor and Chemokine Receptor Activities. *J. Biol. Chem.* **2000**, *275*, 23736-23744.

164. Hatse, S.; Princen, K.; Gerlach, L. O.; Bridger, G.; Henson, G.; Clercq, E.; Schwartz T. W.; Schols, D. Mutation of Asp171 and Asp262 of the chemokine receptor CXCR4 impairs its coreceptor function for human immunodeficiency virus-1 entry and abrogates the antagonistic activity of AMD3100. *Mol. Pharmacol.* **2001**, *60*, 164-173.

165. Hatse, S.; Princen, K.; Vermeire, K.; Gerlach, L.-O.; Rosenkilde, M. M.; Schwartz, T. W.; Bridger, G.; De Clercq, E.; Schols, D. Mutations at the CXCR4 interaction sites for AMD3100 influence anti-CXCR4 antibody binding and HIV-1 entry. *FEBS Lett.* **2003**, *546*, 300-306.

166. Ho, S. N.; Hunt, H. D.; Horton, R. M.; Pullen, J. K.; Pease, L. R. Site-directed mutagenesis by overlap extension using polymerase chain reaction. *Gene* **1989**, *77*, 51-59.

167. Gerlach, L.O.; Jakobsen, J.S.; Jensen, K.P.;Rosenkilde, M.R.;Skerlj, R. T.; Ryde, U.; Bridger, G.J.; Schwartz, T.W. Metal Ion Enhaced Binding of AMD3100 to Asp262 in the CXCR4 Receptor. *Biochemistry* **2003**, *42*, 710-717.

168. Gerlach, L. O.; Skerlj, R. T.; Bridger, G. J.; Schwartz, T. W. Molecular Interaction of Cyclam and Bicyclam Non-peptide Antagonists with the CXCR4 Chemokine Receptor. *J. Biol. Chem.* **2001**, *276*, 14154-14160.

169. Liang, X.; Parkinson, J. A.; Weishaüpl, M.; Gould, R. O.; Paisey, S. J.; Park, H.; Hunter, T. M.; Blindauer, C. A.; Parsons, S.; Sadler, P. J. Structure and Dynamics of Metallomacrocycles: Recognition of Zinc Xylyl-Bicyclam by an HIV Coreceptor. *J. Am. Chem. Soc.* **2002**, *124*, 9105-9112.

170. Trent, J. O.; Wang, Z. X.; Murray, J. L.; Shao, W.; Tamamura, H.; Fujii, N.; Peiper, S. C. Lipid Bilayer Simulations of CXCR4 with Inverse Agonist and Weak Partial Agonist. *J. Biol. Chem.* **2003**, *278*, 47136-47144.

171. Rosenkilde, M. M.; Gerlach, L. O.; Jacobsen, J. S.; Skerlj, R. T.; Bridger, G. J.; Schwartz, T. W. Molecular Mechanism of AMD3100 Antagonism in the CXCR4 Receptor. *J. Biol. Chem.* **2004**, *279*, 3033- 3041.

172. Dragic, T.; Trkola, A.; Thompson, D. A.; Cormier, E. G.; Kajumo, F. A.; Maxwell, E.; Lin, S. W.; Ying, W.; Smith, S. O.; Sakmar, T. P.; Moore, J. P. A binding pocket for a small molecule inhibitor of HIV-1 entry within the transmembrane helices of CCR5. *Proc. Natl. Acad. Sci., U.S.A.* **2000**, *97*, 5639-5644.

173. Seibert, C.; Ying, W.; Gavrilov, S.; Tsamis, F.; Kuhmann, S. E.; Palani, A.; Tagat, J. R.; Clader, J. W.; McCombie, S. W.; Baroudy, B. M.; Smith, S. O.; Dragic, T.; Moore, J. P.; Sakmar, T. P.; Interaction of small molecule inhibitors of HIV-1 entry with CCR5. *J. Virol.* **2006**, *349*, 41-54.

174. Paterlini, M. G. Structure Modeling of the Chemokine Receptor CCR5: Implications for Ligand Binding and Selectivity. *Biophys. J.* **2002**, *83*, 3012-3031.

175. Zhou, N.; Luo, Z.; Hall, J. W.; Luo, J.; Han, X.; Huang, Z.; Molecular modeling and site-directed mutagenesis of CCR5 reveal residues critical for chemokine binding and signal transduction. *Eur. J. Immunol.* **2000**, *30*, 164-173.

176. Baba, M.; Nishimura, O.; Kanzaki, N.; Okamoto, M.; Sawada, H.; Iizawa, Y.; Shiraishi, M.; Aramaki, Y.; Okonogi, K.; Ogawa, Y.; Meguro, K.; Fujino, M. A small-molecule, nonpeptide CCR5 antagonist with highly potent and selective anti-HIV-1 activity. *Proc. Natl. Acad. Sci., U.S.A.* **1999**, *96*, 5698-5703.

177. Fano, A.; Ritchie, D. W.; Carrieri, A. Modelling the structural basis of human CCR5 chemokine receptor function: from homology model-building and molecular dynamics validation to agonist and antagonist docking. *J. Chem. Inf. Model.* **2006**, *46*, 1223-1235.

178. Liang, M.; Mallari, C.; Rosser, M.; Ng, H. P.; May, K.; Monahan, S.; Bauman, J. G.;Islam, I.;Ghannam, A.;Buckman, B.; Shaw, K.; Wei, G. P.;Xu, W.; Zhao, Z.; Ho, E.; Shen, J.; Oanh, H.; Subramanyam, B.; Vergona, R.; Taub, D.; Dunning, L.; Harvey, S.; Snider, R. M.; Hesselgesser, J.; Morrissey, M. M.; Perez, H. D. Identification and characterization of a potent, selective, and orally active antagonist of the CC chemokine receptor-1. *J. Biol. Chem.* **2000**, *275*, 19000-19008.

179. Mirzadegan, T.; Diehl, F.; Ebi, B.; Bhakta, S.; Polsky, I.; McCarley, D.; Mulkins, M.; Weatherhead, G. S.; Lapierre, J. M.; Dankwardt, J.; Morgans, D.; Wilhelm, R.; Jarnagin, K. Identification of the binding site for a novel class of CCR2b chemokine receptor antagonists:

binding to a common chemokine receptor motif within the helical bundle. *J. Biol. Chem.* **2000**, *275*, 25562-25571.

180. Naya, A.; Sagara, Y.; Ohwaki, K.; Saeki, T.; Ichikawa, D.; Iwasawa, Y.; Noguchi, K.; Ohtake, N. Design, synthesis, and discovery of a novel CCR1 antagonist. *J. Med. Chem.* **2001**, *44*, 1429–1435.

181. Sabroe, I.; Peck, M. J.; Van Keulen, B. J.; Jorritsma, A.; Simmons, G.; Clapham, P. R.; Williams Pease, J. E. A small molecule antagonist of chemokine receptors CCR1 and CCR3. Potent inhibition of eosinophil function and CCR3-mediated HIV-1 entry. *J. Biol. Chem.* **2000**, 275, 25985–25992.

182. Kellenberger, E.; Springael, J.-Y.; Parmentier, M.; Hachet-Haas, M.; Galzi, J.-L.; Rognan, D. Identification of nonpeptide CCR5 receptor agonists by structure-based virtual screening. *J. Med. Chem.* **2007**, *50*, 1294–1303.

183. Wang, T.; Duan, Y. Binding modes of CCR5-targeting HIV entry inhibitors: Partial and full antagonists. *J. Mol. Graphics Modell.* **2008**, *26*, 1287–1295.

184. Castonguay, L. A.; Weng, Y.; Adolfsen, W.; Di Salvo, J.; Kilburn, R.; Caldwell, C. G.; Daugherty, B. L.; Finke, P. E.; Hale, J. J.; Lynch, C. L.; Mills, S. G.; MacCoss, M.; Springer, M. S.; DeMartino, J. A. Binding of 2-aryl-4-(piperidin-1-yl)butanamines and 1,3,4-trisubstituted pyrrolidines to human CCR5: A molecular modeling guided mutagenesis study of the binding pocket. *Biochemistry* **2003**, *42*, 1544–1550.

185. Maeda, K.; Das, D.; Ogata-Aoki, H.; Nakata, H.; Miyakawa, T.; Tojo, Y.; Norman, R.; Takaoka, Y.; Ding, J.; Arnold, G. F.; Arnold, E.; Mitsuya, H. Structural and Molecular Interactions of CCR5 Inhibitors with CCR5. *J. Biol. Chem.* **2006**, *281*, 12688–12698.

186. Nishikawa, M.; Takashima, K.; Nishi, T.; Furuta, R. A.; Kanzaki, N.; Yamamoto, Y.; Fujisawa, J.-I. Analysis of binding sites for the new small-molecule CCR5 antagonist TAK-220 on human CCR5. *Antimicrob. Agents Chemother.* **2005**, *49*, 4708–4715.

187. Ballesteros, J. A.; Weinstein, H. Integrated methods for the construction of three dimenisonal models and computational probing of structure-function relations in G-protein coupled receptors. Methods. *Neurosci*. **1994**, *25*, 366-428.

188. Hermans, J.; Berendsen, H. J.; Van Gunsteren, W. F.; Postma, J. P. A Consistent Empirical Potential for Water-Protein Interactions. *Biopolimers* **1984**, *23*, 1.

189. Allinger, N. L. Conformational Analysis. 130. MM2. A Hydrocarbon Force Field Utilizing V1and V2 Torsional Terms. *J. Am. Chem. Soc.* **1977**, *89*, 8127-8134.

190. Allinger, N. L.; Yuh, Y. H.; Lii, J. H. Molecular Mechanics. The MM3 Force Field for Hydrocarbons. *J. Am. Chem. Soc.* **1989**, *111*, 8551-8566.

191. Allinger, N. L.; Chen, K.; Lii, J. H. An Improved Force Field (MM4) for Saturated Hydroarbons. *J. Comput. Chem.* **1996**, *17*, 642-668.

192. Clark, M.; Cramer, R. D.; Van Opdenhosch, N. Validation of the General Purpose Tripose 5.2 Force Field. *J. Comput. Chem.* **1989**, *10*, 982-1012.

193. Halgren, T. A. Merck Molecular Force Field. I. Basis, Form, Scope, Parametrization, and Performance of MMFF94. *J. Comput. Chem.* **1996**, *17*, 490-519.

194. Cornell, W. D.; Cieplak, P.; Bayly, C., I; Gould, I. R.; Merz, K. M.; Ferguson, J.; Spellmeyer, D. C.; Fox, T.; Caldwell, J. W.; Kollman, P. A. A second generation force field for the simulation of proteins, nucleic acids and organic molecules. *J. Am. Chem. Soc.* **1995**, *117*, 5179- 5197.

195. Brooks, B. R.; Bruccoleri, R. E.; Olafson, B. D.; States, D. J.; Swaminathan, S.; Karplus, M. CHARMM: A program for macromolecular energy, minimization and dynamics calculations. *J. Comput. Chem.* **1983**, *4*, 187-217.

196. Hermans, J.; Berendsen, H. J.; Van Gunsteren, W. F.; Postma, J. P. A Consistent Empirical Potential for Water-Protein Interactions. *Biopolymers* **198**4, *23*, 1513-1518.

197. Damm, W.; Frontera, A.; Tirado-Rives, J.; Jorgensen, W. L. OPLS All-Atom Force Field for Carbohydrates. *J. Comput. Chem.* **1997**, *18*, 1955-1970.

198. MacKerell, A. D. Jr. Empirical Force Fields for Biological Macromolecules: Overview and Issues. *J. Comput. Chem.* **2004**, *25*, 1584-1604.

199. Krieger, E.; Nabuurs, S. B.; Vriend, G. Homology modelling. *Structural Bioinformatics* **2003**. Edited by Philip E. Bourne and Helge Weissig ISBN 0-471-20199-5 Copyright 2003 by Wiley-Liss, Inc.

200. Fiser, A.; Sali, A. Modeling of loops in protein structures. *Protein Science* **2000**, *9*, 1753-1773.

201. Sanchez, R.; Sali, A. Advances in comparative protein-structure modelling. *Current Opinion in Structural Biology* **1997**, *7*, 206-214.

202. Jones, D. T. A Practical Guide to Protein Structure Prediction. Para: *Methods in Molecular Biology*, 143. Protein Structure Prediction: Methods and Protocols. Editado por Webster, D.; Ed. Humana Press Inc.,Totowa, NJ **2000**. Pág. 131 -154.

203. Berstein, F. C.; Koetzle, T. F.; Williams, G. J.; Meyer, E.; Brice, M. D.; Rodgers, J. R.; Kennard, O.; Shimanouchi, T.; Tasumi, M. The protein data bank: a computer based archival file for macromolecular structures. *J. Mol. Biol.* **1977**, *112*, 535-542. En línea (3/12/08). Accesible a través de internet: http://www.rcsb.org/pdb/Welcome.do

204. Abola, E. E.; Bernstein, F. C.; Bryant, S. H.; Koetzle, T.; Weng, J. Protein data bank, in *Crystallographic Databases – Information, Content, Software Systems, Scientific Applications*, **1987** (Allen, F. H.; Bergerhoff, G.; Sievers R.; eds.), Data Comission of the International Union Crystallography, Cambridge, pp.107-132.

205. Blundell, T. L.; Sibanda, B. L.; Sternberg, M. J. E.; Thornton, J. M. Knowledge-based prediction of protein structures and the design of novel molecules. *Nature* **1987**, *326*, 347-352.

206. Levitt, M. Accurate modeling of protein conformation by automatic segment matching. *J. Mol. Biol.* **1992**, *226*, 507-533.

207. Sali, A.; Blundell, T. L. Comparative protein modelling by satisfaction of spatial restrains. *J. Mol. Biol.* **1993**, *234*, 779-815.

208. Pincus, M.; Klausner R. D.; Scheraga H. A.; Calculation of the three-dimensional structure of the membrane-bound portion of melittin from its amino acid sequence. *Proc. Natl. Acad. Sci. USA* **1982**, *79*, 5107-5100.

209. Bajorath, J.; Stenkamp, R.; Aruffo, A. Knowledge-based model building of proteins: concepts and examples. *Protein Sci.* **1993**, *2*, 1798-1810.

210. Collura, V.; Higo, J.; Garnier, J. Modeling of loops by simulated annealing. *Protein Sci.* **1993**, *2*, 502-1510.

211. Li, H.; Tejero, R.; Monleon, D.; Bassolino-Klimas, D.; Abate-Shen, C.; Bruccolieri, R. E.; Montelione, G. T. Homology modeling using simulated annealing of restrained molecular dynamics and conformational search with CONGEN: aplication in predicting the three-dimensional structure of murine homeodomain Msx-1. *Protein Sci.* **1997**, *6*, 956-970.

212. Bruccoleri, R. E. Application of Systematic Conformational Search to Protein Modeling. *Mol. Simul.* **1993**, *10*, 151-174.

213. Lüthy, R.; Bowie, J. U.; Eisenberg, D. Assessment of protein models with three-dimensional profiles. *Nature* **1992**, *356*, 83-85.

214. Sippl, M. J. Recognition of Errors in Three-Dimensional Structures of Proteins. *Proteins* **1993**, *17*, 355-362. El programa PROSAII es gratuito a través de la dirección http://www.came.sbg.ac.at/typo3/index.php?id=prosa En línea (10/12/08)

215. Laskowski, R. A.; McArthur, M. W.; Moss, D. S.; and Thornton, J. M.; PROCHECK: a program to check the stereochemical quality of protein structures. *J. Appl. Cryst* **1993**, *26*, 283-291. El

programa PROCHECK es gratuito a través de la dirección http://www.biochem.ucl.ac.uk/~roman/procheck/procheck.html En línea (10/12/08)

216. Hooft, R.; Vriend, G.; Sander, C.; Abola, E. Errors in protein structures. *Nature* **1996**, *381*, 272. El programa WHATCHECK es gratuito a través de la dirección http://swift.cmbi.kun.nl/swift/whatcheck/ En línea (10/12/08)

217. Allen, F. H.; Bellard, S.; Brice, M. D.; Cartwright, B. A.; Doubleday, A.; Higgs, H.; Hummelink, T.; Hummelink-Peters, B. G.; Kennard, O.; Motherwell, W. D. S.; Rodgers, J. R.; Watson, D. G. The Cambridge Crystallographic Data Centre: computer-based search, retrieval, analysis and display of information. *Acta Cryst.* **1979**, *B35*, 2331-2339.

218. Bernstein, F. C., Koetzle, T. F., Williams, G. J., Meyer, E. F. J., Brice, M. D., Rodgers, J. R., Kennard, O., Shimanouchi, T. and Tasumi, M. The Protein Data Bank: a computer-based archival file for macromolecular structures. *J. Mol. Biol.* **1977**, *112*, 535-542.

219. Miller, M.; Wales, D. Energy landscape of a model protein. *J. Chem. Phys.* **1999**, *111*, 6610-6616.

220. Levitt, M. A simplified representation of protein conformations for a rapid simulation of protein folding. *J. Mol. Biol.* **1976**, *104*, 59-107.

221. Verlet, L. Computer Experiments on Classical Fluids. I. Thermodynamical Properties of Lennard-Jones Molecules. *Phys. Rev.* **1967**, *159*, 98.

222. Hockney, R. W. The Potential Calculation and Some Applications. *Methods in Computational Physics* **1970**, *9*, 136-211.

223. Case, D. A.; Pearlman D. A.; Caldwell J. W.; Cheatham III.; Wang, J.; Ross, W. S.; Simmerling, C. L.; Darden, T. A.; Merz, K. M.; Stanton, R. V.; Cheng, A. L.; Vincent, J. J.; Crowley, M.; Tsui, V.; Gohlke, H.; Radmer, R. J.; Duan, Y.; Pitera, J.; Massova, L.; Seibel G. L., Singh, U. C.; Weiner, P. K.; Kollman, P. A. *AMBER*, version 8, University of California, San Francisco **2008**.

224. Shields, G. C.; Laughton, C. A.; Orozco, M. Molecular dynamics simulations of the d(T·A·T) triple helix. *J. Am. Chem. Soc.* **1997**, *119*, 7463-7469.

225. Berendsen, H.J.C.; Postma, J.P.M.; Vangunsteren, W.F.; Dinola, A.; Haak, J.R. Molecular Dynamics with Coupling to an External Bath. *J. Chem. Phys.* **1984**, *81*, 3684-3690.

226. Anderson, H. C. Molecular Dynamics Simulation at Constant Pressure and / or Temperature. *J.Chem.Phys.* **1980**, *72*, 2384-2393.

227. Nosé, S. A Molecular Dynamics Method for Simulations in the Canonical Ensemble. *Molecuar Physics* **1984**, *53*, 255-268.

228. Hoover, W. G. Canonical Dynamics: Equilibrium Phase-space Distributions. *Phys. Rev. A* **1985**, *31*, 1695-1697.

229. Leach, A. R. Molecular Modelling. Principles and Applications. Pearson Education Limited. Prentice Hall: Dorchester, Dorset, Great Britain, **2001**.

230. Gilson, M. K.; Sharp, K.; Honig, B. Calculating the Electrostatic Potential of Molecules in Solution: Method and error assessment. *J. Comput. Chem.* **1987**, *9*, 327-335.

231. Rocchia, W.; Alexov, E.; Honig, B. Extending the Applicability of the Nonlinear Poisson-Boltzmann Equation: Multiple Dielectric Constants and Multivalent Ions. *J. Phys. Chem. B* **2001**, *28*, 6507-6514.

232. Jayaram, B.; Sprous, D.; Beveridge, D. L. Solvatation Free Energy of Biomacromolecules: Parameters for a Modified Generalized Born Model Consistent with the AMBER Force Field. *J.Phys.Chem.B* **1998**, *102*, 9571-9576.

233. Halperin, I.; Ma, B.; Wolfson, H.; Nussinov, R.; Principles of Docking: An Overview of Search Algorithms and a Guide to Scoring Functions. *Proteins: Structure, Function and Genetics* **2002**, *47*, 409-443.

234. Kaapro, A.; Ojanen, J. Protein docking. November 27, **2002**. Accesible a través de internet: http://www.lce.hut.fi/teaching/S-114.500/k2002/Protdock.pdf

235. Fisher, E. Einfluss der Konfiguration auf die Wirkung der Enzyme. *Ber. Dtsch. Chem. Ges.* **1894**, *27*, 2985-2993.

236. Kuntz, I. D.; Blaney, J. M.; Oatley, S. J.; Langridge, R.; Ferrin, T. E. A Geometric Approach to Macromolecule-Ligand Interactions. *J. Mol. Biol.* **1982**, *161*, 269-288.

237. Warren, G. L.; Andrews, C. V.; Capelli, A.; Clarke, B.; LaLonde, J.; Lambert, M. H.; Lindvall, M.; Nevins, N.; Semus, S. F.; Senger, S.; Tedesco, G.; Wall, I. D.; Woolven, J. M.; Peishoff, C. E.; Head, M. S. A critical assessment of docking programs and scoring functions. *J. Med. Chem.* **2006**, *49*, 5912-5931.

238. Gutiérrez de Terán Castañón, H. Tesis Doctoral, Universitat Pompeu Fabra (Barcelona, España), **2004**.

239. Autodock 3.0.5 User Guide. En línea (3/12/08). Accesible a través de internet: http://autodock.scripps.edu/faqs-help/manual/autodock-3-user-s-guide/Autodock3.0.5_auserGuide.pdf

240. Kollman, P. A.; Massova, I.; Reyes, C.; Kuhn, B.; Huo, S.; Chong, L.; Lee, M.; Lee, T.; Duan, Y.; Wang, W.; Donini, O.; Cieplak, P.; Srinivasan, J.; Case, D. A.; Cheatham, T. E. Calculating Strutures and Free Energies of Complex Molecules: Combining Molecular Mechanics and Continuum Models. *Acc. Chem. Res.* **2000**, *33*, 889-897.

241. Srinivasan, J.; Cheatham III; Kollman, P.; Case, D. A. Continuum Solvent Studies of the Stability of DNA, RNA, and Phosphoramidate–DNA Helices. *J. Am. Chem. Soc.* **1998**, *120*, 9401-9409.

242. Åqvist, J.; Medina, C.; Samuelsson, J. E. A New Method for Predicting Binding Affinity in Computer-Aided Drug Design. *Protein Eng.* **1994**, *7*, 385-391.

243. Pérez, C.; Ortiz, A. R. Evaluation of Docking Functions for Protein-Ligand Docking. *J. Med. Chem.* **2001**, *44*, 3768-3785.

244. Ajay, W.; Murcko, M. A. Computational Methods to Predict Binding Free Energy in Ligand-Receptor Complexes. *J. Med. Chem.* **1995**, *38*, 4953-4967.

245. Charifson, P. S.; Corkery, J. J.; Murcko, M. A.; Walters, P. W. Consensus Scoring: A Method for Obtaining Improved Hit Rates from Docking Databases of Three-Dimensional Structures into Proteins. *J. Med. Chem.* **1999**, *42*, 5100-5109.

246. Ferrara, P.; Gohlke, H.; Price, D. J.; Klebe, G.; Brooks, C. L. Assessing Scoring Functions for Protein-Ligand Interacctions. *J. Med. Chem.* **2004**, *47*, 3032-3047.

247. Wang, R.; Wang, S. How does consensus scoring work for virtual library screening? An idealized computer experiment. *J. Chem. Inf. Comput. Sci.* **2001**, *41*, 1422-1426.

248. Pearlman, D. A.; Charifson, P. S. Are Free Energy Calculations Useful in Practice? A Comparison with Rapid Scoring Functions for the p38 MAP Kinase Protein System. *J. Med. Chem.* **2001**, *44*, 3417-3423.

249. Pearlman, D. A. Evaluating the Molecular Mechanics Poisson-Boltzmann Surface Area Free Energy Method Using a Congeneric Series of Ligands to p38 MAP Kinase. *J. Med. Chem.* **2005**, *48*, 7796-7807

250. Wang, R.; Lu, Y.; Wang, S. Comparative Evaluation of 11 Scoring Functions for Molecular Docking. *J. Med. Chem*. **2003**, *46*, 2287-2303.

251. Böhm, H.-J.; The Development of a Simple Empirical Scoring Function to Estimate the Binding Constant for a Protein-Ligand Complex of Known Three-Dimensional Sturcture. *J. Comput.-Aided Mol. Design* **1994**, *3*, 243-256.

252. *AutoDock*, versions 3.0 and 4.0, Department of Molecular Biology, The Scripps Research Institute, MB-5, La Jolla, CA (USA), **1996**. Morris, G. M.; Goodsell, D. S.; Huey, R.; Olson, A.

J. Distributed automated docking of flexible ligands to proteins: Parallel applications of AutoDock 2.4. *J. Computer-Aided Molecular Design* **1996**, *10*, 293-304.

253. *Gold*, versions 3.1 and 4.0, The Cambridge Crystallographic Data Centre, Cambridge (UK) **2003**. Verdonk, M. L.; Cole, J. C.; Hartshorn, M. J.; Murray, C. W.; Taylor, R. D. Improved Protein-Ligand Docking Using GOLD. *Proteins: Structure, Function, and Genetics* **2003**, *52*, 609-623.

254. *Fred*, version 2.2, OpenEye Scientific Software, Inc.: Santa Fe, NM., **2006**. McGann, M. R.; Almond, H. R.; Nicholls, A.; Grant, J. A.; Brown, F. K. Gaussian docking functions. *Biopolymers* **2003**, *68*, 76-90.

255. *Hex*, version 4.8, Department of Computing Science, University of Aberdeen, Aberdeen, Scotland (UK), to be found under http://www.biochem.abdn.ac.uk/hex/, **2007**. Ritchie, D. W.; Kemp, G. J. L. Protein docking using spherical polar Fourier correlations. *Proteins: Struct., Funct., Genet.* **2000**, 39, 178–194.

256. Stouten, P. F. W.; Frömmel, C.; Nakamura, H.; Sander, C. An effective solvation term based on atomic occupancies for use in protein simulations. *Mol. Simul.* **1993**, *10*, 97-120.

257. Verdonk, M. L.; Berdini, V.; Hartshorn, M. J.; Mooij, W. T. M.; Murray, C. W.; Taylor, R. D.; Watson, P. Virtual Screening Using Protein-Ligand Docking: Avoiding Artificial Enrichment. *J. Chem. Inf. Comput. Sci.* **2004**, *44*, 793-806.

258. Eldridge, M. D.; Murray, C. W.; Auton, T. R.; Paolini, G. V.; Mee, R. P. Empirical scoring function to estimate the binding affinity of ligands in receptor complexes. *J. Comput-Aided Mol. Des.* **1997**, *11*, 425-445.

259. Baxter, C. A.; C. Murria, W.; Clark, D. E.; Gestead, D. R. and Eldridge, M. D. Flexible Docking Using Tabu Search and an Empirical Estimate of Binding Affinity. *Proteins* **1998**, *33*, 367-382.

260. *MOE (Molecular Operating Environment)*, versions 2006.08 and 2007.09; Chemical Computing Group, Inc.: Montreal, Canada, **2006**.

261. *QikProp*, version 2.3, Schrödinger Inc., New York (USA) **2005**.

262. *GenerateMD*, version 5.1.3; ChemAxon Ltd.: Budapest, Hungary, **2008**.

263. Rohrbaugh, R. H.; Jurs, P. C. Descriptions of Molecular Shape Applied in Studies of Structure/Activity and Structure/Property Relationships. *Anal. Chim. Acta* **1987**, *199*, 99-109.

264. *Discovery Studio*, Version 1.7, Accelrys Inc., San Diego, CA (USA) **2006**.

265. Labute, P.; Williams, C.; Feher, M.; Sourial, E.; Schmidt, J. M. Flexible alignment of small molecules. *J. Med. Chem.* **2001**, *44*, 1483-1490.

266. *ParaSurf* and *ParaFit*, version 8.0, Cepos Insilico Ltd., Erlangen, Germany, to be found under http://www.ceposinsilico.de/Pages/Products.html, **2008**.

267. Ritchie, D. W.; Kemp, G. J. L. Fast computation, rotation, and comparison of low resolution spherical harmonic molecular surfaces. *J. Comput. Chem.* **1999**, *20*, 383-395.

268. *ROCS*, versions 2.2 and 2.3.1, OpenEye Scientific Software, Inc.: Santa Fe, NM., **2007**. Grant, A. J.; Pickup, B. T. A fast method of molecular shape comparison: a simple application of a Gaussian description of molecular shape. *J. Comput. Chem.* **1996**, *17*, 1653-1659.

269. Dalby, A.; Nourse, J. G.; Hounshell, D.; Gushurst, A. K., I; Grier, D. L.; Leland, B. A.; Laufer, J. Description of Several Chemical Structure File Formats Used by Computer Programs Developed at Molecular Design Limited. *J.Chem.Inf.Comput.Sci.* **1992**, *32*, 244-255.

270. Mavridis, L.; Hudson, B. D.; Ritchie, D. W. Toward High Throughput 3D Virtual Screening Using Spherical Harmonic Surface Representations. *J. Chem. Inf. Model.* **2007**, *47*, 1787-1796.

271. Mavridis, L.; Ritchie, D. W. Representing and Comparing Molecules using Spherical Harmonic Expansions. Department of Computing Science, King's College, University of Aberdeen, Aberdeen, UK. En línea (15/01/09). Accesible a través de http://www.csd.abdn.ac.uk/~dritchie/papers/mavridis_ukqsar_2006.pdf

272. Pardo, L.; Deupi, X.; Dölker, N.; López-Rodríguez M. L.; Campillo, M. The role of internal water molecules in the structure and function of the rhodopsin family of G protein-coupled receptors. *Chembiochem* **2007**, *8*, 19-24.

273. Govaerts, C.; Bondue, A.; Springael, J-Y.; Olivella, M.; Deupi, X.; Le Poul, E.; Wodak, S. J.; Parmentier, M.; Pardo, L.; Blanpain, C. Activation of CCR5 by chemokines involves an aromatic cluster between transmembrane helices 2 and 3. *J. Biol. Chem.* **2003**, *278*, 1892-1903.

274. Govaerts, C.; Blanpain, C.; Deupi, X.; Ballet, S.; Ballesteros, J. A.; Wodak, S. J.; Vassart, G.; Pardo, L.; Parmentier M. The TXP motif in the second transmembrane helix of CCR5. A structural determinant of chemokine-induced activation. *J. Biol. Chem.* **2001**, *276*, 13217-13225.

275. Deupi, X.; Dolker, N.; Luz Lopez-Rodriguez, M.; Campillo, M.; Ballesteros, J. A.; Pardo, L. Structural models of class a G protein-coupled receptors as a tool for drug design: insights on transmembrane bundle plasticity. *Curr. Top. Med. Chem.* **2007**, *7*, 991-998.

276. *Maybride Bringing life to drug discovery*, Maybridge Databases Autumn 2005; Fisher Scientific International: England, **2005**.

277. Lu, S.-F.; Chen, B.; Davey, D.; Dunning, L.; Jaroch, S.; May, K.; Onuffer, J.; Phillips, G.; Subramanyam, B.; Tseng, J.-L.; Wei, R. G.; Wei, M.; Ye, B. CCR5 receptor antagonists: Discovery and SAR of novel 4-hydroxypiperidine derivatives. *Bioorg. Med. Chem. Lett.* **2007**, *17*, 1883–1887.

278. Wei, R. G.; Arnaiz, D. O.; Chou, Y.-L.; Davey, D.; Dunning, L.; Lee, W.; Lu, S.-F.; Onuffer, J.; Ye, B.; Phillips, G. CCR5 receptor antagonists: Discovery and SAR study of guanylhydrazone derivatives. *Bioorg. Med. Chem. Lett.* **2007**, *17*, 231–234.

279. Jorgensen, W. L. *QikSim*, version 2.3, Yale University, New Haven, CT (USA) **2005**.

280. Hawkins, P. D. C.; Skillman, G. A.; Nicholls, A. Comparison of Shape Matching and Docking as Virtual Screening Tools. *J. Med.Chem.* **2007**, *50*, 74-82.

281. Kirchmair, J.; Distinto, S.; Markt, P.; Schuter, D.; Spitzer, G. M.; Liedl, K. R.; Wolber, G. How To Optimize Shape-Based Virtual Screening: Choosing the Right Query and Including Chemical Information. *J. Chem. Inf. Model.* **2009**, *49*, Article ASAP, DOI: 10.1021/ci8004226.

282. Taylor, R. D.; Jewsbury, P. J.; Essex, J. W. A Review of Protein-Small Molecule Docking Methods. *J. Comput.-Aided. Mol. Des.* **2002**, *16*, 151-166.

283. Mpamhanga, C. P.; Chen, B.; McLay, I. M.; Willett, P. Knowledge-based interaction fingerprint scoring: a simple method for improving the effectiveness of fast scoring functions. *J. Chem. Inf. Model.* **2006**, *46*, 686-698.

Apéndices

A1. *Modelo 3 CCR5*.

A2. **Colaboración en la comunicación oral** presentada en **IX Congress of the ISJACHEM**, (11-14 July 2006, Barcelona, Spain).

A3. Pérez-Nueno, V. I.; Ros-Blanco, L.; Pettersson, S.; Puig de la Bellacasa, R.; Rabal,O.; Batllori, X.; Clotet, B.; Clotet-Codina, I.; Armand-Ugón, M.; Esté, J.; Borrell, J. I.; Teixidó, J. Structure-Based Design, Virtual Screening, Synthesis, and Biological Evaluation of Novel HIV Entry Inhibitors For The CXCR4 Receptor. *(Draft)*

A4. **Póster** presentado en **4th Joint Sheffield Conference on Chemoinformatics** (18-20 June 2007, University of Sheffield, UK.).

A5. **Colaboración en la comunicación escrita** Avenços en farmacologia. Nous fàrmacs per bloquejar l'entrada del VIH a les cèl·lules. *Teraflop* **2007**, *94*, 14-15.

A6. **Colaboración en la comunicación oral** presentada en **XXth International Symposium on Medicinal Chemistry EFMC-ISMC** (August 31 - September 4 2008, Vienna, Austria).

A7. **Póster** presentado en **Targeting and tinkering with Interaction Networks. From interaction networks to therapeutics** (14-16 April 2008, Barcelona, Spain).

A8. **Póster** presentado en **Virtual Discovery. Computer-Aided Drug Design and Screening** (24-25 October 2007, London, UK).

A9. **Resumen de la comunicación oral** presentada en LORIA (Lorraine Laboratory for Informatics Research and its Applications), Nancy Université, Vandoeuvre-lès-Nancy, France (28 January 2009).

A10. **JCIM Vol. 48 3rd Issue Art Cover**.

Modelo 3 CCR5

Modelo por homología construido con Moe-Align y Moe-Homology utilizando como plantillas la proteína β2-adrenérgico (código PDB 2rh1) y la proteína rodopsina bovina (código PDB 1u19) para los *loops* intermedios.

Rodopsina bovina (código PDB 1u19)

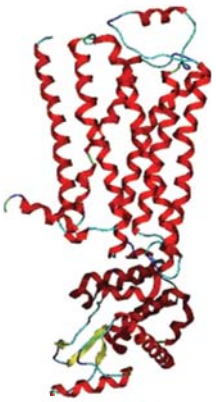

β2-adrenérgico (código PDB 2rh1)

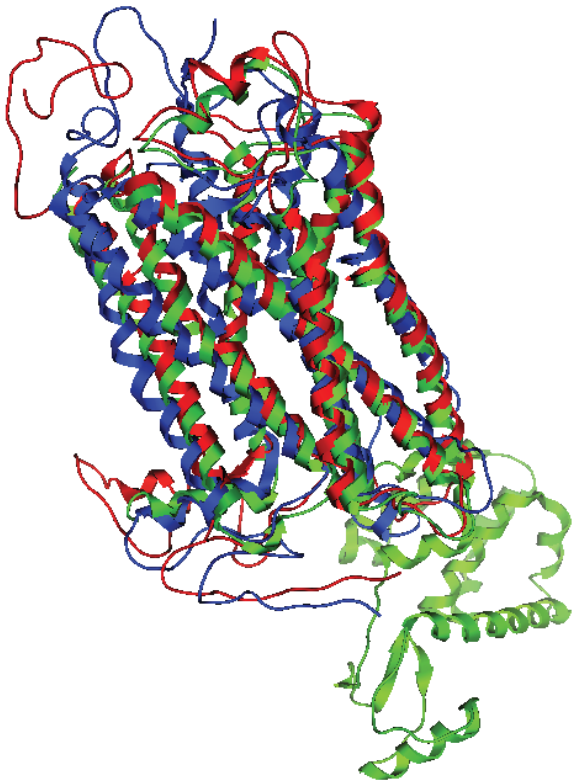

Figura 1 Modelización por homología del co-receptor CCR5. Arriba se muestran las estructuras tridimensionales del β2-adrenérgico y rodopsina bovina. Abajo se muestra la superposición del modelo de CCR5 (rojo) obtenido por homología a partir de las plantillas β2-adrenérgico (verde) y rodopsina bovina (azul).

El modelo se valida con Procheck obteniendo el 70,9% de los residuos en regiones favorables del mapa de Ramachandran y el 26,8% de los residuos en regiones permitidas.

Se realiza un cribado virtual retrospectivo por *docking* utilizando este modelo y una base de datos de 354 inhibidores de CCR5 extraídos de la literatura y 4696 compuestos supuestamente inactivos extraídos de la quimioteca Maybridge Screening Collection (en el Artículo I se detallan estas bases de datos). Primeramente se realiza el *docking* con Moe del compuesto activo TAK779 para comprobar que se detectan las interacciones entre dicho ligando y los residuos claves del co-receptor identificados según los estudios de mutagénesis dirigida (detallados en el Artículo I).

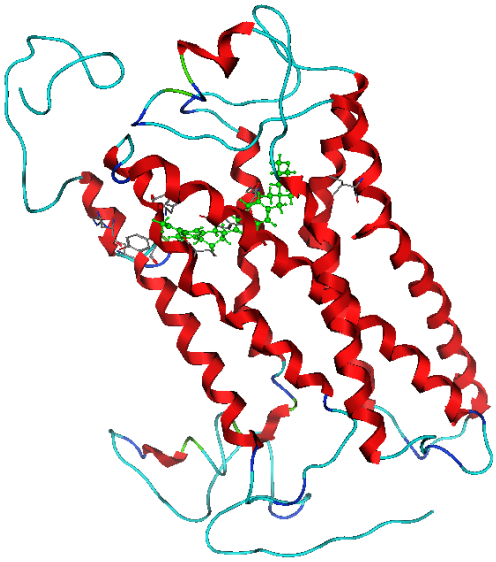

Figura 2 Docking del compuesto activo TAK779 y el *modelo 3 CCR5* con Moe.

El cribado virtual se lleva a cabo con Autodock 4 utilizando los mismos parámetros definidos en el Artículo I. La función de scoring utilizada en este caso es AutoDock41_score.

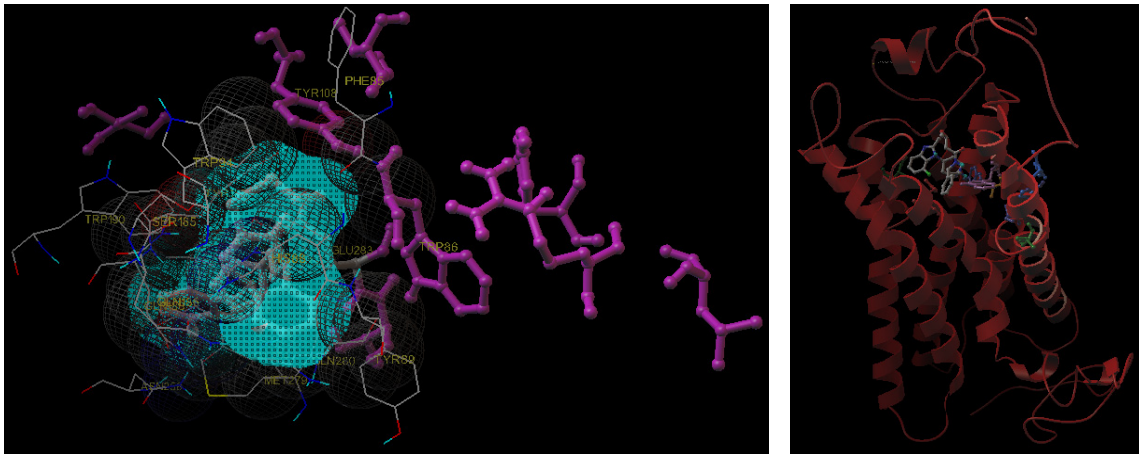

Figura 3 Docking de un compuesto activo de la base de datos con Autodock 4.

Los resultados obtenidos en el cribado virtual no mejoran los obtenidos con los modelos *modelo 1 CCR5* y *modelo 2 CCR5*, mostrando en este caso un comportamiento cercano al aleatorio. Por ello no se utiliza como filtro en el protocolo de cribado de potenciales inhibidores de entrada del VIH llevado a cabo en este estudio.

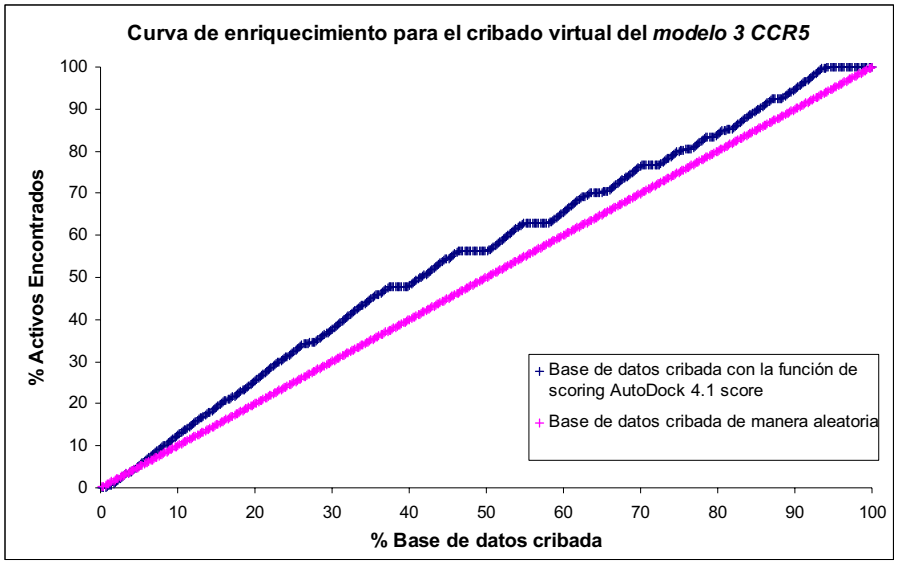

% Base de datos cribada	*EF* (Factor de enriquecimiento)
1	0.30
5	1.08
10	1.26
20	1.28
40	1.20
80	1.06
100	1.00

Figura 3 Curva de enriquecimiento para el cribado virtual retrospectivo por docking utilizando el *modelo 3 CCR5*.

The state of the art in Computational Chemistry: Biomedical Research at GEM

R. Tejedor, O. Rabal, V. Pérez-Nueno, J. Teixidó

Laboratori de Disseny Molecular
Grup d'Enginyeria Molecular (GEM)
Institut Químic de Sarrià, Universitat Ramon Llull

Docking bicyclam AMD3100

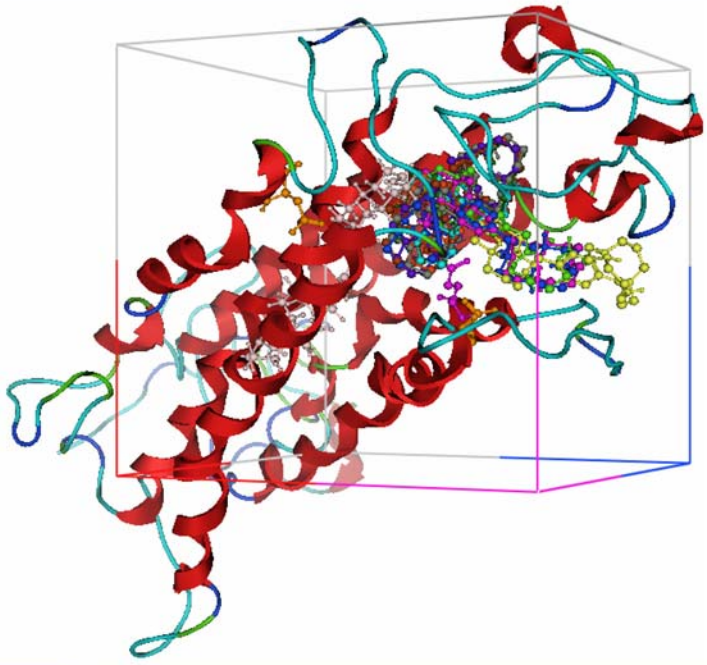

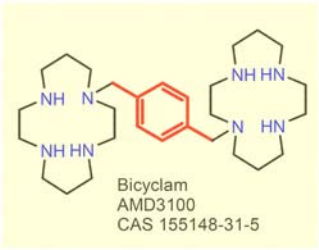

New drugs: **Bicyclam**
Inhib. virus union to membrane receptors

- CXCR4
- CCR5

DOI: 10.1002/cmdc.200((will be filled in by the editorial staff))

Structure-Based Design, Virtual Screening, Synthesis, and Biological Evaluation of Novel HIV Entry Inhibitors For The CXCR4 Receptor

Violeta I. Pérez-Nueno[a], Laia Ros-Blanco[a], Sofia Pettersson[a], Raimon Puig de la Bellacasa[a], María Obdulia Rabal[a], Xavier Batllori[a], Bonaventura Clotet[b], Imma Clotet-Codina[b], Mercedes Armand-Ugón[b], José Esté[b], José I. Borrell[a], and Jordi Teixidó[a]*

The CXCR4 receptor has been shown to interact with the human immunodeficiency viral envelope glycoprotein gp120 leading to fusion of viral and cell membranes. Therefore, ligands which can attach to this receptor represent an important class of therapeutic agents against HIV, thus inhibiting the first step in the cycle of virus infection: the virus-cell entry/fusion. Here we report a structure-based de novo design study and virtual screening structure-based (docking) and ligand-based (pharmacophore modelling, shape matching and similarity searches) tools to find new potential HIV entry inhibitors for the CXCR4 receptor. A library of anti-HIV expected compounds was created from de novo designed ligands. Virtual screening tools were applied to select the hypothetical most active compounds, and some of them were synthesized. In vitro activity testing in cell cultures against HIV strains led to the identification of active CXCR4 inhibitors in the range from x to y µg/ml without cytotoxicity at tested concentrations.

Introduction

According to the Joint United Nations Programme on HIV/AIDS (UNAIDS) and World Health Organization (WHO), a total of 33.2 million [30.6–36.1 million] people were living with human immunodeficiency virus (HIV) in 2007. A total of 30.8 million [28.2–33.6 million] adults' infections, 15.4 million [13.9–16.6 million] women's infections, and 2.1 million [1.9-2.4 million] children's under 15 years infections [1]. There were 2.5 million [1.8–4.1 million] new cases and 2.1 million [1.9–2.4 million] deaths in 2007. The process of HIV entry begins when it binds to a CD4 receptor and one of two co-receptors on the surface of a $CD4^+$ T- lymphocyte (CXCR4 or CCR5) [2]. The virus then fuses with the host cell. After fusion, the virus releases RNA into the host cell. The reverse transcriptase HIV enzyme converts the single-stranded HIV RNA to double-stranded HIV DNA. The newly formed HIV DNA enters the host cell's nucleus, where the HIV enzyme integrase "hides" the HIV DNA within the host cell's own DNA. Host RNA polymerase creates copies of the HIV genomic material, as well as shorter strands of messenger RNA (mRNA). The mRNA is used to make long chains of HIV proteins. The protease HIV enzyme cuts the long chains of HIV proteins into smaller individual proteins. As the smaller HIV proteins come together with copies of HIV's RNA genetic material, a new virus particle is assembled. The newly assembled virus "buds" from the host cell taking part of the cell's outer envelope which acts as a covering studded with HIV glycoprotein's necessary for the subsequent virus CD4 and co-receptors binding [3], [4]. Current antiretroviral therapies (ARTs) against HIV are generally based on the combination of reverse transcriptase and protease inhibitors which is known as highly active antiretroviral therapy (HAART). At the present time there are 8 nucleoside/nucleotide reverse transcriptase inhibitors (NRTIs/NtRTIs), 4 nonnucleoside reverse transcriptase inhibitors (NNRTIs), 10 protease inhibitors (PI), a single fusion inhibitor (Enfuvirtide, Roche Pharmaceuticals), an entry inhibitor (Maraviroc, Pfizer), and an integrase inhibitor (Raltegravir, Merck Sharp & Dohme) available for the treatment of HIV infection [5]. Despite the large number of drugs available, there are several concerns about antiretroviral regimens. The drugs can have serious side effects, regimens can be complicated, requiring patients to take several pills at various times during the day, drug resistance, latent viral reservoirs, and drug induced toxic effects that compromise effective viral control can be developed. Fusion/entry inhibitors have been shown to be effective in patients harbouring resistance to the NRTI, NNRTI, and PI classes [6]. Therefore, there is considerable interest in developing novel ligands that are resistant to the currently used

[a] *V. I. Pérez-Nueno, L. Ros-Blanco, S. Pettersson, Dr. J. I. Borrell, Dr. J. Teixidó*
Grup d'Enginyeria Molecular
Institut Químic de Sarrià, Universitat Ramon Llull
Via Augusta 390, E-08017 Barcelona, Spain
E-mail: j.teixido@iqs.url.edu
[b] *Dr. B. Clotet, Dr. I. Clotet-Codina, Dr. M. Armand-Ugón, Dr. J. Esté*
Retrovirology Laboratory IrsiCaixa
Hospital Universitari Germans Trias i Pujol, Universitat Autònoma de Barcelona
E-08916 Badalona, Spain

*Supporting information for this article is available on the WWW under http://www.chemmedchem.org or from the author.((**Please delete if not appropriate**))*

drugs or new agents belonging to new classes that further heighten the effectiveness and durability of HIV therapy [7], [8].

This article focuses on the design of novel ligands that target virus attachment to CXCR4 receptor and hence block virus-cell entry/fusion. Because no CXCR4 crystal structure currently exist, a *de novo* design structure based was carried out using a built 3D model by homology from the available template structure, bovine rhodopsin [9]. A library of anti-HIV expected compounds was created from the *de novo* designed ligands. Virtual screening (VS) approaches (docking, pharmacophore modelling, shape matching and similarity searches) were performed to select potential active ligands that can interfere with the active site of CXCR4 receptor. Following virtual screening, synthetically accessible compounds were selected, synthesized, and anti-HIV activity was evaluated.

Results and Discussion

Structure-Based Design and Virtual Screening

LUDI [10] interaction sites were generated on CXCR4 binding pocket according to key site directed mutagenesis (SDM)-defined binding residues (Asp171, Asp262, and Glu288) [11], [12], [13], [14].

LUDI approach yielded a total of 200 new ligands based on the 20 highest-ranked scaffolds from standard calculations. The range of Ludi Energy Estimate 3 [15] scores were from 1040 (corresponding with a predicted Ki ~ 0.01 μM) to 280 (mM range). To further prioritize, focus was placed on the ligands that had the best scores and accomplished the necessary molecular interactions to bind CXCR4 receptor. In order to do this selection, the best scoring function to rank-order the hit list and score the docking poses was selected from a training set docking analysis. Ludi Energy Estimate 3 (Ludi_3) [15], PLP2 [16], LigScore2 [17], Jain [18], and PMF [19] scoring functions were calculated. Also, scoring was concatenated after docking, with in situ ligand minimization obtaining Ludi_3_dock, PLP2_dock, LigScore2_dock, Jain_dock, PMF_dock, DockScore and consensus scoring functions. Figure 1 shows the results from this analysis. It can be seen that Ludi_3 and LigScore2 are the functions that perform better, so the final output list was obtained selecting the designed compounds with Ludi_3 scores greater than 700, predicted to be μM inhibitors.

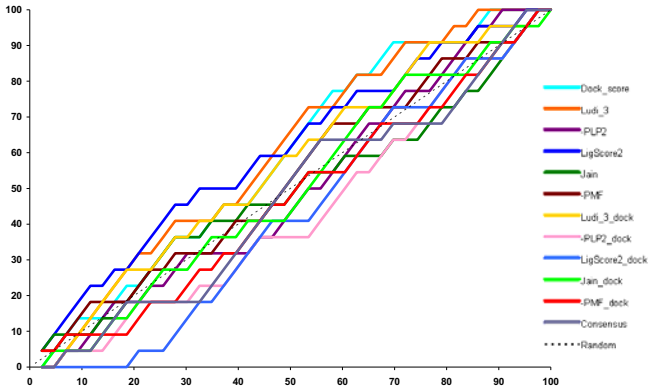

Figure 1. LUDI CXCR4 docking-based enrichments for the training set molecules used in *de novo* design approach. Enrichment curves obtained using several docking protocols for the training set molecules, composed of forty three known CXCR4 inhibitors from the literature, used in *de novo* design. The enrichments are used to assess the best scoring function to score new designed molecules.

Also, visual inspection of the docking results confirmed that selected molecules interact with CXCR4 binding site according to the knowledge of the SDM data. Figure 2 shows a high Ludi_3 compound docked into CXCR4 binding pocket and Figure 3 shows the same compound pose inside the LUDI interaction sites generated for the fragment-based approach. It can be seen that the proposed binding mode fits very well into the interaction sites. All hydrophobic groups of the designed ligand occupy hydrophobic sites on CXCR4, while NH groups at the aromatic rings fit into the hydrogen bond acceptor sites, making it possible to form the hydrogen bond with the carboxylic acids Asp262 and Glu288 of CXCR4.

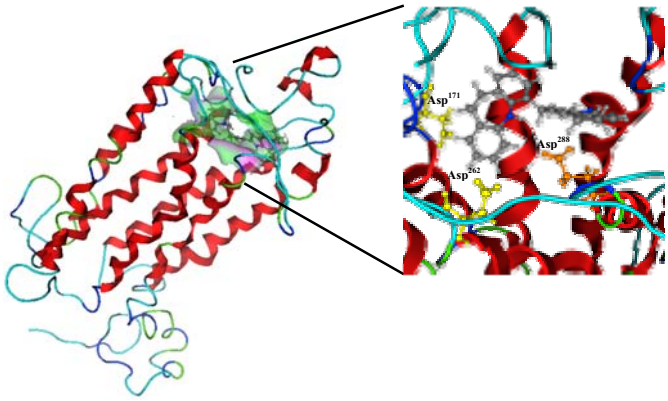

Figure 2. Close-up view of a high Ludi_3 score *de novo* designed compound-CXCR4 binding conformation. The view on the left shows the *de novo* designed compound docked within the CXCR4 pocket. The *de novo* designed compound binding site is depicted using a Gaussian contact surface. The view on the right shows in detail the calculated binding conformation. In this docking prediction, the nitrogen of the seven-membered aromatic ring interacts with the two carboxylic oxygens of Asp171 and Asp262, and the nitrogen of the five-membered aromatic ring interacts with the two carboxylic oxygens of Glu288.

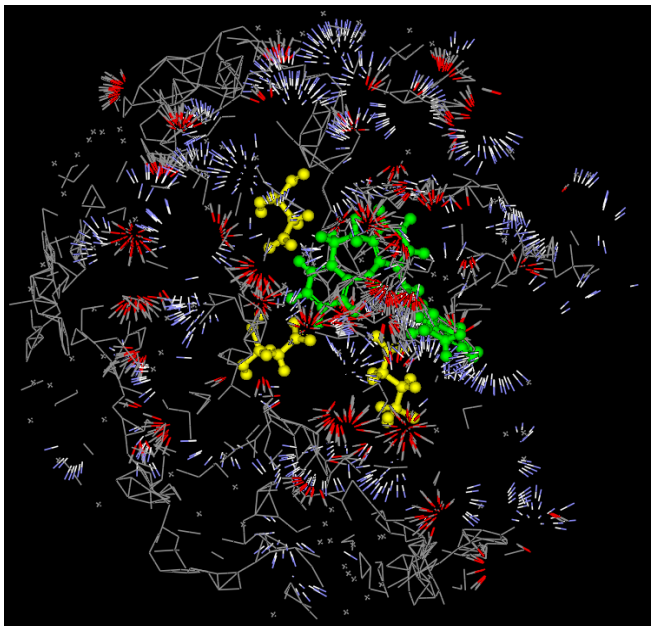

Figure 3. LUDI interaction sites generated on CXCR4 binding pocket: grey – hydrophobic sites, blue-white – hydrogen bond donor sites, red-grey – hydrogen bond acceptor sites. These sites indicate where particular groups of the ligand

molecule should be placed in the protein binding site to make favourable interactions. Proposed binding mode of a high Ludi Energy Estimate 3 score *de novo* designed compound is shown (in green ball and stick representation) to reveal how it fits into the interaction sites. Only Asp171, Asp262, and Glu288 binding site residues of the CXCR4 structure are shown in yellow ball and stick representation for clarity of the figure.

Furthermore, more compounds were *de novo* designed from *p*-xilil and piridone defined scaffolds by binding fragments from LUDI internal library and ZINC fragments database [20]. The scaffolds were pre-docked first onto the CXCR4 active site obtaining poses according to the knowledge of SDM data. Fragments were bound to the scaffolds taking into account a) a defined radius from the pre-docked *p*-xilil and piridone moieties and b) defined linking points selected on the scaffolds as well as a defined radius from the link points. Figure 4 shows the linking points for *p*-xilil and piridone defined scaffolds. Ligands that had the best Ludi_3 scores and accomplished the necessary molecular interactions to bind CXCR4 receptor were selected.

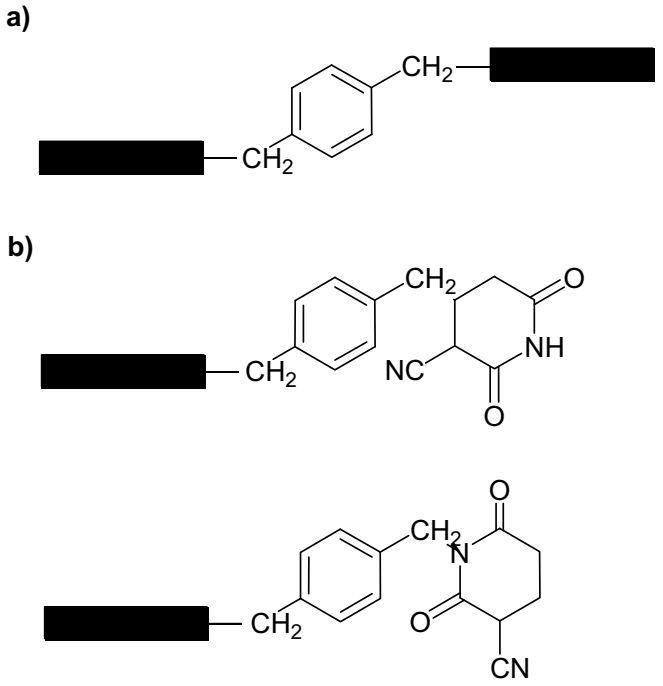

Figure 4. Linking points (black rectangles) selected on *p*-xilil (a) and piridone (b) pre-docked scaffolds for fragments binding.

The final *de novo* list was composed of a total of 208 ligands designed based on CXCR4 structure. Due to the difficult synthetic feasibility of some of the proposed molecules, starting from the commercially available fragments used to virtually build them, a virtual combinatorial library of more synthetically accessible compounds was designed (130 structures) focusing on *de novo* selected fragments, distances between heteroatoms and chemistry of *de novo* ligands. These compound structures were built using MOE [21]. They were protonated at physiological pH (i.e., pH 7), Gasteiger partial charges were assigned [22], and the geometry was optimized using the MMFF94 force field.

The final library of 338 compounds was virtually screened in order to select the best compounds to be synthesized and tested. Structure-based and ligand-based tools that best performed in our previous prospective virtual screening experiments [23] were used. Docking using GOLD [24] and HEX [25], shape matching using PARAFIT [26], ROCS [27] and HEX [25], and pharmacophore modelling using MOE and Discovery Studio [28] were applied.

The different used approaches selected similar molecules at the first percentages of the ranked hit lists. Compounds selected by the different ligand-based virtual screening tools were practically the same, whereas the ones selected by structure-based docking tools included also some others. A consensus "Rank-by-Vote" [29] of all the first hit ranking lists compounds found by the aforementioned approaches was performed. Different descriptors and ADME properties were calculated for these compounds using QIKPROP [30] and similarity searches with respect to a known active compound using QIKSIM [31]. The compounds with the best ADME-tox properties or more similar to the known active properties were selected to be synthesized.

Chemistry

(Results and Discussion)

Synthetic compounds with their names to refer them

((Insert Scheme here. **Note:** Please do **not** combine scheme and caption in a textbox or frame))

Scheme 1. ((Scheme Caption.))

Anti-HIV-Activity

A consensus evaluation of all the virtual screening aforementioned methods led to the selection of x compounds to be synthesized: *1*, *2*, *3*, *4* and *5*. All compounds were classified in the top of the ranked virtually screened lists but we selected the two best ranked and the three best classified *type of compounds*. *1* and *2* compounds showed anti-HIV activity values of x and y µg/ml respectively. *3* and *4* showed anti-HIV activity values of x and y µg/ml respectively. *5* was toxic at a concentration of x µg/ml and showed no activity below this concentration (Table1).

Table 1. Hit selection. Structure, anti-HIV activity (EC_{50}) and cytotoxicity (CC_{50}) of selected hits.

Compound	EC_{50} / µg/ml [a]	CC_{50} / µg/ml [b]
Column 1	Column 2	Column 3
Column 1	Column 2	Column 3

[a] Effective concentration 50 or the concentration required to inhibit HIV-induced cell death by 50% as evaluated with the MTT method in MT-4 cells. [b] Cytotoxic concentration 50 or the concentration required to induce 50% death of non-infected MT-4 cells as evaluated with the MTT method. Reference compounds: AMD3100: EC_{50}=0.001 µg mL^{-1}, CC_{50}=>5 µg mL^{-1}; DS: EC_{50}=0.011 µg mL^{-1}, CC_{50}=>125 µg mL^{-1}.

Conclusion

In summary, we employed a structure-based design followed by a virtual screening structure- and ligand-based selection to identify compounds able to interfere with the active site of CXCR4 receptor. Selected compounds showed anti-HIV activity values below x μg mL^{-1} and displayed no cytotoxic effects at the tested concentrations. Studies on the mode of action of these compounds showed that they inhibited the CXCR4 coreceptor, thus validating the initial target compound design. Therefore, these new ligands might serve as novel leads for further pharmacological investigations as therapeutic agents against HIV.

Experimental Section

De Novo Design Structure-Based

The structure-based design of inhibitors was performed on Discovery Studio (DS) 1.7 environment [28] using CXCR4 structure homology modelled from bovine rhodopsin template (pdb code 1HZX) [9]. We applied *De Novo Receptor* and *Link mode* DS protocols for running LUDI [10] to find fragments in LUDI internal library that bound to the receptor. Starting with the definition of the CXCR4 binding site according to SDM data [9], LUDI derived potential interaction sites for ligand functional groups based on the chemistries presented by the target. First, the receptor-mode LUDI algorithm was used to position a series of small molecules into the CXCR4 active site. Then new chemotypes were built using the LUDI link-mode by attaching small organic fragments to the output molecules (scaffolds) to grow new molecules in the active site via *de novo* design. After defining a scaffold, the LUDI link-mode was activated to search for fragments that could covalently link to the scaffold and contain new non-bonded interactions (hydrogen bond donors, hydrogen bond acceptors, and lipophilic contacts) with the protein. Each fragment was attached and conformational flexibility where two rotatable bonds could be simultaneously moved was allowed. All fragments were automatically fused to the scaffold, bond orders fixed, and duplicates removed. In the final list, 10 molecules for each initial scaffold were generated.

We also applied *De Novo Evolution* DS protocol for running AUTOLUDI [10] to find fragments that increased binding on the defined ligand scaffolds *p*-xilil and piridone. We used both the *Full Evolution* and *Combinatorial* modes to vary the nature of fragment selection and construction of new molecules. On *Full Evolution* mode, fragments from LUDI internal library and ZINC fragment-like library [20] were bound to *p*-xilil and piridone moieties using a radius of 12-14 Å from the pre-docked scaffolds for defining the active site. For *p*-xilil scaffold, AMD3100 CXCR4 known inhibitor (two cyclam moieties tethered by a 1,4-phenylenebis(methylene)-bridge) [32] was used in the pre-docking run. After the calculation, the two cyclam moieties were removed leaving the *p*-xilil linker alone. Scaffolds' pre-docking was carried out with AUTODOCK 4.0 [33] using a 61x61x61 grid with a grid spacing of 0.375 Å and centred on the SDM-defined ligand-binding site. 100 independent Lamarckian genetic algorithm (LGA) runs were performed and pseudo-Solis and Wets minimization methods were applied by using default parameters. Lowest binding energy conformations were selected. Results from docking analyses were assessed by using the knowledge of the SDM data. On *Combinatorial* mode, fragments from LUDI internal library were bound to *p*-xilil and piridone moieties using a radius of 10 Å from selected scaffold linking points. For both modes, 20 molecules for each initial scaffold were generated.

All *de novo* designed compounds were ranked according to a scoring function. Ludi Energy Estimate 3 [15], PLP2 [16], LigScore2 [17], Jain [18], PMF [19], and consensus scoring functions were calculated. In a retrospective docking analysis using forty three active CXCR4 inhibitors from the literature [9], scoring functions Ludi Energy Estimate 3 and Ligscore2 were the ones that scored the resulting hit list better, so these scoring functions were used to select the designed compounds to be synthesized and tested. In order to validate that selected compounds accomplished the necessary molecular interactions to bind CXCR4, LIGANDFIT DS tool [34] was applied to dock them within the co-receptor binding site. DockScore [35] energy function was used. Scoring was also concatenated after docking, with in situ ligand minimization. The satisfactory results obtained were assessed using the knowledge of the SDM data.

Virtual Screening

Docking-based VS was performed using GOLD 4.0 [24] (ChemScore and GoldScore scoring functions) and HEX 4.8 [25] (Docked Energy scoring function) following the protocol described in Pérez-Nueno *et al*. [9]. Shape-based VS was performed using PARAFIT08 [26] (Tanimoto score in single query and consensus query modes), ROCS 2.3.1 [27] (Combo and Tanimoto scores), and HEX 4.8 [25] (Tanimoto score), by superposing each of the database compounds onto AMD3100 query in PARAFIT08 single query mode, ROCS, and HEX, and the consensus of AMD3100 [32], a macrocycle derivative [36], and a KRH derivative [37] in PARAFIT08 consensus query mode as described in Pérez-Nueno *et al*. [38]. Pharmacophore-based VS was performed using MOE [21] (Pharmacophore Elucidate and Pharmacophore Query modules) and Discovery Studio [28] (Hypogen and HipHop algorithms) following the protocol described in Pérez-Nueno *et al*. [23].

The chemical similarity search was carried out using QIKPROP [30] to calculate 46 descriptors and pharmaceutically relevant properties for all database compounds. The Tanimoto coefficient was calculated for all database compounds descriptors with respect to a) AMD3100 descriptors and b) N-(4-((3-(2-Methylpiperidin-1-yl)propylamino)methyl)benzyl)-3-(2-methylpiperidin-1-yl)propan-1-amine [39] descriptors using QIKSIM [31].

Chemistry General Methods

Infrared spectra were recorded in a Nicolet Magna 560 FTIR spectrophotometer. ^{1}H- and ^{13}C-NMR spectra were recorded in a Varian Gemini-300 operating at a field strength of 300 and 75.5 MHz, respectively. Chemical shifts are reported in parts per million (δ) and coupling constants (J) in Hz using, in the case of ^{1}H-NMR, TMS as an internal standard and setting, in the case of ^{13}C-NMR the reference at the signal of the solvent, 77.0 ppm ($CDCl_3$). Standard and peak multiplicities are designated as follows: s, singlet; d, doublet; t, triplet; q, quartet; quint, quintet; m, multiplet; br, broad signal. Mass spectra (m/z (%), EI, 70 eV) were obtained using a Hewlett Packard HP5988A spectrometer and high resolution mass spectra were obtained using a Micromass Autospec spectrometer. Elemental microanalyses were obtained on a Carlo-Erba CHNS-O/EA 1108 analyzer. Thin layer chromatographies (TLC) were performed on precoated sheets of silica 60 Polygram SIL N-HR/UV254 (Macherey Nagel art. 804023). Flash chromatography was performed using silica gel 35-70 μm (SDS art 2000027).

Synthesis of xxx General Procedure

((Experimental Details))

Synthesis of xxx General Procedure

((Experimental Details))

Synthesis of xxx General Procedure

((Experimental Details))

Antiviral Activity Evaluations

HIV-1 strains were titered in MT-4 cells after acute infection, and infectivity was measured by evaluating the cytopathic effect induced after 5-day cultures as described [40]. Anti-HIV activity (EC_{50}) and cytotoxicity (CC_{50}) measurements in MT-4 cells were based on viability of cells that had been infected or not infected with HIV-1, all exposed to various concentrations of the test compound. After the MT-4 cells were allowed to proliferate for 5 days, the number of viable cells was quantified by a tetrazolium-based colorimetric method (MTT method) as described.

Time of Drug Addition Studies

MT-4 cells were infected with HIV-1 NL4-3 at a multiplicity of infection of 0.5 and incubated for 1 h at 20 ºC in the presence or absence of test compounds. Cells were then washed twice in cool PBS and seeded in 96-well plates at a concentration of 2 × 105 cells/well (final volume 200 μL) at a temperature of 37 ºC. Test compounds, dextran sulfate, AMD3100, C34 or AZT were added at various times postinfection or cultured in the absence of drug. Test compounds were added at concentrations that completely block HIV replication (roughly 100-fold higher than the determined EC_{50}) of each drug in the standard assay performed with MT-4 cells. Virus production was measured by p24 antigen determination in the cell supernatant after 30 h postinfection with a commercial p24 antigen ELISA (Innogenetics, Barcelona, Spain) [41].

Acknowledgements

This work was supported in part by the Fundació Marató de TV3 project 020930 and the Spanish Ministerio de Educación y Ciencia project SAF-2007-6322 (J.I.B. and B.C.) and BFU-200600966 (J.A.E.). L. Ros-Blanco and V. I. Pérez-Nueno hold a FI scholarship from Generalitat de Catalunya and S. Pettersson from IQS.

Keywords: *de novo* design · virtual screening · molecular modeling · antiviral agents · medicinal chemistry

[1] UNAIDS. AIDS epidemic update: December 2007. http://www.unaids.org/en/KnowledgeCentre/HIVData/EpiUpdate/EpiUpdArchive/2007/default.asp (accessed Nov. 11, 2008).
[2] J. A. Este, A. Telenti, *Lancet* **2007**, *370*, 81-88.
[3] N. J. Anthony, *Curr. Top. Med. Chem.* **2004**, *4*, 979-990.
[4] I. Markovic, K. A. Clouse, *Curr. HIV Res*. **2004**, *2*, 223-234.
[5] M. R. Nelson, *AIDS 2008: Update on Antiretroviral Therapy: Resistance Issues and Investigational Agents* (Mexico City, Mexico) **2008**, "AIDS 2008: Investigational Antiretroviral Drugs" to be found under http://www.medscape.com/viewarticle/582064, **2008**.
[6] E. De Clercq, *Med. Chem. Res.* **2004**, *13*, 439-478.
[7] E. De Clercq, *Expert Opin. Emerg. Drugs* **2005**, *10*, 241-274.
[8] W. M. Kazmierski, J. P. Peckman, M. Duan, T. P. Kenakin, S. Jenkinson, K. S. Gudmundsson, S. C. Piscitelli, P. L. Feldman, *Curr. Med. Chem. Anti-Infect. Agents* **2005**, *4*, 133-152.
[9] V. I. Pérez-Nueno, D. W. Ritchie, O. Rabal, R. Pascual, J. I. Borrell, J. Teixidó, *J. Chem. Inf. Model.* **2008**, *48*, 509-533.
[10] H.-J. Böhm, *J. Comp. Aided Molec. Design* **1992**, *6*, 61-78.
[11] L.-O. Gerlach, R. T. Skerlj, G. J. Bridger, T. W. Schwartz, *J. Biol. Chem.* **2001**, *276*, 14154-14160.
[12] Hatse, S.; Princes, K.; Vermeire, K.; Gerlach, L.-O.; Rosenkilde, M. M.; Schwartz, T. W.; Bridger, G.; De Clercq, E.; Schols, D. *FEBS Letters* **2003**, *546*, 300-306.
[13] Brelot, A.; Heveker, N.; Montes, M.; Alizon, M. *J. Biol. Chem.* **2000**, *275*, 23736–23744.
[14] S. Hatse,; Princen, K.; Gerlach, L.-O.; Bridger, G.; Henson, G.; Clercq, E.; Schwartz, T. W.; Schols, D. *Mol. Pharmacol.* **2001**, *60*, 164–173.
[15] H. J. Böhm, *J. Comp. Aided Molec. Design* **1994**, *8*, 243-256.
[16] D. K. Gehlhaar, G. M. Verkhivker, P. A. Rejto, C. J. Sherman, D. R. Fogel, L. J. Fogel, S. T. Freer, *Chem. Biol.* **1995**, *2*, 317-324.
[17] M. Waldman, *et al*. U.S. Patent Application No. 20020038184, **2002**.
[18] I. Muegge, Y. C. Martin, *J. Med. Chem.* **1999**, *42*, 791-804.
[19] D. K. Gehlhaar, D. Bouzida, P. A. Rejto, In "Rational Drug Design: Novel Methodology and Practical Applications", *ACS symposium No 719*, (Washington, DC) **1999**; L. Parrill, M. Rami Reddy, Ed.; *American Chemical Society*: Washington, **1999**, 292.
[20] Irwin and Shoichet, *J. Chem. Inf. Model.* **2005**, *45*, 177-82.
[21] MOE, Molecular Operating Environment, Chemical Computing Group Inc., Montreal, QC (Canada) **2006**.
[22] J. Gasteiger, M. Marsili, *Tetrahedron* **1980**, 36, 3219–3228.
[23] V. I. Pérez-Nueno, S. Pettersson, D. W. Ritchie, J. I. Borrell, J. Teixidó, *J. Chem. Inf. Model.* **2008**, *48*, .
[24] GOLD 4.0, The Cambridge Crystallographic Data Centre, Cambridge (UK) **2008**.
[25] D. W. Ritchie, G. J. L. Kemp, *Proteins: Struct., Funct., Genet.* **2000**, *39*, 178- 194.
[26] D. W. Ritchie, G. J. L. Kemp, *J. Comput. Chem.* **1999**, *20*, 383-395.
[27] ROCS 2.3.1, OpenEye Scientific Software, Santa Fe, NM (USA), **2007**.
[28] Discovery Studio, Version 1.7, Accelrys Inc., San Diego, CA (USA) **2006**.
[29] Wang, R.; Wang, S. *J. Chem. Inf. Comput. Sci.* **2001**, *41*, 1422-1426.
[30] QikProp, version 2.3; Schrödinger, Inc.: New York, **2005**.
[31] W. L. Jorgensen, QikSim, version 2.3; Yale University: New Haven, CT, **2005**.
[32] G. A. Donzella, D. Schols, S. W. Lin, J. A. Este, K. A. Nagashima, P. J. Maddon, G. P. Allaway, T. P. Sakmar, G. Henson, E. De Clercq, J. P. Moore, *Nat. Med.* **1998**, *4*, 72-77.
[33] AutoDock 4.0, Department of Molecular Biology, The Scripps Research Institute, MB-5, La Jolla, CA (USA) **2005**.
[34] C.M. Venkatachalam, X. Jiang, T. Oldfield, M. Waldman, *J. Mol. Graph. Modell.* **2003**, *21*, 289-307.
[35] M. Lim-Wilby, J. Jiang, M. Waldman, C. M. Venkatachalam, In "Virtual high throughput screening using LigandFit as an accurate and very fast tool for docking, scoring, and ranking", *224th ACS National Meeting and Exposition*, (Boston, USA) **2002**; Wendy Warr & Associates; *Chemical Information and Computation*: Massachusetts, **2002**, 87-91.
[36] G. J. Bridger, R. T. Skerlj, S. Padmanabhan, S. A. Martellucci, G. W. Henson, S. Struyf, M. Witvrouw, D. Schols, E. De Clercq, *J. Med. Chem.* **1999**, *42*, 3971-3981.
[37] K. Ichiyama, S. Yokohama-Kumakura, Y. Tanaka, R. Tanaka, K. Hirose, K. Bannai, T. Edamatsu, M. Yanaka, Y. Niitani, N. Miyako-Kurosaki, H. Takaku, Y. Koyanagi, N. Yamamoto, *Proc. Natl. Acad. Sci. U.S.A.* **2003**, *100*, 4185-4190.
[38] V. I. Pérez-Nueno, D. W. Ritchie, J. I. Borrell, J. Teixidó, *J. Chem. Inf. Model.* **2008**, *48*, .
[39] S. Pettersson, V. I. Pérez-Nueno, L. Ros-Blanco, R. Puig de La Bellacasa, O. Rabal, X. Batllori, B. Clotet, I. Clotet-Codina, M. Armand-Ugón, J. Esté, J. I. Borrell, J. Teixidó, *ChemMedChem* **2008**, *3*, 1549 – 1557.
[40] G. Moncunill, M. Armand-Ugón, B. Clotet, J. A. Esté, *AIDS* **2008**, *22*, 23–31.
[41] G. Moncunill, M. Armand-Ugón, I. Clotet, E. Pauls, E. Ballana, A. Llano, B. Romagnoli, J. W. Vrijbloed, F. O. Gombert, B. Clotet, S. De Marco, J. A. Esté, *Mol. Pharmacol.* **2008**, *73*, 1264–1273.

Received: ((will be filled in by the editorial staff))
Published online: ((will be filled in by the editorial staff))

Comparison of ligand based shape matching and structure based docking methods for identifying HIV entry inhibitors for the CXCR4 and CCR5 receptors

Violeta Pérez-Nueno[1], Dave Ritchie[2], José I. Borrell[1],Jordi Teixidó[1]

[1] Grup d'Enginyeria Molecular, Institut Químic de Sarrià (IQS), Universitat Ramon Llull, Via Augusta 390, E-08017-Barcelona (Spain). E-mail: j.teixido@iqs.url.edu

[2] Department of Computing Science, King's College, University of Aberdeen, Aberdeen, UK. E-mail: dritchie@csd.abdn.ac.uk

Introduction

G protein-coupled receptors (GPCRs) are one of the most exploited groups of drug targets. We compare the application of structure-based and ligand-based virtual screening tools to find potential HIV entry inhibitors for the CXCR4 and CCR5 receptors using structure-based docking tools (AUTODOCK3.0, GOLD3.0.1) and ligand-based shape matching software (PARASHIFT06, ROCS2.2).

The comparison between these methods was based on virtual screening of a library containing some 4700 drug-like molecules and different known CXCR4 and CCR5 inhibitors as reference sets. For each receptor we determined the enrichment factors and the diversity in the retrieved molecular scaffolds in the virtual hit lists. Overall, we find that ligand based shape matching searches give better results than structure-based docking tools especially for CXCR4.

Ligand Based Shape Matching Virtual Screening (PARASHIFT 06, ROCS 2.2)

PARAFIT [1] superposes and compares molecules using spherical harmonic (SH) expansions of the molecular surface and local surface properties calculated by PARASURF [2]. ROCS superposes molecules by a solid-body optimization process that maximizes their Gaussian volume overlaps [3]. We used the PARAFIT and ROCS Shape Tanimoto scores (shape fit) and the ROCS Combo score (shape fit + chemistry) to screen the databases. This ligand based virtual screening was performed by superposing every one of the *database* compounds onto a given *query* molecule (TAK779 and AMD3100 for CCR5 and CXCR4, respectively). Some example superpositions are shown below. In these figures the *database* compound is in blue/red and the *query* molecule is colour according to atom type (blue:nitrogen, green:carbon, red:oxygen). These examples are shown as spherical harmonic surface overlays drawn using HEX [4].

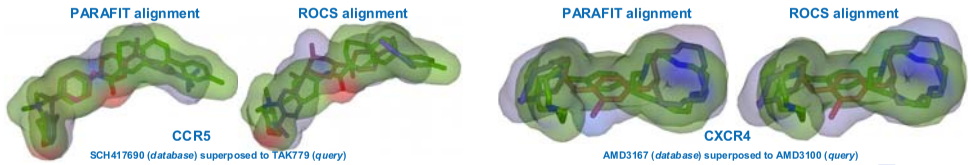

SCH417690 (*database*) superposed to TAK779 (*query*)

AMD3167 (*database*) superposed to AMD3100 (*query*)

Structure Based Docking Virtual Screening (AUTODOCK 3.0, GOLD 3.0.1)

The CCR5 and CXCR4 receptors were homology modelled with MODELLER (backbone + loops) [5] using bovine rhodopsin as the template. The CXCR4 loops were refined with CONGEN [6]. Docking was performed using AUTODOCK [7] and GOLD [8]. In GOLD, constraints were specified in order to obtain binding modes which involved key residues previously identified by site-directed mutagenesis. The Docked Energy scoring function (AUTODOCK), and the GoldScore and ChemScore scoring functions (GOLD) were used to rank the ligand databases. A consensus rank-by-rank score was also calculated using these three scoring functions.

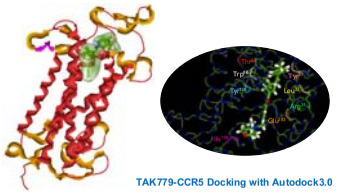

TAK779-CCR5 Docking with Autodock3.0

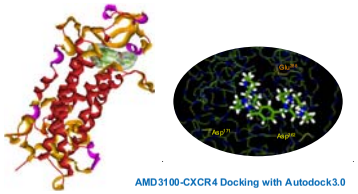

AMD3100-CXCR4 Docking with Autodock3.0

Scaffold Diversity Analysis

The plots below sumarize the retrieval rates for 13 families of CCR5 and 4 families of CXCR4 ligands. The CCR5 families are *SCH derivatives, diketopiperazine, anilide piperidine N/Oxide, AMD derivatives, piperidine, aminopiperidine, 1,3,4-trisubstituted pyrrolidinepiperidine, phenylcyclohexilamine, TAK derivatives, 1-phenyl-1,3-propanodiamine, 1,3,5-trisubstituted five ring, N,N'-diphenylurea, 5-oxopyrrolidine-3-carboxamide*. The CXCR4 families are *tetrahydro-quinolinamines, KRH derivatives, macrocycles, AMD derivatives*.

CCR5

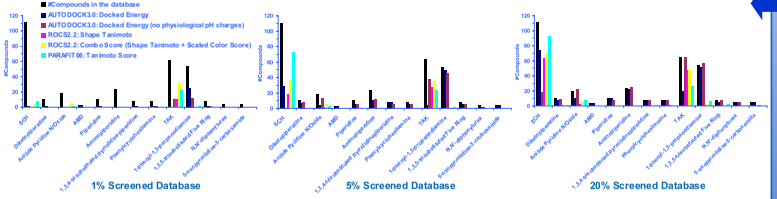

1% Screened Database | 5% Screened Database | 20% Screened Database

CXCR4

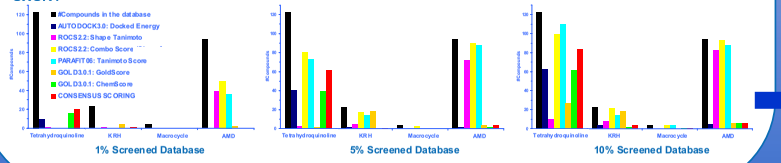

1% Screened Database | 5% Screened Database | 10% Screened Database

Virtual Databases

Our virtual databases comprise 288 actives against CXCR4 [9] (5 different scaffolds), 333 CCR5 actives [9] (13 scaffolds) and around 4700 inactive drug-like compounds from the MAYBRIDGE [10] library.

All ligands were initially protonated at physiological pH, assigned Gasteiger partial charges and energy minimized using the MMFF94 force field. The ligands were then located approximately into their respective receptor binding pockets with the FlexAlign module of MOE06 [11] using the docked TAK779 and AMD3100 as superposition templates for CCR5 and CXCR4, respectively.

Conclusions

The Diversity Analysis graphs (left) show that, at 10% screened database, all of the CXCR4 scaffolds are found, whereas for CCR5 only AUTODOCK find them all. Shape matching methods find first compounds with a scaffold similar to the query. The Enrichment Comparison results (right) for CCR5 show that AUTODOCK, ROCS Combo Score and PARAFIT all give comparable but somewhat modest enrichments. The corresponding results for CXCR4 show that consensus scoring is the best of the docking methods but is nonetheless worse than the ligand based screening and that the similarity based functions give much better enrichments for CXCR4 than for CCR5. For shape-only comparisons, PARAFIT gives generally better results than ROCS and often gives comparable results to the ROCS Combo Score in both cases.

These results demonstrate that for these receptors (especially CXCR4) ligand-based shape matching searches give better results than structure-based docking tools. We are applying these virtual screening tools for the identification of new anti-HIV compounds whose activity is currently being tested [12] [13].

Enrichment Comparison

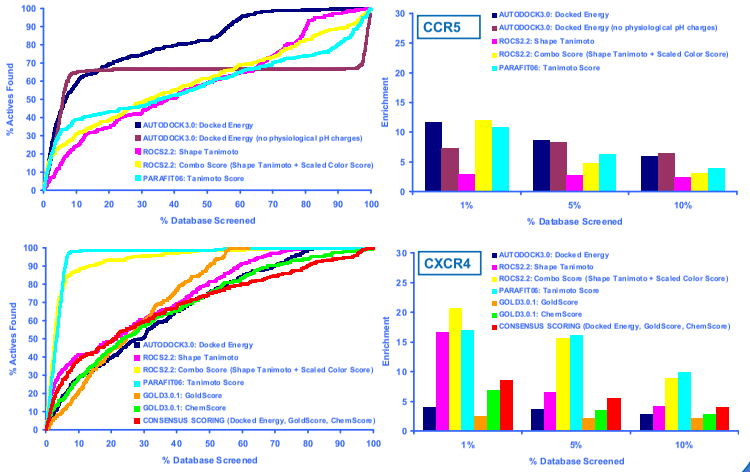

References

1. D. W. Ritchie, G. J. L. Kemp; Fast computation, rotation and comparison of low resolution spherical harmonic molecular surfaces. *J. Comp. Chem.* 1999, 20(4):383-395.
2. L. Mavridis, B. D. Hudson, D. W. Ritchie; Towards High Throughput 3D Virtual Screening Using Spherical Harmonic Representations. (*Accepted*)
3. J. A. Grant, M. A. Gallardo, B. J. Pickup; A fast method of molecular shape comparison. A simple application of a Gaussian description of molecular shape. *J.Comp. Chem.* 1996, 17:1653.
4. D. W. Ritchie, G. J. L. Kemp; Protein docking using spherical polar Fourier Correlations. *Proteins: Struct. Func. Genet.* 2000, 39: 178-194.
5. A. Sali, T. L. Blundell; Comparative protein modelling by satisfaction of spatial restrains. *Proteins* 1989, 5:355-373.
6. R. E. Bruccolieri; Application of Systematic Conformational Search to Protein Modeling. *Molecular Simulations* 1993, 10, 151-174.
7. G. M. Morris, D. S. Goodsell, R. S. Halliday, W. Hart, R. K. Belew, A. J. Olson; Automated Docking Using a Lamarckian Genetic Algorithm and Empirical Binding Free Energy Function. *J. Computational Chemistry* 1998, 19:1639-1662.
8. M. L. Verdonk, J. C. Cole, M. J. Hartshorn, C. W. Murray, R. D. Taylor; Improved Protein-Ligand Docking Using GOLD. *Proteins: Structure, Function, and Genetics* 2003, 52:609-623.
9. W. M. Kazmierski, J. P. Peckman, M. Duan, T. P. Kenakin, S. Jenkinson, K. S. Gudmundsson, S. C. Piscitelli, P. L. Feldman; Recent Progress in the Discovery of New CCR5 and CXCR4 Chemokine Receptor Antagonists as Inhibitors of HIV-1 Entry. Part 2. *Curr Med Chem – Anti Infective Agents* 2005, 4:133-152.
10. Maybride Bringing life to drug discovery TM. Fisher Scientific International. Maybridge CD features: Maybridge Databases Autumn 2005.
11. MOE, Molecular Operating Environment. Distributor: Chemical Computing Group, 1010 Sherbrooke St. West, #910, Montreal, Canada H3A.
12. J. Teixidó, J. I. Borrell, S. Nonell, X. Batllori, S. Pettersson, L. Ros, R. Puig de la Bellacasa, M. O. Rabal, V. Pérez, J. Esté, I. Clotet, M. Armand-Ugón; Nuevos sistemas polinitrogenados como agentes anti-VIH, *Spanish Patent No. ES200602764*, Oct. 26, 2006.
13. S. Pettersson , I. Clotet-Codina , J. A. Esté , J. I. Borrell , J. Teixidó; Recent advances in combinatorial chemistry applied to development of anti-HIV drugs. *Mini Rev Med Chem.* 2006, 6(1):91-108.

Acknowledgements

Violeta Pérez-Nueno would like to thank the Institut Químic de Sarrià (IQS) for a predoctoral grant.

We thank OpenEye Scientific Software Inc. for providing an Academic Licence for ROCS, and we are grateful to Cepos Insilico Ltd. for providing a pre-release version of PARASURF.

This research was supported by the Department of Computing Science, University of Aberdeen, and the Organic Chemistry and Biochemistry Department, Institut Químic de Sarrià, Universitat Ramon Llull, Barcelona.

http://gem.iqs.url.edu

Nous fàrmacs per bloquejar l'entrada del VIH a les cèl·lules

Universitat Ramon Llull

La Síndrome d'Immunodeficiència Adquirida (SIDA) ha esdevingut una terrible malaltia d'abast global. D'acord amb les dades recollides per l'Organització Mundial de la Salut, s'estima que actualment 39 milions de persones conviuen amb aquesta malaltia i que el 2006 han aparegut 4,3 milions de casos nous. La principal causa de la SIDA és la infecció de cèl·lules hoste pel virus de la immunodeficiència humana (VIH). Les teràpies anti-retrovirals actuals (ART) contra la SIDA, basades generalment en inhibidors de la transcriptasa reversa i de la proteasa, poden controlar la propagació del virus i arribar a aconseguir millorar la qualitat de vida dels pacients, però no poden arribar a eliminar el virus del cos i poden tenir efectes secundaris no desitjats. Diversos investigadors del grup de recerca del Prof. Jordi Teixidó de l'Institut Químic de Sarrià (IQS) consideren com a alternativa molt prometedora el desenvolupament de noves teràpies que puguin prevenir l'entrada del VIH a les cèl·lules hoste i, per tant, bloquejar la primera etapa crucial del procés d'infecció del virus.

"El descobriment del procés d'infecció de cèl·lules per VIH mostra que aquest s'inicia mitjançant la fusió del virus amb la cèl·lula diana gràcies a la unió de la glicoproteïna gp120 del virus amb el receptor proteic CD4 i els coreceptors CXCR4 o CCR5 de la cèl·lula diana", explica Jordi Teixidó. A partir d'aquest descobriment ha aparegut un interès considerable pel desenvolupament de nous lligands els quals modulin els canvis conformacionals dels coreceptors i, per tant, bloquegin la fusió del virus a les cèl·lules.

Així, aquest grup de recerca està utilitzant diferents aproximacions computacionals i experimentals per identificar compostos actius bloquejadors dels coreceptors CXCR4 i CCR5 que puguin, per tant, inhibir l'entrada del VIH a les cèl·lules. "Generalment, aquestes aproximacions tenen com a objectiu el cribratge ràpid de grans quimioteques de compostos candidats a possibles fàrmacs. Actualment, hom es refereix a aquestes aproximacions computacionals com a mètodes de cribratge virtual (*virtual screening*). Així, el cribratge virtual de quimioteques de compostos ha esdevingut una alternativa aproximada però útil als mètodes de cribratge real al laboratori de grans quimioteques de compostos (*high-throughput screening methods*)", explica Teixidó. En el cribratge virtual, els compostos poden ser seleccionats i filtrats mitjançant recerques de semblança 2D o 3D, aplicant tècniques d'anàlisi de diversitat i avaluant la interacció o acoblament (*docking*) de compostos contra una proteïna diana. Els compostos poden també ser seleccionats en funció de les seves propietats físiques predites (estudis ADMET) i en funció de la seva accessibilitat sintètica. Aquestes aproximacions poden ser aplicades a conjunts de compostos, ja sigui de manera seqüencial o en paral·lel.

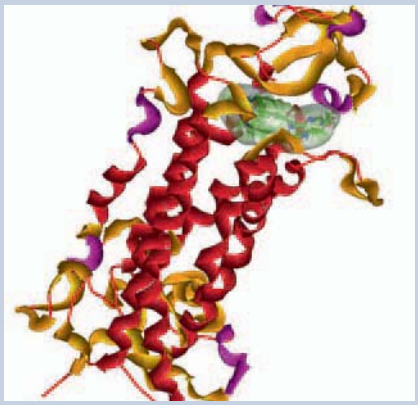

Figura 1. Cribatge virtual basat en l'estructura: *Docking* CXCR4-AMD3100.

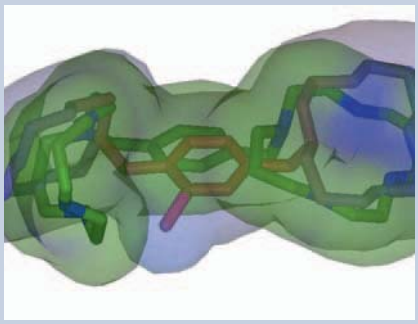

Figura 2. Cribatge virtual basat en els lligands: acarament de forma (*shape matching*). Molècules AMD3100 i AMD 3167.

En termes generals, aquests mètodes poden ser classificats com mètodes basats en l'estructura (*structure-based methods*), utilitzats quan l'estructura del receptor és coneguda, com per exemple els mètodes de *docking* i *ligand-based searches*; o mètodes basats en els lligands, usats quan el procés de cribratge només té en compte la caracterització de compostos actius coneguts, per exemple en la comparació de propietats 2D/3D utilitzant actius coneguts com a referència o en la construcció de models farmacofòrics. Les tècniques de cribratge virtual es poden aplicar a conjunts de compostos actius coneguts, el que s'anomena anàlisi retrospectiva, amb la finalitat d'establir paràmetres apropiats i validar el protocol de cribratge. Un cop validat, també pot ser aplicat per seleccionar compostos dels quals es vol testar la seva activitat i és anomenat anàlisi prospectiva. Aparentment, els mètodes basats en l'estructura, els quals utilitzen estructures de la proteïna diana conegudes o modelades/construïdes, haurien de ser els que proporcionessin els millors models de cribratge, ja que persegueixen avaluar les interaccions proteïna-lligand. No obstant això, l'ús d'aproximacions basades en l'estructura depèn críticament de la qualitat de les estructures de la proteïna d'estudi disponibles i del programari d'acoblament emprat. Per aquest motiu, els diversos mètodes computacionals emprats dins el camp del descobriment de fàrmacs sovint utilitzen una combinació d'ambdues tècniques, basades en l'estructura i basades en els lligands.

Com expliquen els integrants del grup, en aquest projecte s'ha construït una base de dades de compostos actius procedents de la literatura (molècules derivades de l'AMD3100, macrocicles, anàlegs del KRH1636, compostos del tipus complex dipicolilamina-zinc(II) i tetrahidroquinolines com a inhibidors de CXCR4; derivats del SCH-C i 13 famílies més com a inhibidors de CCR5), compostos sintetitzats al grup i compostos inactius *drug like* procedents de la biblioteca Maybridge amb propietats similars als compostos actius.

Els compostos sintetitzats al grup formen part d'una quimioteca virtual dissenyada com a anàlegs de l'AMD3100 (compost de referència inhibidor del coreceptor CXCR4), és a dir, sistemes polinitrogenats separats per un espaiador *p*-fenilènic. D'aquesta quimioteca s'ha seleccionat un conjunt de compostos diversos mitjançant el programari propi del grup, PRALINS, per tal de dur a terme la seva síntesi i assaig de l'activitat (en col·laboració amb el grup del Dr. Esté del laboratori de retrovirologia de l'IrsiCaixa). Els compostos actius trobats s'han inclòs com a actius de la base de dades. Per trobar altres compostos actius s'han emprat les tècniques de cribratge virtual.

Per la banda de mètodes basats en el lligand, s'han realitzat estudis de QSAR (amb el programari MOE), a partir dels quals s'obté una funció que relaciona l'estructura de molècules amb la seva activitat d'una manera quantitativa, disseny de farmacòfors o models tridimensionals en els quals es defineixen les característiques essencials que han de tenir les molècules per interaccionar amb els receptors, *shape matching* (PARASHIFT, ROCS) amb el qual es defineix la forma que han de complir les molècules per presentar activitat.

Per als mètodes basats en l'estructura, és necessari disposar de l'estructura del receptor. Les dianes són els coreceptors CXCR4 i CCR5, els quals pertanyen a la família de les proteïnes GPCR (*G-protein coupled receptors*). L'única estructura que es troba cristal·litzada d'aquesta família és la rodopsina bovina, la qual s'utilitza com a referència en el modelatge per homologia dels coreceptors (MODELLER, CONGEN). Un cop obtinguts els models s'empren les tècniques d'acoblament (AUTODOCK, GOLD, FRED) per avaluar les interaccions proteïna-lligand mitjançant una funció de puntuació (*scoring*). L'ús de tècniques de dinàmica molecular, costoses computacionalment, permeten refinar les conformacions obtingudes a l'acoblament proteïna-lligand.

Noves teràpies per prevenir l'entrada del VIH a les cèl·lules hoste com a possible alternativa a les teràpies antiretrovirals actuals

A més, s'han realitzat estudis de *novo design* (CERIUS) per tal de trobar esquelets (*scaffolds*) candidats a ser actius o modificar les molècules actives ja sintetitzades pel grup. S'utilitza l'estructura dels receptors per identificar la geometria i el tipus d'interacció que han de tenir els lligands per unir-s'hi.

Per validar els models i fixar els millors paràmetres de cadascun d'ells s'ha realitzat una anàlisi retrospectiva del cribratge virtual emprant les bases de dades d'actius i d'inactius confeccionades. Un cop determinats els millors models es realitza l'anàlisi prospectiva per tal d'establir un rànquing de possibles nous inhibidors de CXCR4 i CCR5 per ser sintetitzats als laboratoris de l'IQS. ■

Grup d'Enginyeria Molecular de l'Institut Químic de Sarrià.

Biological Profiling of Anti-HIV Agents using in Silico Techniques: Insights into CCR5 Ligands Binding Through Homology Buildings, 3D-QSAR, Docking and Shape Matching Virtual Screening

Antonio Carrieri, PhD
Faculty of Pharmacy, University of Bari
carrieri@farmchim.uniba.it

XXth International Symposium on Medicinal Chemistry
Vienna, 4th September 2008

SPHERICAL HARMONIC MOLECULAR SURFACES

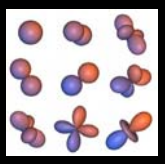

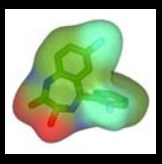

PARAFIT: SCAFFOLD-FREE SUPERPOSITIONS

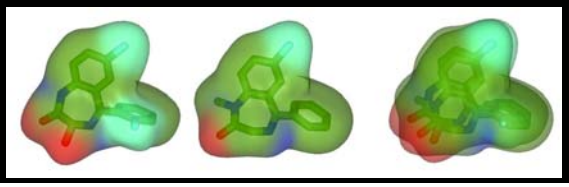

SHAPE-BASED VIRTUAL SCREENING

PARAFIT CONSENSUS SHAPE

- ✓ The three "different scaffold" reference compounds of Berlex dataset (cmpd01x, cmpd02x, cmpd10h).

Consensus shape (3 active compounds) | cmpd1 | cmpd2 | cmpd10h

- ✓ The six PCA selected compounds of Berlex dataset.

Consensus shape (6 PCA compounds) | cmpd1 | cmpd61 | cmpd7g | cmpd9 | cmpd10j | cmpd36

SHAPE-BASED VIRTUAL SCREENING

- ✓ 69 Berlex dataset cmpds
- ✓ 3388 drug like cmpds with 1D properties similar to Berlex active cmpds

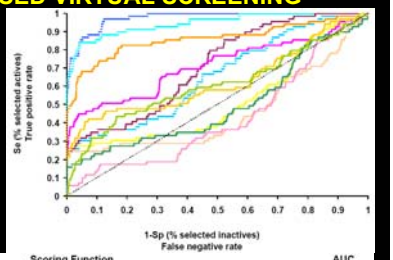

Scoring Function	AUC
PARAFIT08: Shape consensus Tanimoto (3 active compounds)	0.976
PARAFIT08: Shape consensus Tanimoto (6 PCA selected compounds)	0.947
ROCS2.2: Combo Score (Shape Tanimoto + Scaled Color Score) 10 query conf & 10 conf/database compd	0.861
ROCS2.2: Shape Tanimoto 10 query conf & 10 conf/database compound	0.714
HEX4.8: Shape Tanimoto (query cmpd10h from 3D-QSAR)	0.710
PARAFIT08: Shape Tanimoto (query cmpd10h from 3D-QSAR)	0.655
ROCS2.2: Combo Score (Shape Tanimoto + Scaled Color Score) 10 conf/database compound	0.628
QIKPROP/QIKSIM (actives averaged descriptors): Tanimoto Score	0.609
ROCS2.2: Combo Score (Shape Tanimoto + Scaled Color Score) (query cmpd10h from 3D-QSAR)	0.521
QIKPROP/QIKSIM (cmpd10h descriptors): Tanimoto Score	0.495
ROCS2.2: Shape Tanimoto (query cmpd10h from 3D-QSAR)	0.456
ROCS2.2: Shape Tanimoto 10 conf/database compound	0.426

SHAPE-BASED VIRTUAL SCREENING

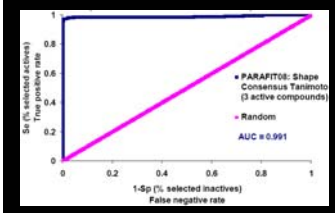

- ✓ 424 CCR5 known inhibitors
- ✓ 4696 commercial cmpds (Maybridge Screening Collection)

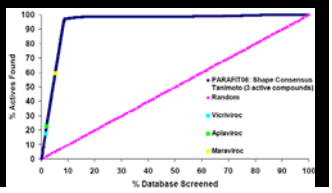

ACKNOWLEDGEMENT

Alessandra Fano
Pharmaceutical Chemistry Department, University of Bari, Italy

Dave Ritchie
Computer Chemistry Department, University of Aberdeen, Scotland

Violeta I. Pérez-Nueno, Jordi Teixidó
Grup d'Enginyeria Molecular, Institut Químic de Sarrià, Barcelona, Spain

Analysis of ligand based shape matching and structure based docking methods for identifying HIV entry inhibitors for the CXCR4 and CCR5 receptors

Violeta I. Pérez-Nueno[1], Dave Ritchie[2], José I. Borrell[1], Jordi Teixidó[1]

[1] Grup d'Enginyeria Molecular, Institut Químic de Sarrià (IQS), Universitat Ramon Llull, Via Augusta 390, E-08017-Barcelona (Spain). E-mail: j.teixido@iqs.url.edu

[2] Department of Computing Science, King's College, University of Aberdeen, Aberdeen, UK. E-mail: dritchie@csd.abdn.ac.uk

Introduction

G protein-coupled receptors (GPCRs) are one of the most exploited groups of drug targets. We compare the application of structure-based and ligand-based virtual screening tools to find potential HIV entry inhibitors for the CXCR4 and CCR5 receptors using structure-based docking tools (AUTODOCK 3.0, GOLD 3.0.1, FRED 2.2.1 and HEX 4.8) and ligand-based shape matching software (PARASHIFT 06, ROCS 2.2 and HEX 4.8).
The comparison between these methods was based on virtual screening of a library containing 4696 presumed inactive drug-like compounds from the MAYBRIDGE [1] library, 248 CXCR4 actives (5 scaffolds) and 354 CCR5 actives (13 scaffolds) compiled from the literature [2] as reference sets. All ligands were initially protonated at physiological pH, assigned Gasteiger partial charges and energy minimized using the MMFF94 force field. The ligands were then located approximately into their respective receptor binding pockets with the FlexAlign module of MOE06 [3] using the docked TAK779 and AMD3100 as superposition templates for CCR5 and CXCR4, respectively. For each receptor we determined the enrichment factors and the diversity in the retrieved molecular scaffolds in the virtual hit lists. Overall, we find that ligand based shape matching searches give better results than structure-based docking tools especially for CXCR4 [4]. A new spherical harmonic shape-based virtual screening approach has been developed to improve CCR5 results.

Ligand Based Shape Matching Virtual Screening (PARASHIFT 06, ROCS 2.2, HEX 4.8)

PARAFIT [5] superposes and compares molecules using spherical harmonic (SH) expansions of the molecular surface and local surface properties calculated by PARASURF [6]. ROCS superposes molecules by a solid-body optimization process that maximizes their Gaussian volume overlaps [7]. We used the PARAFIT and ROCS Shape Tanimoto scores (shape fit) and the ROCS Combo score (shape fit + chemistry) to screen the databases. Similarly, HEX [8] 3D shape Tanimoto scores were calculated by maximizing the 3D density overlap between pairs of colocated molecules using default HEX search parameters. The ligand based virtual screening was performed by superposing every one of the *database* compounds onto a given *query* molecule (TAK779 and AMD3100 for CCR5 and CXCR4, respectively). Some example superpositions are shown below. In these figures the *database* compound is in blue/red and the *query* molecule is colour according to atom type (blue:nitrogen, green:carbon, red:oxygen). These examples are shown as spherical harmonic surface overlays drawn using HEX.

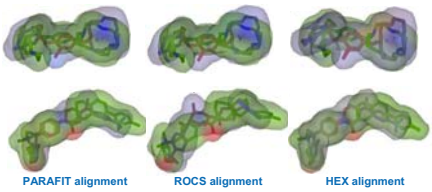

CXCR4

AMD3167 (*database*) superposed to AMD3100 (*query*)

CCR5

SCH417690 (*database*) superposed to TAK779 (*query*)

PARAFIT alignment | ROCS alignment | HEX alignment

Structure Based Docking Virtual Screening (AUTODOCK 3.0, GOLD 3.0.1, FRED2.2, HEX 4.8)

The CCR5 and CXCR4 receptors were homology modelled with MODELLER (backbone + loops) [9] using bovine rhodopsin as the template. The CXCR4 loops were refined with CONGEN [10]. Docking was performed using AUTODOCK [11], GOLD [12], FRED [13] and HEX [8]. In GOLD, constraints were specified in order to obtain binding modes which involved key residues previously identified by site-directed mutagenesis. The Docked Energy scoring function (AUTODOCK), the GoldScore and ChemScore scoring functions (GOLD), the Chemscore, Oechemscore, Shapegauss, Chemgauss3, Screenscore, Plp, a consensus of these scoring functions (FRED), and the Docked energy scoring function (HEX) were used to rank the ligand databases. A consensus rank-by-rank score was also calculated using Autodock Docked Energy, Goldscore and ChemScore scoring functions.

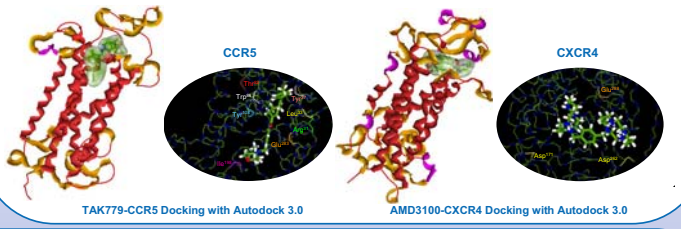

TAK779-CCR5 Docking with Autodock 3.0 | AMD3100-CXCR4 Docking with Autodock 3.0

Ligand Based Shape Matching: Spherical Harmonic Shape-Based Consensus Approach (PARAFIT 8.01)

A new spherical harmonic shape-based virtual screening approach to classify and model diverse groups of molecules has been developed in PARAFIT 8.01. It uses a fast superposition technique based on spherical harmonic decompositions of surface shapes in order to perform rapid and exhaustive comparison and clustering of multiple combinations of ligands in multiple trial superpositions. It allows the construction of a consensus 3D shape query from a set of known binders by calculating the average of their individual expansion coefficient vectors. Two examples of shape consensus superpositions are shown below.

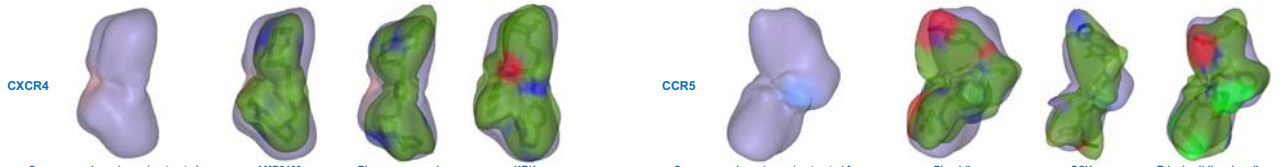

Consensus shape (*query*) extracted from AMD3100, Bisazamacrocycle and KRH derivates | AMD3100 superposed to the consensus shape | Bisazamacrocycle superposed to the consensus shape | KRH superposed to the consensus shape

Consensus shape (*query*) extracted from Piperidine, Trispyrrolidinepiperidine and SCH derivates | Piperidine superposed to the consensus shape | SCH superposed to the consensus shape | Trispirrolidinepiperdine superposed to the consensus shape

Enrichment Comparison and Scaffold Diversity Analysis

The plots below sumarize the comparison of docking and shape matching enrichments for CXCR4 and CCR5 receptors. (a) Enrichment curves obtained using several docking and shape matching protocols. (b) Enrichment factor for actives found within the top-ranking 1%, 5% and 10% compounds of the screened databases. The scaffold diversity plots (c, d, e) sumarize the retrieval rates for 4 families of CXCR4 and 13 families of CCR5 ligands.

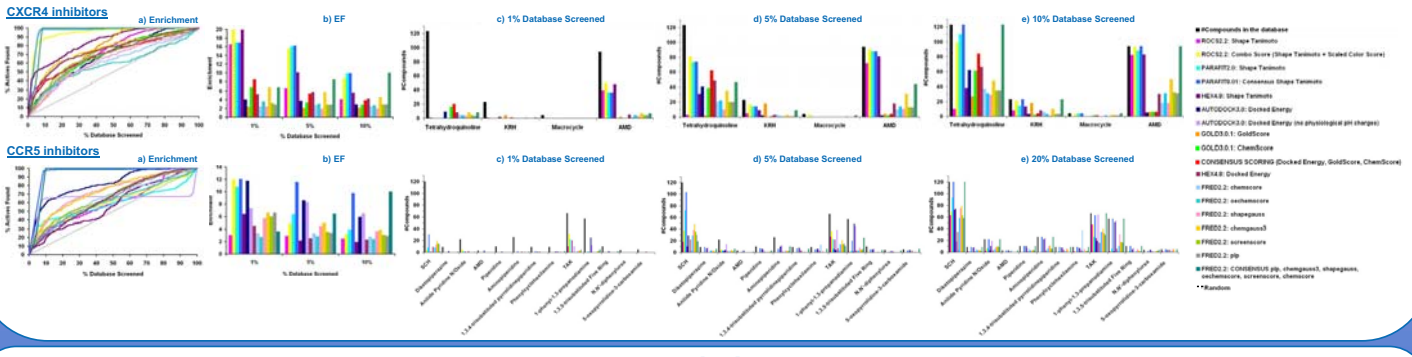

Conclusions

The Diversity Analysis graphs show that, at 10% screened database, all of the CXCR4 scaffolds are found, whereas for CCR5 only AUTODOCK and FRED consensus find them all. Shape matching methods find first compounds with a scaffold similar to the query. The Enrichment Comparison results for CCR5 show that AUTODOCK, ROCS Combo Score, PARAFIT, FRED Chemgauss3, Consensus and Shapegauss all give comparable but somewhat modest enrichments. The corresponding results for CXCR4 show that Consensus Scoring, Chemgauss3 and FRED consensus are the best of the docking methods but are nonetheless worse than the ligand based screening and that the similarity based functions give much better enrichments for CXCR4 than for CCR5. For shape-only comparisons, PARAFIT shape Tanimoto gives generally better results than ROCS and often gives comparable results to the ROCS Combo Score in both cases. We are applying these tools for the identification of anti-HIV compounds whose activity is currently being tested [14] [15].

Overall, our results show that CXCR4 model obtains good enrichments. However, CCR5 enrichments are not as good as those for CXCR4. The CCR5 seems to have a larger binding pocket than CXCR4 and, for this reason, it is difficult for docking algorithms to locate feasible binding modes of the known actives. We are working to investigate a distributed binding site hypothesis by extending the SH-base shape-matching algorithm, to be able to identify clusters of structural scaffolds from a large set of known actives. A first approach is shown here (PARAFIT Shape Consensus Tanimoto), which uses a "consensus shape", extracted from the average of the individual shapes for the most active ligands in the database belonging to different families, as the query for shape matching superpositions. In this way, the consensus query shape constructed from sterically similar known binders should give better virtual screening enrichments than only using a simple shape as the query, as the results for CCR5 shown here. The results obtained seem to corroborate the hypothesis that known CCR5 binders can form two or more groups, that is to say, they have two or more binding modes, and thus, a consensus shape representative of different binding modes can improve virtual screening results.

References

1. Maybride Bringing life to drug discovery, Maybridge Databases Autumn 2005; Fisher Scientific International: England, 2005.
2. W. M. Kazmierski, J. P. Peckman, M. Duan, T. P. Kenakin, S. Jenkinson, K. S. Gudmundsson, S. C. Pisciteli, P. L. Feldman; Recent Progress in the Discovery of New CCR5 and CXCR4 Chemokine Receptor Antagonists as Inhibitors of HIV-1 Entry. Part 2. *Curr Med Chem – Anti Infective Agents* 2005, 4:133-152.
3. MOE (Molecular Operating EnVironment), 2006.08 Release; Chemical Computing Group, Inc.: Montreal, Canada, 2004.
4. V. I. Pérez-Nueno, D. W. Ritchie, O. Rabal, R. Pascual, J. I. Borrell, J. Teixidó; Comparison of Ligand-Based and Receptor-Based Virtual Screening of HIV Entry Inhibitors for the CXCR4 and CCR5 Receptors Using 3D Ligand Shape Matching and Ligand-Receptor Docking. *J. Chem. Inf. Model.* 2008, 48:509-533.
5. D. W. Ritchie, G. J. L. Kemp; Fast computation, rotation and comparison of low resolution spherical harmonic molecular surfaces. *J. Comp. Chem.* 1999, 20(4):383-395.
6. L. Mavridis, B. D. Hudson, D. W. Ritchie; Toward High Throughput 3D Virtual Screening Using Spherical Harmonic Surface Representations. *J. Chem. Inf. Model.* 2007, 47:1787-1796.
7. J. A. Grant, M. A. Gallardo, B. J. Pickup; A fast method of molecular shape comparison. A simple application of a Gaussian description of molecular shape. *J.Comp. Chem.* 1996, 17:1653.
8. D. W. Ritchie, G. J. L. Kemp; Protein docking using spherical polar Fourier Correlations. *Proteins: Struct. Func. Genet.* 2000, 39: 178-194.
9. A. Sali, T. L. Blundell; Comparative protein modelling by satisfaction of spatial restrains. *Proteins* 1989, 5:355-373.
10. R. E. Bruccolieri; Application of Systematic Conformational Search to Protein Modeling. *Molecular Simulations* 1993, 10, 151-174.
11. G. M. Morris, D. S. Goodsell, R. S. Halliday, W. Hart, R. K. Belew, A. J. Olson; Automated Docking Using a Lamarckian Genetic Algorithm and Empirical Binding Free Energy Function. *J. Comp. Chem.* 1998, 19:1639-1662.
12. M. L. Verdonk, J. C. Cole, M. J. Hartshorn, C. W. Murray, R. D. Taylor; Improved Protein-Ligand Docking Using GOLD. *Proteins: Structure, Function, and Genetics* 2003, 52:609-623.
13. McGann, M. R.; Almond, H. R.; Nicholls, A.; Grant, J. A.; Brown, F. K. Gaussian docking functions. *Biopolymers* 2003, 68, 76-90.
14. J. Teixidó, J. I. Borrell, S. Nonell, X. Batllori, S. Pettersson, L. Ros, R. Puig de la Bellacasa, M. O. Rabal, V. I. Pérez-Nueno, J. Esté, I. Clotet, M. Armand-Ugón; Nuevos sistemas polinitrogenados como agentes anti-VIH, Patent PCT/ES2007/000613 N. Ref. 20070968, 2007.
15. S. Pettersson, I. Clotet-Codina, J. A. Esté, J. I. Borrell, J. Teixidó; Recent advances in combinatorial chemistry applied to development of anti-HIV drugs. *Mini Rev Med Chem.* 2006, 6(1):91-108.

Acknowledgements

Violeta I. Pérez-Nueno would like to thank the Generalitat de Catalunya – DURSI for a grant within the Formació de Personal Investigador (2008FI) program.

We thank OpenEye Scientific Software Inc. for providing an Academic Licence for ROCS, and we are grateful to Cepos Insilico Ltd. for providing a pre-release version of PARASURF.

This research was supported by the Department of Computing Science, University of Aberdeen, and the Organic Chemistry and Biochemistry Department, Institut Químic de Sarrià, Universitat Ramon Llull, Barcelona.

http://gem.iqs.url.edu

Virtual Screening tools applied to HIV entry inhibitors

Violeta I. Pérez-Nueno[1], Sofia Pettersson[1], María Obdulia Rabal[1], Laia Ros-Blanco[1], Raimon Puig de la Bellacasa[1], José Esté[2], Imma Clotet-Codina[2], Mercedes Armand-Ugón[2], Xavier Batllori[1], José I. Borrell[1] and Jordi Teixidó[1]

[1] Grup d'Enginyeria Molecular (GEM), Institut Químic de Sarrià (IQS), Universitat Ramon Llull, Via Augusta 390, E-08017-Barcelona (Spain). E-mail: j.teixido@iqs.url.edu

[2] Laboratori de Retrovirologia IrsiCaixa, Hospital Universitari Germans Trias i Pujol, Universitat Autònoma de Barcelona, E-08916-Badalona (Spain). E-mail: jaeste@irsicaixa.es

Introduction

G protein-coupled receptors (GPCRs) are one of the most exploited groups of drug targets. Here, we compare the application of structure-based and ligand-based virtual screening tools to find potential HIV entry inhibitors for the CXCR4 receptor using structure-based docking tools (AUTODOCK3[1], GOLD[2], FRED[3], HEX[4]), ligand-based pharmacophore modelling (MOE[5]), and ligand-based shape matching approaches (PARASHIFT[4], ROCS[6], HEX). The comparison between these methods was based on a retrospective virtual screening of a library containing some 4700 drug-like molecules[7] and different known CXCR4 inhibitors[8] as reference sets. We determined the enrichment factors and the diversity in the retrieved molecular scaffolds in the virtual hit lists.

A library of anti-HIV expected compounds was designed, selected and some of their compounds were synthesized in our group. The activity tests led to the identification of actives in the range from 20 to 0.008 μg/ml[9]. Experimental binding assays confirmed that the mode of action of the active synthesized compounds was blocking CXCR4 receptor. Activity values were used for the development of ligand-based QSAR models (MOE). Prospective virtual screening, using the same protocol as in retrospective virtual screening analysis, was applied for the identification of new anti-HIV compounds. Compounds selected using these computational tools were synthesized and are currently being tested. Also, we are applying *de novo design* to improve activity values of synthesized molecules.

Library design

Current CXCR4 antagonist

Current most active leads, such as AMD3100 (bicyclam, a CXCR4 antagonist), TAK-779 or SCH-D (CCR5 antagonists), contain nitrogenated heterocyclic systems separated by an aromatic or aliphatic linker. Among all compounds under study, bicyclams appear to be the most active ones.

We have designed a combinatorial library preserving the main features of AMD3100: the benzylic nitrogen on both sides of the p-phenylene moiety and the distance between the nitrogens in the heterocyclic systems, using commercially available nitrogenated building blocks and terephthalaldehyde or 4-(diethoxymethyl)benzaldehyde as precursors of the core structure.

The virtual combinatorial library has been built and enumerated with CERIUS2[10] and a reduced diverse set of compounds to be synthesized has been selected with PRALINS[11] (*Program for Rational Analysis of Libraries in Silico*).

AMD3100

EC50 = 0.001 μg/ml

CC50 > 5 μg/ml

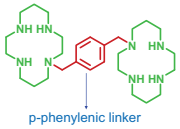

nitrogen-containing heterocyclic system

Target library

Retrosynthetic analysis

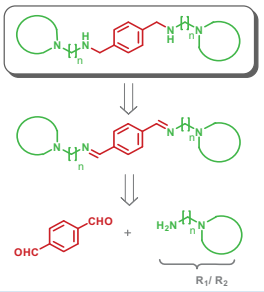

Library building blocks

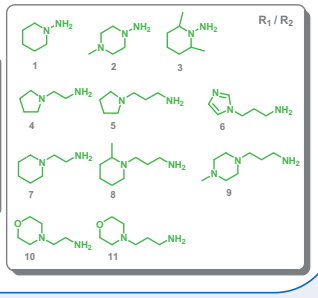

Ligand-based Virtual Screening

QSAR (MOE)

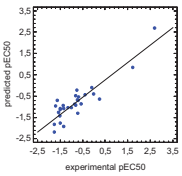

pEC_{50}= -3.47414 +0.00940·Q_VSA_HYD +0.00507·SlogP_VSA8 +0.10611·dipoleY

N=29, k=3, R^2=0.81, RMSE=0.42, F=36.45 (2.99), p=10^{-9}

R^2_{LOO}=0.75, $RMSE_{LOO}$=0.49

n=9, R^2_{test}=0.69, $RMSE_{test}$=0.57

PHARMACOPHORE MODELLING (MOE)

PHARMACOPHORE MODEL

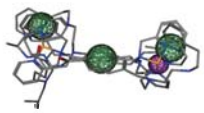

SCAFFOLD DIVERSITY ANALYSIS

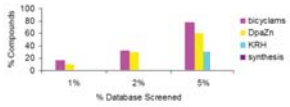

A	D	H_a	H_t	false +	false -	ef	%Y	%A	GH
151	1613	142	142	0	9	10.68	100.00	94.04	0.99

SHAPE MATCHING APPROACHES (PARASHIFT, ROCS, HEX)

RETROSPECTIVE ANALYSIS

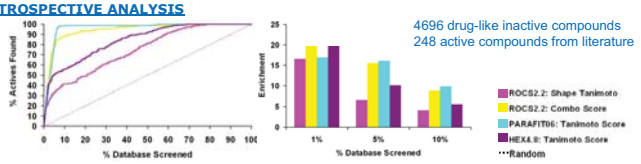

4696 drug-like inactive compounds
248 active compounds from literature

PROSPECTIVE ANALYSIS

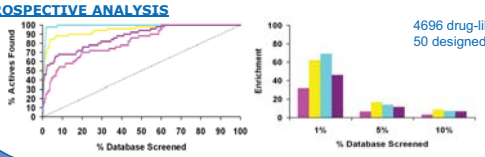

4696 drug-like inactive compounds
50 designed-library compounds

Structure-based Virtual Screening

DOCKING (AUTODOCK3, GOLD, FRED, HEX)

RETROSPECTIVE ANALYSIS

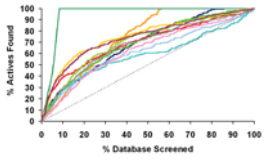

4696 drug-like inactive compounds
248 active compounds from literature

PROSPECTIVE ANALYSIS

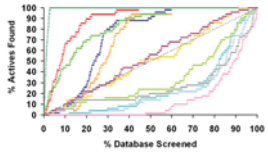

4696 drug-like inactive compounds
50 designed-library compounds

Receptor-based *de Novo Design*

We applied *de novo design* receptor-based (LUDI and LIGANDFIT modules of CERIUS2[10]) tools in order to find new active scaffolds and modify active molecules synthesized in our group. Receptor structure was used to identify the geometry and the kind of interactions that active ligands need to bind the target.

De novo designed compounds were selected according to a scoring function. In a retrospective docking analysis using 43 active compounds from the literature, scoring functions Ludi_3 and Ligscore2 were the ones that performed better, so these scoring functions were used to select the designed compounds to be synthesized and tested.

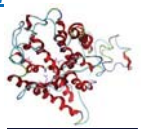

Conclusion

Some anti-HIV expected compounds from our designed library were synthesized and tested giving activity values in the range from 20 to 0.008 μg/ml. For the identification of new HIV entry inhibitors a combination of the aforementioned virtual screening tools helped us to select other molecules from the library; they show activity values in the range from 4 to 0.4 μg/ml and other are currently being tested.

Retrospective virtual screening shows that in this study ligand-based searches give better results than structure-based docking. Prospective virtual screening is consistent with this. Compounds selected by the different ligand-based virtual screening tools are practically the same, whereas the ones selected by structure-based docking tools include also some others.

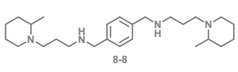

EC_{50} = **0.008** μg/ml
CC_{50} > **25** μg/ml

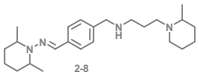

EC_{50} = 0.603 μg/ml
CC_{50} = 14.6 μg/ml

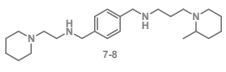

EC_{50} = 0.443 μg/ml
CC_{50} > 25 μg/ml

References

1. Morris *et al.*; ***J. Computational Chemistry*** 1998, 19:1639-1662.
2. Verdonk *et al.*; ***Proteins: Structure, Function, and Genetics*** 2003, 52:609-623.
3. McGann *et al.*; ***Biopolymers*** 2003, 68, 76-90.
4. D. W. Ritchie, G. J. L. Kemp; ***J. Comp. Chem.*** 1999, 20(4):383-395.
5. MOE, Molecular Operating Environment. Distributor: Chemical Computing Group, 1010 Sherbrooke St. West, #910, Montreal, Canada H3A.
6. J. A. Grant, M. A. Gallardo, B. J. Pickup; ***J.Comp. Chem.*** 1996, 17:1653.
7. Maybride Bringing life to drug discovery TM. Fisher Scientific International. Maybridge CD features: Maybridge Databases Autumn 2005.
8. Kazmierski *et al.*; ***Curr Med Chem – Anti Infective Agents*** 2005, 4:133-152.
9. J. Teixidó *et al.*; ***Spanish Patent No. ES200602764***, Oct. 26, 2006.
10. CERIUS2 Version 6.6. Accelrys Inc. 2001-2006
11. Pascual *et al.*; Mol. Divers. 2003, 6, 85-92.

Acknowledgments

This work was supported in part by the Fundació Marató de TV3 project 020930 and the Spanish Ministerio de Educación y Ciencia project BFI-2003-00405. I. Clotet-Codina and R. Puig de la Bellacasa hold a FI scholarship from Generalitat de Catalunya; and S. Pettersson, L. Ros-Blanco and V. Perez-Nueno from IQS.

We thank OpenEye Scientific Software Inc. for providing an Academic Licence for ROCS, and we are grateful to Cepos Insilico Ltd. for providing a pre-release version of PARASURF and PARAFIT.

http://gem.iqs.url.edu

Virtual screening tools applied to the discovery of novel HIV entry inhibitors for the CXCR4 and CCR5 receptors

Violeta Isabel Pérez Nueno
Grup d'Enginyeria Molecular, Institut Químic de Sarrià (IQS), Universitat Ramon Llull, Barcelona, Spain

Oral communication, 28th January 2009, Vandoeuvre-lès-Nancy, France

HIV entry inhibitors have emerged as a new generation of antiretroviral drugs that block viral fusion with the CXCR4 and CCR5 membrane co-receptors. Several small molecule antagonists for these co-receptors have been developed, some of which are currently in clinical trials. However, because no crystal structures for the co-receptor proteins are available, the binding modes of the known inhibitors within the co-receptor extracellular pockets need to be analyzed by means of site-directed mutagenesis and computational experiments. Here, we describe a detailed comparison of the performance of receptor-based and ligand-based virtual screening approaches to find CXCR4 and CCR5 antagonists that could potentially serve as HIV entry inhibitors [1].

For receptor-based virtual screening, homology models of CXCR4 and CCR5 have been built, using bovine rhodopsin as the template. For ligand-based virtual screening, several shape-based and property-based molecular comparison approaches have been compared, using high-affinity ligands as query molecules. Also, a novel consensus shape-based virtual screening approach has been developed and used to investigate and add further evidence for multiple binding sites within the CCR5 extracellular pocket hypothesis [2] [3].

All the receptor-based and ligand-based methods were compared by retrospective virtual screening, using a library assembled by us consisting of 672 known CXCR4 and CCR5 inhibitors and some 4700 similar presumed inactive molecules. For each receptor, the library was queried using known binders, and the enrichment factors and diversity of the resulting virtual hit lists were analyzed. Overall, ligand-based shape-matching searches yielded higher enrichments than receptor-based docking. Moreover, receiver-operator-characteristic performance analyses for both CXCR4 and CCR5 inhibitors showed that the new consensus shape matching approach gives better virtual screening enrichments than existing shape matching and docking virtual screening techniques.

Once the different virtual screening approaches had been validated and the best parameters had been selected, prospective virtual screening of a combinatorial library designed by us, derived from AMD3100 (one of the most potent CXCR4 antagonists), was applied to identify new anti-HIV compounds. The actives identified in this way had activities in the range 20 to 0.008 μg/ml. Experimental binding assays of those compounds confirmed that their mode of action was to block the CXCR4 receptor. Activity values were used for the development of ligand-based QSAR models in order to use them to predict activity of hitherto unsynthesised molecules. Prospective virtual screening, using the same protocol as in retrospective screening analysis, was then used to guide the selection of other molecules from the virtual combinatorial library. Molecules found at the first positions of the consensus ranked hit list showed activity values in the range from 4 to 0.022 μg/ml [4] [5] [6].

1. Pérez-Nueno, V. I.; Ritchie, D. W.; Rabal, O.; Pascual, R.; Borrell, J. I.; Teixidó, J. Comparison of Ligand-Based and Receptor-Based Virtual Screening of HIV Entry Inhibitors for the CXCR4 and CCR5 Receptors Using 3D Ligand Shape-matching and Ligand-Receptor Docking. *J. Chem. Inf. Model.* **2008**, *48*, 509-533.

2. Pérez-Nueno, V. I.; Ritchie, D. W.; Borrell, J. I.; Teixidó, J. Clustering and classifying diverse HIV entry inhibitors using a novel consensus shape based virtual screening approach: Further evidence for multiple binding sites within the CCR5 extracellular pocket. *J. Chem. Inf. Model.* **2008** , *48*, 2146-2165.

3. Carrieri, A.; Pérez-Nueno, V. I.; Fano, A.; Pistone, C.; Ritchie, D. W.; Teixidó, J.; Biological profiling of anti-HIV agents and insights into CCR5 antagonist binding using *in silico* techniques. *ChemMedChem* **2009**, *4* (Submitted).

4. Pérez-Nueno, V. I.; Pettersson, S.; Ritchie, D. W.; Borrell, J. I.; Teixidó, J. Discovery of Novel HIV Entry Inhibitors for the CXCR4 Receptor by Prospective Virtual Screening. *J. Chem. Inf. Model.* **2009**, 49 (Accepted).

5. Pettersson, S.; Pérez-Nueno, V. I.; Ros-Blanco, L.; Puig de la Bellacasa, R.; Rabal,O.; Batllori, X.; Clotet, B.; Clotet-Codina, I.; Armand-Ugón, M.; Esté, J.; Borrell, J. I.; Teixidó, J. Discovery of novel non-cyclam polynitrogenated CXCR4 coreceptor inhibitors. *ChemMedChem* **2008**, *3*, 1549 – 1557.

6. Teixidó, J.; Borrell, J. I.; Nonell, S.; Pettersson, S.; Ros, L; Puig de la Bellacasa, R.; Rabal, M. O.; Pérez-Nueno, V. I.; Esté, J.; Clotet-Codina, I.; Armand-Ugón, M.; Nuevos sistemas polinitrogenados como agentes anti-VIH. ES Patent ES200602764, **2006** (filing date: October 26, 2006).

JOURNAL OF CHEMICAL INFORMATION AND MODELING

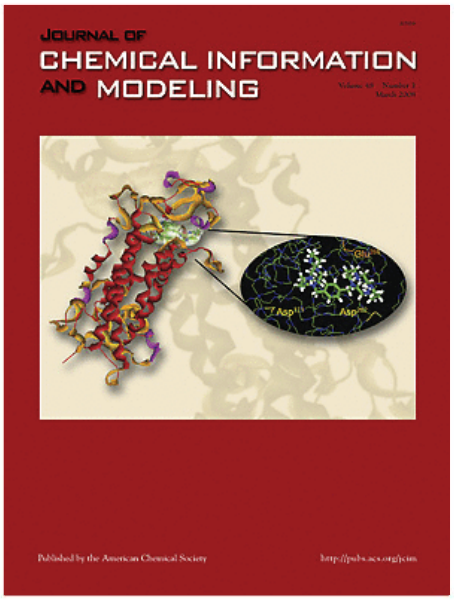

Volume 48, Issue 3
March 24, 2008 Cover

Virtual screening of HIV-blocking antagonists: the figure depicts the lowest energy CXCR4/AMD3100 binding conformation identified by AUTODOCK. The view on the left shows AMD3100 docked within the extracellular binding pocket of the CXCR4 receptor, shown as a ribbon cartoon. The AMD3100 molecular volume is depicted using a semitransparent spherical harmonic surface. The view on the right shows in more detail the calculated binding conformation. In this docking prediction, two nitrogens of one AMD3100 cyclam ring interact with the two carboxylic oxygens of Asp262, and two nitrogens of the other cyclam ring interact with the two carboxylic oxygens of Glu288. See V. I. Pérez-Nueno, D. W. Ritchie, O. Rabal, R. Pascual, J. I. Borrell, and J. Teixidó, p 509.

Close Window | Print Window